

DEVELOPMENT OF MECHANICAL PROPERTIES AND
BIOCOMPATIBILITY OF CALCIUM PHOSPHATE BONE CEMENT
FOR BONE SUBSTITUTION



A Thesis Submitted in Partial Fulfillment of the Requirements for the
Degree of Doctor of Philosophy in Materials Engineering
Suranaree University of Technology
Academic Year 2021

การพัฒนาคุณสมบัติเชิงกลและความเข้ากันได้ทางชีวภาพของซีเมนต์กระดูก
ชนิดแคลเซียมฟอสเฟตสำหรับการทดแทนกระดูก



วิทยานิพนธ์นี้เป็นส่วนหนึ่งของการศึกษาตามหลักสูตรปริญญาวิศวกรรมศาสตรดุษฎีบัณฑิต
สาขาวิชาวิศวกรรมวัสดุ
มหาวิทยาลัยเทคโนโลยีสุรนารี
ปีการศึกษา 2564

DEVELOPMENT OF MECHANICAL PROPERTIES AND
BIOCOMPATIBILITY OF CALCIUM PHOSPHATE BONE CEMENT FOR
BONE SUBSTITUTION

Suranaree University of Technology has approved this thesis submitted in
partial fulfillment of the requirements for a Doctor of Philosophy

Thesis Examining Committee

Dujreutai P. Kashima

(Asst. Prof. Dr. Dujreutai Pongkao Kashima)

Chairperson

Sir Rattanach

(Assoc. Prof. Dr. Sirat Tubsungnoen Rattanachan)

Member (Thesis Advisor)

S. Jiansirisomboon

(Assoc. Prof. Dr. Sukanda Jiansirisomboon)

Member

Nitinat Suppakarn

(Asst. Prof. Dr. Nitinat Suppakarn)

Member

Sanong Suksaweang

(Dr. Sanong Suksaweang)

Member

Chatchai Jothityangkoon

(Assoc. Prof. Dr. Chatchai Jothityangkoon)

Vice Rector for Academic

Affairs and Quality Assurance

Pornsiri Jongkol

(Assoc. Prof. Dr. Pornsiri Jongkol)

Dean of Institute of Engineering

ปารีทัศน์ ไทยทะเล: การพัฒนาคุณสมบัติเชิงกลและความเข้ากันได้ทางชีวภาพของซีเมนต์กระดูกชนิดแคลเซียมฟอสเฟตสำหรับการทดแทนกระดูก (DEVELOPMENT OF MECHANICAL PROPERTIES AND BIOCOMPATIBILITY OF CALCIUM PHOSPHATE BONE CEMENT FOR BONE SUBSTITUTION) อาจารย์ที่ปรึกษา: รองศาสตราจารย์ ดร. ศิริรัตน์ ทับสูงเนิน รัตนจันทร์, 207 หน้า.

คำสำคัญ: แคลเซียมฟอสเฟตซีเมนต์/ อะพาไทต์-ไตรแคลเซียมฟอสเฟตซีเมนต์/ ซีเมนต์กระดูก/ วิศวกรรมเนื้อเยื่อกระดูก

ถึงแม้ว่าอะพาไทต์ (apatite, HA)/เบต้า-ไตรแคลเซียมฟอสเฟต (β -TCP) ซีเมนต์จะเป็นหนึ่งในวัสดุสังเคราะห์ทดแทนกระดูกที่มีประสิทธิภาพสูง แต่สมบัติทางกลที่ไม่ดีนั้นกลายเป็นข้อจำกัดสำหรับการใช้งานภายใต้สภาวะรับแรงกดอัดสูง และได้กลายเป็นปัญหาที่สำคัญในการรักษาความผิดปกติของกระดูกต่างๆ เช่น โรคกระดูกพรุน ดังนั้นวิทยานิพนธ์นี้จึงมีวัตถุประสงค์ที่จะปรับปรุงคุณสมบัติทางกลของ apatite/ β -TCP ซีเมนต์เพื่อก้าวข้ามข้อจำกัดในการใช้งานได้เฉพาะภายใต้สภาวะรับแรงกดดันต่ำในความหลากหลายของวิศวกรรมเนื้อเยื่อกระดูก ซึ่งในสูตรซีเมนต์นี้ อัลฟา-ไตรแคลเซียมฟอสเฟต (α -TCP) เป็นสารตั้งต้นหลักที่สามารถสังเคราะห์ได้จากวิธีสังเคราะห์แบบปฏิกิริยาของแข็ง (solid state reaction) และวิธีสังเคราะห์แบบปฏิกิริยาของเหลว (wet chemical reaction) ซึ่งวิธีสังเคราะห์แบบปฏิกิริยาของเหลวเป็นวิธีการอีกทางเลือกที่มีประสิทธิภาพเนื่องจากความสะดวกและค่าใช้จ่ายในการเตรียมที่ต่ำกว่าวิธีสังเคราะห์แบบปฏิกิริยาของแข็ง อย่างไรก็ตามสารละลายที่ได้จากวิธีสังเคราะห์แบบปฏิกิริยาของเหลวนั้นมีความเป็นกรดสูง จึงเป็นปัญหาต่อเครื่องมือและอาจเป็นพิษต่อสิ่งแวดล้อมใกล้เคียง ดังนั้นจึงได้ทำการปรับค่าความเป็นกรดของสารละลายให้เป็นกลางโดยวิธีการนี้มีชื่อว่าวิธีการตกตะกอน (precipitation)

ในส่วนถัดมาจึงได้ทำการศึกษาผลของขนาดอนุภาคของ α -TCP ต่อคุณสมบัติต่างๆของซีเมนต์ ซึ่งพบว่าอนุภาค α -TCP ขนาดเล็กสามารถลดเวลาในการเซตตัว เพิ่มความแข็งแรง และกระตุ้นการเปลี่ยนแปลงเฟส HA ของซีเมนต์ นอกจากนี้ วิธีการฆ่าเชื้อของซีเมนต์นี้ด้วยวิธีการอบความร้อนแห้ง (dry heat sterilization) ได้ถูกตรวจสอบเนื่องจากวิธีการนี้อาจเป็นสาเหตุให้เกิดความเสียหายของเส้นใยไคโตซาน (chitosan) ที่อยู่ในผงซีเมนต์นี้ ซึ่งอาจจะนำไปสู่ผลกระทบที่ไม่พึงประสงค์ต่อการตอบสนองของเซลล์ ผลการทดลองแสดงให้เห็นว่าสภาวะวิธีการฆ่าเชื้อด้วยการอบความร้อนแห้งที่เหมาะสมคืออบที่อุณหภูมิ 121 องศาเซลเซียสเป็นเวลา 10 ชั่วโมง เนื่องจากสภาวะนี้ไม่ทำให้เกิดความเปลี่ยนแปลงของคุณสมบัติของซีเมนต์หรือความเสียหายของเส้นใยไคโตซาน

เพื่อจะเพิ่มความแข็งแรงให้กับซีเมนต์ apatite/ β -TCP ในส่วนต่อมาจึงได้ทำเติมพอลิอะคริลิกแอซิด (PAA) ที่ความเข้มข้นต่างๆ ตั้งแต่ 0 ถึง 50 เปอร์เซ็นต์โดยปริมาตร (v/v%) ลงไปในส่วนผสมของเหลว ซึ่งพบว่า 30 v/v% เป็นจุดวิกฤต ซึ่งสามารถเพิ่มความแข็งแรง และลดเวลาในการเซตตัวของซีเมนต์ อย่างไรก็ตาม PAA ในปริมาณที่มากขึ้นจะรบกวนการเปลี่ยนแปลงเฟส HA ของซีเมนต์ซึ่งจะไปลดความว่องไวทางชีวภาพของซีเมนต์ ดังนั้น ความเข้มข้นของ PAA ในซีเมนต์จึงถูกจำกัดให้แคบลงจากความเข้มข้นที่ 20 ถึง 35 v/v% และพบว่า ที่ 25 v/v% PAA แสดงความแข็งแรงของซีเมนต์สูงสุด

หลังจากนั้นจึงได้ทำการเติมแก้วที่มีความว่องไวทางชีวภาพสูง (bioactive glass, BG) ที่อัตราส่วน 0.5 ถึง 1.5 เปอร์เซ็นต์โดยน้ำหนัก (wt.%) เข้าไปในซีเมนต์เพื่อจะปรับปรุงคุณสมบัติความว่องไวทางชีวภาพที่ต่ำลงของซีเมนต์ ซึ่งพบว่า BG ช่วยลดเวลาในการเซตตัวและเพิ่มความแข็งแรงของซีเมนต์ ยิ่งไปกว่านั้นยังสามารถปรับปรุงความว่องไวทางชีวภาพของซีเมนต์ ซึ่งสามารถระบุได้จากการสร้าง HA บนผิวของชิ้นซีเมนต์มากขึ้นเมื่อเพิ่มปริมาณ BG ในซีเมนต์ เนื่องจากความแข็งแรงสูงสุดถูกพบในสูตร 1 wt.% BG ผสมซีเมนต์ (p-CPC/1.0BG) จึงได้นำสูตรนี้ไปศึกษาต่อในการทดลองทางชีวภาพกับเซลล์ต่างๆ 3 ชนิด คือเซลล์ตัวอ่อนกระดูก (osteoblast cell) เซลล์ต้นกำเนิดมีเซนไคม์ (mesenchymal stem cell) และเซลล์ต้นกำเนิดที่ได้จากไขมัน (adipose-derived stem cell) เพื่อเปรียบเทียบกับสูตรซีเมนต์ที่ไม่เติม BG (p-CPC) และสูตรซีเมนต์ควบคุมที่ไม่ได้เติมทั้ง BG และ PAA (CPC) ซึ่งผลแสดงให้เห็นว่าเซลล์ทั้ง 3 ชนิดชอบสูตร p-CPC/1.0BG และ p-CPC มากกว่า CPC ซึ่งสามารถวัดได้จาก ปริมาณการเจริญเติบโตและปริมาณการสร้างสารสำหรับเหนี่ยวนำการสร้างกระดูกของเซลล์ที่สูงกว่าในขณะที่อยู่บนชิ้นงาน p-CPC/1.0BG และ p-CPC เมื่อเทียบกับสูตร CPC ซึ่งปริมาณสารสำหรับการเหนี่ยวนำการสร้างกระดูกสูตรสูงสุดถูกพบในสูตรซีเมนต์ p-CPC/1.0BG เนื่องจากซีเมนต์ที่ถูกปรับปรุงด้วยการเติม PAA และ BG ในปริมาณที่เหมาะสมนั้น แสดงให้เห็นถึงความเข้ากันได้ดีกับเซลล์และมีความแข็งแรงสูง จึงสามารถเป็นสูตรซีเมนต์ที่มีโอกาสสำหรับการใช้งานภายใต้แรงกดสูงได้

PARITAT THAITALAY: DEVELOPMENT OF MECHANICAL PROPERTIES AND
BIOCOMPATIBILITY OF CALCIUM PHOSPHATE BONE CEMENT FOR BONE
SUBSTITUTION. THESIS ADVISOR: ASSOC. PROF. SIRIRAT TUBSUNGNOEN
RATTANACHAN, Ph.D., 207 PP.

Keyword: CALCIUM PHOSPHATE CEMENT/ APATITE-TRICALCIUM PHOSPHATE CEMENT/
BONE CEMENT/ BONE TISSUE ENGINEERING

Although apatite/ β -TCP cement is one of the highly effective synthetic bone grafts, its poor mechanical performance is limited for use under loadbearing condition. This is a major issue in the treatment of bone disorders such as osteoporosis. Therefore, this work aimed to improve the mechanical properties of apatite/ β -TCP cement to overcome its limited use only under non-loadbearing conditions in a variety of bone tissue engineering. In this cement formular, alpha-tricalcium phosphate (α -TCP) is a major phase that could be synthesized by conventional (solid state reaction) and new (wet chemical reaction) method. Thus, the wet chemical reaction method was an effectively alternative route due to its convenience in preparation with the less cost when compared with the solid state reaction. However, the wet chemical reaction still had some issues of strongly acidic solution during the manufacturing process, causing damage of instrument or toxic environment nearby. Therefore, the strong acid of wet chemical reaction was adjusted to neutral pH, naming as a precipitation method.

Afterward, the effect of particle size of α -TCP on the cement properties were investigated. Thus, the smaller size of α -TCP resulted in a reduced setting time, increased compressive strength, and enhanced hydroxyapatite (HA) phase conversion of cement. In addition, the effective dry heat sterilization was examined for this cement due to it could cause a damage of chitosan content in this cement system, leading to unfavorable effect to cellular responses. The result showed that the appropriate condition of dry heat sterilization was the condition of 121 °C for 10 h due to there

were no significant changes in physical properties of cement or significant damages in chitosan fibers.

Consequently, various concentration of PAA (0 to 50 v/v%) was added to the liquid phase to improve the compressive strength of apatite/ β -TCP cement. It was found that 30 v/v% PAA was a critical point, resulting in increased compressive strength and reduced setting time. However, higher PAA inhibited the HA conversion, which consequently downregulated the bioactivity of the cement. Therefore, the concentration of PAA was varied in narrower range from 20 to 35 v/v%, indicating the highest compressive strength at 25 v/v% PAA.

Afterward, the poor bioactivity of PAA-apatite/ β -TCP cement was improved by the addition of 0.5-1.5 wt.% bioactive glass (BG) to the cement powder. The results showed that BG reduced setting time and increased compressive strength of the cement. Moreover, the poor bioactivity of PAA-apatite/ β -TCP cement was improved, indicating higher HA formation on the surface of cement when increasing the BG content. Due to the highest compressive strength of modified cement was detected at 1 wt.% BG addition, the unmodified PAA-apatite/ β -TCP (p-CPC) and 1 wt.% BG (p-CPC/1.0BG) were selected for further analysis of cellular responses to these cements by using different cells (osteoblast, mesenchymal, and adipose-derived stem cell). In addition, the control cement (CPC) without modification of PAA and BG was used as a control sample. It was found that those cells favored both p-CPC/1.0BG and p-CPC more than the control CPC, indicating induced cell proliferation, and supported osteogenic differentiation. Thus, p-CPC/1.0BG presented the highest level of osteogenic differentiation production. As a result, p-CPC/1.0BG with excellent biocompatibility seemed to be the most promising formula for use under loadbearing condition.

School of Ceramic Engineering
Academic Year 2021

Student's Signature Paritot Thnitalny
Advisor's Signature Dr. Pethanadran

ACKNOWLEDGEMENTS

First of all, I would like to show my thankfulness to the Royal Golden Jubilee Ph.D. scholarship for their financial assistance and support throughout this program.

Secondly, I would like to express my appreciation to my advisor, Associate Professor Dr. Sirirat Tubsungnoen Rattanachan, for her exceptional guidance and assistance, not only in terms of "how to work or conduct research efficiently," but also in terms of other crucial life prospects. She's like a second mother to me. And it is because of her that I have had this great opportunity so far. I can't thank her enough for everything she's done for me. I would also like express my gratitude to the committee members, Assistant Professor Dr. Dujreutai Pongkao Kashima, Associate Professor Dr. Sukanda Jiansirisomboon, Associate Professor Dr. Nitinat Suppakarn, and Dr. Sanong Suksaweang for their insightful comments and recommendations.

Next, I would like to show my thankfulness to Professor Dr. Julie Elizabeth Gough for allowing me to join her research group at the University of Manchester as a visiting student. I'd also like to give special thanks to Dr. Thunyaporn Srisubin and the rest of the Gough group for their kind welcome, valuable guidance, and priceless expertise during my visit to their lab. I would also like to express my sincere thanks to Associate Professor Dr. Anna Teresa Brini for allowing me to participate as a visiting student in her research group at the University of Milano. Thank you to all of the Brini group members for their assistance and support, as well as all of the vital expertise. Dr. Chiara Giannasi deserves a special thanks for her assistance throughout my visit. I can't express how grateful I am for everything she has done for me.

Without my wonderful family's unending love, tolerance, and encouragement, I would never have come this far. I would dedicate my Ph.D. to Mr. Prayoot and Mrs. Kannika Thaitalay, my dear parents. Thanks to all of my dear close friends from my childhood who have always believed in me, supported me, cheered me up, and even

pulled me back when I had fallen too far. Without them, I would not have made it this far. And a huge thank you to Oranich Thongsri, a wonderful friend from the same lab group who has been really helpful throughout this long program. Without your assistance, I would not have come this far.

Finally, I would like to thank myself for not giving up despite all of the challenges I have faced and for always standing up for what I believe in. And I would like to thank everyone else who has helped me in some manner, whether directly or indirectly, that I have not mentioned. That means a lot to me.

Paritat Thaitalay

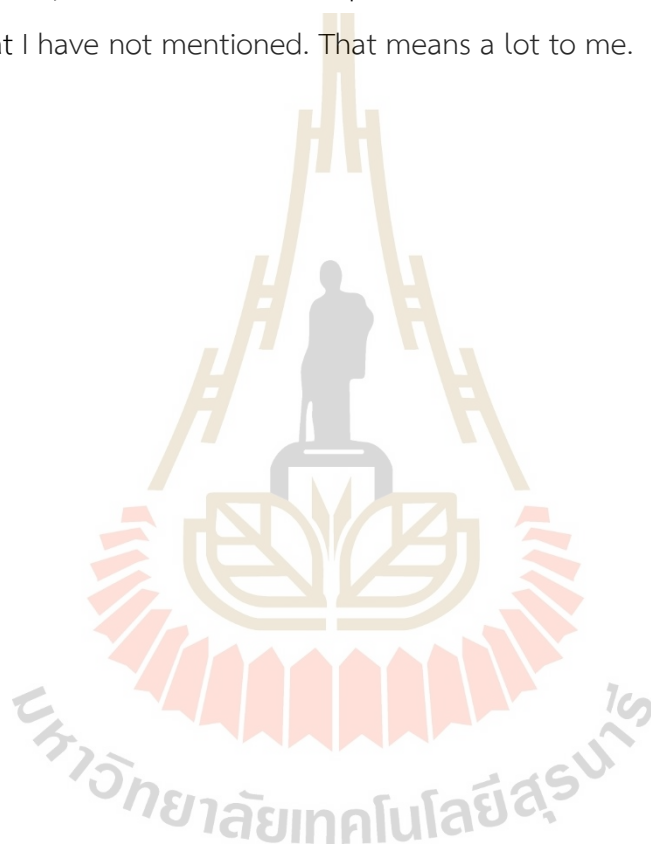


TABLE OF CONTENTS

	Page
ABSTRACT (THAI).....	I
ABSTRACT (ENGLISH).....	III
ACKNOWLEDGEMENT.....	V
TABLE OF CONTENTS.....	VII
LIST OF TABLES.....	XV
LIST OF FIGURES.....	XVI
LIST OF ABBREVIATIONS.....	XXVII
CHAPTER	
I. INTRODUCTION.....	1
1.1 GENERAL INTRODUCTION.....	1
1.2 BONE CEMENT.....	2
1.3 CALCIUM PHOSPHATE CEMENTS.....	3
1.4 CALCIUM PHOSPHATE COMPOUND AND SOLUBILITY.....	4
1.5 PROPERTIES AND LIMITATION OF CALCIUM PHOSPHATE CEMENTS.....	7
II. LITERATURE REVIEWS.....	11
2.1 Research background, rationale, and significance.....	11
2.2 Reinforcement of calcium phosphate cements.....	13
2.2.1 Addition of biopolymer.....	13
2.2.2 Addition of bioactive reagent.....	14
2.3 Literature reviews.....	15
2.3.1 Improvement of calcium phosphate cement by addition of PAA.....	15
2.3.2 Improvement of calcium phosphate cement by	

TABLE OF CONTENTS (Continued)

	Page
addition of BG.....	16
2.4 Starting chemical compounds of the modified apatite/ β -TCP Cement.....	22
2.4.1 Starting cement powder.....	22
2.4.2 Cement liquid.....	26
2.5 Thesis aims.....	28
2.6 Research objective.....	31
2.7 Scope and limitation.....	31
2.8 Expected benefit.....	31
III. INFLUENCED OF DIFFERENT SYNTHESSES OF ALPHA-TRICALCIUM PHOSPHATE POWDER ON APATITE/β-TCP CEMENT.....	33
3.1 Research background, rationale, and significance.....	34
3.2 Experimental procedure.....	35
3.2.1 Synthesis of α -TCP powder.....	35
3.2.2 Characterization of α -TCP powde.....	36
3.2.2.1 Phase composition and chemical functional group analysis.....	36
3.2.2.2 particle size distribution analysis.....	36
3.2.2.3 Morphology analysis.....	36
3.2.3 Characterization of cement.....	37
3.2.3.1 Cement preparation.....	37
3.2.3.2 Phase composition analysis.....	37
3.2.3.3 Setting time measurement.....	38
3.2.3.4 Compressive strength.....	38
3.2.3.5 Microstructure analysis... ..	39

TABLE OF CONTENTS (Continued)

	Page
3.3	Result and discussion 39
3.3.1	Characterization of α -TCP powder 39
3.3.1.1	Phase composition and chemical functional group analysis 39
3.3.1.2	Chemical functional group analysis 40
3.3.1.3	Particle size distribution analysis 43
3.3.1.4	Morphology analysis 43
3.3.2	Characterization of cement 45
3.3.2.1	Setting time measurement 45
3.3.2.2	Phase composition analysis 45
3.3.2.3	Compressive strength 47
3.3.2.4	Morphology analysis 48
3.4	Conclusions 50
IV.	SEVERAL PARAMETERS INFLUENCED ON APATITE/ β -TCP CEMENT: PARTICLE SIZE OF ALPHA-TRICALCIUM PHOSPHATE POWDER AND DRY-HEAT STERILIZATION 51
4.1	Research background, rationale, and significance 52
4.2	Experimental procedure 53
4.2.1	Effect of particle size of α -TCP powder on Apatite/ β -TCP cement 53
4.2.1.1	Synthesis and characterization of α -TCP powder 53
4.2.1.2	Preparation of cements 54
4.2.1.3	Properties testing and characterization of cement 54
4.2.2	Effect of dry heat sterilization on Apatite/ β -TCP cement 54
4.2.2.1	Preparation of cements 54

TABLE OF CONTENTS (Continued)

	Page
4.2.2.2	Properties testing and characterization of cement 55
4.2.2.3	pH measurement..... 55
4.3	Result and discussion..... 55
4.3.1	Effect of particle size of α -TCP powder on Apatite/ β -TCP cement..... 55
4.3.1.1	Phase composition of α -TCP powder..... 55
4.3.1.2	Particle size distribution of α -TCP powder..... 56
4.3.1.3	Morphology of α -TCP powder..... 57
4.3.1.4	Setting time measurement 58
4.3.1.5	Compressive strength..... 59
4.3.1.6	Phase composition of cement..... 60
4.3.2	Effect of dry heat sterilization on Apatite/ β -TCP cement..... 62
4.3.2.1	Phase composition and chemical functional group analysis..... 62
4.3.2.2	Compressive strength..... 64
4.3.2.3	Setting time measurement 65
4.3.2.4	pH measurement 66
4.3.2.5	Morphology analysis..... 67
4.4	Conclusions..... 68
V.	EFFECT OF POLYACRYLIC ACID/DISODIUM HYDROGEN PHOSPHATE MIXTURE ON APATITE/ β -TCP CEMENT 69
5.1	Research background, rationale, and significance 69
5.2	Experimental procedure 71
5.2.1	Cement liquid preparation 71
5.2.2	Preparation of cements..... 72

TABLE OF CONTENTS (Continued)

	Page
5.2.3 Properties testing and characterization of cement	73
5.2.4 Cell viability	73
5.3 Result and discussion.....	74
5.3.1 Phase composition.....	74
5.3.2 Chemical functional group analysis	76
5.3.3 Setting time measurement.....	79
5.3.4 Compressive strength	82
5.3.5 pH measurement and in vitro bioactivity	83
5.3.6 Cell viability	89
5.4 Conclusions.....	91
VI. EFFECT OF NANO-BIOACTIVE GLASS ON POLYMERIC APATITE/β-TCP	
CEMENT	92
6.1 Research background, rationale, and significance	93
6.2 Experimental procedure	95
6.2.1 Preparation of nano-bioactive glass.....	95
6.2.2 Preparation of cement	96
6.2.3 Properties testing and characterization of cement	97
6.2.4 In vitro testing.....	97
6.2.4.1 hASCs and culture conditions	97
6.2.4.2 Indirect cell culture	98
6.2.4.3 Direct cell culture	99
6.2.4.4 pH changes and ion concentration in culture medium.....	99
6.2.4.5 Alamarblue assay	99
6.2.4.6 BCA protein assay.....	100

TABLE OF CONTENTS (Continued)

	Page
6.2.4.7 Alkaline phosphatase assay.....	100
6.2.5 Statistical analysis.....	100
6.3 Result and discussion.....	100
6.3.1 Characterization of n-BG.....	100
6.3.2 Setting time measurement.....	103
6.3.3 Mechanical testing.....	105
6.3.4 Phase composition analysis.....	107
6.3.5 Morphology analysis.....	110
6.3.6 In vitro testing.....	111
6.3.6.1 Ion releasing/adsorption and pH measurement.....	111
6.3.6.2 Indirect cell culture: metabolic activity.....	115
6.3.6.3 Direct cell culture: metabolic activity.....	117
6.3.6.4 Direct cell culture: total protein contents.....	119
6.3.6.5 Direct cell culture: ALP activity.....	120
6.4 Conclusions.....	122
VII. SELF-SETTING NANO-BIOACTIVE GLASS ADDED POLYMERIC APATITE/β-TCP CEMENT FOR BONE FIXATION AND REGERATION.....	124
7.1 Research background, rationale, and significance.....	125
7.2 Experimental procedure.....	127
7.2.1 Preparation of precursors.....	127
7.2.2 Preparation of cement.....	136
7.2.3 Properties testing and characterization of cement.....	128
7.2.4 Injectability testing.....	128
7.2.5 Degradation.....	129
7.2.6 Nitrogen adsorption/desorption analysis.....	129

TABLE OF CONTENTS (Continued)

	Page
7.2.7 In vitro biocompatibility.....	130
7.2.7.1 Cell culture conditions.....	130
7.2.7.2 Live/Dead assay.....	130
7.2.7.3 pH changes, ion release/adsorption, and surface roughness.....	131
7.2.7.4 Cell morphology.....	132
7.2.7.5 Cell proliferation.....	132
7.2.7.6 DNA quantification.....	133
7.2.7.7 Alkaline phosphatase (ALP) assay.....	133
7.2.7.8 Total collagen secretion.....	134
7.2.7.9 Statistical analysis.....	134
7.3 Result and discussion.....	134
7.3.1 Setting time measurement.....	134
7.3.2 Injectability.....	136
7.3.3 Mechanical testing.....	137
7.3.4 Phase composition analysis.....	139
7.3.5 FT-IR.....	144
7.3.6 Degradation.....	147
7.3.7 Nitrogen adsorption/desorption analysis.....	148
7.3.8 Cement morphology analysis.....	151
7.3.9 In vitro biocompatibility.....	155
7.3.9.1 Live/Dead assay.....	155
7.3.9.2 Cell morphology.....	160
7.3.9.3 pH changes, ion release/adsorption, and surface roughness.....	162

TABLE OF CONTENTS (Continued)

	Page
7.3.9.4 Cell proliferation and Picogreen DNA quantification	167
7.3.9.5 Alkaline phosphatase (ALP) assay	167
7.3.9.6 Total collagen secretion.....	169
7.4 Conclusions.....	172
VIII. CONCLUSIONS.....	174
8.1 Effect of different synthesis of α -TCP powder on physical properties of apatite/ β -TCP cement.....	174
8.2 Effect of particle size of α -TCP and dry heat sterilization on physical properties of apatite/ β -TCP cement.....	175
8.3 Effect of PAA added into apatite/ β -TCP cement on its physical properties and cytotoxicity	175
8.4 Effect nano-BG added into polymeric apatite/ β -TCP cement on its physical performances and adipose-derived stem (ASC) cells behaviors.....	176
8.5 Nano-BG incorporated polymeric apatite/ β -TCP cement for bone regeneration.....	176
REFERENCES	179
APPENDIX I LIST OF PUBLICATIONS	205
BIOGRAPHY	207

LIST OF TABLES

Table	Page
1.1 Calcium phosphate compounds and solubility	5
2.1 The improvement of cement properties by the incorporation of various polymer	13
2.2 Composition and properties of PAA modified calcium phosphate bone cements.....	19
2.3 Composition and properties of BG modified calcium phosphate bone cements.....	20
3.1 Main bands and characteristic wave number of α -TCP (α -solid and α -wet) compared with α -TCP from literature review	42
3.2 Particle size distribution of powders.....	43
3.3 The quantitative results of two different powder of α -TCP, using EDX spectrum analyzer	44
3.4 Setting time measurement of cement at different L/P ratio	45
3.5 Percentage of hydroxyapatite after immersion of cement in SBF solution over 14 days.....	47
4.1 Dry heat sterilized conditions	55
5.1 The mixture of cements liquid comprising of the different ratio of PAA and Na ₂ HPO ₄	72
5.2 EDS analysis of Ca/P mole ratio of sample surface at 0, 7 days of immersion.....	87
7.1 Compositions of cement with different solid and liquid phase, and L/P ratio	128
7.2 Conditions of cement with different preparation process.....	131

LIST OF FIGURES

Figure	Page
1.1 Solubility diagrams of (a) Ca and (b) P ions for each calcium orthophosphate compounds.....	7
1.2 Comparison of compressive strength of natural bone and different type of calcium phosphate cements: apatite cement (HA), monophasic (m) and biphasic (b) as setting product of Sr substituted apatite cement, brushite cement (brushite), and Sr substituted brushite cement (s).....	10
3.1 XRD pattern of α -TCP obtained by solid state reaction (α -solid), and wet chemical reaction (α -wet).....	40
3.2 FTIR spectra of α -TCP obtained by two methods (α -solid, α -wet).....	41
3.3 SEM images of α -TCP powder obtained by solid state reaction and wet chemical reaction synthesis at magnification of x1000 and x5000.....	44
3.4 XRD patterns of cement containing α -TCP powder obtained by solid state reaction and wet chemical reaction synthesis at L/P ratio of (a) 0.35 and (b) 0.40 after soaking in SBF solution for 7 and 14 days.....	46
3.5 Compressive strength of cement containing α -TCP powder obtained by solid state reaction and wet chemical reaction synthesis at L/P ratio of 0.35 and 0.40 after soaking in SBF solution for 7 days.....	48
3.6 Fracture surface micrographs of cement containing α -TCP powder obtained by solid state reaction and wet chemical reaction synthesis at L/P ratio of 0.35 and 0.40 after soaking in SBF solution for 7 days.....	49

LIST OF FIGURES (Continued)

Figure	Page
3.7	SEM images of surface area of cement containing α -TCP powder obtained by solid state reaction and wet chemical reaction synthesis at L/P ratio of 0.35 and 0.40 after soaking in SBF solution for 7 days.....
	50
4.1	XRD patterns of α -TCP powder with various milling times of 0, 4, 6, and 8 hours.
	56
4.2	Particle size distribution of α -TCP powder with different milling times of 0, 4, 6, and 8 hours, respectively.....
	57
4.3	SEM micrographs of α -TCP powder at different milling times of 4, 6, and 8 hours
	58
4.4	Initial and final setting time of apatite/ β -TCP cement with various milling times of α -TCP powder at L/P ratio of 0.40.
	59
4.5	Compressive strength of apatite/ β -TCP cement with various milling times of α -TCP powder at L/P ratio of 0.40 after soaking in SBF solution for 7 days.
	60
4.6	XRD patterns of apatite/ β -TCP cement with various milling times of α -TCP powder at L/P ratio.....
	61
4.7	Weight percent of α -TCP and HA phases in apatite/ β -TCP cement with various milling times of α -TCP powder at L/P ratio of 0.40 after soaking in SBF solution for 7 days
	61
4.8	XRD patterns of starting cement powder with various dry heat-sterilized conditions
	63

LIST OF FIGURES (Continued)

Figure	Page
4.9 XRD patterns of cement with various dry heat-sterilized conditions at L/P ratio of 0.40 after soaking in SBF solution for 7 days.63
4.10 FT-IR patterns of chitosan fiber with various dry heat-sterilized conditions, each band region was referred to previous study.....	.64
4.11 Compressive strength of cement with various dry heat-sterilized conditions at L/P ratio of 0.40 after soaking in SBF solution for 7 days65
4.12 Initial and final setting time of cement before and after dry heat sterilization at 121 °C for 10 hours with L/P ratio of 0.4066
4.13 pH changes in SBF at different period of time after immersion of both cements (Non-sterilized and sterilized sample).....	.67
4.14 SEM micrographs of the surface of the cements (Non-sterilized and sterilized sample) after incubation in SBF solution for 7 days68
5.1 XRD patterns of the bone cement containing of the different PAA contents (0-100PAA) at 0.35 L/P ratio after soaking in SBF solution for 7 days75
5.2 XRD patterns of the bone cement containing of the different PAA contents (0-50PAA) at 0.35 L/P ratio after soaking in SBF solution for 7 days76
5.3 Percentage of Phase composition after immersion of cement (0.35 L/P ratio) in SBF solution for 7 days using Rietveld refinement analysis.....	.76
5.4 FT-IR patterns of the bone cement containing of the different PAA contents at 0.35 L/P ratio.....	.78

LIST OF FIGURES (Continued)

Figure	Page
5.5	Enlarge FT-IR patterns of the bone cement containing of the different PAA contents for wavelength of 1500-1600 cm ⁻¹78
5.6	The relationship between the setting time of bone cement with the content of PAA with the L/P ratio of 0.35 and 0.4, respectively (****p < 0.0001)..... .81
5.7	Setting mechanism and phase conversion of apatite cement based on α -TCP powder, interacted with aqueous solution and PAA81
5.8	Compressive strength of the bone cement containing of the different PAA contents with L/P ratio of 0.35 and 0.4 ml/g Mean \pm SD, n = 9 replicates. (**p < 0.01 and ****p < 0.0001)..... .83
5.9	pH change of SBF in a period of time after immersion of bone cement samples with the different of PAA contents..... .85
5.10	SEM micrographs of the surface of the bone cements with different PAA concentrations from 0-50 v/v%, (a) 0PAA, (b) 10PAA, (c) 20PAA, (d) 30PAA, (e) 40PAA, (f) 50PAA as prepared before soaking in SBF (day0). Sample surface of (g) 0PAA, (h) 10PAA, (i) 20PAA, (j) 30PAA, (k) 40PAA, (l) 50PAA soaked in SBF for 7 days.86
5.11	Schematic drawing illustrating the effect of the setting reaction related to setting time, compressive strength, and bioactivity on the concentration of PAA88
5.12	Cell viability of NIH 3T3 fibroblast cells after culturing with precondition medium of each samples including 0PAA, 30PAA, and biphasic granule from days 1, 2 and 7. Mean \pm SD, n = 3 replicates. (NS = no significance, *p < 0.05, and ****p < 0.0001).90

LIST OF FIGURES (Continued)

Figure	Page
6.1	Schematic drawing illustrating the procedure of two different hASCs culture conditions (Indirect and Direct culture)..... 98
6.2	SEM image of n-BG powders, magnification of x50,000..... 102
6.3	TEM image of n-BG powders, magnification of x100,000 102
6.4	Particle size distribution of n-BG powders..... 103
6.5	XRD pattern of n-BG powders 103
6.6	Initial and final setting time of polymeric apatite/ β -TCP cement containing the different n-BG contents 105
6.7	Compressive strength of cement containing the different n-BG contents after immersion in the SBF solution for 7 days..... 107
6.8	Young's modulus of cement containing the different n-BG contents after immersion in the SBF solution for 7 days..... 107
6.9	XRD patterns of the apatite/ β -TCP cement containing the different n-BG contents after immersion in SBF solution for 7 days..... 109
6.10	Phase composition of apatite/ β -TCP cement containing the different n-BG contents after immersion in SBF solution for 7 days. The experiment was repeated in duplicate with n = 6..... 109
6.11	SEM micrographs of the surface (1 and 14 days) and fracture (14 days) of the cements with different n-BG concentrations from 0-1.5 wt.% soaking in SBF solution at different time points, magnification of x10,000 111
6.12	pH change in (a) control (-OS) and (b) osteogenic (+OS) media after soaking samples in cell culture media at different immersion time points (Day 0 is preconditioned overnight)..... 113

LIST OF FIGURES (Continued)

Figure	Page
6.13 Ion changes of Mg ions in (a) control (-OS) and (b) osteogenic (+OS) media. All ions of each condition were subtracted by the control cell culture medium as a blank, showing the ions in the medium adsorbed by samples (negative values) and ions released from sample to medium (positive values).	113
6.14 Ion changes of Na ions in (a) control (-OS) and (b) osteogenic (+OS) media. All ions of each condition were subtracted by the control cell culture medium as a blank, showing the ions in the medium adsorbed by samples (negative values) and ions released from sample to medium (positive values).	114
6.15 Ion changes of P ions in (a) control (-OS) and (b) osteogenic (+OS) media. All ions of each condition were subtracted by the control cell culture medium as a blank.....	114
6.16 Ion changes of Ca ions in (a) control (-OS) and (b) osteogenic (+OS) media. All ions of each condition were subtracted by the control cell culture medium as a blank, showing the ions in the medium adsorbed by samples (negative values) and ions released from sample to medium (positive values).	115
6.17 Ion changes of Si ions in (a) control (-OS) and (b) osteogenic (+OS) media. All ions of each condition were subtracted by the control cell culture medium as a blank.....	115
6.18 Indirect culture: hASCs proliferation on tissue plastic plate cultured with sample-conditioned medium at different time points (The comparison between complete (-OS) and osteogenic (+OS) medium within each condition	

LIST OF FIGURES (Continued)

Figure	Page
	(CPC, CPC/1.0BG, and control) is shown as ns = no significance, *p < 0.05, and ****p < 0.0001/ The comparison among samples grown in -OS medium as \$\$\$p < 0.01/ The comparison among samples grown in +OS medium as ++++p < 0.0001).....
6.19	Direct culture: hASCs proliferation on samples. The comparison between complete (-OS) and osteogenic (+OS) medium within each condition (CPC, CPC/1.0BG, and control) is shown as ns = no significance, **p < 0.01, and ****p < 0.0001/ The comparison among samples grown in -OS medium as \$\$\$p < 0.01, \$\$\$p < 0.001, and \$\$\$p < 0.0001/ The comparison among samples grown in +OS medium as +p < 0.05, ++p < 0.01, and ++++p < 0.0001).....
6.20	Direct culture: hASCs protein content (day 21) on samples. The comparison between complete (-OS) and osteogenic (+OS) medium within each condition (CPC, CPC/1.0BG, and control) is shown as ***p < 0.001 and ****p < 0.0001/ The comparison among samples grown in -OS medium as \$\$\$p < 0.0001/ The comparison among samples grown in +OS medium as +p < 0.05 and ++++p < 0.0001).....
6.21	Direct culture: hASCs differentiation (day 21) on samples. The comparison between complete (-OS) and osteogenic (+OS) medium within each condition (CPC, CPC/1.0BG, and control) is shown as *p < 0.05.....
7.1	Setting time of all cement conditions at different L/P ratio of 0.35 and 0.40. The un moldable sample was denoted as X.

LIST OF FIGURES (Continued)

Figure	Page	
7.2	Injectability percentage of each cement condition with an appropriate selective L/P ratio 0.35; p-CPC and p-CPC/BG, 0.40; CPC). The statistical comparison among sample conditions: ns = no significance, **p < 0.01, and ***p < 0.001.....	137
7.3	Compressive strength of each cement condition after immersion in SBF solution over 28 days. The statistical comparison among sample conditions is shown as ns = no significance, *p < 0.05, ***p < 0.001, and ****p < 0.0001.....	138
7.4	Young's Modulus of each cement condition after immersion in SBF solution over 28 days. The statistical comparison among sample conditions is shown as ns = no significance, *p < 0.05, **p < 0.01, and ***p < 0.001.....	139
7.5	XRD patterns of (a) CPC, (b) p-CPC, and (c) p-CPC/BG cement after immersion in SBF solution over 28 days.....	140
7.6	Remaining phases of (a) HA, (b) α -TCP, (c) DCPA, (d) CaCO ₃ , and (e) β -TCP in cement matrix of each cement condition after immersion in SBF solution over 28 days	142
7.7	FTIR patterns of (a) CPC, (b) p-CPC, and (c) p-CPC/BG cement after immersion in SBF solution over 28 days.....	145
7.8	Weight loss percentage of each cement condition after immersion in SBF solution over 28 days	147
7.9	N ₂ adsorption-desorption isotherms and (b) pore size distribution curves of each cement condition, as comparing samples before (0d) and after immersion in SBF for 28 days (28d).....	149

LIST OF FIGURES (Continued)

Figure	Page
7.10 Cumulative pore volume (Macropore and mesopore) of each cement condition, as comparing samples before (0d) and after immersion in SBF for 28 days (28d). The statistical comparison among sample conditions is shown as * $p < 0.05$, ** $p < 0.001$, and **** $p < 0.0001$	150
7.11 Specific surface area of each cement condition, as comparing samples before (0d) and after immersion in SBF for 28 days (28d).....	151
7.12 SEM micrographs of the fracture (magnification of x100 and x5,000) and surface (magnification of x5,000) of the CPC cement before and after soaking in SBF solution over 28 days.....	153
7.13 SEM micrographs of the fracture (magnification of x100 and x5,000) and surface (magnification of x5,000) of the p-CPC cement before and after soaking in SBF solution over 28 days.....	154
7.14 SEM micrographs of the fracture (magnification of x100 and x5,000) and surface (magnification of x5,000) of the p-CPC/BG cement before and after soaking in SBF solution over 28 days.....	155
7.15 Live/Dead assay of HObs on coverslip cultured with preconditioned media and control medium for 1 day (Day0), magnification of x10. Green stain represents live cells and red stain represents dead cells. The scale bar was 100 μm	156
7.16 Live/Dead assay of HObs cultured on each cement condition with different sample preparation for 1 day, magnification of x10. Green stain represents live cells and red stain represents dead cells. The scale bar was 100 μm	158

LIST OF FIGURES (Continued)

Figure		Page
7.17	Live/Dead assay of HObs cultured on each cement condition with different sample preparation for 7 days, magnification of x10. Green stain represents live cells and red stain represents dead cells. The scale bar was 100 μ m.	159
7.18	Live/Dead assay of MSCs cultured on each cement condition with different sample preparation for 1 (Day1) and 7 (Day7) days, magnification of x10. Green stain represents live cells and red stain represents dead cells. The scale bar was 100 μ m.	159
7.19	HObs morphology cultured on each cement condition with control medium for 7 days. 2D images of cells spreading stained with phalloidin for actin cytoskeleton (green) and DAPI for the nucleus (blue), original magnification of x40. SEM images show cells adhesion on each cement at magnification of x1000.....	161
7.20	MSCs morphology cultured on each cement condition with control medium for 7 days. 2D images of cells spreading stained with phalloidin for actin cytoskeleton (green) and DAPI for the nucleus (blue), original magnification of x40. SEM images show cells adhesion on each cement at magnification of x1000.....	161
7.21	pH value of sample-conditioned medium after soaking in culture medium at different time points.	163
7.22	Ion changes of (a) Ca, (b) Si, (c) P, (d) Na, and (e) Mg ions of sample-conditioned medium after soaking in culture medium at different time points. All ions of each condition were subtracted by the control cell culture medium as a blank, showing the ions in	

LIST OF FIGURES (Continued)

Figure	Page
the medium adsorbed by samples (Grey area: negative value) and ions released from sample to medium (White area: positive value).....	164
7.23 Surface roughness of each cement condition after immersion in culture medium overnight	165
7.24 Metabolic activity of (a) HObs and (b) MSCs cultured for 1, 7, 14, 21, and 28 days in the control medium.....	166
7.25 DNA content of (a) HObs and (b) MSCs cultured for 1, 7, 14, 21, and 28 days in the control medium.....	167
7.26 ALP activity of (a) HObs and (b) MSCs cultured on cement sample with control medium (OS-) and osteogenic medium (OS+) for 1, 7, 14, 21, and 28 days (The statistical comparison among sample conditions is shown as *p < 0.05, **p < 0.01, ***p < 0.001, and ****p < 0.0001/ The comparison between complete (OS-) and osteogenic (OS+) medium as \$p < 0.05 and \$\$p < 0.01).....	169
7.27 Total collagen secretion of (a) HObs and (b) MSCs cultured on cement sample with control medium (OS+) and osteogenic medium (OS+) for 14 and 28 days (The statistical comparison among sample conditions is shown as *p < 0.05, **p < 0.01, and ***p < 0.001/ The comparison between complete (OS-) and osteogenic (OS+) medium as \$p < 0.05, \$\$p < 0.01, and \$\$\$p < 0.001).	171

LIST OF ABBREVIATIONS

PMMA	=	Polymethyl methacrylate
PAA	=	Polyacrylic acid
Na ₂ HPO ₄	=	Disodium hydrogen phosphate
NaH ₂ PO ₄	=	Sodium dihydrogen phosphate
BG	=	Bioactive glass
CPCs	=	Calcium phosphate cements
α -TCP	=	Alpha-tricalcium phosphate
β -TCP	=	Beta-tricalcium phosphate
HA	=	Hydroxyapatite
CDHA	=	Calcium deficient hydroxyapatite
OCP	=	Octacalcium phosphate
CaCO ₃	=	Calcium carbonate
MCPM	=	Monocalcium phosphate monohydrate
MCPA	=	Monocalcium phosphate anhydrous
DCPD	=	Dicalcium phosphate dihydrate
DCPA	=	Dicalcium phosphate anhydrous
TTCP	=	Tetracalcium phosphate
L/P	=	Liquid to powder
Ca/P	=	Calcium to phosphate
XRD	=	X-ray diffraction
FTIR	=	Fourier transform infrared spectroscopy
SEM	=	Scanning electron microscopy
BET	=	Brunauer-Emmett-Teller
ICP-OES	=	Inductively coupled plasma optical emission spectrometry
UTM	=	Universal testing machine

LIST OF ABBREVIATIONS (Continued)

EDX	=	Energy dispersive X-ray
SBF	=	Simulated body fluid
PBS	=	Phosphate-buffered saline
Mw	=	Molecular weight
CO ₂	=	Carbon dioxide
hASCs	=	human Adipose-derived Stem/Stromal cells
MSCs	=	Mesenchymal Stem/Stromal cells
HObs	=	Primary human osteoblast cells
ALP	=	Alkaline phosphatase
MPa	=	Megapascal
mM	=	Millimolar
PO ₄ ³⁻	=	phosphate ions
Na ⁺	=	Sodium ions
Ca ²⁺	=	Calcium ions
Mg ²⁺	=	Magnesium ions
Si ⁴⁺	=	Silicon ions
n-BG	=	Nanoparticle bioactive glass

CHAPTER I

INTRODUCTION

1.1 General introduction

The elderly population is currently increasing and will continue to grow in the future worldwide. The most common unavoidable consequence is osteoporosis, which causes older people's bones to become weaker. In addition, general orthopaedic accidents can happen to anyone. Furthermore, congenital deformity, infection, and tumour treatment can all result in large orthopaedics and maxillofacial bone abnormalities (Laurencin, 2006).

As a result, they frequently require the use of bone grafts for bone replacement. Bone grafts can be classified into four different kinds, which include autografts (from patients), allografts (from other humans), xenografts (from other species), and alloplasts (synthetic materials) (Suneelkumar, 2008).

(i) Autograft or autogenous bone graft has traditionally been known as gold standard for bone grafting materials due to its osteoconductive, osteoinductive, and osteogenic properties. It was transplanted from one location to another by the same person, and it was the patient's own bone. The drawback of autograft is the inherent morbidity or complex procedure, despite the fact that there is no immune reaction or infection connected to hazards. (Campana, 2014).

(ii) Allograft or allogenic bone graft is a type of bone graft obtained from people that is utilized as a second option. It can be obtained from either living or non-living donors who have been submitted to a bone bank. Allograft bone has some drawbacks, such as expense, infection risk, and sterilization requirements (gamma irradiation).

(iii) Xenograft or xenogenic bone graft is known as a graft made of other species, such as bovine bone or porcine bone. It can be freeze dried or demineralized or deproteinized.

(iv) Alloplast or alloplastic bone graft (synthetic) is defined as the synthetic materials, such as hydroxyapatite, TCP, and bioglass. These synthetic bone grafts overcome a need for secondary operation for autograft harvest. Thus, both sophisticated osteoconduction and degradability of synthetic bone graft could be achieved by mixing TCP with HA (Kumar, 2013).

Consequently, synthetic biomaterials appeared to be the most effective bone replacement and fixation options because they could be customized for each patient with different types of bone defects. Bone cements have been famously used for bone fixation due to their various advantages, such as injectability, cementation at room temperature, degradability, osteoconductivity.

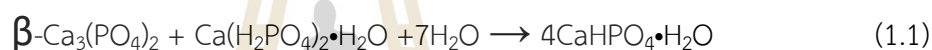
1.2 Bone cements

Bone cements were first discovered by J. Charnley, and have been used in orthopaedic surgery since the late 1950s. (Mitzner, 2009). Polymethyl methacrylate (PMMA) bone cement has been used as the gold standard for bone fixation in various orthopaedic treatments, while other several bone cements have been developing (L. Evans, 2006). However, long-term implantation could result in a foreign-body reaction (rejection risk) or failure of the synthetic bone replacement with a failure rate of up to 10% after 15 years (Ayre, 2014). This could be due to the poor bioactivity of non-degradable PMMA, which does not support cell and new bone ingrowth in the material after implantation (Mitzner, 2009, Sun, 2017). Furthermore, PMMA could produce heat during the cementation process, causing serious harm to living tissue (Santos Jr., 2013). Meanwhile, calcium phosphate bone cements have been receiving more attention in orthopaedic and dental treatments because they are biodegradable, biocompatible, and bioactive (Xu, 2017).

1.3 Calcium phosphate cements

Calcium phosphate cements (CPCs) are commonly produced by blending crystalline or amorphous calcium phosphate with an aqueous solution, which finally generates a hardening cement mechanism via a dissolution-precipitation process. Generally, the end-setting products of CPCs could be divided into two categories: dicalcium dihydrate (DCPD, brushite) and hydroxyapatite/calcium deficient hydroxyapatite (HA/CDHA, apatite) (Geffers, 2015, O'Neill, 2017), as shown in following equations (Dorozhkin, 2008).

- Brushite cement (DCPD) was formed by the acid-base reaction of beta-tricalcium phosphate (β -TCP) and monocalcium phosphate monohydrate (MCPM)



- Apatite cement (HA) was form by the acid-base reaction of tetracalcium phosphate (TTCP) + dicalcium phosphate anhydrous (DCPA)



- Apatite cement (CDHA) was formed by the hydrolysis reaction of alpha-tricalcium phosphate (α -TCP)



Among these cements, the degradation of brushite cements was faster than that of apatite cements. Previous work showed that because of the poor biodegradability of apatite cement, the new bone could grow only on the surface of nonporous apatite cement (Kanter, 2014). Herein, bone restoration materials require a specific microstructure (microporosity and macroporosity) to facilitate both body fluid

and bone cell growth for newly formed bone inside the structure. Nevertheless, more porosity could reduce the mechanical properties of cement. As a result, the optimization of materials with high mechanical performance and porosity will be carefully considered (Zhang, 2011).

1.4 Calcium phosphate compound and solubility

Self-setting calcium phosphate formulations appear to be a potential tool for bone healing because calcium phosphate is an inorganic component of bone mineral. Table 1.1 shows a list of calcium phosphates compounds, along with their Ca/P ratios, chemical formulas, and solubility. In addition, the solubility diagram of calcium phosphate compounds in Figure 1.1 revealed the concentration of Ca and P ions (at pH = 7.3) for each calcium phosphate compound in decreasing order: TTCP > α -TCP > DCPD > DCPA > OCP > β -TCP > HA (HAP). Thus, HAP was the least soluble compound with respect to other calcium orthophosphates (Carrodegua and De Aza, 2011).

In terms of solubility, most cement formulations will harden to either precipitated crystalline apatite (HA or CDHA at pH > 4.2) or brushite (DCPD at pH < 4.2). It was found that apatite cement is formed in a basic environment (pH > 6.5), while brushite cement is formed in an acidic environment (pH < 6). According to the stability of apatite (pH > 4.2) and brushite (pH < 4.2), this can predict the *in vivo* biodegradation of each cement formula following their different solubility.

Table 1.1 Calcium phosphate compounds and solubility (Carrodeguas and De Aza, 2011, Schamel, 2017).

Compound	Formula	Ca/P Molar ratio	-log K _{sp}		Solubility mg L ⁻¹
			25°C	37°C	
Monocalcium phosphate monohydrate (MCPM)	Ca(H ₂ PO ₄) ₂ ·H ₂ O	0.5	1.14	n.a.	66204.3
Monocalcium phosphate anhydrous (MCPA)	Ca(H ₂ PO ₄) ₂	0.5	1.14	n.a.	61477.3
Dicalcium phosphate dihydrate (DCPD)	CaHPO ₄ ·H ₂ O	1.0	6.59	6.63- 6.73	74-87
Dicalcium phosphate anhydrous (DCPA)	CaHPO ₄	1.0	6.9	7.04	41-48
Octacalcium phosphate (OCP)	Ca ₈ (HPO ₄) ₂ (PO ₄) ₄ · 5H ₂ O	1.33	96.6	95.9- 98.6	0.18-0.5

Table 1.1 Calcium phosphate compounds and solubility (Carrodeguas and De Aza, 2011, Schamel, 2017). (Continued)

Compound	Formula	Ca/P Molar ratio	-log K _{sp}		Solubility mg L ⁻¹
			25°C	37°C	
Tricalcium phosphate (α - TCP)	α -Ca ₃ (PO ₄) ₂	1.5	25.5	28.5	0.24-2.5
Tricalcium phosphate (β - TCP)	β -Ca ₃ (PO ₄) ₂	1.5	28.9	29.5- 29.6	0.15-0.4
Hydroxyapatite (HA)	Ca ₁₀ (PO ₄) ₆ (OH) ₂	1.67	116.8	117.2	0.000096- 0.2
Tetracalcium phosphate (TTCP)	Ca ₄ (PO ₄) ₂ O	2	38-44	37-42	0.038-0.39

n.a. = not applicable

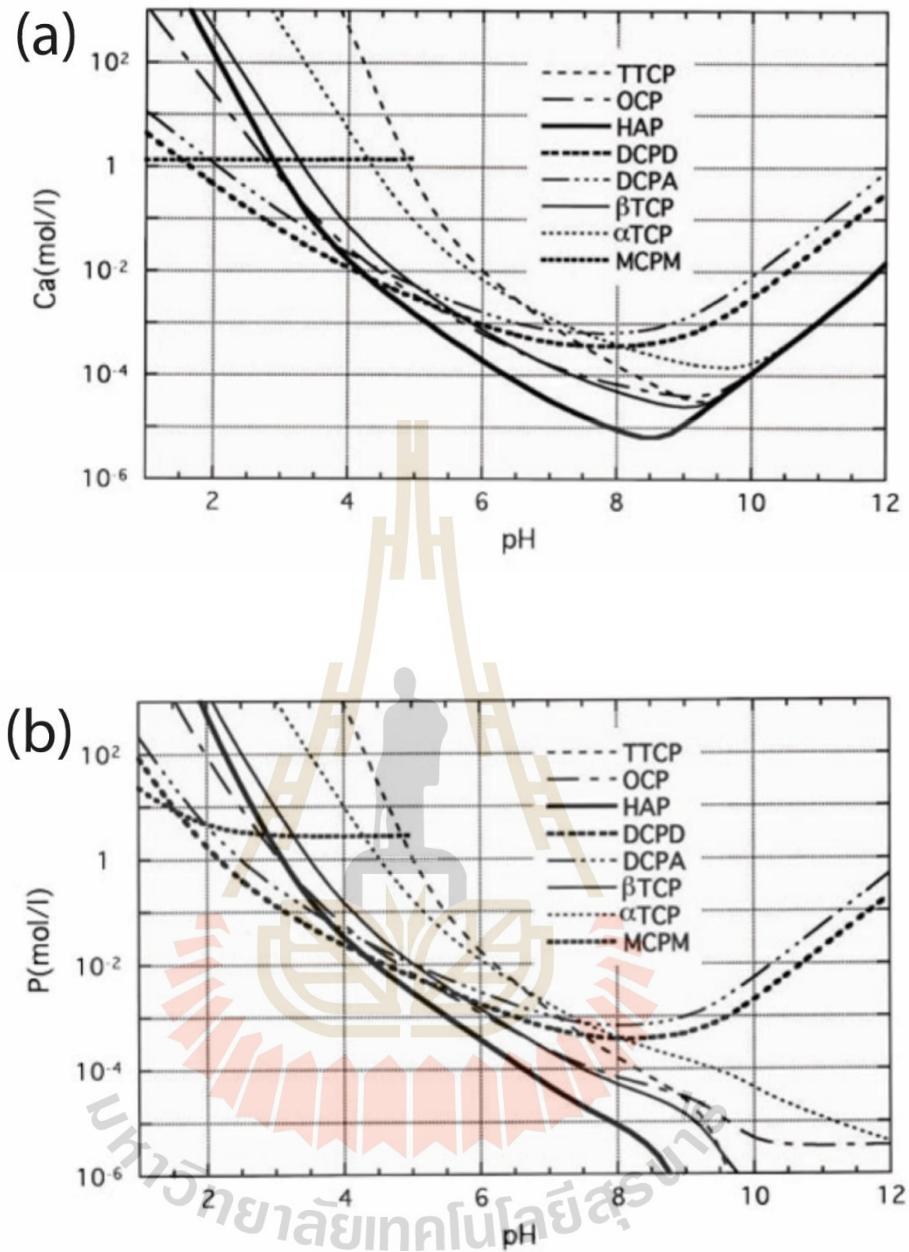


Figure 1.1 Solubility diagrams of (a) Ca and (b) P ions for each calcium orthophosphate compounds (Ishikawa, 2010).

1.5 Properties and limitation of calcium phosphate cements

- Setting time

Setting time is referred to as the cement hardening time. After mixing cement liquid and powder, the setting time of cement is measured when the cement

paste is formed and able to resist force. Setting time is usually measured as the initial and final setting time by using the Gillmore apparatus. During the setting process, cement samples should not change their shape, as this could result in a broken structure (Zhang, 2014). Furthermore, cement paste should be injectable prior to the initial setting time (< 8 min), and surgeons should be able to close the bone defect after the final setting time (< 15 min) of cement (Khairoun, 1998, Dorozhkin, 2013). However, the setting time of cement could take a few minutes or hours to complete the hardening sample. It was found that the prolonged setting time of cement could be adjusted by several parameters, including the optimized particle size of starting powder, accelerators, and lower liquid to powder ratio (L/P ratio) (Zhang, 2014).

- Injectability

The injection of cement paste could be influenced by different factors such as the type of syringe, needle size, and injection speed. During the injection process, phase separation may appear and affect a variation of the cement phase composition (Zhang, 2014), resulting in poor injectability of cement. It was reported that the phase separation during injection could be improved by different factors, such as a higher L/P ratio, increased repulsive force between particles, and gently shaking the cement paste during injection (O'Neill, 2017). The percentage of injectability could be measured following Equation 1.4 (Arkin, 2021).

$$\% \text{ Injectability} = \frac{W_p - W_f}{W_p - W_s} \times 100 \quad (1.4)$$

Where the W_p is the weight of syringe full of cement paste, W_f is the weight of syringe after injection test with remaining paste, W_s is the weight of the empty syringe

- Bioresorbability and biocompatibility

Bioresorption has been examined in terms of the degradation rate of cements. The bioresorbability of cement should be optimized for new bone

regeneration through a combination of osteogenic, osteoinductive, or osteoconductive processes. Bone regeneration is first induced by bone resorption, followed by new bone formation in the sample. Thus, the sample structure should be degradable to allow cells' penetration for the new bone formation inside the samples (Sheikh, 2015). Apart from bioresorbability, the cement sample must be biocompatible with the human body, which could be initially demonstrated on the lab scale both *in vitro* (using various cellular assays) and *in vivo* (animal test) investigation before the next step of the clinical trial process. In addition, the biocompatibility of cement can be proved when there is no inflammatory effect after the implantation process (O'Neill, 2017).

- Mechanical properties

Although the biological properties of calcium phosphate cement were excellent, its mechanical properties were a drawback for use in orthopedics (Habraken, 2016). The mechanical properties of calcium phosphate cement have been characterized and correlated to microstructural parameters including porosity, apatite crystal quantity, size, shape, and distribution. Furthermore, the mechanical performance of cement is also correlated to the production and processing techniques. As a result, all parameters such as cement composition, accelerator additives, particle sizes, and L/P ratio will have an impact on the mechanical performance of cement (Dorozhkin, 2008).

However, other mechanical characteristics such as tensile strength and fracture toughness have received much less attention than compressive strength (Zhang, 2014), and may be worth investigating in the future. It was found that most calcium phosphate cements have low mechanical strength, which limits their use in load-bearing applications (Unosson and Engqvist, 2014). According to the cement types (apatite and brushite), apatite has been enhanced and shown to have greater compressive strength than brushite (Zhang, 2014, Schumacher and Gelinsky, 2015), as shown in Figure 1.

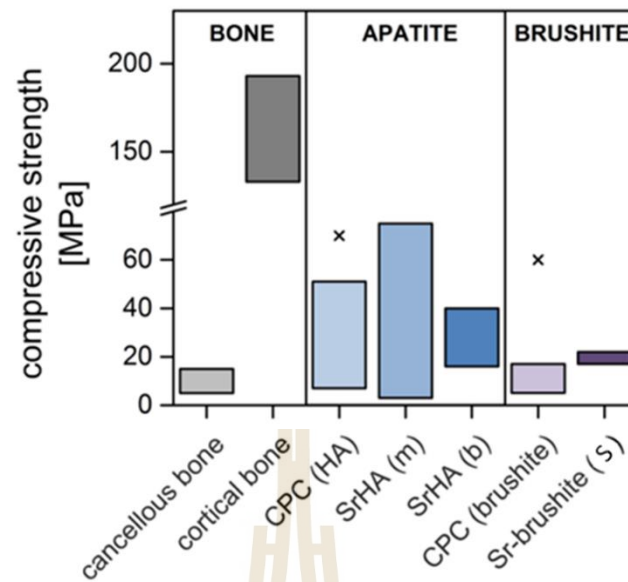


Figure 1.2 Comparison of compressive strength of natural bone and different type of calcium phosphate cements: apatite cement (HA), monophasic (m) and biphasic (b) as setting product of Sr substituted apatite cement, brushite cement (brushite), and Sr substituted brushite cement (s) (Schumacher and Gelinsky, 2015).

It was reported that the compressive strength of both apatite (up to 75 MPa) and brushite cements (10-60 MPa) was stronger than cancellous bone (5-15 MPa) but weaker than cortical bone (30-230 MPa) (Tan, Samper Gaitán, 2011, Henkel, 2013, Mondal, 2014, Schumacher and Gelinsky, 2015). Therefore, the compressive strength of calcium phosphate cement needs to be improved in order to overcome its limitations in nonload-bearing treatments.

CHAPTER II

LITERATURE REVIEW

Hydroxyapatite (HA)/or calcium deficient hydroxyapatite (CDHA) and brushite (dicalcium phosphate dehydrate, DCPD) cement have been investigated and used as bone substitutes, in which brushite presented a higher *in vivo* resorption for cell ingrowth during implantation (O'Neill, 2017). However, brushite may generate an acidic environment in the surrounding environment, which is harmful to living cells. Brushite is also unsuitable for load-bearing applications because of its lower mechanical performance than apatite (Dorozhkin, 2008). The calcium to phosphate (Ca/P) ratio of apatite materials (HA/or CDHA) could be varied in general from 1.5 to 1.67. Although apatite materials consistently remained after long term implantation, CDHA (Ca/P ratio is 1.5) presented a greater degradation rate with respect to HA (Ca/P ratio is 1.67) (Victor and Kumar, 2008). From this view, CDHA is receiving more attention for use in the long term as bone fixation. Thus, CDHA could be prepared by the hydrolysis of alpha-tricalcium phosphate (α -TCP) into CDHA cement at room temperature (Gbureck, 2004, Hurle, 2014). However, it was found that nonporous CDHA cement with poor biodegradability showed new bone growth only on the surface of the cement, while the samples with a porous structure could allow new bone growth inside the samples after 10 months of implantation (Kanter, 2014). This led to the idea of a new cement formula based on apatite cement and modified with biodegradable reagents in order to overcome the poor resorbability of apatite cement.

2.1 Research background, rationale, and significance

Biphasic (HA/ β -TCP) cement concept has been widely studied in numerous orthopedic applications due to their biocompatibility (HA and β -TCP) and *in vivo* biodegradability (β -TCP). A previous study (Rattanachan, 2020) evaluated biphasic

HA/ β -TCP cement both *in vitro* and *in vivo* and found that it produced more new bone than commercial biphasic granules and a control empty defect with no substituted material. Herein, the biphasic HA/ β -TCP cement could be a promising tool for bone regeneration. Due to the high solubility of β -TCP, the biphasic HA/ β -TCP cement concept has been suggested for improving degradability (Daculsi, 1998). It was reported that the presence of β -TCP significantly increased the resorption rate of apatite cement, which consequently reduced its mechanical strength (Sariibrahimoglu, 2014, Srakaew and Rattanachan, 2014, Rattanachan, 2018).

According to the low mechanical performance of HA/ β -TCP, this cement can only be utilized in non-load bearing applications. The poor mechanical properties of biphasic HA/ β -TCP could be improved by the reinforcement of biodegradable polymers, such as chitosan. Chitosan has been used in various medical treatments for bone tissue engineering in various forms (such as micro/nano particles and hydrogel) because it has biocompatible and biodegradable properties (Pillai, 2009, Dash, 2011). Previous work (Pan, 2006) showed the improvement of the flexural strength of tetracalcium phosphate/dicalcium phosphate (TTCP/DCPA) apatite cement by the addition of chitosan fiber. In addition, the new bone formation could be induced by the chitosan fiber modified apatite TTCP/DCPA cement (Wu, 2014).

As a result, the addition of chitosan fiber to apatite/ β -TCP cement in this study could be a promising solution for improving its mechanical and biodegradable performance. However, this biphasic apatite/ β -TCP with poor mechanical strength (approximately 25 MPa (Rattanachan, 2020)) could be used only in non-loadbearing environment due to its strength was lower than cortical bone (30-230 MPa) (Tan, Samper Gaitán, 2011, Henkel, 2013, Mondal, 2014, Schumacher and Gelinsky, 2015). To overcome this limitation, the compressive strength of apatite/ β -TCP cement needs to be improved, including other physical and biological properties.

2.2 Reinforcement of calcium phosphate cements

2.2.1 Addition of biopolymer

The mechanical strength could be effectively improved by different parameters, including cement composition, particle size distribution of starting powder, liquid phase, L/P ratio, and porosity (Dorozhkin, 2008, Zhang, 2014). Furthermore, some other methods could also enhance the poor mechanical properties of cement such as the addition of biopolymers, as shown in Table 2.1. The incorporation of polymers to calcium phosphate cement has shown outstanding results (Mickiewicz, 2002, Canal and Ginebra, 2011). These added polymers could be used in different forms of solid and liquid phase, which were mixed with the cement starting powder (Xu, 2000, Perez, 2012, Geffers, 2015).

Table 2.1 The improvement of cement properties by the incorporation of various polymers (Perez, 2012).

Cement properties	Polymer forms	
	Solid	liquid
Setting time	-	Alginate Chitin Polyethylene glycol
Injectability	-	Hyaluronate Cellulose
Porosity	Gelatin Polyesters	Soybean Albumen

Table 2.1 The improvement of cement properties by the incorporation of various polymers (Perez, 2012). (Continued)

Cement properties	Polymer forms	
	Solid	liquid
Degradation	Gelatin Chitosan Polyesters	-
Biological performance	Alginate Polyesters	Gelatin Collagen

2.2.2 Addition of bioactive reagent

The addition of bioactive reagents such as bioactive glass (BG) could be another solution to improve the compressive strength of calcium phosphate cement. Previous studies (Yu, 2013, Medvecky, 2017) presented the higher compressive strength of BG added apatite cement with respect to the control cement without BG. Moreover, both *in vitro* and *in vivo* studies revealed that BG has remarkable bioactive and biocompatible characteristics (Hoppe, 2011). Afterward, the incorporation of BG in calcium phosphate cement and its great biological activity have been established earlier (Renno, 2013, Sadiasa, 2014, Lee, 2016). Due to the high specific surface area of BG, it could enhance the growth factor delivery (Schumacher, 2017) and protein absorption feature (El-Fiqi, 2015) of cement, promoting the cellular responses.

2.3 Literature reviews

2.3.1 Improvement of calcium phosphate cement by addition of PAA

The influence of PAA on apatite cements based on TTCP/DCPA or α -TCP powder has been explored in order to improve their mechanical performance (Miyazaki, 1993, Kodera, 2005). Majekodunmi et al. (Majekodunmi, 2003) studied the influence of varied concentration (10-25 wt./vol%) and molecular weight (up to 100,000) of PAA on setting time and mechanical properties of apatite (TTCP/DCPA) cement since 2003. They indicated the optimum concentration of PAA (Molecular weight = 30,000) at 20 wt./vol.% for maximum compressive strength (56 MPa) and at 10 wt./vol% for shortest setting time of cement. Afterward, Majekodunmi et al. (O Majekodunmi and Deb, 2007) continuously explored the setting time and mechanical properties of PAA (10-25 vol./vol.%) modified TTCP/DCPA-apatite cement by investigating the various ratio of TTCP and DCPA powder and molecular weight of PAA. They found that the initial setting time was affected by the starting TTCP/DCPA powder ratio, but not the final setting time. The initial setting time decreased when the TTCP concentration in the powder phase was increased. In addition, the higher molecular weight PAA (100,000) revealed the shorter initial and final setting time of cement when compared with lower molecular weight PAA (30,000). Meanwhile, the different concentration of PAA did not present a significant trend of setting time results. According to a various concentration of PAA (10-25 vol./vol.%), the maximum compressive strength of TTCP/DCPA-apatite cement was measured at 20 vol./vol.% PAA.

Watanabe et al. (Watanabe, 2005) also studied PAA incorporation apatite cement prepared from different precursors of TTCP and α -TCP powder. They found that the compressive strength of PAA/ α -TCP cement was higher than that of PAA/TTCP cement. Furthermore, the exothermic release of PAA/ α -TCP cement was below 30 °C at room temperature, whereas PAA/TTCP cement was above 30 °C. In another previous work (Chen, 2008), the brittleness of apatite (TTCP/DCPA) cement was improved by

the addition of PAA from 0.25 to 1 wt./wt.%, although the compressive strength of PAA modified cement was lower than the control cement.

In terms of biological performance, previous work (Chen, 2012) found that PAA modified apatite (TTCP/HA) cement made the surrounding environment liquid at a neutral pH of approximately 7, which could be favourable for cell behaviour. They also indicated the biocompatibility of PAA modified cement by fibroblast cell viability and proliferation on cement. Khashaba et al. also (Khashaba, 2010) studied the addition of PAA and Polymethyl-vinyl ether-maleic anhydride (PMVE-Ma) copolymer to apatite cement based on TTCP/DCPD/TCP powder. They found that the PAA incorporated cement (highest strength, 70 MPa) was a non-toxic material, as witnessed by the remarkable *in vitro* and *in vivo* results. It showed that PAA-modified cement was not harmful to osteoblast cells and allowed them to grow and proliferate over time. Furthermore, this composite PAA-apatite cement was compatible with the connective tissue of rats, with less inflammatory effect than other candidates in the *in vivo* investigation.

2.3.2 Improvement of calcium phosphate cement by addition of BG

It has been proven that BG is bioactive and biocompatible in both cellular and animal tests (Hoppe, 2011). It was reported that BG with different formulas and microstructures could be produced by various techniques (Wang, 2019). For the past decade, researchers have been studying the effects of BG on calcium phosphate cement based on different starting powders. Renno et al. (Renno, 2013) studied the addition of 30-50 wt.% BG to apatite (α -TCP/DCPA/HA) cement. They found that the setting time (initial setting time: 4-8 min, final setting time: 6-16 min) of cement increased when the BG content was increased in the system. In contrast, the other groups found that the higher BG content decreased the setting time of TTCP/DCPD/gypsum (Sadiasa, 2014) and α -TCP/HA (El-Fiqi, 2015) cement. This difference in setting time of BG modified cement could be influenced by various factors, such as cement and BG formula, amount of BG.

Afterward, it was found that the compressive strength of cement could be increased by the addition of BG. Yu et al. (Yu, 2013) showed that 20 wt.% BG (45SiO₂-24.5Na₂O-24.5CaO-6P₂O₅) could increase about 2 times the compressive strength (40 MPa) with respect to the control cement without BG after incubation in 100% humidity for 7 days. Another research group (Medvecky, 2017) also found that the small amount (1-5 wt.%) of BG (36.7SiO₂-50CaO-13.3P₂O₅ system) could increase the compressive strength (up to 70 MPa) of TTCP-apatite cement. They assumed that the fine particles of BG could fulfil the porous structure of cement, resulting in a more compact structure with a higher strength.

Furthermore, the addition of BG to apatite (TTCP/DCPD (Nezafati, 2013), α -TCP/HA (Lee, 2016)) cement could enhance their bioactivity. They reported that BG could release extra ions (such as Ca and Si) into the surrounding environment, which could enhance the HA formation on the surface of cement samples. Moreover, BG could adsorb some essential proteins (El-Fiqi, 2015) or growth factors (Schumacher, 2017), which were favourable for cellular responses. Nezafati et al. (Nezafati, 2013) demonstrated that TTCP/DCPD cement reinforced with 5–25 wt.% BG fibres could increase osteoblastic cell activity. Schumacher et al. (Schumacher, 2017) also found that mesoporous BG (80SiO₂-15CaO-5P₂O₅) could adsorb growth factors from the surrounding solution, which facilitated cell activities and enhanced osteoblast proliferation. However, the addition of BG to cement could result in reduced cell viability due to the rapid changes in pH and ions of the surrounding environment influenced by the released ions from BG (Stulajterova, 2017). Consequently, the *in vivo* testing of BG modified apatite cements was investigated (Yu, 2013, Sadiasa, 2014, El-Fiqi, 2015). They found that the BG incorporated apatite cement could enhance newly formed bone after implantation in rats at different time points. Moreover, it was found that the newly formed bone was interface-interaction inside the BG modified cement sample, while the new bone could form on the surface of the control cement without BG. This could be contributed to the higher degradation aspect of BG modified cement when compared with control cement. Their findings proved that the incorporation of

BG into calcium phosphate cement is another promising solution for use in various medical treatments.

However, those results from the literature still lack some investigation (such as degradation and injection testing of PAA modified cements) in order to confirm the possibility of using these composite materials in orthopaedic treatments. According to the literature reviews, the development of apatite/ β -TCP cement in this study by the addition of PAA and BG could be a new finding and possible for use under loadbearing conditions.

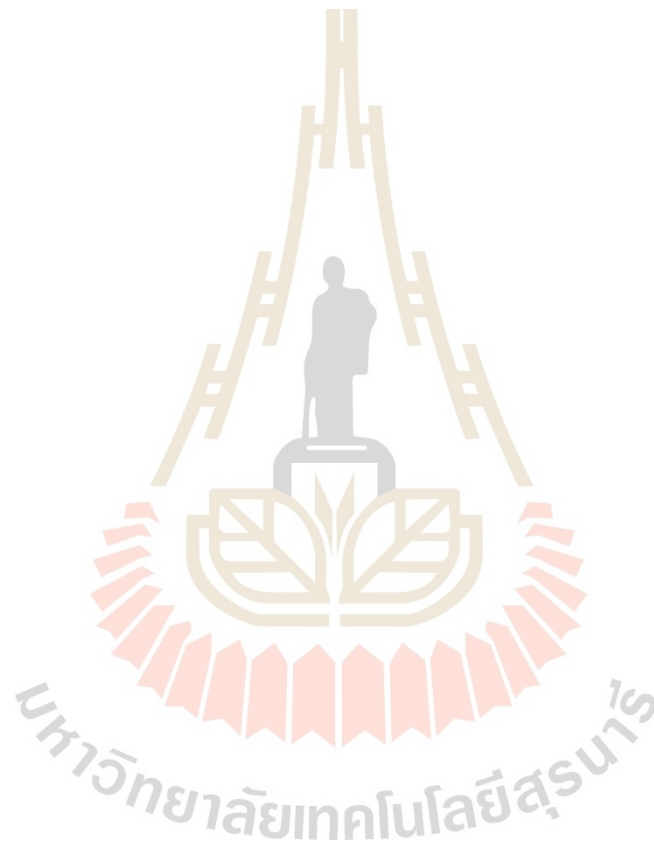


Table 2.2 Composition and properties of PAA modified calcium phosphate bone cements

Powder composition	Additive	Liquid phase	Setting time (min)		Compressive strength (MPa)	End product	Note/ References
			Initial setting time	Final setting time			
TTCP, DCPA		50 w/w% PAA			53.6-55.2 (increased 28-30 MPa) after 1-28 days immersion	HA	Small amount of converted HA was detected after 1 month (Miyazaki, 1993).
TTCP, DCPA		10-25 w/v% PAA	2-17	5-90	56 (increased 24 MPa) after 16h immersion	N.A.	Mw 30,000 and 100,000 at 20% PAA provided the highest strength. Setting time increased when PAA increased (Majekodunmi, 2003).
α -TCP, Na ₂ SiO ₃ glass		25 w% PAA			30 (increased 1.5 times of control)	N.A.	PAA modified cement presented higher strength with respect to both PVA modified cement and control cement without PAA (Kodera, 2005).
TTCP or α -TCP		10-25 w/v% PAA	2.4-3.3 (TTCP), 12-50 (α -TCP)		5.9-21.3 (TTCP), 6.4-29.2 (α -TCP)	HA	Exothermic temperature of α -TCP cements was about room temp (below 30 °C), while that of TTCP cements was above 30 °C. Setting time reduced when PAA increased (α -TCP) (Watanabe, 2005).
TTCP, DCPA		10-25 v/v% PAA	1.5 - 11	7.5 - 32	55 after 20h immersion	N.A.	Composition of powder, PAA concentration and molecular weight altered setting time and strength. Setting time did not have a specific trend (O Majekodunmi and Deb, 2007).
TTCP, DCPA	0.25-1 w/w% PAA, CaF ₂ , Tataric acid	Water			57.9 ± 2.9 (reduced 8 MPa)	DCPA, DCPD, CaF ₂	PAA modified cement was more ductile with respect to the control sample. However, HA conversion was interrupted by PAA (Chen, 2008).
TTCP, DCPD, TCP		10w/w% PAA	5 ± 1.4	12 ± 1.7	90.57 ± 4.09 after 24h immersion	N.A.	PAA modified cement resulted in the highest strength and greater biocompatibility as compared with other candidates, PMVE-Ma, and commercial HA (Khashaba, 2010).
TTCP, HA	9 w% PAA, 3 w% Citric acid, 2 w% Sodium citrate		11		25.6-38.2, 1-7 days	HA	Wash-outed resistance, neutral pH range during incubation in solution, biocompatible to fibroblast cells (Chen, 2012).

TTCP, Tetracalcium phosphate; DCPA, Dicalcium phosphate anhydrous; DCPD, Dicalcium phosphate dihydrate; HA, Hydroxyapatite; α -TCP, Alpha-tricalcium phosphate; CaF₂, Calcium fluoride; PAA, Polyacrylic acid; PMVE-Ma, Polymethyl-vinyl ether-maleic anhydride copolymer; N.A. Not applicable.

Table 2.3 Composition and properties of BG modified calcium phosphate bone cements

Powder composition	Additive	Liquid phase	Setting time (min)		Compressive strength (MPa)	Degradation	Injection	End product	Note/ References
			Initial setting time	Final setting time					
α -TCP, DCPA, HA	30-50 w% BG	Na ₂ HPO ₄	4-8	6-16		10% mass loss after 9 weeks		α -TCP, DCPA, HA, BG	Setting time increased when BG increased. BG increased pH of PBS (Renno, 2013).
TTCP, DCPD, Gypsum	10-30 w% BG (60Si:36Ca:4P)	2% chitosan, 4%HPMC, 10% Citric acid	24.67-43.25		7.97-15.04 (increased about 2 times of control) after 7 days in 100% humidity		Injectable through syringe	HA	Setting time reduced when BG increased. BG induced osteoblast cell proliferation, gene expression, and new bone formation (Sadiasa, 2014).
TTCP, DCPA	10-20 w% BG (45S5, 45Si:24.5Na:24.5Ca:6P)	potassium phosphate buffers	15-25		40 (increased about 2 times of control), after 7 days of immersion	15% mass loss after 4 weeks (increased 2 times of control)	Injectable through syringe (increased 40% from control)	HA, Calcium silicate	Setting time, compressive strength, injectability, and degradation increased when BG increased. BG doped cement enhanced osteoblast cell activities and new bone formation (Yu, 2013).
TTCP, DCPD	5-25 w% BG fibres	Na ₂ HPO ₄						HA	BG doped cement improved bioactivity and enhanced cellular responses (Nezafati, 2013).
α -TCP, HA	2-10 w% mesoporous nano-BG (85Si:15Ca)	Na ₂ HPO ₄	25-108		26 (increased about 2 times of control)	Increased degradability (sign of interface interaction with bone)	Injectable through syringe (increased 15% from control)	HA	Setting time reduced and compressive strength increased when BG increased. BG increased surface area of cement and improved wash-outed resistance and injectability. More released Si ions, higher pH of PBS, and protein adsorption ability of BG doped cement. BG doped cement showed more sign of interface interaction with bone (El-Fiqi, 2015).
α -TCP, HA	2-10 w% nano-BG (85Si:15Ca)	Na ₂ HPO ₄	37-123		25.6 ± 1.74			HA	Bioactivity was improved with higher BG addition. Setting time reduced when BG increased. BG cement released more Ca and Si ions. Greater cellular activities of BG cement (Lee, 2016).

Table 2.3 Composition and properties of BG modified calcium phosphate bone cements. (Continued)

Powder composition	Additive	Liquid phase	Setting time (min)		Compressive strength (MPa)	Degradation	Injection	End product	Note/ References
			Initial setting time	Final setting time					
α -TCP, HA	2-10 w% nano-BG (85Si:15Ca)	Na_2HPO_4	37-123		25.6 ± 1.74			HA	Bioactivity was improved with higher BG addition. Setting time reduced when BG increased. BG cement released more Ca and Si ions. Greater cellular activities of BG cement (Lee, 2016).
TTCP	7.5-15 w% BG (45S5, 45Si:24.5Na:24.5Ca:6P)	H_3PO_4	4-10		52 (increased 7 MPa)			HA	Higher released Si ions and pH in BG cement. Setting time increased when BG increased. BG reduced rMSC viability (Stulajterova, 2017).
α -TCP, DCPA, CaCO_3 , HA	5-10 w% mesoporous BG (80Si:15Ca:5P)	Na_2HPO_4	12.6-13.2	41.6	42 (increased 12 MPa)	51.4 v% porosity (increased 17%)		HA	BG doped cement increased growth factor delivery and induced osteoblast proliferation (Schumacher, 2017).
TTCP	1-5 w% BG (36.7Si:50Ca:13.3P)	H_3PO_4 , NaH_2PO_4	4-7		70 (increased about 2 times of control) after 7 days immersion			HA	Setting time and compressive strength increased, but porosity reduced when BG increased (Medvecky, 2017).

TTCP, Tetracalcium phosphate; DCPA, Dicalcium phosphate anhydrous; DCPD, Dicalcium phosphate dihydrate; HA, Hydroxyapatite; α -TCP, Alpha-tricalcium phosphate; CaCO_3 , Calcium carbonate; BG, bioactive glass; Na_2HPO_4 , Disodium hydrogen phosphate; NaH_2PO_4 , Sodium dihydrogen phosphate; H_3PO_4 , Phosphoric acid; HPMC, Hydroxyl-propyl-methyl-cellulose; rMSC, rat mesenchymal stem cell.

2.4 Starting chemical compounds of the modified apatite/ β -TCP cement

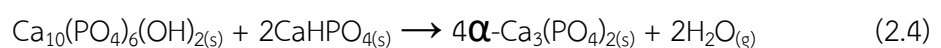
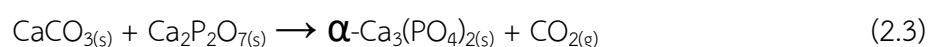
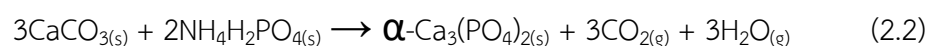
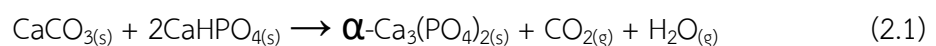
In this work, calcium phosphate cement referred to the composite apatite/ β TCP cement was produced by the mixture of cement powder and liquid as follow:

2.4.1 Starting cement powder

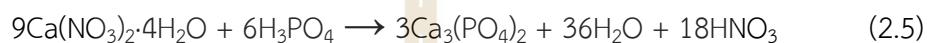
- Alpha-tricalcium phosphate

α -TCP was frequently employed in self-setting bone cements, which formed calcium-deficient hydroxyapatite (CDHA) when contacted to an aqueous solution. Because of its inconstancy at ambient temperature, α -TCP (stable at 1140-1470 °C) is difficult to synthesize (Kolmas, 2015).

(i) Solid state reaction method has been widely used to synthesize synthesis α -TCP powder (C.L. Camire´ a, 2005, Duncan, 2014). It was reported that α -TCP could be produced by using the different starting reagents (mole ratio of Ca/P is 1.5), as presented in Eq (2.1-2.4). Briefly, the reagents were mixed through a wet-milling process, followed by the calcination at high temperature ranging from 1250 to 1500 °C with a long holding time. Finally, the high temperature was quickly reduced to room temperature (quenching process) due to α -TCP is able to convert to unfavoured β -TCP phases (~ 1125 °C). Thus, the obtained α -TCP powder may consist of the purity phases (β -TCP or HA) (Carrodegua and De Aza, 2011).



(ii) Wet chemical reaction has been a new approach to produce α -TCP powder with a high purity phase for the past decade (Thürmer, 2012, Kolmas, 2015, Thürmer, 2016). In this method, α -TCP could be prepared by mixing calcium nitrate and phosphoric acid with Ca/P ratio of 1.5 (Eq 2.5). This technique could be prepared at high temperature with a shorter holding time when compared with the conventional solid state reaction. Furthermore, the quenching process is not necessarily required for this synthesis.



- Dicalcium phosphate anhydrous

Dicalcium phosphate anhydrous/or monetite (DCPA) has been utilized in various orthopedics treatment. In term of calcium phosphate cement, DCPA has been utilized and mixed with other precursors (such as TTCP or α -TCP powders) to form apatite cement systems (Dorozhkin, 2013). Previous work found that DCPA increased the compressive strength of α -TCP based apatite cement by approximately 1.8 times compared to the control cement without DCPA (Gbureck, 2005). In addition, DCPA could be an extra source of Ca and P ions in the setting reaction during the cement hardening process. The presence of DCPA could increases the resorption rate of α -TCP based apatite cement due to the degradability of DCPA. Moreover, the degradable DCPA could enhance the new bone formation after in vivo experiments (Sheikh, 2017). This has proved that DCPA is biocompatible and suitable for new bone regeneration.

- Calcium carbonate

Calcium carbonate (CaCO_3) has been used as one of the starting cement powders in various apatite cement formular. CaCO_3 could supply extra Ca ions during the setting reaction, which could finally form both precipitated CDHA or carbonate apatite (Dorozhkin, 2013). The addition of CaCO_3 to α -TCP based apatite cement could increase its mechanical strength, and setting time (Kon, 2005). Although the presence of CaCO_3 prolonged the setting time of apatite cement, it increased the injectability

and degradation rate of cement (Sariibrahimoglu, 2012). Thus, the increased degradation of CaCO_3 incorporated apatite cement resulted in more extra Ca ions to the surrounding environment. This could be more favorable for cellular responses as witnessed in the previous study (Farley, 1994), indicating the enhanced osteoblastic cell activities.

- Precipitated hydroxyapatite

Hydroxyapatite/or precipitated hydroxyapatite (HA/or PHA) has been widely used in a variety of bone tissue engineering due to its similarity of chemical compound when compared with the human bone. The cytotoxicity and biocompatibility of HA with different forms has been investigated both *in vitro* and *in vivo*. Thus, HA is the essential compound to promote the new bone regeneration (Kattimani, 2016). For the cementation, small amount of HA has been used and added to the starting cement powder as a seed. It was reported that the higher HA seed could enhance the HA phase conversion rate in the apatite cement (Tsuru, 2015). However, the high concentration of HA seed could result in a decreased compressive strength, prolonged setting time (Yang, 2002). Therefore, HA seed should be added to the cement precursors only a small amount, as presented in other works (Schumacher, 2013, Rattanachan, 2020).

- Beta-tricalcium phosphate

Beta-tricalcium phosphate (β -TCP) has been studied and used in orthopedics application for many years (Lu, 2021). Although β -TCP has a similar Ca/P ratio (1.5) to α -TCP, their characteristics are different, such as crystal structure, calcined temperature, degradation rate. β -TCP is a stable phase below 1100 °C, while α -TCP is stable above 1125 °C (Jeong, 2019). It was reported that the degradation rate of β -TCP was higher than that of α -TCP over 86 weeks of implantation in minipig (Wiltfang, 2002). This could facilitate new bone formation inside the β -TCP scaffold. However, β -TCP with excellent degradation leads to the lack of use under load-bearing application. Meanwhile, the compressive strength of poorly degradable apatite cement

could be up to 75 MPa (Schumacher and Gelinsky, 2015). At this view, the combination of β -TCP and apatite components at different ratios has received more attention for bone tissue regeneration (Gallinetti, 2014, Arahira, 2017, Rattanachan, 2018, Rattanachan, 2020). It was found that the higher β -TCP content in biphasic (β -TCP/HA) system could enhance more new bone formation in dog implantation (Fariña, 2008).

- Chitosan fiber

Chitosan is one of natural biopolymer that has been used in numerous medical applications due to its excellent biocompatibility and biodegradability (Pillai, 2009). Chitosan is soluble in acidic environment (pH is about 6.5), in which the solubility of chitosan is controlled by the degree of deacetylation. Because of its soluble characteristics, chitosan became an excellent alternative for biofabrication. Chitosan has been fabricated and used in various forms, such as nanoparticle, and hydrogel (Dash, 2011). Chitosan can also be used in the fiber form. A number of researchers have studied the addition of chitosan fiber to calcium phosphate cement, indicating the increased mechanical strength of modified cement (Pan, 2006, Pan, 2007). Moreover, the chitosan fiber incorporated cement has been found to promote newly formed bone after implantation (Wu, 2014, Rattanachan, 2020). Due to the degradation aspect of chitosan fiber, the manufacture process of the composite chitosan/calcium phosphate cement should be further investigated in order to confirm the toxicity of degraded chitosan product. It was reported that chitosan could be excreted via chemical and enzymatic systems in the body, which most of the degraded chitosan was excreted through the urine after 14 h (Pillai, 2009). Thus, most chitosan with the different degree of deacetylation and molecular weight presented no significant toxicity *in vitro* cellular and *in vivo* testing.

- Bioactive glass

Bioactive glass (BG) has been widely studied for use in various medical cares. Thus, both *in vitro* and *in vivo* experiments demonstrated that bioactive glass (BG) has excellent bioactive and biocompatible abilities (Hoppe, 2011). It has been known that bioactive BG could degrade when it attaches the simulated body fluid (SBF

solution) and enhances the HA formation on its surface, representing bioactive capacity. In the previous work (Siqueira, 2017), it was reported that the higher SiO₂ (80SiO₂-15CaO-5P₂O₅, 80Si) content in BG could result in less resorption rate and HA formation on its surface when compared with the BG with the lower content of SiO₂ (60SiO₂-36CaO-4P₂O₅, 60Si). However, the pH of SBF solution was not quickly changed by 80Si glass (7.4-7.7), whereas the pH of SBF solution was rapidly changed by 60Si glass to a strong basic (up to 8.4). As a result, 80Si glass became more favourable for cell responses. Other previous work also presented excellent bioactivity and biocompatibility of 80Si glass (Yan, 2006, Phetnin, 2020). Moreover, 80Si was found to be highly osteoconductive for osteoblast cells, leading to an excellent new bone bonding (K, 2011). According to a variety of BG formular based on SiO₂: CaO: P₂O₅, they presented a different degradation rate. At this point, their difference resorption rate could be beneficial for use in a number of medical application needs.

Afterward, the addition of BG to calcium phosphate cements has been studied for their improvement of physical properties, including setting time (Lee, 2016, Medvecky, 2017, Stulajterova, 2017, Hasan, 2019), and compressive strength (Yu, 2013, Medvecky, 2017). Furthermore, the utilization of BG in CPCs and its remarkable biological activity have already been demonstrated (Renno, 2013, Sadiasa, 2014, Lee, 2016). However, previous study found a negative cell response on BG modified cement due to the high concentration of BG influenced a rapid change of ions and pH in the culture medium (Stulajterova, 2017). Therefore, the addition of BG (80SiO₂-15CaO-5P₂O₅) to apatite/ β -TCP cement in this study must be carefully optimized.

2.4.2 Cement liquid

- Disodium hydrogen phosphate

Disodium hydrogen phosphate (Na₂HPO₄) has been utilized as the accelerator in the apatite cement system. Thus, it was shown to enhance the setting reaction, resulting in the formation of CDHA as a cement end product (Fernández, 1994). Previous works also found that Na₂HPO₄ could reduce the setting time of α -TCP

(Ginebra, 1995, Khairoun, 1997, Khairoun, 1998), and TTCP/DCPD (Komath, 2000) based apatite cement. Moreover, Na_2HPO_4 modified cement showed a faster rate of HA formation with respect to the control cement without Na_2HPO_4 (Chow, 1999). This could suggest that Na_2HPO_4 provided extra phosphate ions to the system during the setting reaction, resulting in a shortening setting time and promoted HA conversion of cement. However, the presence of Na_2HPO_4 could also affect other cement properties, including the solubility of starting powder, and compressive strength of cement (Ginebra, 1994).

- Polyacrylic acid

Polyacrylic acid (PAA) is a water soluble polymer that has been employed in a variety of medical treatments (Kadajji and Betageri, 2011). There were several works that studied the effect of PAA addition on the properties of apatite cement. Thus, PAA modified apatite cement was found to be nontoxic in both *in vitro* cellular and *in vivo* animal tests (Khashaba, 2010). Previous work (Watanabe, 2005) also found that PAA could decrease the setting time of α -TCP based apatite cement. Moreover, some studies (Majekodunmi, 2003, Majekodunmi and Deb, 2007) examined the effect of PAA loaded apatite (TTCP/DCPA) cement, finding a significantly improved mechanical performance of cement with an appropriate concentration of PAA. However, the presence of PAA could strongly affect the HA phase conversion in the cement system (Miyazaki, 1993). They found only a few HA conversions after the cement had set over a month. Therefore, the concentration of PAA must be carefully optimized in the composite apatite/ β -TCP cement system in this current study to approach the clinical needs.

2.5 Thesis aims

In order to solve the limitations of apatite/ β -TCP cement, this thesis work will consist of 8 chapters, including Chapter I (introduction), II (literature reviews), III-VII (development of apatite/ β -TCP cement), and VIII (conclusion). The brief idea of the improvement of apatite/ β -TCP cement was listed as follows:

- Chapter III: Influence of different synthesis of alpha-tricalcium phosphate powder on apatite/ β -TCP cement

According to the biphasic apatite/ β -TCP cement system, the apatite content in this cement system was converted by alpha-tricalcium phosphate (α -TCP) after mixing cement powder and aqueous solution. Thus, α -TCP prepared by the conventional solid state reaction method could be inconvenient due to its complicated synthesis procedure of quenching step after calcination at high temperature (Famery, 1994, Durucan and Brown, 2002, Camiré, 2005, Camiré, 2006). This led to the new synthesis routes of wet chemical reactions (Thürmer, 2012, Thürmer, 2013, Thürmer, 2016) and precipitation methods without a quenching step during the calcination process. Therefore, the new route of α -TCP synthesis (wet chemical reaction and precipitation) could be beneficial for this cement system.

- Chapter IV: Several parameters influenced on apatite/ β -TCP cement: particle size of alpha-tricalcium phosphate powder and dry-heat sterilization

To overcome the limitations of calcium phosphate cement with nonload-bearing performances, the improvement of the mechanical properties of this cement is required. In comparison to compressive strength, other mechanical parameters such as tensile strength and fracture toughness have received less attention (Zhang, 2014). These characteristics might be worthwhile to investigate further in the future. It was reported that various parameters, such as cement formula, L/P ratio, and particle size distribution, could significantly improve the mechanical strength of cement. As a result, the particle size of the starting cement powder had a significant impact on the apatite

cement setting process (Zhang, 2014). Previous work showed that a smaller particle size of α -TCP powder increased the compressive strength of cement (Ginebra, 2004).

Furthermore, the appropriate sterilization method is also mandatory for using this apatite/ β -TCP cement in medical applications. Various methods of sterilization, such as steam under pressure (autoclave), dry heat, gamma radiation (γ -ray), and ethylene oxide (EO), have been widely utilized [10]. The appropriate sterilization must be carefully selected for this apatite/ β -TCP cement due to it contains chitosan fiber. Thus, it was reported that chitosan fiber was decomposed by several sterilizations (autoclave, γ -ray, and EO) (Yang, 2007). In addition, damages of chitosan fiber could be found at high temperature (>254.6 °C) (Arora, 2011). The decomposition of chitosan fiber could minimize physical properties of apatite/ β -TCP cement. Therefore, dry heat sterilization seemed to be the most promising method with respect to others for this cement formula. Dry heat sterilization is one of the effective processes, which was proved in previous studies of apatite cement (Tsai, 2008, Goldberg, 2018). Thus, the different conditions of dry heat sterilization should be investigated to indicate the appropriate condition for the apatite/ β -TCP cement in this current work.

- Chapter V: Effect of polyacrylic acid/hydrogen phosphate mixture on apatite/ β -TCP cement

In order to overcome the low mechanical properties of apatite/ β -TCP cement, the incorporation of polymer content into cement seemed to be promising for use in load bearing applications. The polymer content could be used in different forms of both solutions and solids (Xu, 2000, Geffers, 2015). Polyacrylic acid (PAA) has been studied in some previous works (Majekodunmi, 2003, Majekodunmi and Deb, 2007) of apatite cement, presenting the increased compressive strength of PAA modified cement due to the crosslink reaction between PAA and cement powder. In addition, PAA modified apatite cement showed excellent biocompatibility both *in vitro* and *in vivo* (Khashaba, 2010). However, the presence of PAA could significantly interfere with the transformation of the HA phase during the setting reaction, indicating a few

converted HA after the cement had set for 1 month (Miyazaki, 1993). Consequently, the poor HA formation could also affect other properties of cement, such as bioactivity. Therefore, the concentration of PAA added to apatite/ β -TCP cement should be optimized.

- Chapter VI: Effect of nano-bioactive glass on polymeric apatite/ β -TCP cement

In a subsequent study, the unsatisfied performance of PAA added apatite/ β -TCP cement in this work could be improved by the addition of bioactive reagents. Bioactive glass (BG) has been found to have outstanding bioactivity and biocompatibility (Hoppe, 2011). Previous studies (Renno, 2013, Sadiasa, 2014, Lee, 2016) have examined the incorporation of BG in calcium phosphate cements and its significant biological success. In order to prove the possible use of this apatite/ β -TCP cement in bone tissue engineering, biological *in vitro* testing on the lab scale is an important step before the analysis of *in vivo* and clinical trials. Thus, cellular testing with different human cells (such as osteoblast and stem cells) using various assays will be required to provide precise and comprehensive data before further *in vivo* experiments.

- Chapter VII: Self-setting nano-bioactive glass added polymeric apatite/ β -TCP cement for bone fixation and regeneration

To improve some drawbacks (poor mechanical strength) of unmodified apatite/ β -TCP cement, the cement formula was modified and optimized by the addition of promising PAA and BG with an appropriate concentration. This work aimed to produce the new formula of polymeric apatite/ β -TCP cement, including raw material synthesis, characterization, and testing. Afterward, the physical and cellular testing of these composite cements were investigated at different time points. Developing degradable apatite/ β -TCP modified with PAA and BG that improves physical and biological performance could be a significant step forward from currently available commercial products.

2.6 Research objective

- To improve the mechanical properties of calcium phosphate cements for bone substitution and tissue engineering.
- To explore and develop the new bone cement formula consisting of α -TCP synthesized by precipitation method for a controllable and cost-effective process.
- To study the effect of additives (PAA and BG) on the properties of apatite/ β -TCP.

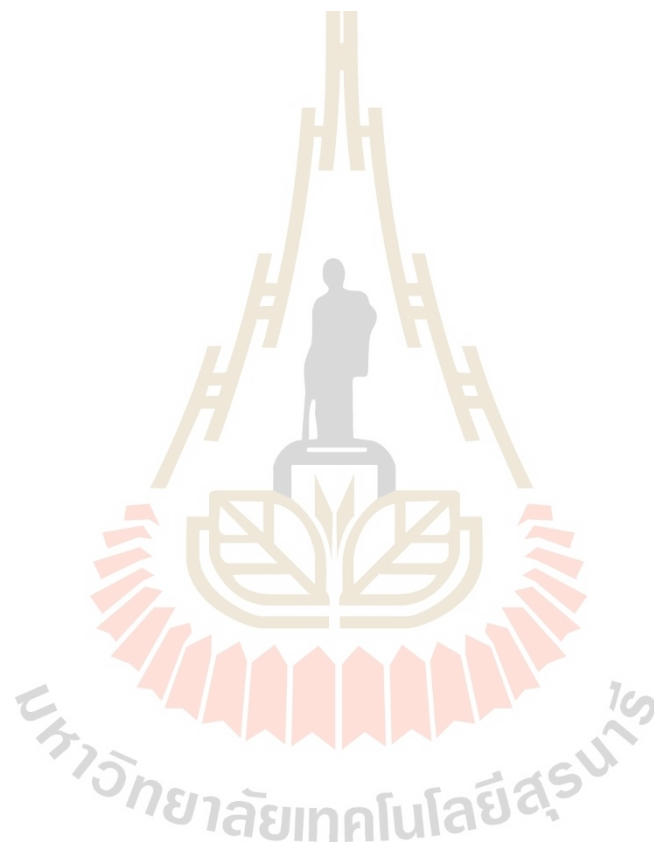
2.7 Scope and limitation

- To synthesize α -TCP, precipitated hydroxyapatite (PHA) by precipitation and BG by sol-gel method for the preparation of apatite/ β -TCP cement.
- To study and understand the effect of additives such as biopolymer (PAA), and bioactive reagent (BG) on the apatite/ β -TCP cement properties, including physical and biological properties.
- To investigate and improve the mechanical properties, bioactivity, biocompatibility, and cytotoxicity of composite apatite/ β -TCP cement, as compared with the unmodified cement.
- To achieve a compressive strength of apatite/ β -TCP cement that is comparable to that of natural human bone (more than 30 MPa).
- To investigate the cellular responses (such as osteoblast and stem cells) to the composite cements by using various assays.

2.8 Expected benefit

- To obtain the new composite cement formula for bone substitution and regeneration.
- To understand how to produce and develop the composite bone cement

- To understand how the combination of reinforced materials on the calcium phosphate cement structure affects mechanical properties, biodegradability, bioactivity, biocompatibility, and cytotoxicity for the development of composite cement for tissue engineering.



CHAPTER III

INFLUENCES OF DIFFERENT SYNTHESSES OF ALPHA-TRICALCIUM PHOSPHATE POWDER ON APATITE/ β -TCP CEMENT

Recently, calcium phosphate cement has been used in bone tissue engineering and regenerative medicine due to its bioactivity and biocompatibility. Alpha-tricalcium phosphate (α -TCP) has been known previously to be an essential raw material of self-setting calcium phosphate cement. The most established method for α -TCP synthesis is the solid state reaction of Dicalcium phosphate anhydrous (DCPA) and Calcium carbonate (CaCO_3) at high temperatures, followed by immediate quenching to room temperature. It has been reported that α -TCP synthesized by wet chemical reaction from calcium nitrate ($\text{Ca}(\text{NO}_3)_2 \cdot 4\text{H}_2\text{O}$) and phosphoric acid (H_3PO_4) at high temperature, being unnecessary quenching to obtain high purity α -TCP. The aim of the present work was to study the effect of comparative α -TCP powder obtained by solid state reaction and wet chemical reaction on the properties of calcium phosphate cements. The obtained powder was characterized by particle size analysis and X-ray diffraction. Cement powders consisting of the different syntheses of α -TCP and other calcium phosphate compounds were mixed with the liquid solution to obtain cement paste. Afterward, set cement samples were determined by setting time measurement, compressive strength, phase analysis in vitro test (simulated body fluid). Although the calcium phosphate cement containing α -TCP from solid state reaction showed a slightly better performance with respect to the cement containing α -TCP from wet chemical reaction, it was likely that the resulting cement from both syntheses was not significantly different.

3.1 Research background, rationale, and significance

Alpha-tricalcium phosphate (α -TCP) has been used as the one component for bone cements, reacting with water and converting into calcium-deficient hydroxyapatite (CDHA), which has a similar chemical and composition of the mineral phase of bones. Hydroxyapatite (HA) could induce the new bone formation due to the positive connection between HA and bone, leading to the proliferation of bone cells (Webster, 2001, Zhao, 2017). It was found that α -TCP is difficult to synthesize because of its instability at ambient temperature. This α -TCP is stable in the temperature range of 1140-1470 °C. Although it was quite difficult to obtain the pure α -TCP, it has been investigated in other methods and applications (Kolmas, 2015). There are many methods of synthesis which have been published. The synthesis of α -TCP is most basically described as the thermal transformation of a precursor with a molar ratio Ca/P \sim 1.5 or by solid state reaction of a mixture of solid component at high temperatures. The solid state reaction, mixing solid precursors was a popular method in the publications, which have been reported so far (Famery, 1994, Durucan and Brown, 2002, Camiré, 2005, Camiré, 2006).

The solid state reaction is synthesized by the mixture of solid reagents, followed by wet milling for the homogenous phase. After mixing, the mixture must be heated above the transformation temperature between 1250 and 1500 °C. After long holding calcination time, it must be quenched suddenly to room temperature to avoid the conversion of α -TCP phase which could transform to beta-tricalcium phosphate (β -TCP) at \sim 1125 °C. The obtained powder often displays some of other phases, mostly β -TCP or HA (Carrodeguas and De Aza, 2011). Camiré et al. (Camiré, 2005) produced the purity of α -TCP from a mixture of dicalcium phosphate (DCPA) and calcium carbonate (CaCO_3) at 2:1 molar ratio, followed by heating at 1350 °C for 4 h. Duncan et al. (Duncan, 2014) obtained the pure phase of α -TCP by solid state reaction, mixing monetite (DCPA, dicalcium phosphate) and CaCO_3 in acetone, in which DCPA was prepared by aqueous precipitation method using calcium hydroxide (Ca(OH)_2) and

phosphoric acid (H_3PO_4) as the reagents. After mixing DCPA and CaCO_3 , the mixture was dried at 80 °C and then directly heated at 1300 °C for 16 h, then reground and heated again at 1300 °C for another 8-12 h, followed by quenching to room temperature.

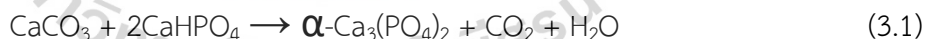
The wet chemical reaction has been known as the new method for the synthesis of α -TCP, as this method was able to synthesize the α -TCP without quenching step. This method has been improved to produce the high purity of α -TCP. Some researchers have evaluated and identified the appropriated factors to provide the α -TCP since 2012 (Thürmer, 2012). However, it is critically important to obtain α -TCP by the new method of synthesis in order to improve material properties and/or reduce cost. The purpose of this work is to study the influence of α -TCP obtained by different routes of synthesis on the properties of bone cements.

3.2 Experimental procedure

3.2.1 Synthesis of α -TCP powder

Two different routes of α -TCP synthesis were prepared by (a) solid state reaction method and (b) by wet chemical reaction method as followed by Eq. (3.1) and (3.2) respectively, representing the α -solid and α -wet to be used as one of the precursors for cement preparation.

Solid state reaction (Famery, 1994, Durucan and Brown, 2002, Camiré, 2005):



Wet chemical reaction (Thürmer, 2012, Thürmer, 2013, Thürmer, 2016):



The α -solid was obtained by solid state reaction as originally described by Srakaew et al. (Srakaew and Rattanachan, 2014). Briefly, dicalcium phosphate anhydrous (CaHPO_4) was mixed with calcium carbonate (CaCO_3) at a 2:1 molar ratio.

The mixture was heated to 1350 °C, left to dwell for 4 h and then rapidly quenched to room temperature. The α -wet from wet chemical reaction was prepared as followed Thürmer et al. (Thürmer, 2016), 0.5 M calcium nitrate ($\text{Ca}(\text{NO}_3)_2 \cdot 4\text{H}_2\text{O}$) was mixed with 0.5 M phosphoric acid (H_3PO_4) at Ca/P ratio of 1.5. After 1 h of mixing, the obtained solution was aged at 90 °C for 24 h and dried at 120 °C. The obtained powder was calcined in an alumina crucible at 1400 °C for 1 h without quenching in air. The obtained powder from both methods was milled and sieved through 325 mesh to achieve a fine powder.

3.2.2 Characterization of α -TCP powder

3.2.2.1 Phase composition and chemical functional group analysis

The phase composition of α -TCP powder from two different syntheses (α -solid and α -wet) was determined by X-ray diffraction (XRD Bruker/D2-phaser) in the range 2θ of 10 to 40, and in step size of 0.02. The chemical functional groups were characterized by using Fourier transform infrared spectroscopy (ATR-FTIR Bruker/Tensor27-Hyperion) with the range of 4000 to 400 cm^{-1} .

3.2.2.2 particle size distribution analysis

Particle size distribution of both α -solid and α -wet was detected by using laser scattering particle size distribution analyser (Horiba/LA-950V2). 100 mg of powder was dispersed in 200 ml isopropanol by applying ultrasound for 15 min (Gbureck, 2004).

3.2.2.3 Morphology analysis

The morphologies of α -TCP powder were observed by the scanning electron microscopy (SEM JEOL/JSM-6010LV) coupled with an energy dispersive X-ray (EDX OXFORD INSTRUMENTS/X-max20) analyser. All specimens were mounted on stubs and coated with gold.

3.2.3 Characterization of cement

3.2.3.1 Cement preparation

The cement powder consisted of two main components, β -TCP/apatite at a weight ratio of 1:5. The apatite component consisted of 62.5 wt.% α -TCP, 26.8 wt.% DCPA, 8.9 wt.% CaCO_3 , and 1.8 wt.% precipitated hydroxyapatite (PHA), as followed the previous work (Rattanachan, 2020). PHA was synthesized in house by precipitation method as followed previous study (Srakaew and Rattanachan, 2014). All precursors powder was homogenously mixed for 45 min using a ball mill (NITTO/ANZ10D Rotation, Japan). The powder mixing was performed in a polyethylene pot mill containing zirconia balls with a diameter of 10 mm. The cement powder and zirconia balls were dried in the oven at 110 °C to avoid the moisture before mixing in the pot mil. After mixing α -TCP from different syntheses (α -solid and α -wet) with other calcium phosphate compounds, the cement powder was homogenously mixed with cement liquid, denoted as CPC-solid and CPC-wet. The cement liquid was the mixture of 1 M disodium hydrogen phosphate (Na_2HPO_4) and 1 M sodium dihydrogen phosphate (NaH_2PO_4). In this work, the L/P ratios of 0.35-0.40 were fixed, which were suitable to handle this cement. The cement pastes were packed into the cylindrical mold with a size diameter of 6 mm and height of 12 mm for compressive strength testing and phase composition analysis. Another set of samples was prepared in the same size of mold, followed by cutting for 3 pieces (6 mm diameter, 4mm height) for bioactivity and pH measurement. All samples were incubated at 37 °C under 100% humidity for 24 h before the test mentioned above, to avoid some incomplete reaction of the sample before soaking in simulated body fluid (SBF).

3.2.3.2 Phase composition analysis

The cement powder was mixed with cement liquid with liquid to powder ratio (L/P) of 0.35 and 0.40 ml/g. Afterward, the set cement was soaked in SBF solution at 37 °C for 7 and 14 days. After incubation, the specimens were ground into fine powder before the analysis. The phase composition of samples was determined by X-ray diffraction (XRD Bruker/D2-phaser) with the Cu K α radiation ($\lambda =$

1.5406 Å). The data were analysed in the range of 2θ from 20 to 40, and in increments of 0.02 with the counting time per step of 0.5. The quantitative phase compositions of cements were measured by means of Rietveld refinement analysis using the TOPAS software (Bruker AXS, Karlsruhe, Germany). Rietveld refinement was accomplished in triplicate for the phase composition following the database of the Inorganic Crystal Structure Database (ICSD). The structures of α -TCP (ICSD No. 923 (Yashima and Sakai, 2003)), β -TCP (ICSD No. 6191 (Yashima, 2003)), CaCO_3 (ICSD No. 73446 (Maslen, 1993)), DCPA (ICSD No. 917 (Catti, 1980)), and Hydroxyapatite (ICSD No.87668 (Wilson, 1999)) were used to measure the composition of cement.

3.2.3.3 Setting time measurement

The cement powder was mixed with cement liquid for 1 minute in mortar. The homogenous paste of each condition was poured into the mold using a spatula. The setting time was measured when the Gilmore needles were pressed on the surface and there is no visible mark on the surface of cements. The standard Gillmore needles with a light-thick needle (2.13 mm, 113.4 g) and a heavy-thin needle (1.06 mm diameter, 453.6 g) was used to measure the initial and final setting of cement pastes, respectively, in accordance with the standard ASTM C266-99. The measurement was repeated twice.

3.2.3.4 Compressive strength

The cement sample was prepared in a Teflon mold (6 mm diameter and 12 mm height) according to the standard ASTM F451-95. The specimens were removed from the mold and maintained in 100 % humidity at 37 °C for 24 h, then immersed in SBF solutions for 7 days. For sample incubation in SBF solutions, the volume of SBF to the surface area of specimen ratio of 0.1 mL/mm² was used, as followed (Kokubo and Takadama, 2006). The compressive strength of all specimens was tested using Universal testing machine (UTM capacity 100 kN/MUL-125 TTR: THAI, according to ISO/IEC 17025) with a 10 kN load cell at a cross speed of 1 mm/min⁻¹. Eight specimens were tested for each condition.

3.2.3.5 Microstructure analysis

The fracture surfaces of cement after compression test and the surface of the samples (bioactivity) after incubation in SBF solution for 7 days were observed by using the scanning electron microscopy (SEM JEOL/JSM-6010LV). The bioactivity was investigated by detecting whether the precipitated hydroxyapatite occurred on the surface of samples or not after immersion in SFB solution. All specimens received a gold coating before observation.

3.3 Result and discussion

3.3.1 Characterization of α -TCP powder

3.3.1.1 Phase composition and chemical functional group analysis

As shown in Figure 3.1, it can be seen that there is no significant difference between the XRD pattern of both α -TCP obtained by solid state reaction and wet chemical reaction. The high purity phase of α -TCP was detected, with corresponding to the standard file (α -TCP: JCPDS 09-0348 and 29-0359 (Thürmer, 2016)).

The α -TCP obtained by wet chemical reaction was calcined at varying temperatures from 1300-1500 °C, has been published in Thürmer et al. (Thürmer, 2016) providing the higher pure phase of α -TCP with the increasing of temperature calcination to 1500 °C. However, this study showed the high purity phase of α -TCP at 1400 °C which is unnecessary for the higher calcination (1500 °C) to obtain the higher pure phase of α -TCP. The synthesis of α -TCP with high purity phase has been studied with the use of long dwell time at high temperature (greater than 1200 °C) not less than 4 h, was known as the standard method. Moreover, the quenching to room temperature was the main point to inhibit the transformation of β -TCP in α -TCP after cooling period. Duncan et al. (Duncan, 2014) studied the effect of cooling rate on the quantitative transformation of β -TCP, resulting the higher β -TCP with the increasing of cooling rate. As the result, it should be noted that the high purity phase

of α -TCP could be obtained by the wet chemical method under heat treatment at high temperature without quenching step.

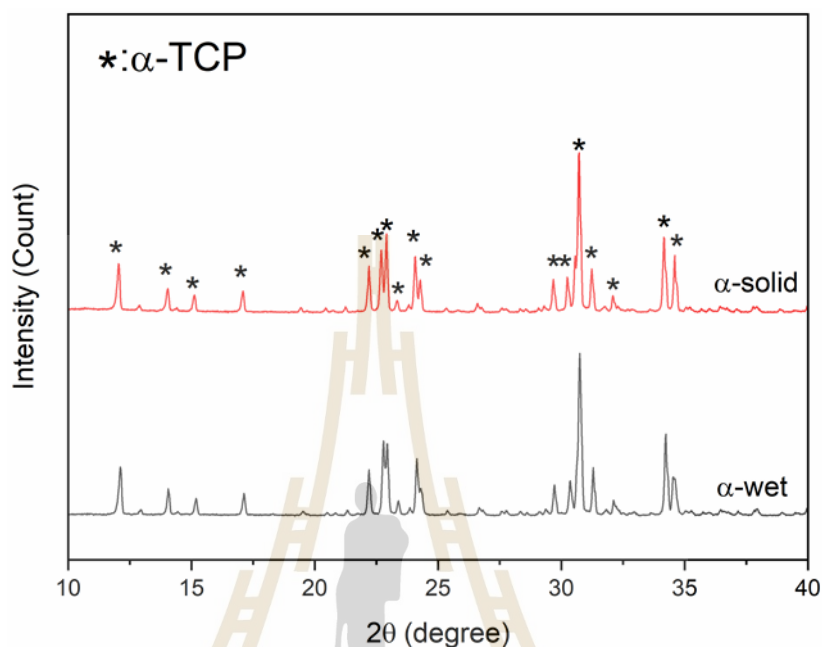


Figure 3.1 XRD pattern of α -TCP obtained by solid state reaction (α -solid), and wet chemical reaction (α -wet).

3.3.1.2 Chemical functional group analysis

The spectra of α -solid and α -wet were also investigated in transmission mode using the ATR technique of FTIR, as shown in Figure 3.2. The spectra of α -TCP powder from literature reviews (Carrodegua and De Aza, 2011, Kolmas, 2015) compared with α -solid and α -wet, bands were identified in accordance with the vibrations of phosphate groups that consisted of ν_1 bands determined to symmetric P-O stretching and ν_3 bands determined anti-symmetric P-O stretching triply degenerate ($1200-900\text{ cm}^{-1}$), ν_2 bands determined symmetric P-O bending double degenerate ($410-470\text{ cm}^{-1}$), and ν_4 bands determined anti-symmetric P-O bending triply degenerate ($650-500\text{ cm}^{-1}$), illustrated in Table 3.1.

FTIR spectrum of the α -solid powder was similar to that of the α -wet, but some bands in the region of ν_2 , ν_3 , and ν_4 vibrations were not identified comparing to the bands of α -wet and α -TCP from literature reviews, as shown in Table 3.1. Some noticeable bands are poorly resolved showing very low intensity. This may be due to the low intensive bands overlapped with other higher intensive bands (Kolmas, 2015).

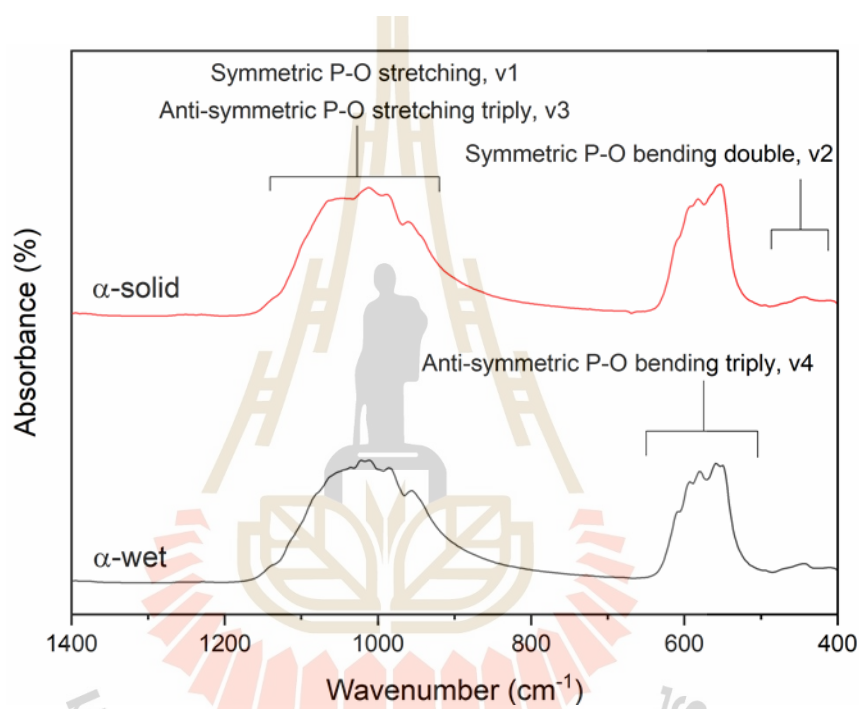


Figure 3.2 FTIR spectra of α -TCP obtained by two methods (α -solid, α -wet)

Table 3.1 Main bands and characteristic wave number of α -TCP (α -solid and α -wet) compared with α -TCP from literature review.

Normal mode	Free PO_4^{3-} (cm^{-1})	α -solid (cm^{-1})	α -wet (cm^{-1})	α -literature (cm^{-1}) (Carrodegus and De Aza, 2011, Kolmas, 2015)
Symmetric P-O stretching, ν_1	938	960	955	954
Symmetric P-O bending double degenerate, ν_2	420	412	412	415
		443	444	430
			463	454
			470	463
				471
Anti-symmetric P-O stretching triply degenerate, ν_3	1017	988	984	984
		1012	1012	997
		1038	1022	1013
		1047	1036	1025
			1045	1039
				1055
Anti-symmetric P-O bending triply degenerate, ν_4	567	553	550	551
		582	559	563
			580	585
			593	597
			609	613

3.3.1.3 Particle size distribution analysis

Particle size distributions of both α -TCP powders (α -solid and α -wet) were narrow distribution (data not shown). α -solid and α -wet had mean particle size of 13.739 μm , and 16.9 μm , respectively. Although the mean size of α -solid is smaller than that of α -wet, it was not a significant difference, as displayed in Table 3.2.

The obtained α -solid and α -wet powders in our current work were in a similar range to the particle size of α -TCP powder (13.33 μm and 16.80 μm by milling time at 30 and 60 min (Thürmer, 2016)), which was determined by light scattering.

Table 3.2 Particle size distribution of powders

Samples	Particle size (μm)		
	mean	median	mode
α -solid	13.74	12.48	12.43
α -wet	16.90	14.30	14.16

3.3.1.4 Morphology analysis

The scanning electron microscope (SEM) was used for morphological determination of α -TCP, both powders (α -solid and α -wet) presented irregular shape crystals without agglomeration. The size range of α -solid and α -wet represented in Figure 3.3, which the size of both powders was related to the results of particle size distribution analysis.

The Ca/P molar ration of powders was examined by energy dispersive X-ray (EDX) to ensure that Ca/P molar ratio of both synthesized α -TCP was about 1.5 as calculated from the ratio of starting reagents, resulting in Table 3.2.

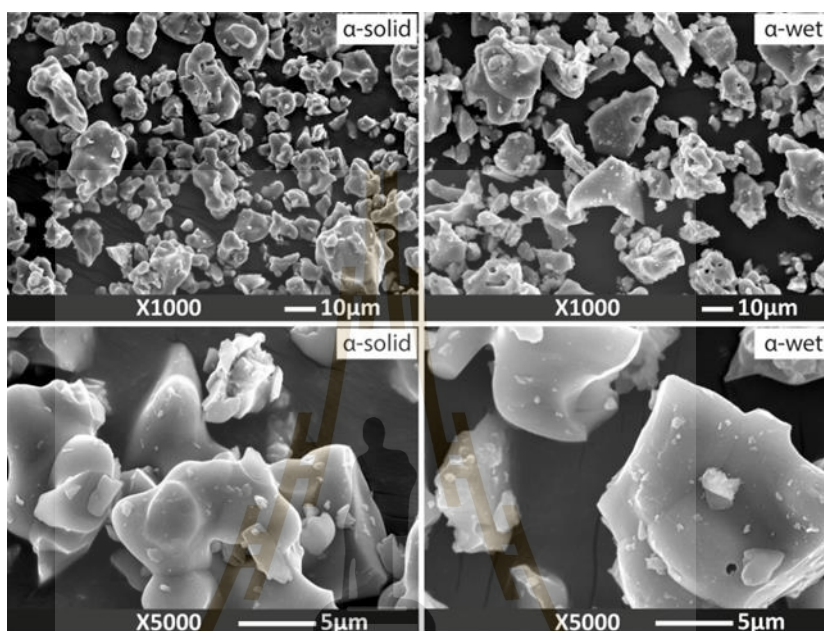


Figure 3.3 SEM images of α -TCP powder obtained by solid state reaction and wet chemical reaction synthesis at magnification of x1000 and x5000.

Table 3.3 The quantitative results of two different powder of α -TCP, using EDX spectrum analyzer.

Samples	P (Atomic%)	Ca (Atomic%)	Ca/P ratio
α -solid	40.03	59.97	1.498
α -wet	39.93	60.07	1.504

3.3.2 Characterization of cement

3.3.2.1 Setting time measurement

The setting time of cements was measured at room temperature with constant L/P ratio values of 0.35 and 0.40 ml/g in order to observe which ratio was the most suitable for moldability of cements after mixing powder and liquid phase. The results showed that the setting time of CPC-solid raised up from 13.5 min to 25 min and that of CPC-wet raised up from 15 min to 26.5 min when the L/P ratio was increased from 0.35 to 0.40 ml/g.

As a result, the CPC-solid specimen contained a smaller mean particle size of α -solid powder, which resulted in a slight shorter setting time than that of CPC-wet. The particle size of reactants and liquid to powder ratio were reported as the factor that involved the setting time performance. These factors became a strategy to reduce the setting time of cements (Zhang, 2014).

Table 3.4 Setting time measurement of cement at different L/P ratio.

Samples	Setting time (min)			
	L/P = 0.35 ml/g		L/P = 0.40 ml/g	
	Initial time	Final time	Initial time	Final time
CPC-solid	13.5	55	25	80
CPC-wet	15	58	26.5	86

3.3.2.2 Phase composition analysis

XRD patterns of both cements indicated the phase compositions of HA (09-0432), β -TCP (09-0169), α -TCP (09-0348 and 29-0359), DCPA (70-0359), and CaCO_3 (47-1743), as followed the data sheet number of the powder diffraction

standard. It was found that HA phase in both cements similarly increased after incubation in SBF solution from 7 to 14 days, as shown in Table 3.5.

After mixing cement powder and liquid, the released Ca^{2+} and PO_4^{3-} from starting powder reacted with PO_4^{3-} in the cement liquid (Na_2HPO_4 and NaH_2PO_4), following by the crystal nucleation as the cement set (Burguera, 2006). The higher L/P ratio of 0.40 provided more PO_4^{3-} from the cement liquid during the setting reaction, which could result in the higher HA formation when compared with L/P ratio of 0.35. Here, α -TCP from different syntheses did not affect the phase conversion of α -TCP into HA over incubation time in SBF solution.

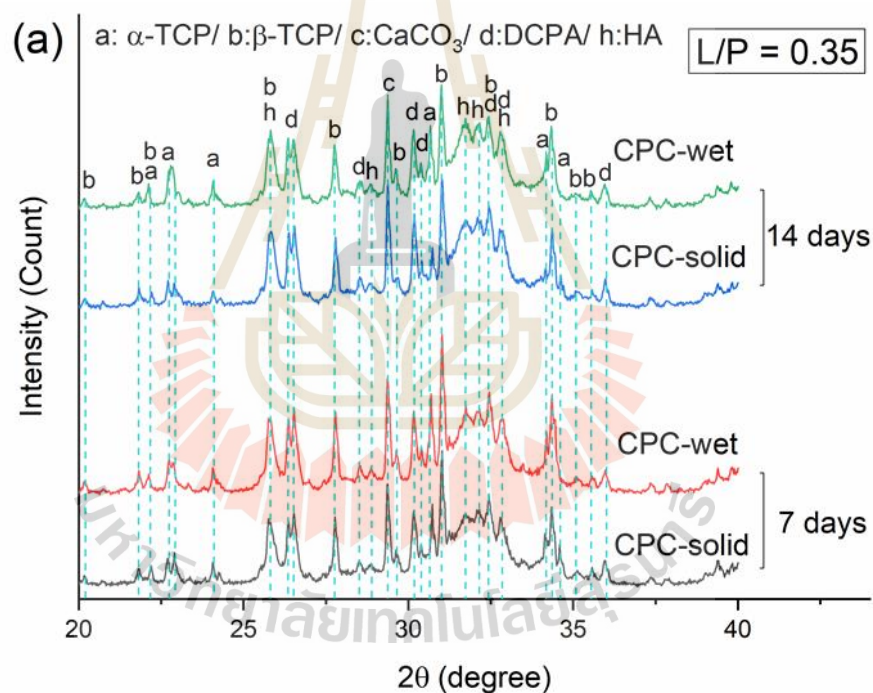


Figure 3.4 XRD patterns of cement containing α -TCP powder obtained by solid state reaction and wet chemical reaction synthesis at L/P ratio of (a) 0.35 and (b) 0.40 after soaking in SBF solution for 7 and 14 days.

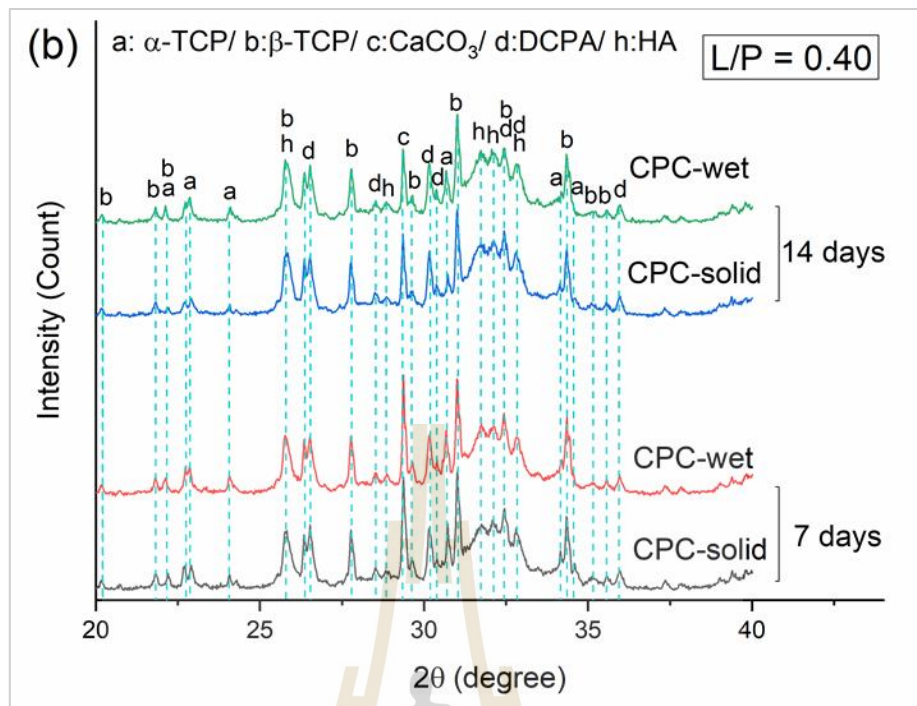


Figure 3.4 XRD patterns of cement containing α -TCP powder obtained by solid state reaction and wet chemical reaction synthesis at L/P ratio of (a) 0.35 and (b) 0.40 after soaking in SBF solution for 7 and 14 days. (Continued)

Table 3.5 Percentage of hydroxyapatite after immersion of cement in SBF solution over 14 days.

Samples	HA formation wt.% (Rietveld refinement)			
	L/P = 0.35 mL/g		L/P = 0.40 mL/g	
	7 days	14 days	7 days	14 days
CPC-solid	31.67	37.94	33.96	41.67
CPC-wet	31.65	36.58	34.03	39.17

3.3.2.3 Compressive strength

The result of compressive strength was presented as mean \pm standard deviation (SD). The statistical comparison between each data group was performed by One-way ANOVA coupled with Tukey's multiple comparison test with

the confidence interval of $p < 0.05$. The compressive strength of CPC-wet was slightly lower than that of CPC-solid. However, the mean of one-way analysis statically presented compressive strength of both cements with no significant difference at the same L/P ratio, as displayed in Figure 5.

It has been proved that the particle size of α -TCP and liquid to powder ratio affected the properties of cements (Montufar, 2013). It can be seen that a slightly bigger size of particle (Ginebra, 2004) and increasing of L/P ratio (O'Hara, 2010) reduced the compressive strength after immersion in SBF solution, while setting time increased. Their findings are similar to the result trend of the current work.

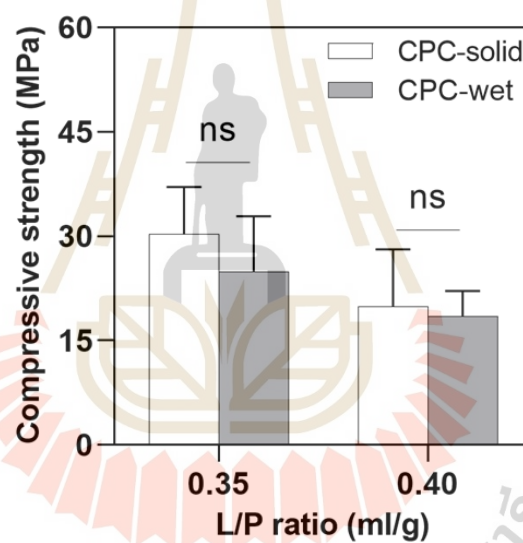


Figure 3.5 Compressive strength of cement containing α -TCP powder obtained by solid state reaction and wet chemical reaction synthesis at L/P ratio of 0.35 and 0.40 after soaking in SBF solution for 7 days.

3.3.2.4 Morphology analysis

Figure 3.6 shows the SEM images of the fracture surface micrograph of cements (CPC-solid, and CPC-wet) at L/P ratio of 0.35 and 0.40 ml/g after immersion in SBF solution for 7 days. As the results, needle-like crystals were observed surrounding some of the incompletely solubilized starting powder phases. In

addition, the HA formation covered on the surface area of the cement was observed after soaking in SBF solution over time, as presented in Figure 3.7.

The HA conversion was formed by the dissolution of α -TCP and other powders after mixing with liquid phase, followed by the reprecipitation process of the network of entangled crystals on the starting powder, which the HA became a thicker layer as the reaction time continued [16]. It can be seen that both cements consisting of different α -TCP powder as one of the starting powders transformed to HA phase, as described above. After soaking the sample in SBF solution for various periods of time, the deposition of the HA layer on the surface of materials has been measured as evidence of bioactivity (Morejón-Alonso, 2012). In this study, the surface of sample was covered by the visibly dense hydroxyapatite after the immersion of cement in SBF solution for 7 days. The formation of precipitated HA on the surface of cement containing α -TCP from different syntheses presented an excellent bioactivity of material.

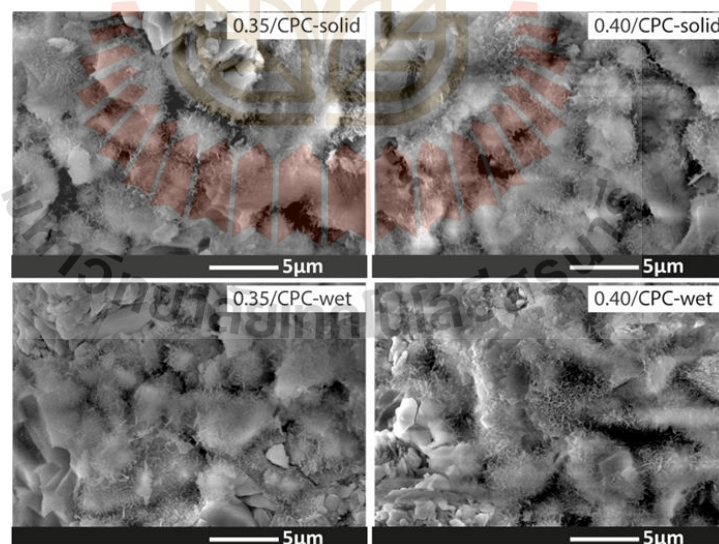


Figure 3.6 Fracture surface micrographs of cement containing α -TCP powder obtained by solid state reaction and wet chemical reaction synthesis at L/P ratio of 0.35 and 0.40 after soaking in SBF solution for 7 days.

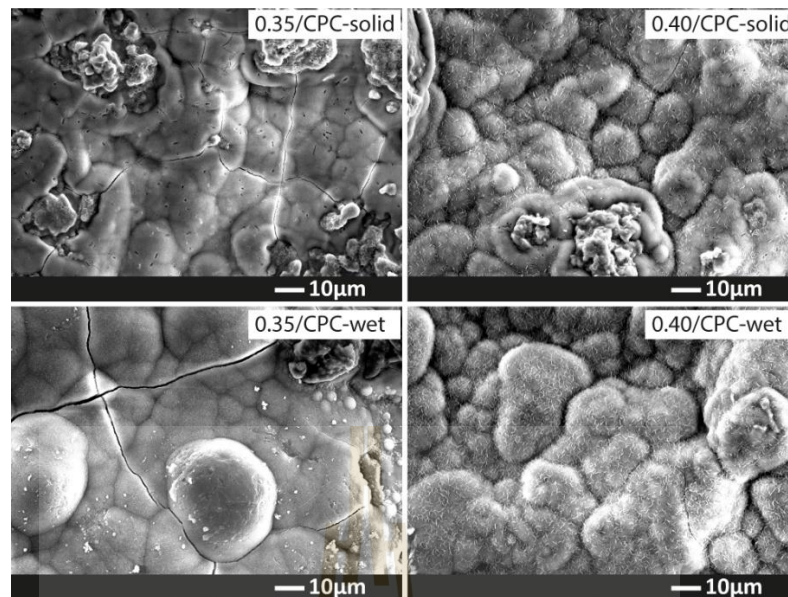


Figure 3.7 SEM images of surface area of cement containing α -TCP powder obtained by solid state reaction and wet chemical reaction synthesis at L/P ratio of 0.35 and 0.40 after soaking in SBF solution for 7 days.

3.4 Conclusions

α -TCP powder with high purity phase was successfully synthesized by both conventional solid state reaction and optional wet chemical reaction. Although α -solid powder displayed slightly better performances of cements including setting time, compressive strength, and percentage of hydroxyapatite formation as the final product, it can be proved that the high purity of α -TCP from different syntheses (solid state reaction and wet chemical reaction) presented the properties of calcium phosphate cement with no significant difference. This is possibly another choice for the use of α -TCP from wet chemical reaction instead of the solid state reaction method due to time efficiency and the reduced cost of the process. However, further analysis must be investigated with more comprehensive results in order to support the results in current study.

CHAPTER IV

SEVERAL PARAMETERS INFLUENCED ON APATITE/ β -TCP CEMENT: PARTICLE SIZE OF ALPHA-TRICALCIUM PHOSPHATE POWDER AND DRY-HEAT STERILIZATION

Apatite/beta-tricalcium phosphate (β -TCP) cements have been enormously studied for use in various medical applications due to their osteoconductive and in vivo biodegradable ability. However, apatite/ β -TCP mostly presented poor mechanical properties, which were suitable only for use under non-load bearing conditions. Herein, the improvement of this cement by reducing the size of the starting powder has become a promising method. Consequently, the major phase of alpha-tricalcium phosphate (α -TCP) was ground at different time points, resulting in smaller particle size when increasing milling time from 4 to 8 h. The physical properties of apatite/ β -TCP cement consisting of different sizes of α -TCP were characterized throughout setting time, compressive strength, and phase composition after soaking in SBF solution for 7 days. The cement containing a smaller size of α -TCP showed decreased setting time, higher compressive strength, and enhanced apatite conversion. Therefore, cement with α -TCP powder ground for 8 h was then used for further experiments. The sterilization process of biomaterials is mandatory for use in biological processes. Dry heat sterilization was selected for this study due to its advantages of having no moisture or released residuals during the process. Afterward, the effect of dry heat sterilization at different conditions of temperature on the physical properties of apatite/ β -TCP cement was detected. As a result, the sterilized sample (121 °C, 10 h) was a suitable condition for this cement formula, showing no significant difference in physical properties of cement including phase composition, compressive strength, setting time, pH changes, and bioactivity.

4.1 Research background, rationale, and significance

Calcium phosphate cements (CPCs) are a potential bone fixing material that is also well-established in clinical care. The chemical components in this material are identical to the hydroxyapatite (HA) found in human bone, which assists in the production of new bone after surgery (O'Hara, 2014). However, the low degradation rate of apatite cement could not completely allow the new bone ingrowth (Frankenburg, 1998). Therefore, the apatite cement incorporated with a highly resorbed beta-tricalcium phosphate (β -TCP) component has received a lot of attention (Daculsi, 1998). Although β -TCP showed a higher resorption aspect of cement, it could lead to a decrease in mechanical strength of cement (Srakaew and Rattanachan, 2014).

The mechanical strength could be significantly improved by various factors, such as cement formula, L/P ratio, and particle size distribution. Thus, the particle size of the starting cement powder plays an important role in the setting reaction of apatite cement (Zhang, 2014). The effect of particle size of α -TCP powder on the properties of apatite cement has been studied (Hurle, 2014). It was found that the smaller size of α -TCP increased the compressive strength of cement (Ginebra, 2004). However, the smaller could result in lower strength due to the more amorphous phase of α -TCP when increasing milling time (Gbureck, 2004). It was reported that the more amorphous phase of α -TCP could provide the heat release during the setting reaction of cement (C.L. Camire´ a, 2005). Therefore, the suitable milling time for α -TCP should be considered to avoid heat release during the reaction.

In general, the biomaterials must be sterilized in order to prevent any harmful microorganisms found in the materials before being used in *in vitro/in vivo* biological testing and clinical use. Sterilization has been commonly used in various methods, including steam under pressure (autoclave), dry heat, gamma radiation (γ -ray), and ethylene oxide (EO) (Hasirci and Hasirci, 2018). The appropriate sterilization method is required for each material due to their different characteristics. Previous work (Morejón-Alonso, 2007) has studied the effect of different sterilization on calcium phosphate cement. They found that EO sterilization seemed to be the most appropriate method, indicating less effect on cement properties with respect to other sterilizations. Surprisingly, the residual gas could still be found in the materials after EO sterilization,

which was toxic to livings (Takechi, 2004). Furthermore, γ -ray appeared to be an alternative sterilization of calcium phosphate cement (Chen, 2013, Meng, 2018). However, the chitosan fiber content in the cement of the current study could be damaged by γ -ray, as evidenced in previous study (Yang, 2007). Dry heat sterilization was another promising method, which has been used in some previous studies for in vitro (Goldberg, 2018) and in vivo (Tsai, 2008) experiments with apatite cement. However, the higher temperature of dry heat sterilization could result in the decomposition of chitosan (Lim, 1999, Kim, 2004). This work aimed to examine the effect of particle size of α -TCP powder on cement properties and to indicate the appropriate dry heat sterilization for the apatite/ β -TCP cement.

4.2 Experimental procedure

4.2.1 Effect of particle size of α -TCP powder on Apatite/ β -TCP cement

4.2.1.1 Synthesis and characterization of α -TCP powder

α -TCP powder was synthesized by the precipitation method, which was modified from the wet chemical reaction method in topic 3.2.1 of Chapter III. Briefly, 0.5 M calcium nitrate ($\text{Ca}(\text{NO}_3)_2 \cdot 4\text{H}_2\text{O}$) was mixed with 0.5 M phosphoric acid (H_3PO_4) at Ca/P ratio of 1.5. After 30 min of mixing, the pH of the obtained solution was adjusted to 10.5 by the addition of ammonium solution (NH_4OH). The white precipitated particles were washed and filtrated with deionized water for 5 times. The obtained particles were incubated at 90 °C for 24 h and dried at 120 °C. The particles were calcined in an alumina crucible at 1400 °C for 1 h without quenching in air. The obtained powder was ground in mortar and sieved through 325 mesh to achieve a fine α -TCP powder (denoted as 0 h). Afterward, the α -TCP powder was added to an alumina grinding jar with a ratio of 1 g α -TCP powder/1 zirconium ball (10 mm diameter) and milled at different period of times (4, 6, and 8 h) using planetary ball mill. The grinding speed was set at 400 rpm with bidirectional milling for every 5 min.

The phase composition was measured by X-ray diffraction (XRD Bruker/D2-phaser) according to the topic 3.2.2.1 of Chapter III. Particle size distribution of α -TCP powder at different time milling was measured laser scattering particle size

distribution analyser (Horiba/LA-950V2), as followed the topic of 3.3.2.2 of Chapter III. The morphologies of α -TCP powder were detected by the scanning electron microscopy (SEM JEOL/JSM-6010LV) following the topic of 3.3.2.3 of Chapter III.

4.2.1.2 Preparation of cements

The cement powder composition consisted of 62.5 wt.% α -TCP, 26.8 wt.% dicalcium phosphate anhydrous (DCPA), 8.9 wt.% calcium carbonate (CaCO_3), 1.8 wt.% precipitated hydroxyapatite (PHA), 20 wt.% beta-tricalcium phosphate (β -TCP), and 1 wt.% chitosan fiber (Rattanachan, 2020). The cement powder and liquid was prepared in accordance with the topic 3.2.3.1 of Chapter III. The L/P ratios of 0.40 were chosen in this chapter since it enabled for cement fabrication. After mixing powder and liquid, the cement paste was poured into the cylindrical mold and allowed to set at room temperature for 30 min before further analysis. The cement consisted of α -TCP from different milling time from 4 to 8 h was denoted as 4h, 6h, and 8h, respectively.

4.2.1.3 Properties testing and characterization of cement

The condition and analysis procedures of calcium phosphate cement properties, including setting time, compressive strength, and phase composition were performed according to topic 3.2.3 of Chapter III.

4.2.2 Effect of dry heat sterilization on Apatite/ β -TCP cement

4.2.2.1 Preparation of cements

The cement powder composition consisting of ground α -TCP powder (8 h) from section 4.2.1.1 was used in this part. Some of the starting cement powder was sterilized using dry heat sterilization at various conditions (Talaro, 2008), as shown in Table 4.1. To prepare the cement samples, the sterilized cement powder was mixed with cement liquid at L/P ratio of 0.40 ml/g following the section 3.3.1.2. The control sample was denoted as non-sterilized, while other sterilized conditions were denoted as 121°C/10, 140°C/3, 160°C/2, and 170°C/1, respectively.

Table 4.1 Dry heat sterilized conditions.

Conditions	Temperature (°C)	Soaking time (hours)
121°C/10h	121	10
140°C/3h	140	3
160°C/2h	160	2
170°C/1h	170	1

4.2.2.2 Properties testing and characterization of cement

The setup and analysis methods of calcium phosphate cement characteristics, comprising phase composition, compressive strength, setting time, and bioactivity were conducted following the topic 3.2.3 of Chapter III. In addition, the chemical functional groups of the starting chitosan fiber under various dry heat sterilized conditions was separately characterized using FTIR analysis, as followed the topic 3.2.2.1 of Chapter III.

4.2.2.3 pH measurement

The pH changes in SBF solution were measured at various time intervals without changing the solution during the sample incubation in the solution. The volume of SBF to the surface area of the specimen ratio of 0.1 ml/mm² was employed for sample incubation in SBF solution.

4.3 Result and discussion

4.3.1 Effect of particle size of α -TCP powder on Apatite/ β -TCP cement

4.3.1.1 Phase composition of α -TCP powder

The XRD patterns of α -TCP at different milling time from 0 to 8 h were detected with no noticeable difference, as illustrated in Figure 4.1. All conditions were matched with the high purity phase of α -TCP according to the standard JCPDS files of 09-0348 and 29-0359.

In the previous works (Camiré, 2006, Wang, 2007), the milling process could affect the crystallinity of α -TCP, resulting in a higher amorphous aspect of α -TCP when increasing milling time. However, the prolonged grinding time from 0 to 8 h under the dry milling process in this current study did not significantly affect the crystallinity of α -TCP powder. This contrast aspect could be attributed to the difference in grinding procedure, as presented in the previous study (Gbureck, 2004). They found that wet milling in ethanol produced more amorphous fractions of α -TCP powder than dry milling conditions.

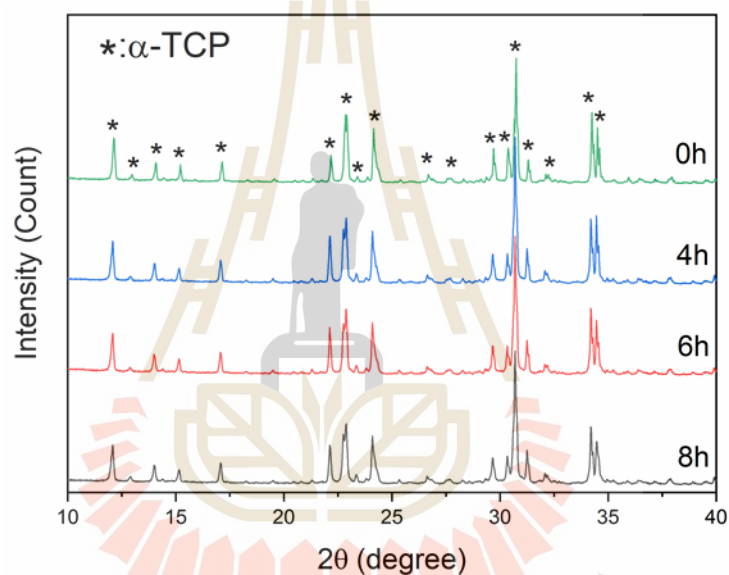


Figure 4.1 XRD patterns of α -TCP powder with various milling times of 0, 4, 6, and 8 hours.

4.3.1.2 Particle size distribution of α -TCP powder

The influence of prolonged milling time on the particle size distribution of α -TCP powder was presented Figure 4.2. The result showed that the particle size distribution of α -TCP powder widened to smaller size distribution after milling over 8 h. The mean size of α -TCP particles for 0, 4, 6, and 8 h were 52.5, 15.7, 4.4, and 3.2 μm , respectively. In addition, the starting α -TCP powder condition was bimodal distribution, while other conditions were monomodal distribution.

After 8 h of grinding process, the mean size of α -TCP particle decreased from 52.5 to 3.2 μm , which was much smaller than previous study (Thürmer, 2016) in the same periods. Gbureck et al. (Gbureck, 2004) could reduce the particle size of α -TCP from 17.48 to 5.76 (ground in ethanol) and to 6.42 (ground in dry state). Moreover, the particle size distribution of α -TCP was monomodal after grinding, while the other works were still mostly bimodal (Bohner, 2006). These differences in particle size distribution of α -TCP could be due to the different grinding procedure between the current work and others.

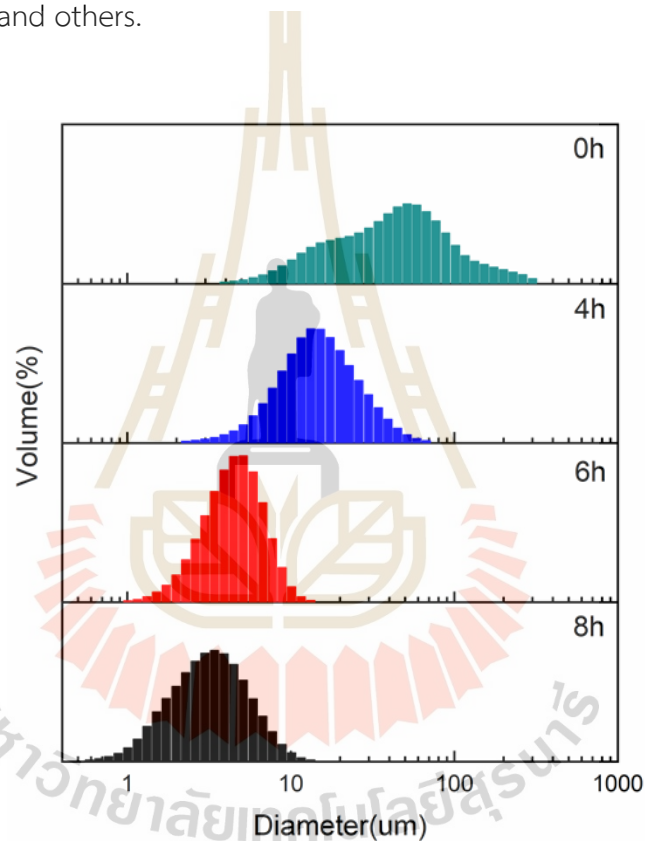


Figure 4.2 Particle size distribution of α -TCP powder with different milling times of 0, 4, 6, and 8 hours, respectively.

4.3.1.3 Morphology of α -TCP powder

SEM micrographs presented the effect of prolonged milling process on the morphology of α -TCP powder. It was found that the particle size of α -TCP decreased when increasing milling from 4 to 8 h. Furthermore, all conditions had

an irregular shape without agglomeration, and their size range was similar to the particle size distribution result.

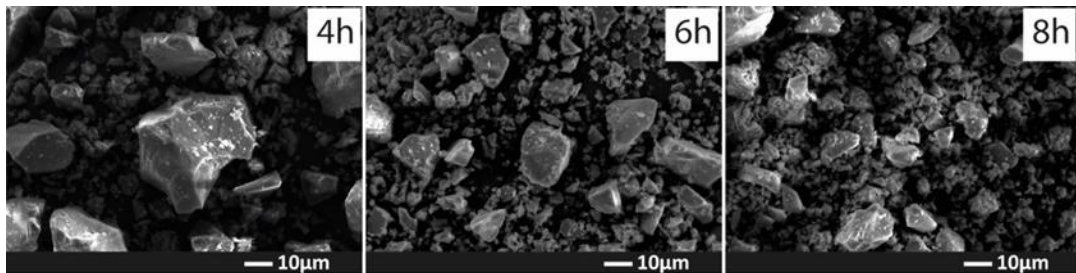


Figure 4.3 SEM micrographs of α -TCP powder at different milling times of 4, 6, and 8 hours.

4.3.1.4 Setting time measurement

The results showed that the longer milling time of α -TCP powder had an effect on the cement's initial (t_i) and final (t_f) setting time, as demonstrated in Figure 4.4. It was found that both t_i and t_f times significantly decreased when milling time was increased from 4 to 8 h.

This work investigated the influence of a longer milling time of α -TCP powder on the setting time of cement. Ginebra et al. (Ginebra, 2004) presented that the longer milling time provided a smaller particle size of α -TCP, resulting in shorter setting time. Another previous study also revealed the reduced setting time of cement when the α -TCP starting powder was smaller (Wang, 2007). Their findings are similar to our current work. Thus, the t_i (3.8 ± 0.4 min) and t_f (24 ± 2.8 min) times of 8h cement were closer to the clinical requirements ($t_i < 8$ min, $t_f < 15$ min (Khairoun, 1998)) with respect to 4h ($t_i = 12.5 \pm 2.1$ min and $t_f = 47 \pm 2.8$ min) and 6h ($t_i = 6.5 \pm 0.7$ min and $t_f = 36.5 \pm 2.1$ min) cements.

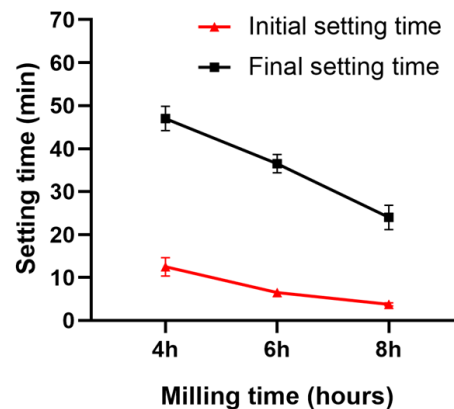


Figure 4.4 Initial and final setting time of apatite/ β -TCP cement with various milling times of α -TCP powder at L/P ratio of 0.40.

4.3.1.5 Compressive strength

After soaking samples in SBF solution for 7 days, the compressive strength of all conditions was measured. Figure 4.5 shows that the compressive strength of both 6h (36.3 ± 4.6 MPa) and 8h (36.5 ± 5.8 MPa) cement was significantly higher than that of 4h (29.7 ± 4.0 MPa). Meanwhile, there was no statistic difference between 6h and 8h cement.

In this work, the compressive strength was improved by a smaller size of α -TCP from prolonged milling time of 6 and 8 h with respect to 4 h. This aspect is relevant to the previous work (Ginebra, 2004), which indicates that fine α -TCP cement has a higher compressive strength than coarse α -TCP cement. They reported that the smaller particles led to more contact sites and reduced the porosity, providing a higher strength of cement. Although the prolonged milling time (1 to 4 h) of α -TCP powder could result in the higher compressive strength of cement, the decreased strength was found with longer milling (> 4 h) due to the lower crystallinity of α -TCP powder (Gbureck, 2004). However, this feature did not influence the strength of cement in the present work as it was presented without a significant difference in the crystallinity of α -TCP powder after milling over 8 h. A similar strength in both 6h and 8h conditions could be attributed to the similar range of mean particle size (6h = $4.4\mu\text{m}$, 8h = $3.2\mu\text{m}$).

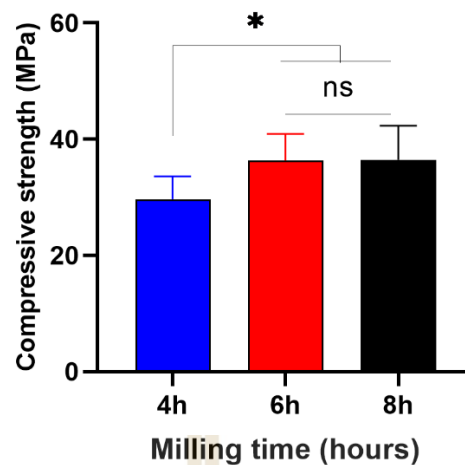


Figure 4.5 Compressive strength of apatite/ β -TCP cement with various milling times of α -TCP powder at L/P ratio of 0.40 after soaking in SBF solution for 7 days.

4.3.1.6 Phase composition of cement

The XRD patterns of all cement conditions composed of various peaks, including 09-0432 (HA), 29-0359 (α -TCP), 09-0169 (β -TCP), 47-1743 (CaCO_3), and 70-0359 (DCPA). After soaking sample in SBF solution at 37 °C for 7 days, the different intensity of α -TCP and HA among each condition was noticeable. The XRD pattern showed a lower intensity of α -TCP and a higher intensity of HA when milling time was increased. Afterward, this different composition of α -TCP and HA of all conditions was quantitatively analyzed by Rietveld refinement, as shown in Figure 4.7.

Previous studies (Gbureck, 2004, C.L. Camire´ a, 2005) found that a longer milling time resulted in a more amorphous phase of α -TCP. This amorphous aspect presented a higher reactivity, resulting in the higher nucleation rate of CDHA (Brunner, 2007). However, the longer times (4 to 8 h) did not affect the crystallinity of α -TCP in this work, as previously described. Therefore, the higher CDHA should be attributed to the higher specific surface area of the smaller particle size when milling time was increased. This consideration is in agreement with the previous work (Ginebra, 2004). They ascribed that the smaller particle size of α -TCP had a higher specific surface area dissolved and provided a higher supersaturation in the solution. This led to more precipitated CDHA crystal formation. After cement was set in SBF for 7 days,

the major phases of these current cements were composed of HA/CDHA and β -TCP with respect to other residuals of α -TCP, DCPA, and CaCO_3 . This was comparable to the result of Chapter III.

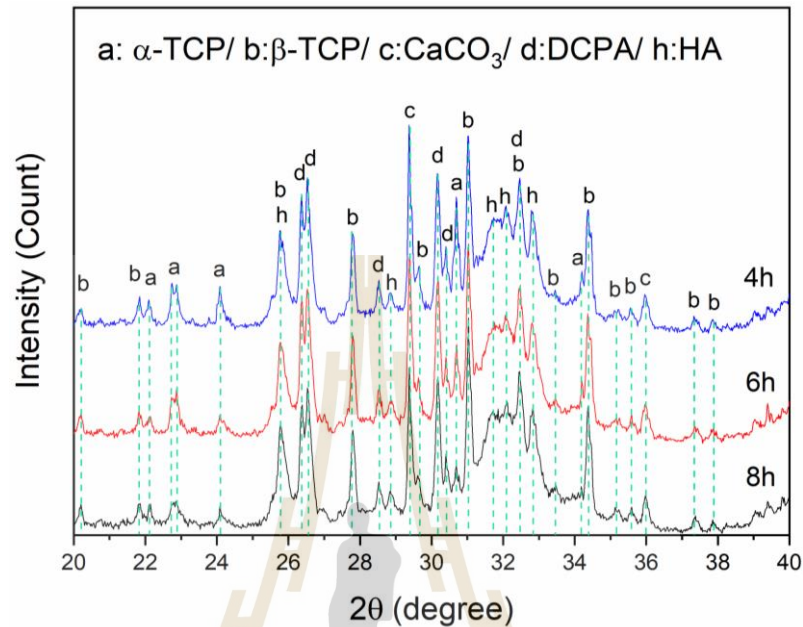


Figure 4.6 XRD patterns of apatite/ β -TCP cement with various milling times of α -TCP powder at L/P ratio.

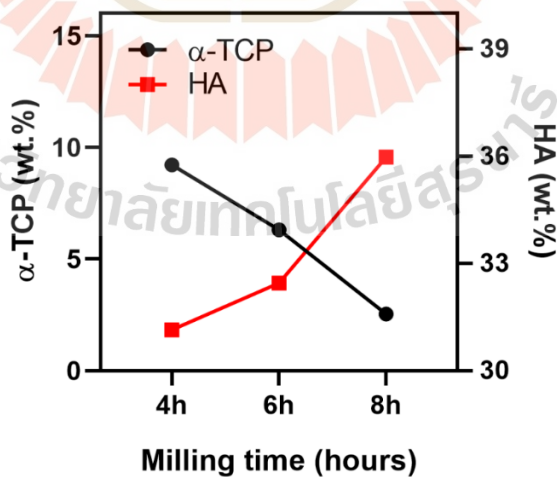


Figure 4.7 Weight percent of α -TCP and HA phases in apatite/ β -TCP cement with various milling times of α -TCP powder at L/P ratio of 0.40 after soaking in SBF solution for 7 days.

4.3.2 Effect of dry heat sterilization on Apatite/ β -TCP cement

4.3.2.1 Phase composition and chemical functional group analysis

In Figure 4.8, the starting powder from different dry heat sterilized conditions presented similar XRD patterns, comprising of the major phase of α -TCP with other minor components. After forming cement and soaking in SBF for 7 days, all set cement (Figure 4.9) exhibited XRD patterns with no significant difference, revealing the main phases of apatite and β -TCP with other remaining residuals. In addition, the chemical functional group of all starting chitosan fibers from different dry heat sterilized conditions was analyzed using FT-IR technique, as shown in Figure 4.10. It was found that FT-IR peaks of all sterilized chitosan fiber conditions were similar to the control non-sterilized condition.

The effect of dry heat sterilization with different conditions on the properties of apatite/ β -TCP cement, including phase composition, compressive strength, setting time, pH changes, and bioactivity, was investigated. The temperature and holding time of dry heat sterilization are shown in Table 4.1. Morejón-Alonso et al. (Morejón-Alonso, 2007) found that the dry heat sterilization (190 °C, 2 h) did not affect the CDHA and β -TCP contents in the cement, revealing a similar XRD peak between the dry heat sterilized condition and control condition. Their findings were comparable with this current work, presenting no difference in XRD patterns among the conditions of sterilized samples and non-sterilized ones. In addition, each condition of the dry heat sterilization did not affect the phase conversion of apatite/ β -TCP cement, presenting similar XRD patterns (Figure 4.9).

The apatite/ β -TCP cement contained the chitosan fiber (1 wt.%) content in a small concentration, which could be influenced by the high temperature of dry heat sterilization. Therefore, chitosan fiber under various conditions of dry heat sterilization was analyzed using FT-IR analysis. Despite the fact that the early (254.6 °C) and significant (296 °C) decomposition temperatures of chitosan were established (Arora, 2011), some researchers were able to identify chitosan damage with a darker color at higher temperatures (> 120 °) (Lim, 1999). In this current work, the FT-IR peaks of each condition showed a similar trend. Meanwhile, the color of the chitosan fiber became slightly darker when increasing temperature. This aspect of the slight change

in color was related to the previous study (Lim, 1999). They reported that the color of chitosan changed from yellow to brown with the increase in temperature and holding time, which could be due to interchain rearrangement after heat treatment (above 120 °C). However, this feature did not affect the phase composition of apatite/ β -TCP cement in this work.

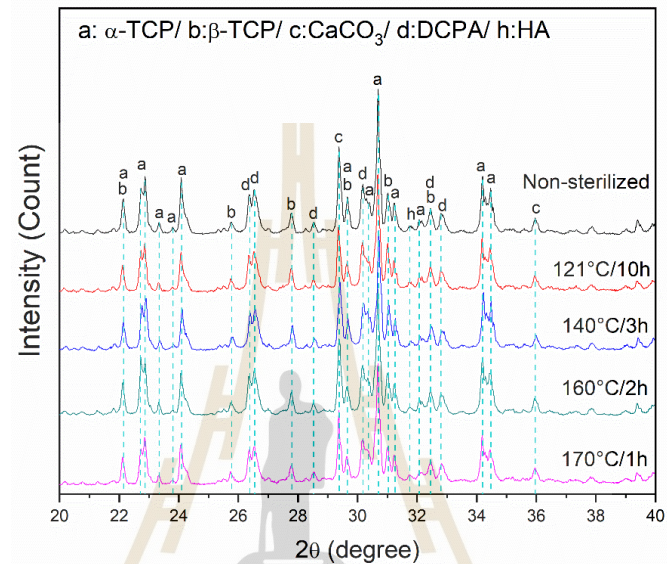


Figure 4.8 XRD patterns of starting cement powder with various dry heat-sterilized conditions.

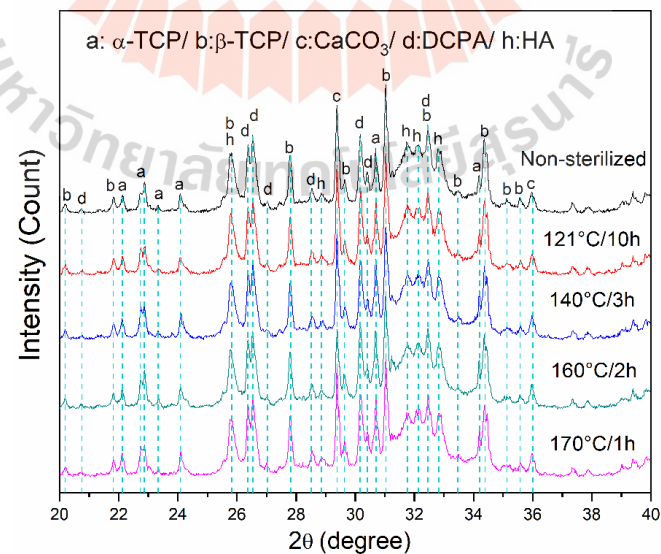


Figure 4.9 XRD patterns of cement with various dry heat-sterilized conditions at L/P ratio of 0.40 after soaking in SBF solution for 7 days.

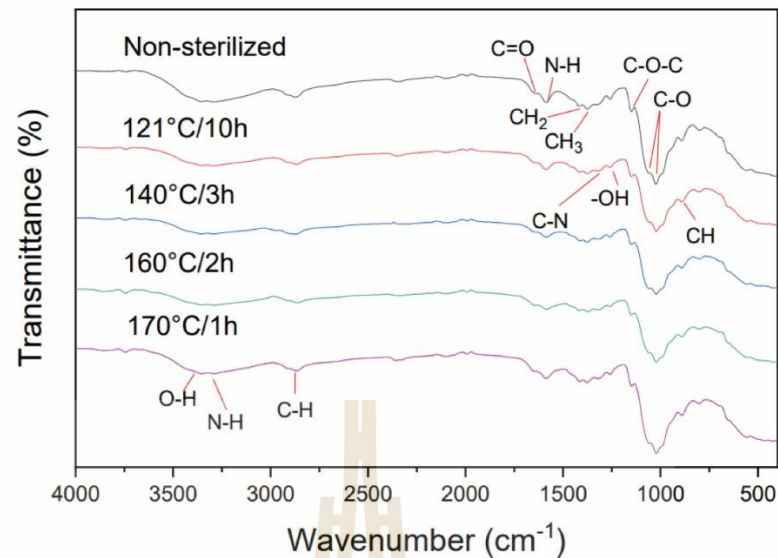


Figure 4.10 FT-IR patterns of chitosan fiber with various dry heat-sterilized conditions, Each band region was referred to previous study (Queiroz, 2014).

4.3.2.2 Compressive strength

After soaking samples in SBF over 7 days, the compressive strength of set cement was measured. The results showed that the compressive strength of 140°C/3h, 160°C/2h, and 170°C/1h cement was significantly lower than that of 121°C/10h and non-sterilized ones. Meanwhile, there was no statistical difference between 121°C/10h and non-sterilized cement condition.

The difference in compressive strength of these cements was not affected by the phase composition due to the fact that the dry heat sterilization from 121 to 170 °C did not influence the phase composition of cement powders or set cements as presented in XRD results. Therefore, the reduced compressive strength of some sterilized samples could be attributed to the decomposition of chitosan fiber content at high temperature (> 121 °C), as witnessed by the previous findings of chitosan decomposition at high temperature (> 120 °) (Lim, 1999). This decomposition feature could result in the lower deacetylation degree of chitosan when increasing temperature (Zawadzki and Kaczmarek, 2010) or holding time (Kim, 2004). Consequently, the reduced deacetylation degree could decrease the mechanical properties of chitosan (Zhuang, 2019, Tavares, 2020). Their findings are related to the

result of the cements containing chitosan fiber in this study, indicating the decreased compressive strength of sterilized cement with higher temperature (>121 °C). Therefore, the 121°C/10h cement condition was selected for further investigation since it maintained a similar compressive strength to the non-sterilized control cement, whereas the strength of other sterilized cements was decreased after dry heat sterilization.

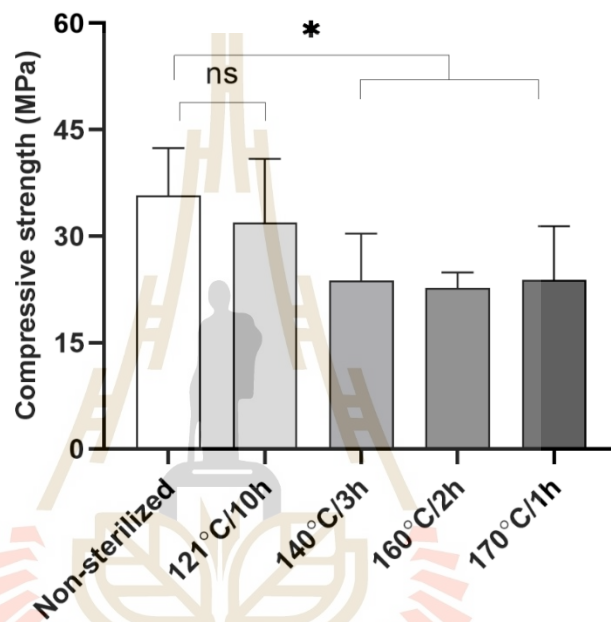


Figure 4.11 Compressive strength of cement with various dry heat-sterilized conditions at L/P ratio of 0.40 after soaking in SBF solution for 7 days.

4.3.2.3 Setting time measurement

As the result of compressive strength, the setting times of selective 121°C/10h cement were measured and compared with the non-sterilized control cement. The result presented that the t_i and t_f times of both non-sterilized control and 121°C/10h cement did not differ significantly.

As a result, there was no difference in setting time between sterilized 121 °C/10h cement and non-sterilized cement in this study. This suggests that the temperature range employed in this study (121 to 170 °C) was more appropriate when compared with the previous work (200 °C) (Takechi, 2004). They discovered that some DCPA content in apatite TTCP/DCPA cement might degrade to

pyrophosphate at a high temperature of 200 °C. Afterward, pyrophosphate retarded the production of apatite, resulting in a prolonged setting time. This discrepancy could be attributed to a difference in temperature or cement formula between the previous and present work.

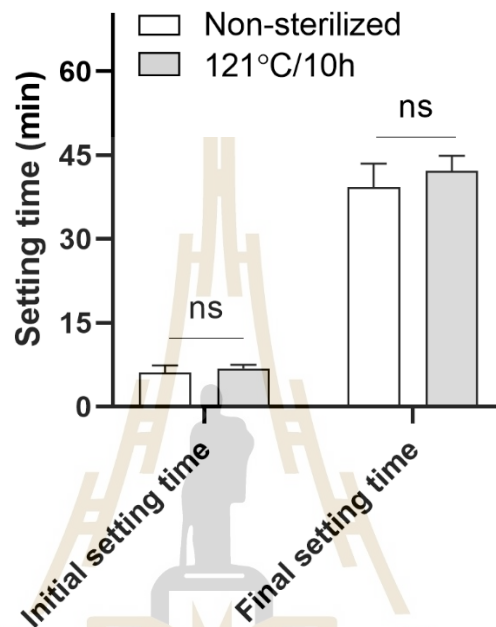


Figure 4.12 Initial and final setting time of cement before and after dry heat sterilization at 121 °C for 10 hours with L/P ratio of 0.40.

4.3.2.4 pH measurement

After soaking both cements in SBF solution for 12 h, the pH of the solution appeared to be more acidic, as indicated in Figure 4.13. The pH trend of both conditions was similar, ranging from 7.45 to 7.32 (Non-sterilized cement) and 7.46 to 7.32 (121°C/10h cement).

As a result, the more basic at the early time point of the incubation could be correlated to the residual from the cement liquid containing Na_2HPO_4 (pH = 8.92) released into the SBF solution. After that, the pH of both cement conditions decreased slightly and became more neutral after 12 hours of incubation, reflecting a more biocompatible range. This could assure that the dry heat sterilization (121 °C, 10 h) did not significantly influence the pH change of the sample.

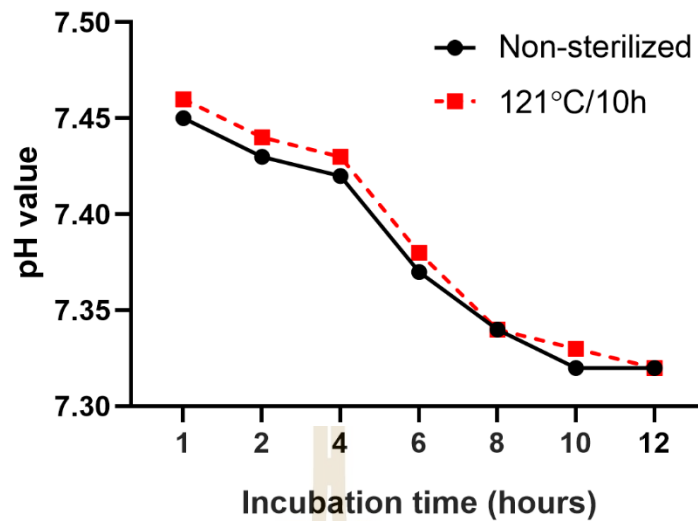


Figure 4.13 pH changes in SBF at different period of time after immersion of both cements (Non-sterilized and sterilized sample)

4.3.2.5 Morphology analysis

Figure 4.14 shows SEM images of the sample surfaces over 7 days of immersion in SBF solution at 37 °C. On the surface of samples, needle-like crystals were observed in both non-sterilized and sterilized 121 °C/10h cements.

Bone-like apatite deposition on the surface of the specimen in SBF solution was used to determine the bioactivity of bioactive materials (Kokubo and Takadama, 2006). This work assured that the dry heat sterilization at 121 °C for 2 h was suitable for this apatite/ β -TCP cement, presenting excellent bioactivity in both sterilized and non-sterilized ones.

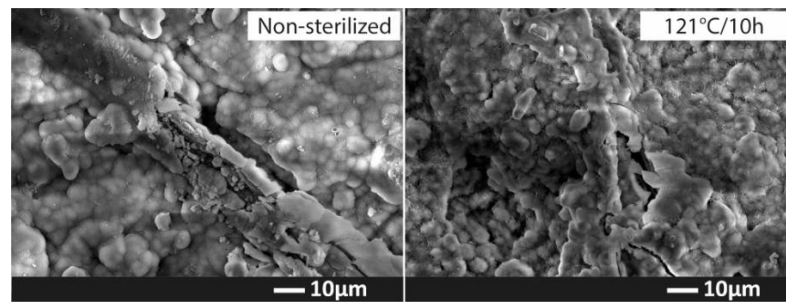


Figure 4.14 SEM micrographs of the surface of the cements (Non-sterilized and sterilized sample) after incubation in SBF solution for 7 days.

4.4 Conclusions

This study presented that the smaller particle size of α -TCP improved the physical properties of apatite/ β -TCP bone cement, including reduced setting time, increased compressive strength, and higher CDHA phase conversion. Afterward, the influence of dry heat sterilization at various temperatures on the physical properties of apatite/ β -TCP bone cement was investigated. The higher temperature from 121 to 170 °C did not affect the phase composition of either the starting powder or the set cement for 7 days in the SBF solution. Although there was no significant difference in FT-IR peaks of each condition, the color of chitosan fiber became darker after dry heat sterilization, representing the decomposition of chitosan. Thus, this damage to chitosan at higher temperatures (> 121 °C) resulted in a decreased compressive strength. However, the sterilized condition at 121 °C for 10 h still presented similar results of compressive strength, setting time, pH changes, and bioactivity with respect to the control non-sterilized cement. As a result, this suggests that dry heat sterilization (121 °C, 10 h) could be effectively used as an alternative method for sterilization of the apatite/ β -TCP cement or other materials with similar characteristics.

CHAPTER V

EFFECT OF POLYACRYLIC ACID/DISODIUM HYDROGEN PHOSPHATE MIXTURE ON APATITE/ β -TCP CEMENT

This chapter has investigated the effect of combination of new liquid phase mixture of disodium hydrogen phosphate (Na_2HPO_4) and polyacrylic acid (PAA) on the compressive strength, setting time, bioactivity, and cytotoxicity of apatite/beta-tricalcium phosphate (β -TCP) cement. The PAA was known as one of water-soluble and biocompatible polymers to improve the mechanical performances of the bone cement, but it usually inhibits the phase conversion to hydroxyapatite after the cement has already set. The aim of this work was to evaluate the incorporation of the mixture of PAA and Na_2HPO_4 into apatite/ β -TCP cement. It was found that the crucial concentration for adding PAA/ Na_2HPO_4 at 30:70 v/v% to enhance the mechanical strength, cell viability and maintain bioactivity. The phase composition and crosslinking reaction between PAA and alpha-tricalcium phosphate (α -TCP) powder was detected by XRD and FTIR techniques. The β -TCP was added in the formula to achieve the biphasic cement, which composed of β -TCP and Apatite/Calcium Deficient-Hydroxyapatite in the final product. The biphasic granule commercial product was used as comparison in the cell viability test. This work had been confirmed that the cement was a non-toxic material. Therefore, these results suggest that the PAA/ Na_2HPO_4 could be beneficial for further clinical applications.

5.1 Research background, rationale, and significance

The self-setting calcium phosphate bone cements have been extensively investigated for decades, due to their distinguished properties for use in biomedical applications (Dorozhkin, 2017). This material could be simply prepared by mixing a variety of solids with liquid phases. The cement paste was obtained by the dissolution of the starting powder in the solution, it then hardened by the re-precipitation and

allowed crystal growth respectively (Ginebra, 2008, O'Neill, 2017). This bone cement was theoretically classified in two groups of different final cement products, Apatite and Brushite. The apatite cement produced the hydroxyapatite (HA) or Calcium deficient-HA (CD-HA), which is similar to the bone mineral compounds (O'Hara, 2014). This feature was the advantage of the apatite cement, which was effectively compatible with the bone tissue (Wagh, 2016).

Although the calcium phosphate cement was outstanding in biological properties, its mechanical properties became the weakness for the orthopedics (Habraken, 2016). In consideration of the porosity, the brushite cement generally presented the lower strength when compared with apatite cement (Dorozhkin, 2008). There are many other factors that can affect the mechanical properties, such as the precursor composition, particle size distribution, liquid phase (Zhang, 2014), etc. To improve the mechanical properties, the addition of polymer in the calcium phosphate cement has revealed excellent results (Mickiewicz, 2002, Canal and Ginebra, 2011). The strategies of using polymer as the cement reinforcement were presented by both processes, the polymer in the solution or solid form mixed with cement powder (Xu, 2000, Geffers, 2015).

PAA is one of the aqueous soluble polymers which has been widely used in medical applications (Kadajji and Betageri, 2011). It was reported that the PAA doped calcium phosphate cement could improve the mechanical properties and the setting reaction due to the crosslinking reaction between the functional group of PAA and the precursor (Khashaba, 2010). Furthermore, some researchers (Majekodunmi, 2003, Majekodunmi and Deb, 2007) have studied the influence of PAA doped apatite cement based on the starting powder of tetracalcium phosphate/dicalcium phosphate (TTCP/DCPA). However, it has been reported that the addition of PAA in cement could inhibit the HA phase conversion (Miyazaki, 1993). They reported that less HA conversion was detected after setting for 1 month. The Na_2HPO_4 has been used to accelerate the setting time of the apatite cement based on the main phase of α -TCP powder (Ginebra, 1995, Khairoun, 1997, Khairoun, 1998), and TTCP/DCPD powder (Komath, 2000). Chow et al (Chow, 1999) reported that the HA formation in cement incorporated with Na_2HPO_4 solution was faster than that of cement mixed with water. It could be due to

the presence of more phosphate ions in the solution reacted with the cement powder, resulting the increasing rate of HA formation, and shortening setting time. However, the amount of Na_2HPO_4 could affect to the compressive strength of bone cement. To optimize the properties of bone cement for medical application, the combination of PAA and Na_2HPO_4 mixture was studied in terms of setting mechanism and phase analysis.

In this study, the cement solution comprised of Na_2HPO_4 and PAA at various ratios was studied. Both reagents were used for enhancing the properties of apatite/ β -TCP cement, such as setting time, mechanical properties, etc. The Na_2HPO_4 has been frequently used as one of the liquids for the apatite cement in terms of monophasic, biphasic, and multiphasic systems for many years. This chemical was demonstrated to activate the setting reaction, which provided the calcium-deficient hydroxyapatite (CD-HA) precipitation as a final product of cement (Fernández, 1994). To reach the properties of calcium phosphate cement for clinical requirements, this study was examined the optimal condition from the range of PAA and Na_2HPO_4 mixtures, incorporated with this calcium phosphate cement based on α -TCP with other precursors. This formula consisted of β -TCP content for improving the biodegradability after setting as converted to HA and β -TCP for the biphasic calcium phosphate cement. From the previous result, the complete setting reaction has reached to be biphasic calcium phosphate (β -TCP+ HA) after 3 months (Rattanachan, 2020). However, the multiple phases had still found including α -TCP, DCPA, β -TCP, calcium carbonate (CaCO_3), and precipitated hydroxyapatite (PHA) as the residuals from the starting powder after the cement setting for 7 days.

5.2 Experimental procedure

5.2.1 Cement liquid preparation

The liquid phase of cement was the mixture of PAA ($M_w = 100,000$, Sigma Aldrich) and Na_2HPO_4 (Merck) at various concentration, as shown in Table 5.1. The 10 w/w% PAA solution was mixed with 1M Na_2HPO_4 for 10 min using magnetic stirrer, the mixed solutions were stored at room temperature. The pH value of the solution was measured by using an electrolyte-type pH meter (Denver pH/mV/Temp. Meter, UB-10).

Table 5.1 The mixture of cements liquid comprising of the different ratio of PAA and Na_2HPO_4

Conditions	Liquid(%v/v)		pH value
	10%w/w PAA	1M Na_2HPO_4	
0PAA	0	100	8.87
10PAA	10	90	7.38
20PAA	20	80	6.70
30PAA	30	70	6.34
40PAA	40	60	5.78
50PAA	50	50	5.33

5.2.2 Preparation of cements

The cement powder consisted of two main components, β -TCP/apatite at a weight ratio of 1:5. The apatite component consisted of 62.5 wt.% α -TCP, 26.8 wt.% DCPA, 8.9 wt.% CaCO_3 , and 1.8 wt.% precipitated hydroxyapatite (PHA), as followed the topic 3.2.3.1 of Chapter III. The cement powder was homogenously mixed with cement liquid (Table 5.1). In this work, the L/P ratios of 0.35-0.4 were suitable to handle this cement. Thus, the setting time and compressive strength were evaluated for the L/P ratio in the range of 0.35 and 0.4. The cement pastes were packed into the cylindrical mold size diameter of 6mm and height of 12 mm for compressive strength testing. Another set of samples was prepared in the same size of mold, followed by cutting for 3 pieces (6 mm diameter, 4mm height) for bioactivity and pH measurement. All samples were incubated at 37 °C under 100% humidity for 24 h before the test mentioned above, to avoid some incomplete reaction of the sample before soaking in simulated body fluid (SBF).

5.2.3 Properties testing and characterization of cement

Setting time, phase composition (XRD, Rietveld refinement), FT-IR, compressive strength, and bioactivity of cement were performed using the same protocol as followed topic 3.2 of Chapter III. The pH measurement was tested in accordance with topic 4.2.2.3 of Chapter IV.

5.2.4 Cell viability

The cement powder was sterilized by dry heat sterilization at 121 °C for 10 h. The cement liquid was sterile by membrane filtration (0.22 µm sterile filter). The specimens were molded into the cylindrical shape with a diameter of 2 mm and 12 mm in height. After 30 min, the sample were immersed in culture medium consisting of 44 v/v% Dulbecco's Modified Eagle Medium (DMEM (1X) from Invitrogen, USA), 44 v/v% F-12 Nutrient mixture (HAM form Invitrogen, USA), 10 v/v% Fetal Bovine Serum (FBS from Invitrogen, USA) 1 v/v% L-glutamine and 1 v/v% Penicillin streptomycin (Invitrogen, USA) for 7 days, the medium solution was changed every day. The precondition medium at 1, 2 and 7 days was collected, and stored in the fridge at 4 °C for subsequent experiment including cell viability by MTS assay. The standard surface area to exact liquid volume ratio conditions were fixed at 1.25 cm²/ml. The biphasic granules (60 wt.% HA and 40 wt.% β-TCP) from the commercial (KYERON, Netherlands) was used to compare in this study, the ratio of extract medium was 0.1 g/ml, followed ISO 10993. NIH/3T3 fibroblast cell line (NIH 3T3) was used as cell model for checking the cytotoxicity of the cement samples. NIH 3T3 fibroblast cell with 3x10³ cells were seeded into each well of 96-well plate and cultured in 37 °C, 5% CO₂ incubator for 24 h. The culture medium was removed and replaced with 100 µl precondition medium from each cement samples, then cultured in 37 °C, 5% CO₂ incubator for another 24 h. After incubation for 24 h, 20 µl MTS solution (The CellTiter 96® AQueous One Solution Cell Proliferation Assay, Promega) was added into each well of the 96-well assay plate containing 100 µl precondition medium and then incubated in 37 °C 5% CO₂ for 2 h. The optical density value at the absorbance of 490 nm was measured. The results were compared with the control medium. The percentage of cell viability was measured according to the equation 5.1, as shown below

$$\% \text{ cell viability} = \frac{\text{O.D value (exact of tested sample)}}{\text{O.D value of control (Control medium)}} \times 100 \quad (5.1)$$

5.2.5 Statistical analysis

GraphPad Prism 8 was used to investigate the results presented as mean \pm standard deviation. The statistical comparisons of Setting time, Compressive strength, and Cell viability were performed by Two-way ANOVA coupled with Tukey's multiple comparison test. All results were statistically considered with the confidence interval of $p < 0.05$.

5.3 Result and discussion

5.3.1 Phase composition

In order to examine the effect of PAA doping on the reaction and phase composition of this cement, the X-ray diffraction was used to observe, as shown in Figure 5.1 and 5.2. The XRD patterns from the results corresponded to the data sheet number 09-0432 (HA), 09-0169 (β -TCP), 09-0348 and 29-0359 (α -TCP), 70-0359 (DCPA), and 47-1743 (CaCO_3) of the powder diffraction standards. After the compressive strength testing, the broken samples were finely ground before analysis. XRD analysis indicated that some of the α -TCP phase converted to hydroxyapatite phase but some of the other phases in the starting powder had remained after immersion in SBF solution for 1 week. At 0-40 v/v% PAA, the reaction of hydroxyapatite formation still occurred but there was no change at 50 v/v% PAA, as compared with the dried starting precursors.

In this work, the cement incorporated with PAA could convert most of α -TCP to hydroxyapatite after 1 week. This was compared with the starting powder. Moreover, the XRD peak of cements was estimated quantitatively by Rietveld refinement (Figure 5.3). In preliminary study, we found that the XRD result (Figure 5.1) showed poor phase conversion from α -TCP to CD-HA after 7 days of immersion for samples including 60-100PAA. Therefore, the concentration of PAA in range of 0-50 v/v% was selected to investigate in the further experiment, as shown in Figure 5.2. The

result presented the phase transformation of α -TCP powder converted to hydroxyapatite after the sample was immersed in SBF solution for 1 week. Figures 5.1 and 5.2 show that there were no significant differences from 0-40 v/v% PAA which confirmed the transformation of the sample to hydroxyapatite. In contrast, the amount of hydroxyapatite was dramatically lower at 50 v/v% PAA, which was similar with that of the starting cement powder.

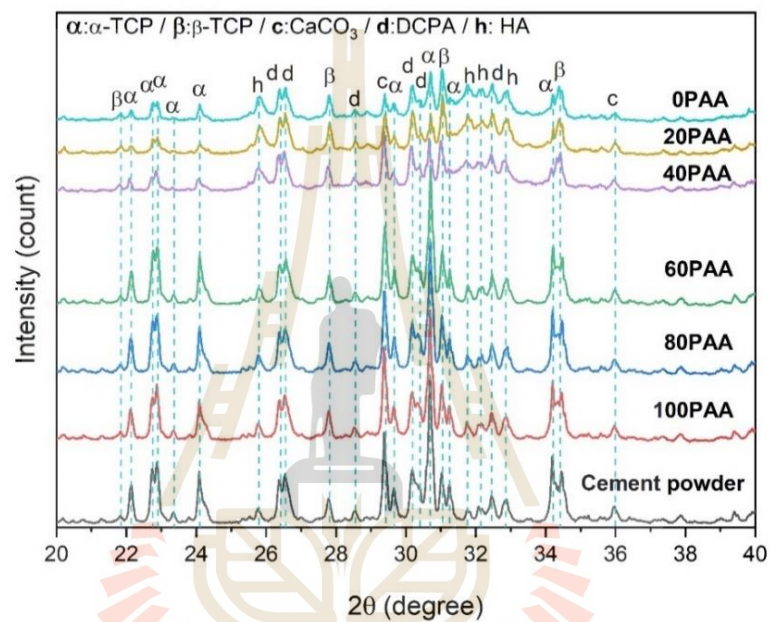


Figure 5.1 XRD patterns of the bone cement containing of the different PAA contents (0-100PAA) at 0.35 L/P ratio after soaking in SBF solution for 7 days.

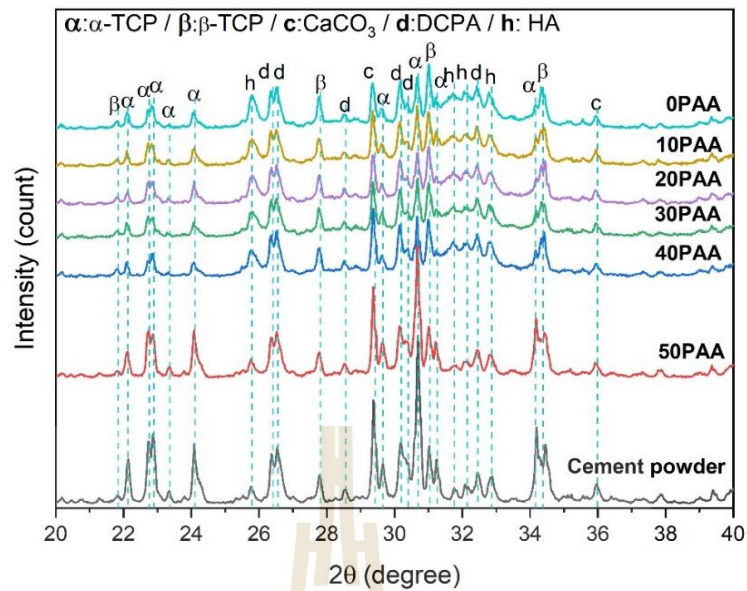


Figure 5.2 XRD patterns of the bone cement containing of the different PAA contents (0-50PAA) at 0.35 L/P ratio after soaking in SBF solution for 7 days.

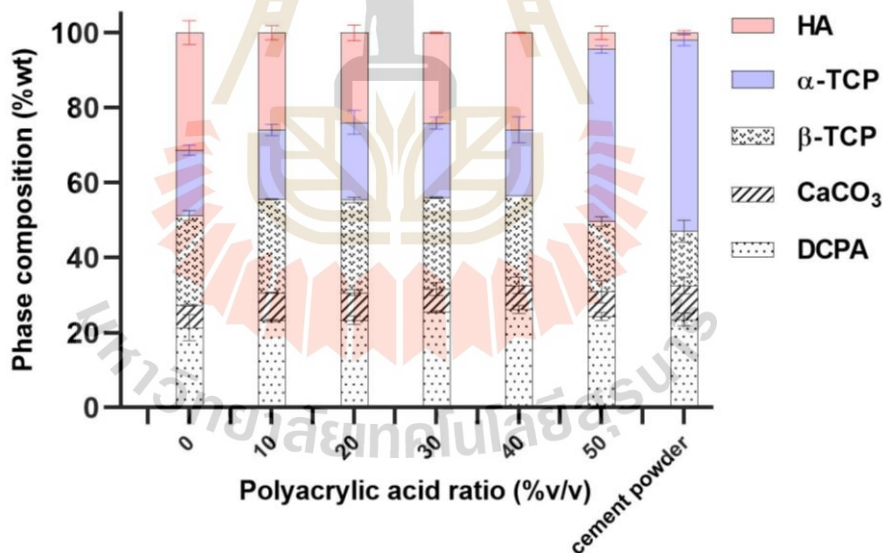


Figure 5.3 Percentage of Phase composition after immersion of cement (0.35 L/P ratio) in SBF solution for 7 days using Rietveld refinement analysis.

5.3.2 Chemical functional group analysis

From XRD pattern of the phase composition of cement after soaking in SBF for 1 week, the results indicated some important feature of cement interaction with the addition of PAA. However, this cement system required more essential

evidence to confirm the reaction between the precursor and the PAA. After XRD analysis was completed, the fine ground cement powder was analysed using FT-IR. Figure 5.4 and 5.5 display the FT-IR spectra of cement at 0.35 L/P ratio after soaking in SBF solution for 7 days. From the previous study (Kolmas, 2015), the researcher revealed the peaks of standard α -TCP powder at 548, 581, 1024, and 1036 cm^{-1} , etc. Since the spectra of 50PAA cement showed at the bands of 550, 580, 1025, and 1037 cm^{-1} , the FT-IR peaks of 50PAA could be considered as similar to the starting powder and indicated as the remaining α -TCP. In contrast, the visible bands of hydroxyapatite formation were found at 0-40 v/v% PAA. The 50 v/v% PAA displayed the more intense peak of calcium polyacrylate band at about 1568 cm^{-1} than that of other cement conditions which were observed. This related to the result in (Watson, 1999).

The reaction of PAA in the apatite cement (TTCP/DCPA) (Majekodunmi, 2003) has been reported via both neutralization and chelation reaction, this is similar to glass ionomer or zinc polycarboxylate cements. The neutralization occurred by the dissociation of the hydrogen ions from polyacrylic acid which react with the calcium phosphate starting powder, thus enhancing the dissolution, and releasing calcium ions. These are followed by cross linking reaction resulting in the formation of a poly acrylate network. In the previous works (Verma, 2006, Shen, 2011), the peak at 1567 and 1580 cm^{-1} were assigned to the symmetric stretching vibration modes of protonated carboxylate groups, showing the reaction between COO^{-1} of PAA and Ca^{2+} of hydroxyapatite particle. This could be attributed to the crosslink reaction between Ca^{2+} and COO^{-1} in the cement of 0-50 v/v% PAA around 1568 cm^{-1} in this work. This could be proved that there was some amount of crosslink reaction in the cement at 0-50 v/v% PAA. Nevertheless, the researcher (Chen, 2012) reported that calcium carboxylate salt appeared at the peak 1570 cm^{-1} in apatite cement based on the TTCP/HA system. This peak distinctly indicated the reaction between TTCP and PAA, which it partially converted to HA after it was stored in 100% humidity at 37 °C for 7 days.

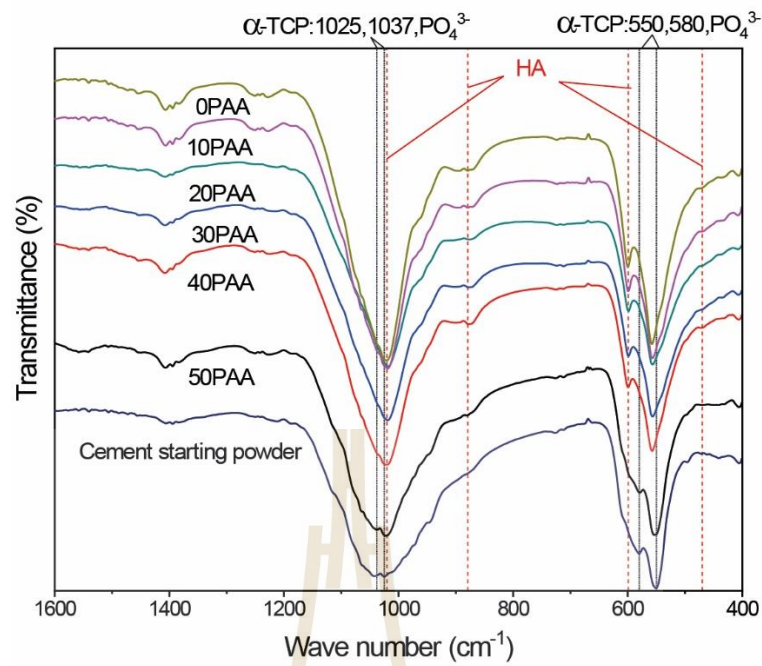


Figure 5.4 FT-IR patterns of the bone cement containing of the different PAA contents at 0.35 L/P ratio.

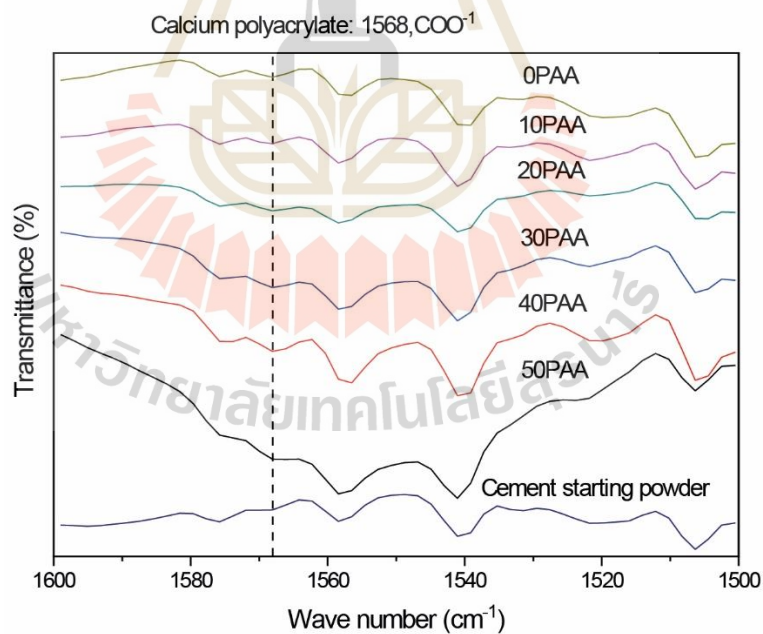


Figure 5.5 Enlarge FT-IR patterns of the bone cement containing of the different PAA contents for wavelength of 1500-1600 cm^{-1} .

5.3.3 Setting time measurement

The results determined that the addition of PAA significantly influenced the initial and final setting time of this cement system, as shown in Figure 5.6. 10 w/w% PAA was mixed with 1M Na₂HPO₄ at different concentrations, represented as a liquid phase. The higher concentration of PAA aqueous solution reduced the pH value of cement liquid, as shown in Table 5.1. The setting time trended to decrease with the increasing of PAA at the ratio of 0-30 v/v%. However, it slightly increased at 40 v/v% and finally decreased again at 50 v/v%. This trend appeared at both initial and final setting in two different L/P ratios of 0.35 and 0.4 ml/g, respectively.

The setting reaction of cement was the dissolution of α -TCP reacted with both the aqueous solution of PAA and Na₂HPO₄. The cement powder released Ca²⁺ and PO₄³⁻ ions during the dissolution. Those ions from the starting powders would combine with PO₄³⁻ ions from Na₂HPO₄, followed by the nucleation of crystal as the cement hardened (Burguera, 2006). The Na₂HPO₄ was a common ion effect reagent for the faster setting time in the early hardening stage (Fernández, 1994, Khairoun, 1997), but it could slightly lower the strength compared with the cement using the solution without the accelerator (Ginebra, 1994). However, the transformation of HA in the apatite cement based on α -TCP cement has been explained in the following hydrolysis reaction (Yubao, 1997), as presented in equations (5.2-5.5).



Furthermore, the surface of the precursor could react with the COO⁻ functional group of PAA to form the cross-linking reaction. Khashaba et al. (Khashaba, 2010) revealed the setting reaction between cement powder and carboxylic group (P-

COOH). In this similar aspect, it could be assumed in the following equations (5.6-5.7) where P-COOH represents PAA.



Equation 5.7 shows that the functional group of PAA reacted with Ca^{2+} from the starting powder. The higher concentration of COO^- would interact with released Ca^{2+} from the Equation 5.2. This feature could reduce the HA conversion. Moreover, the increasing of PAA concentration in the liquid phase appeared more acidic which was measured in Table 1. According to the solubility diagram of calcium orthophosphate or calcium phosphate salt (Chow, 2001), the lower pH of cement liquid could affect the dissolution of cement powder. The setting reaction of apatite cement was started from the hydrolysis of α -TCP powder, which provided Ca^{2+} and PO_4^{3-} ions, as shown in Figure 5.7. The intense ions led to the faster precipitation of HA, showing in terms of a faster setting time. This study was similar to the previous work. Watanabe et al. (Watanabe, 2005) studied the addition of PAA aqueous solution with various concentrations from 10-25 wt.% into cement based on α -TCP compared with TTCP. They showed that the setting times of cement based on α -TCP decreased with increasing PAA concentration from 10-25%. Their findings are relevant to the results of this study that showed a decreased setting time of PAA (10-50 v/v%) incorporated cement. At 10-30 v/v% PAA concentration, they could facilitate the particle distribution in the cement paste during the setting reaction. However, the higher concentration of PAA (40-50v/v%) could increase the viscosity of liquid. This higher viscosity could possibly result in the lower mobility of Ca^{2+} ions dissolved in solution (Majekodunmi and Deb, 2007). This lower mobility of ions could be attributed to poor solubility. Consequently, the setting times of 40 and 50 v/v% PAA were slightly higher than 30 v/v% due to the lower solubility of starting powder. Herein, 30 v/v% PAA was an optimum concentration, showing a shortest setting time with respect to other conditions.

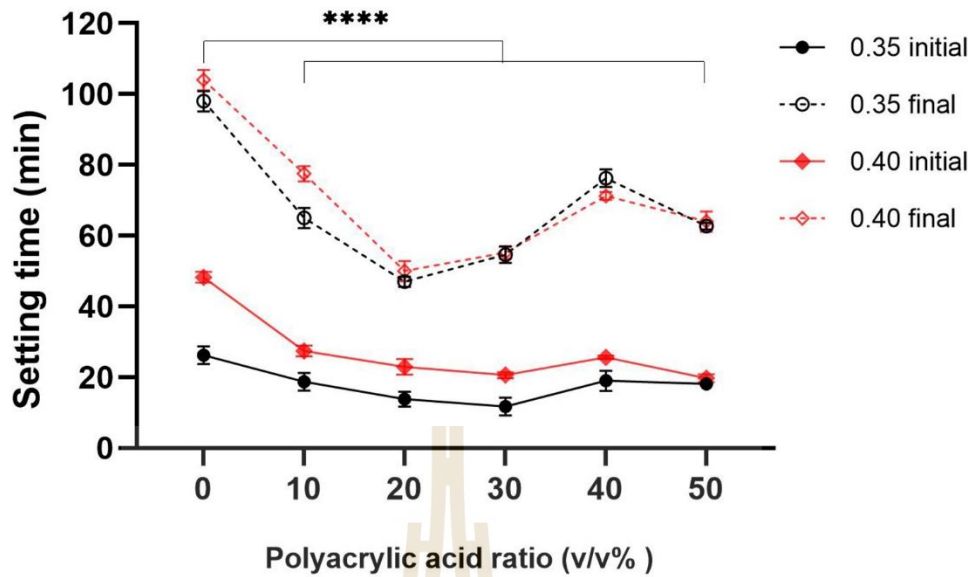


Figure 5.6 The relationship between the setting time of bone cement with the content of PAA with the L/P ratio of 0.35 and 0.4, respectively (**** $p < 0.0001$).

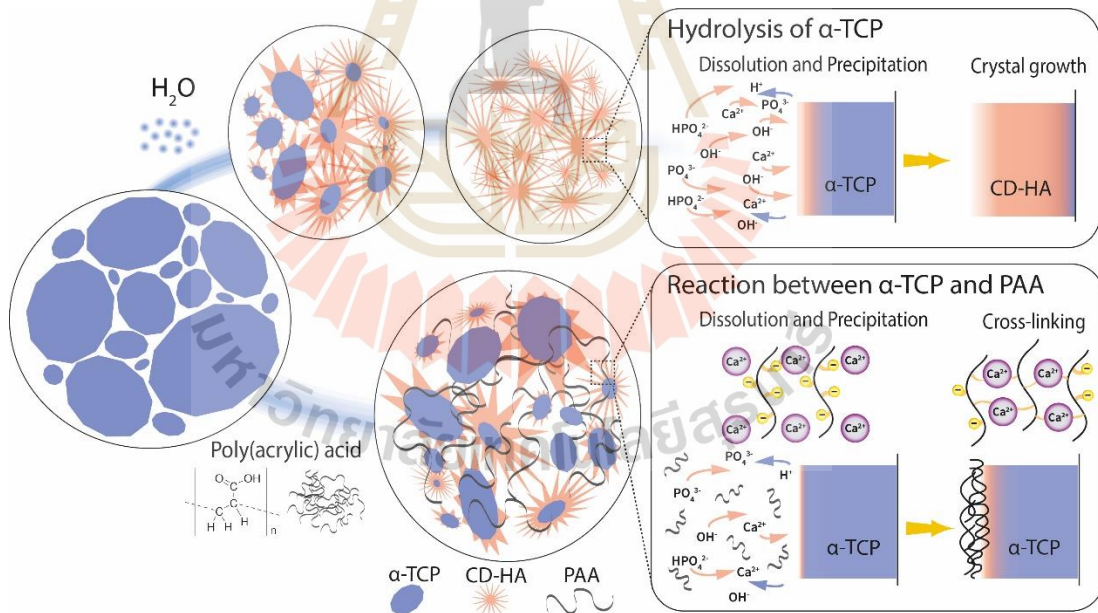


Figure 5.7 Setting mechanism and phase conversion of apatite cement based on α -TCP powder, interacted with aqueous solution and PAA.

5.3.4 Compressive strength

Figure 5.8 displays the results of the mean compressive strength of sample cements at different concentrations of PAA aqueous solution in the liquid phase mixture. The cement liquid was blended with cement powder in L/P ratio of 0.35 and 0.4 ml/g, respectively. There was no significant difference in compressive strength at 0, 10, 20 v/v% PAA. The highest compressive strength in this experiment was found at 30 v/v% PAA, then decreased at 40, and 50 v/v% PAA, respectively. At 30 v/v% PAA, the compressive strength of both L/P ratios of 0.35 and 0.4 ml/g (40.3 ± 5.9 MPa, 36.4 ± 4.3 MPa) were significantly higher than that of other concentrations. This ratio (30 v/v% PAA) was revealed to be the optimum point of these two reagents combined in cement liquid, which provided the higher compressive strength in this cement system.

There are various parameters to improve compressive strength of calcium phosphate cement, such as composition of cements, additives, particle sizes, liquid to powder ratio (L/P), (Zhang, 2014) etc. In this study, the GraphPad Prism 8 was used to determine statistically the main effect of each parameter on the samples, the performance of the concentration ratio of PAA in liquid phase and the two different L/P ratios on this calcium phosphate cement system were investigated. Both parameters were significant factors ($P < 0.05$), which influenced the compressive strength of the sample. However, the most significant parameter was PAA concentration (P-value is 0.001), as compared with L/P ratio (P-value is 0.0027).

The trend in these results was similar to some conditions of (Majekodunmi and Deb, 2007), which reported that the crosslinking reaction of this cement improved the compressive strength by adding 20 w/v% PAA, resulting the best condition. Kodera et al. (Kodera, 2005) also presented that the addition of PAA into cement could improve the compressive strength. They reported that polyacrylic acid would ionize in the solution and then produced positive and negative ions that neutralized the charges presenting on the surface of α -TCP particles. This aspect is related to the reaction between PAA and α -TCP powder (Figure 5.7), which could enhance compressive strength by crosslink reaction in this current work. However, the addition of PAA at 40 and 50 v/v% in the liquid solution reduced the compressive

strength due to the excessive concentration of PAA which interrupted the setting reaction. In these cases, the PAA would encapsulate the insoluble α -TCP particles. This feature could relate to a reduction in the release of Ca ions, forming less of the crosslinking reaction between the boundary of each particle.

Besides enhancing the mechanical properties reported from another work, the brittle/ductile property was also adjusted by the addition of PAA incorporated with tartaric acid into apatite cement (TTCP/DCPA system) (Chen, 2008). The researcher reported that PAA was added to 25 wt% causing a dramatic change of compressive strength as compared with the lower concentrations (5 wt%, and 11 wt% PAA). However, the desired final product of apatite cement was also inhibited by PAA blocking the acid-based reaction of TTCP/DCPA starting powder.

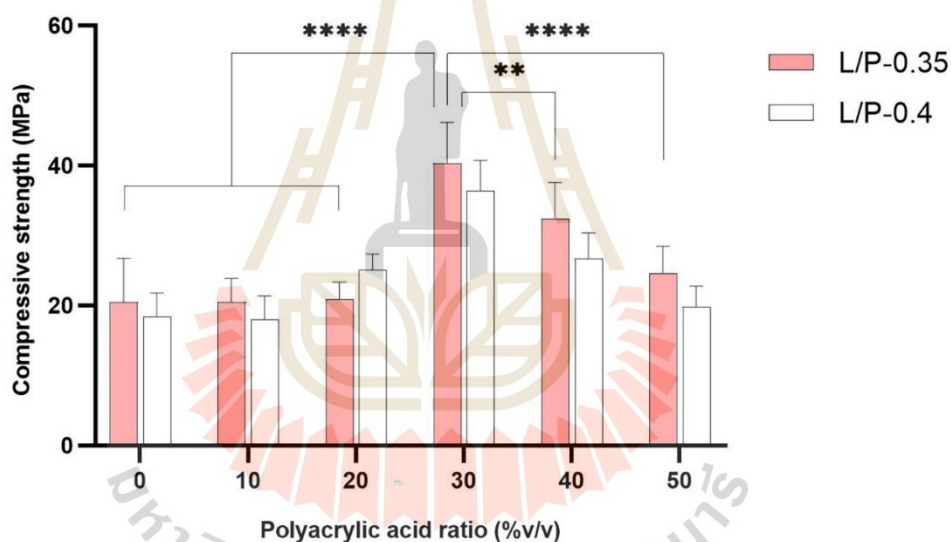


Figure 5.8 Compressive strength of the bone cement containing of the different PAA contents with L/P ratio of 0.35 and 0.4 mL/g Mean \pm SD, n = 9 replicates. (**p < 0.01 and ****p < 0.0001).

5.3.5 pH measurement and *in vitro* bioactivity

The pH changes of SBF after soaking the bone cement samples as shown in Figure 5.9 indicated that the pH in the range of 7.33-7.46 provided for biocompatibility. The pH change was similar among all sample conditions. After the samples soaking in SBF with the initial pH of about 7.39, the pH of 0-50PAA samples slightly rose up to approximately 7.44 - 7.47 after 12 h and dropped to around 7.32 -

7.36 at 24 h. The pH range eventually reached to neutral range of 7.35 - 7.39 after 72 h.

The pH change in this study was similar to the previous works (Oliveira, 2015), in which they reported that the increase in pH resulted in the supersaturation of SBF solution. This aspect could provide the precipitation of an HA-like layer on the surface of the sample, as shown in Figure 5.10.

The deposition of the HA layer on the surface of materials has been monitored as evidence of bioactivity after soaking the sample in SBF solution for different periods of time (Morejón-Alonso, 2012). Figure 5.10 presents the SEM micrographs of the sample surface after immersion in SBF at 0 and 7 days. Before immersion in SBF, the samples of all conditions presented no appearance of any tiny particles precipitation as shown in Figure 5.10 (a-f). In contrast, the needle-like particles were seemingly presented on the sample surfaces of 0-30PAA (Figure 5.10 (g-j)) after immersion for 7 days while there were no needle-like particle formations on the surface of 40-50PAA samples as presented in Figure 5.10 (k-l). Furthermore, the SEM results could be supported by EDS analysis on sample surface after immersion for 7 days as shown in Table 5.2. From EDS result at day 0, the Ca/P ratio was not significantly different for all samples. After soaking in SBF for 7 days, the Ca/P ratio on the sample surface of 0-30PAA was 1.55-1.69. In addition, these Ca/P ratios of sample surface (0-30PAA) were higher than that of the set cement (0-50PAA) in the range of 1.40-1.47 according to the phase compositions result in Figure 5.3. It can be indicated that CD-HA was precipitated on the 0-30PAA sample surface after soaking in SBF for 7 days. Besides, the Ca/P ratio of 40-50PAA showed no significant difference between 0 and 7 days. This could be considered that the CD-HA particles precipitated on the sample surface of 0-30PAA after soaking in SBF for 7 days.

The addition of PAA to cement has significantly influenced on the setting reaction, compressive strength, and bioactivity, as shown in Figure 5.11. The setting time reduced due to the higher dissolution of α -TCP in the solution with a lower pH. Nonetheless, the setting time can slightly increase if the PAA concentration is too high, as described above. The PAA also interacted with the starting powder which formed the crosslink reaction, increasing the compressive strength. However, the strength

could also decrease if the amount of PAA is immoderate. Furthermore, this could reduce and interfere with the HA phase transformation because the surface of starting powder was covered by PAA, leaving more unreacted powder in the sample. Nevertheless, the increasing of PAA appeared to reduce the bioactivity because less HA crystals were detected on the surface of the cement. As a result, the surface of the sample was not able to release and exchange ions in the SBF solution in order to establish HA crystals on the sample. Therefore, the dissolution of the sample would control the exchange of ions, causing more or less of apatite crystal deposition on the material surface (Lu, 2018).

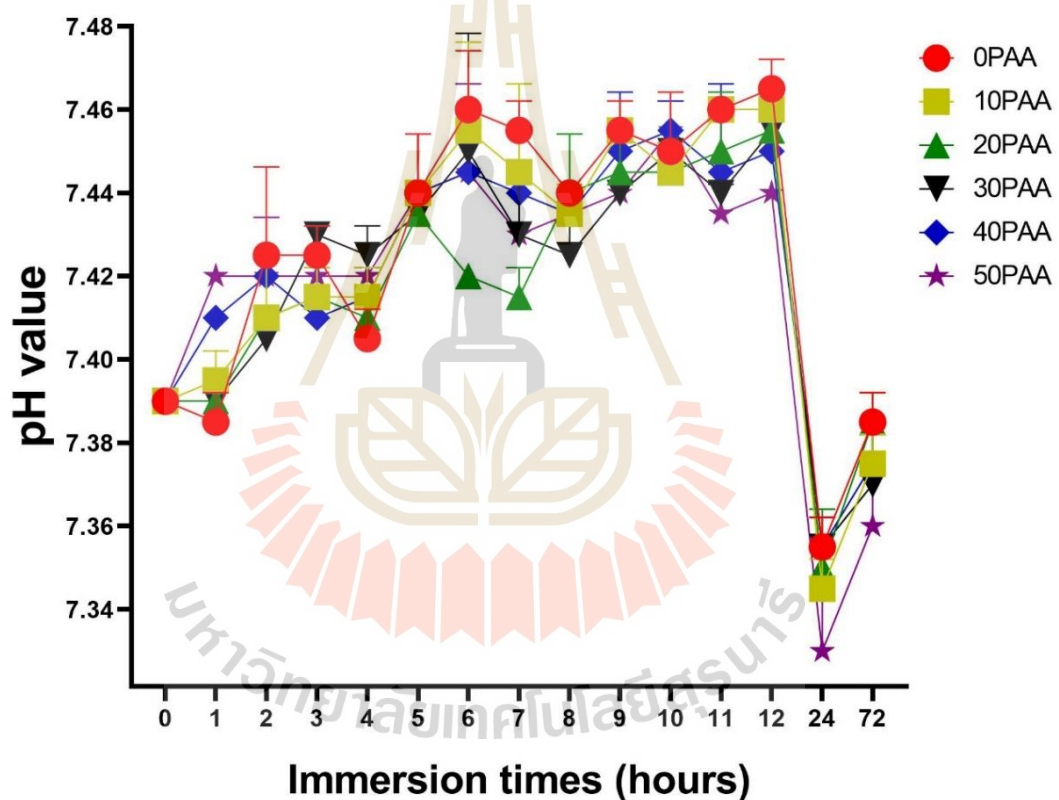


Figure 5.9 pH change of SBF in a period of time after immersion of bone cement samples with the different of PAA contents.

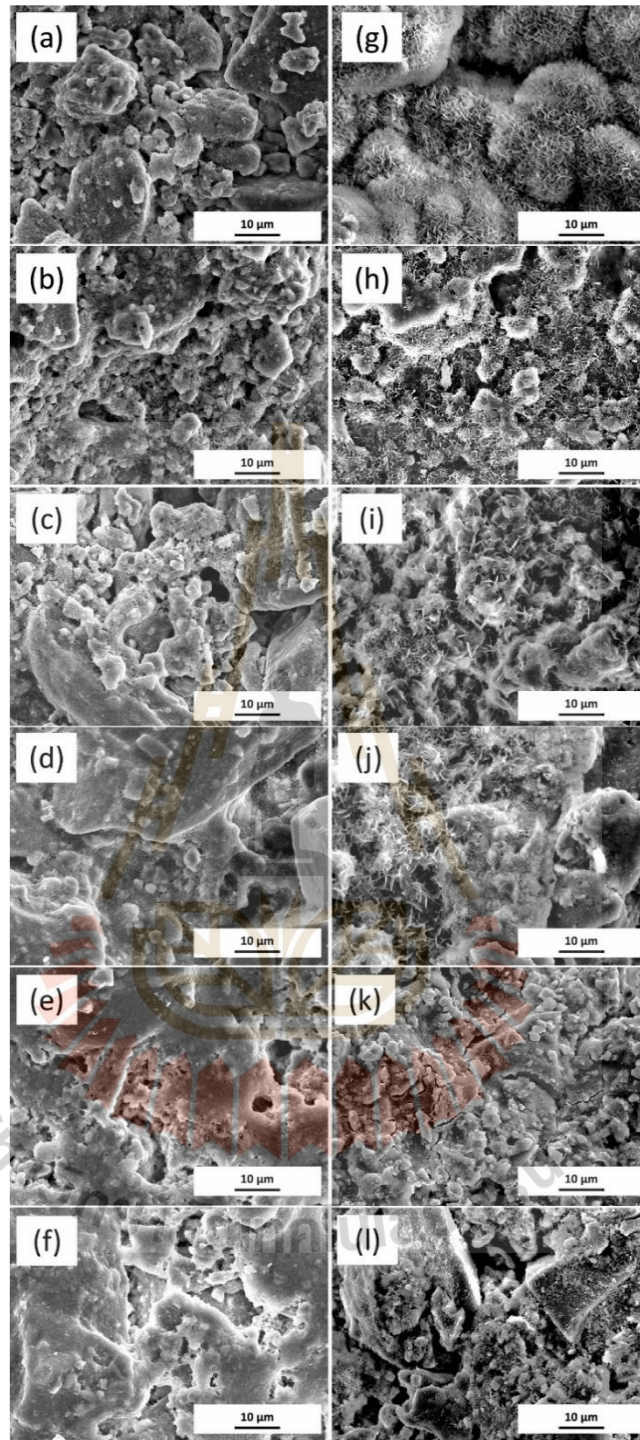


Figure 5.10 SEM micrographs of the surface of the bone cements with different PAA concentrations from 0-50 v/v%, (a) 0PAA, (b) 10PAA, (c) 20PAA, (d) 30PAA, (e) 40PAA, (f) 50PAA as prepared before soaking in SBF (day0). Sample surface of (g) 0PAA, (h) 10PAA, (i) 20PAA, (j) 30PAA, (k) 40PAA, (l) 50PAA soaked in SBF for 7 days.

Table 5.2 EDS analysis of Ca/P mole ratio of sample surface at 0, 7 days of immersion.

Cement condition	Ca/P ratio	
	Day 0	Day 7
0PAA	1.40 ± 0.05	1.69 ± 0.12
10PAA	1.46 ± 0.03	1.65 ± 0.01
20PAA	1.32 ± 0.03	1.64 ± 0.06
30PAA	1.41 ± 0.03	1.55 ± 0.02
40PAA	1.41 ± 0.03	1.48 ± 0.06
50PAA	1.39 ± 0.00	1.38 ± 0.00

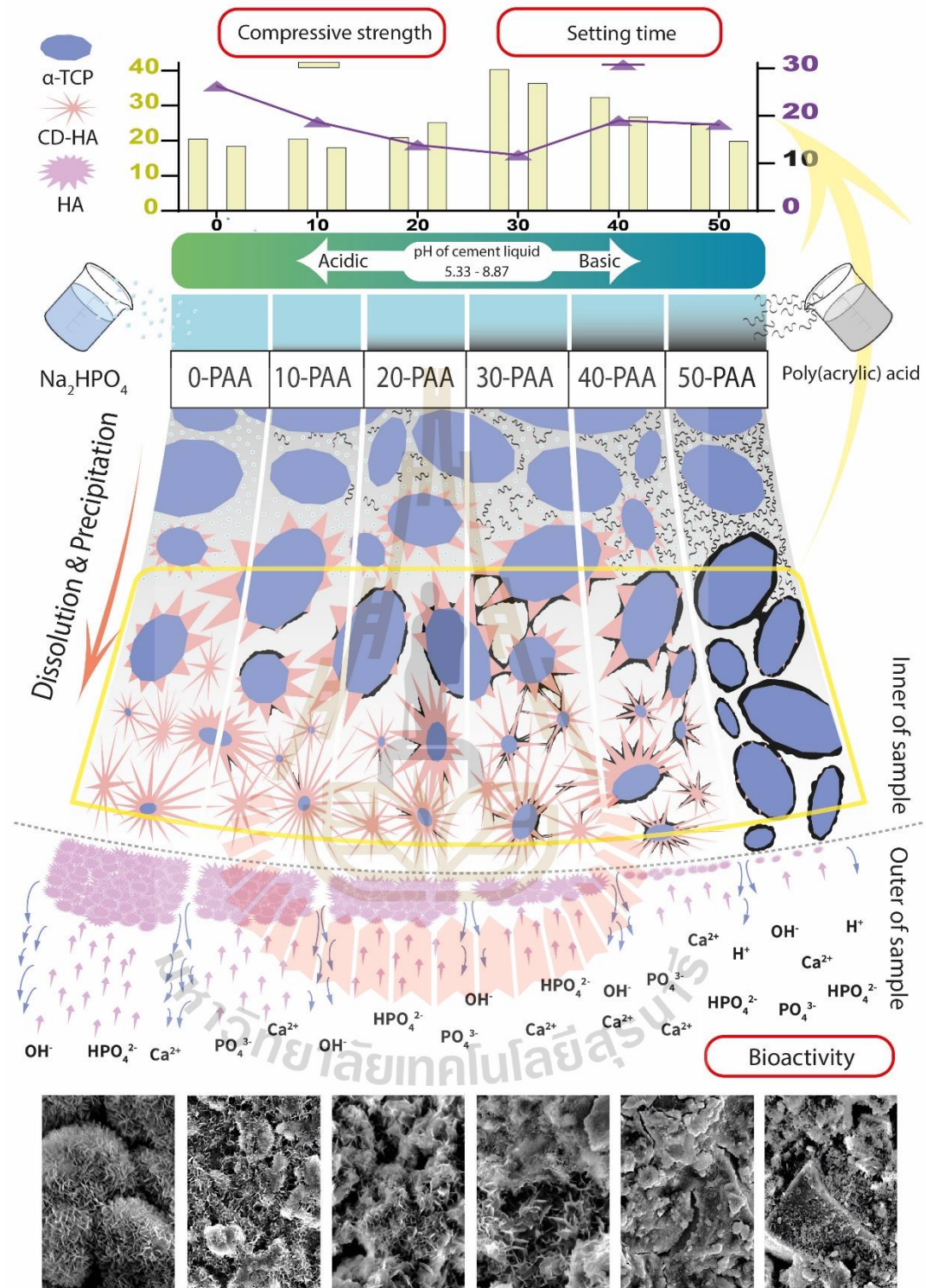


Figure 5.11 Schematic drawing illustrating the effect of the setting reaction related to setting time, compressive strength, and bioactivity on the concentration of PAA.

5.3.6 Cell viability

Firstly, the cement powder and liquid were sterilized as described in the method, then the discs were freshly prepared in the sterilized cabinet. The samples were soaked in the culture medium for 7 days, during which the medium was collected and replaced with fresh medium every day. The extracted medium was collected carefully using a filter in order to avoid transferring some small pieces of broken sample into the medium. In addition, the extracted medium at 1, 2 and 7 days were used to culture cells in 96-well plate. After 24 h of cells incubation with the extracted medium, the cell viability was performed by MTS solution, which resulted in the O.D. value. The percentage of cell viability was calculated using Eq.1. The results in Figure 5.12 show that all of the samples displayed a wide range of cell viability values at day 1. The percentage of cell viability of all samples were significantly different at P value < 0.0001. The cell viability increased in order from 0 v/v% PAA ($31.3 \pm 2.4\%$), 30 v/v% PAA cement ($87.1 \pm 4.5\%$) to biphasic granule commercial ($108.4 \pm 6.6\%$), respectively. It was found that the cell viability of both samples, 30 v/v% PAA cement and biphasic granule commercial were apparently higher than that of cement without PAA. It displayed no significant difference on day 2. Nonetheless, the cell viability percentage on day 7 appeared significantly greater in the 30 v/v% PAA sample than that of the biphasic granule.

The various procedures of sample preparation have been demonstrated for the *in vitro* testing. The researcher (Xu, 2007) soaked the specimen in fresh medium overnight and replaced it with new medium before analysis. Horiuchi et al. stored the sample under 100% humidity, then sterilized the samples by autoclave before testing, where the steam rinsed any residue that could affect the cell (Horiuchi, 2014). Some research also reported that the cement was cured for 3 days before cell culture testing to inhibit the unexpected releasing of ions from the materials (Lode, 2017). In this study, all samples have been freshly prepared without soaking in 100% humidity or other solutions prior to testing with cells. This procedure aimed to mimic real life use of these cements in the operation. In some research, the samples were prepared according to different procedures prior to cell culture testing. This was possibly in order to prevent the release of undesired toxic ions in the medium. In addition, these sample

preparations could have provided results with a high value of cell viability. In different circumstances, the result in the early stage could have affected the cell viability, as shown in the condition 0PAA at day1 in this study.

In this work, the cement samples of 0PAA and 30PAA were selected to investigate for biocompatibility. At day 1 of testing, 30 v/v% PAA presented as a non-toxic material whereas 0 v/v% PAA presented toxic in accordance with the criteria of cytotoxicity index as followed the ref. (Szymonowicz, 2017). The cell viability of 0PAA cement at day 1 was lower than 70% indicating toxic according to the cytotoxicity index. It can be due to high alkaline of Na_2HPO_4 at pH 8.87, resulting in severity of setting reaction at 1 day. However, the cell viability after 2 days of incubation was increased as similar to a control medium. At day 2 of testing, each condition presented a similar trend to nontoxic material (Higher than 70%). Nevertheless, the biphasic commercial material provided a higher value than that of other conditions, but reduced slightly at 2 and 7 days, respectively. This could be evidence that the cement in this study (30PAA) would be a promising material for using in bone fixation, which could be tested *in vitro* and *in vivo* in the future.

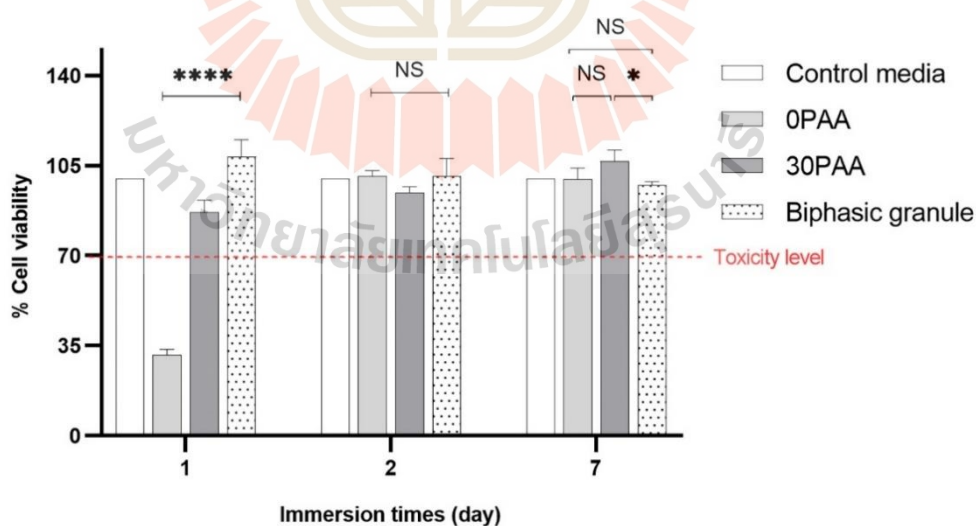


Figure 5.12 Cell viability of NIH 3T3 fibroblast cells after culturing with precondition medium of each samples including 0PAA, 30PAA, and biphasic granule from days 1, 2 and 7. Mean \pm SD, n = 3 replicates. (NS = no significance, * $p < 0.05$, and **** $p < 0.0001$).

5.4 Conclusions

This work has demonstrated that the new mixture of PAA and Na_2HPO_4 liquid for the calcium phosphate cement dramatically affected their properties for bone cement. 30 v/v% PAA addition in the liquid mixture presented as a crucial concentration for improving of the mechanical properties of this cement. Among the L/P ratio of 0.35 and 0.40, a L/P ratio of 0.35 met the shortest setting time and highest compressive strength. In addition, the pH slightly changed in range of the neutral level for 72 h of sample immersion. The concentration of PAA in the liquid influenced on the bioactivity, which reduced the HA deposition on the surface of sample for more than 40 v/v% PAA concentration. Surprisingly, 30 v/v% PAA added cement displayed excellent cell viability result at the first day and better result at 7 days as compared with the biphasic granule commercial. Despite the addition of PAA could inhibit the phase transformation from α -TCP to HA, this study explored the appropriate ratio of 30 v/v% PAA and 70 v/v% Na_2HPO_4 liquid mixture for enhancing compressive strength and cell viability, while the phase transformation had still maintained for bioactivity. This polymeric/calcium phosphate composite cement performed as non-toxic material resulting high cell viability. The cement in this study could be compromised as a bone substitution material for tissue engineering, which would be investigated more *in vitro* and *in vivo* in future work.

CHAPTER VI

EFFECT OF NANO-BIOACTIVE GLASS ON POLYMERIC APATITE/ β -TCP CEMENT

Apatite/Tricalcium phosphate composite cement composed with polyacrylic acid (PAA-apatite/TCP) has previously been reported to be a great promise for orthopedic applications. However, it was investigated that PAA could inhibit apatite phase conversion and result in poor bioactivity. To improve those limitations, PAA-apatite/TCP cement modified with the bioactive glass nanoparticle (0 to 1.5 wt.%) was investigated for physical properties, phase formation after setting and bioactivity. In addition, human Adipose-derived Stem/Stromal cells (hASCs), which were isolated from human adipose tissue and represent a widely implemented cell type for tissue engineering applications, were selected to determine their biological response to the bioactive glass modified PAA-apatite/TCP cement. The results indicated that the PAA-apatite/TCP cement added with bioactive glass cement decreased setting time and enhanced apatite phase transformation and bioactivity, as compared with the control cement. For in vitro testing, hASCs viability, proliferation, and differentiation potential were assessed under two cell culture conditions. In details, cells were either cultured with cement-preconditioned medium (indirect setting) or with cement (direct setting). The indirect culture presented a lower proliferation rate as compared with the control medium. In contrast, the result of direct culture indicated a higher proliferation rate on both control cement and 1 wt.% bioactive glass incorporated cement, as compared with coverslip control. Moreover, the increase in Alkaline Phosphatase activity following osteogenic stimuli indicated that both cements supported osteogenic commitment. In conclusion, these in vitro data lay the basis for a deeper investigation of 1 wt.% bioactive glass incorporated cement as a promising formula for clinical applications in bone engineering and orthopedic.

6.1 Research background, rationale, and significance

In the early 1980s, the self-setting calcium phosphate cements (CPCs) consisting of tetracalcium phosphate (TTCP) and dicalcium phosphate anhydrous (DCPA)/or dicalcium phosphate dihydrate (DCPD) discovered by Brown and Chow (Brown and Chow, 1983, Brown, 1987) and Legeros et al. (Legeros, 1982). Later, the CPCs have become promising materials in a wide variety of medical applications and bone engineering (Xu, 2017) due to their excellent bioactivity and biocompatibility (Ginebra, 2012). Although the CPCs present several useful biological properties, the improvement of their limited biodegradability and mechanical properties is still required (Habraken, 2016). This cement can be divided into two types of end-products: hydroxyapatite (HA) or calcium deficient hydroxyapatite (CD-HA, apatite cement) and dicalcium phosphate dihydrate (DCPD, brushite cement). It was noted that the degradation rate of apatite cement was slower than that of brushite cement (Gisep, 2003). Afterward, the biphasic cement concept (apatite/beta-tricalcium phosphate) has been considered for enhancing biodegradability due to the high dissolution of beta-tricalcium phosphate (β -TCP) by cells via an acid-release mediated process (Daculsi, 1998). According to the cement formula in the current work, β -TCP was added to the cement to improve its biodegradability. In previous works (Gallinetti, 2014, Sariibrahimoglu, 2014, Srakaew and Rattanachan, 2014), it was found that the addition of β -TCP into apatite cement could provide a higher degradation rate, though leading to a decrease in compressive strength. However, the mechanical properties could be improved by numerous factors such as the addition of polymers, and the decrease in porosity or liquid to powder ratio (Dorozhkin, 2008). Previous works (Majekodunmi, 2003, Majekodunmi and Deb, 2007) investigated the improvement of apatite cement with the addition of polyacrylic acid (PAA). In addition, the biocompatibility of PAA incorporated apatite cement was also proved to reduce the inflammatory responses *in vivo* (Khashaba, 2010). In the previous work (Thaitalay, 2021), the compressive strength of apatite/ β -TCP cement was increased with the addition of PAA aqueous

solution. Consequently, the higher concentration of PAA significantly decreased HA phase conversion and bioactivity of cement.

Bioactive glass (BG) has revealed excellent bioactive and biocompatible properties in both *in vitro* and *in vivo* testing (Hoppe, 2011). In addition, the integration of BG in CPCs and its good biological performance have been previously described (Renno, 2013, Sadiasa, 2014, Lee, 2016). Nonetheless, Stulajterova et al. (Stulajterova, 2017) have investigated the responses of rat primary Mesenchymal Stem/Stromal cells (rMSCs) on 45S5-BG incorporated apatite cement and they observed a reduced cell viability and proliferation when the BG content was increased of 7.5-15 wt.%. They reported that increased cytotoxicity of cement with a higher BG content was induced by toxicity of culture media following ion release or a pH change. Some researchers also reported that the addition of mesoporous BG into the apatite cement enhanced the growth factor delivery (Schumacher, 2017), and protein absorption ability (El-Fiqi, 2015), which could be due to the high surface area of BG. In this view, the influence of mesoporous BG/CPCs composite loaded with growth factor (rhBMP-2) on bone marrow MSCs (BMSCs) was examined (Li, 2015), demonstrating the induction of osteogenic differentiation *in vitro*, and the increase in osteointegration *in vivo*.

Although BMSCs have been the most commonly studied MSCs for tissue repair and/or regeneration, they hold some limitations, such as the low cell yield and the donor site morbidity linked to bone marrow harvesting procedure (Lindroos, 2011). Human adipose-derived stem/stromal cells (hASCs) represent a good alternative MSCs type for tissue engineering since they are abundantly and easily isolated from adipose tissue with a minor donor discomfort (Baer and Geiger, 2012, Canciani, 2016). Additionally, hASCs can self-renew and differentiate into several cell types, including osteoblast-like cells (Dai, 2016). Afterward, the studies of hASCs responses on various biomaterials have become promising for a large number of clinical applications due to their multipotential differentiation capacity (Liu, 2021). It was reported that hASCs growth and differentiation could be promoted both *in vitro* and *in vivo* by polymer/BG scaffold (Lu, 2014). In addition, some researchers have presented hASCs responses on

CPCs, resulting in the enhanced differentiation of hASCs on brushite/PLGA fiber cement (Kunisch, 2019) and apatite/pectin cement (Zhao, 2016). Corsetti et al. (CORSETTI, 2017) reported that rat ASCs-loaded α -TCP scaffold significantly increased bone repair in a rat model testing, as compared with the control α -TCP scaffold without ASCs.

In this current work, the BG nanosphere with porous structure was added into the PAA-apatite/ β -TCP cement for improving physical and biological properties. It was noted that the glass formula and type influenced the dissolution rate of BG involved with the HA layer precipitation for new bone formation (Jones, 2013). Furthermore, the nano-size (Lei, 2012) and spherical shape of the particle (Lei, 2011) could affect the biocompatibility, resulting in more viable cells. In previous studies (Yan, 2006, Phetnin, 2020), the mesoporous ($80\text{SiO}_2\text{-}15\text{CaO}\text{-}5\text{P}_2\text{O}_5$) glass showed excellent bioactivity and biocompatibility. In addition, the mesoporous BG showed a higher specific surface area, as compared with the standard BG (Yan, 2005). The mesoporous BG with a higher specific surface area could also enhance the apatite-like formation, presenting superior bioactivity (Yan, 2004). Therefore, present work aimed to evaluate the influence of the incorporation of developed porous BG nanospheres ($80\text{SiO}_2\text{-}15\text{CaO}\text{-}5\text{P}_2\text{O}_5$) into PAA-apatite/ β -TCP cement on hASCs responses, such as cell viability, proliferation, and differentiation potential. In addition, here the *in vitro* testing was performed under different environmental conditions (direct and indirect cell culture). Both hASCs responses on cement and the surrounding environment of the sample (Conditioned medium) have been monitored and investigated.

6.2 Experimental procedure

6.2.1 Preparation of nano-bioactive glass

The nano-bioactive glass (n-BG) based on $80\text{SiO}_2\text{-}15\text{CaO}\text{-}5\text{P}_2\text{O}_5$ system (Phetnin and Rattanachan, 2015) was prepared by the the wet chemical process in accordance with the previous study (Hu, 2014). Briefly, 0.598 g Cetyltrimethylammonium Bromide (CTAB, Sigma-Aldrich) was dissolved in the mixture of 330 ml deionized water and 156 ml absolute ethanol (EtOH, Carlo Erba reagents). 5 ml

ammonia solution (30% NH₃ in water, Carlo Erba reagents) was added to the solution. Then, 12.5 ml tetraethyl orthosilicate (TEOS, Acros), triethylphosphate (TEP, Acros), and 2.5 g calcium nitrate tetrahydrate (CN, Kemaus) were added to the solution under stirring for 3 h, respectively. The obtained white precipitated particle was calcined at 650 °C for 3 h. The morphology of the n-BG was observed by scanning electron microscope (SEM, Carl Zeiss: Auriga, Germany) and Transmission electron microscope (TEM, FEI/Tecnaig2 20S-TWIN). The particle size distribution of n-BG was determined by counting partial size in SEM images using ImageJ software (NIH, USA). The average particle size of n-BG was calculated from the number of particles (~900 particles), and reported as the mean value ± standard deviation. The phase identification of n-BG was analysed using X-ray diffraction (XRD Bruker/D2-phaser) in the range of 2 Θ from 10 to 60, and in the increments of 0.02.

6.2.2 Preparation of cement

The cement powder was prepared consisting of two main components of apatite and β -TCP (Sigma-Aldrich) with a weight ratio of 5:1. The apatite content consisted of 62.5 wt.% α -TCP, 26.8 wt.% DCPA (Sigma-Aldrich), 8.9 wt.% CaCO₃ (Carlo Erba reagents), 1.8 wt.% precipitated hydroxyapatite (PHA), and 1 wt.% chitosan fiber (G.T.C. Union group), as explained in previous work (Rattanachan, 2020). α -TCP (6±0.13 μ m) and PHA (12±1.5 μ m) powder were in-house synthesized by precipitation method. Afterward, the different concentration of n-BG (0.5, 1.0, 1.5 wt.%) was added to the cement powder. The cement liquid consisted of 1M disodium hydrogen phosphate (Na₂HPO₄, Merk) and 10 wt./wt.% PAA (Sigma-Aldrich) in a volume ratio of 3:1, as reported in the previous work (Thaitalay, 2021). The sample was prepared by mixing the cement powder and liquid with a liquid to powder ratio (L/P ratio) of 0.35 ml/g, following the topic 3.2.3.1 of Chapter III. Afterward, cement samples containing different n-BG concentrations were indicated as CPC, CPC/0.5BG, CPC/1.0BG, and CPC/1.5BG, respectively.

6.2.3 Properties testing and characterization of cement

Setting time, phase composition (XRD, Rietveld refinement), mechanical properties (compressive strength and young's modulus), and morphology (bioactivity, fracture surface) of cement were investigated using the same procedure as discussed in Chapter III (Topic 3.2).

6.2.4 *In vitro* testing

6.2.4.1 hASCs and culture conditions

Human waste tissues were collected from the surgery room following the procedure PQ 7.5.125 approved by IRCCS Istituto Ortopedico Galeazzi institutional review board. Prior to donation, all patients provided written informed consent. For *in vitro* testing, the hASCs were derived from subcutaneous adipose tissue of two female donors (mean age 58 ± 2 years) after written consent. The cells were cultured in complete medium consisting of high glucose Dulbecco's Modified Eagle Medium (Sigma Aldrich) supplemented with 10% Fetal Bovine Serum, 2 mM L-glutamine, 50 U/ml penicillin, 50 $\mu\text{g/ml}$ streptomycin at 5% CO_2 and 37 °C in the absence of any osteogenic stimuli (therefore, herein this medium is indicated as '-OS medium').

hASCs behaviour on cement and in the presence of cement-conditioned medium was determined. The cell response to culture condition was investigated in two different environments (Direct and Indirect culture), as shown in Figure 6.1.

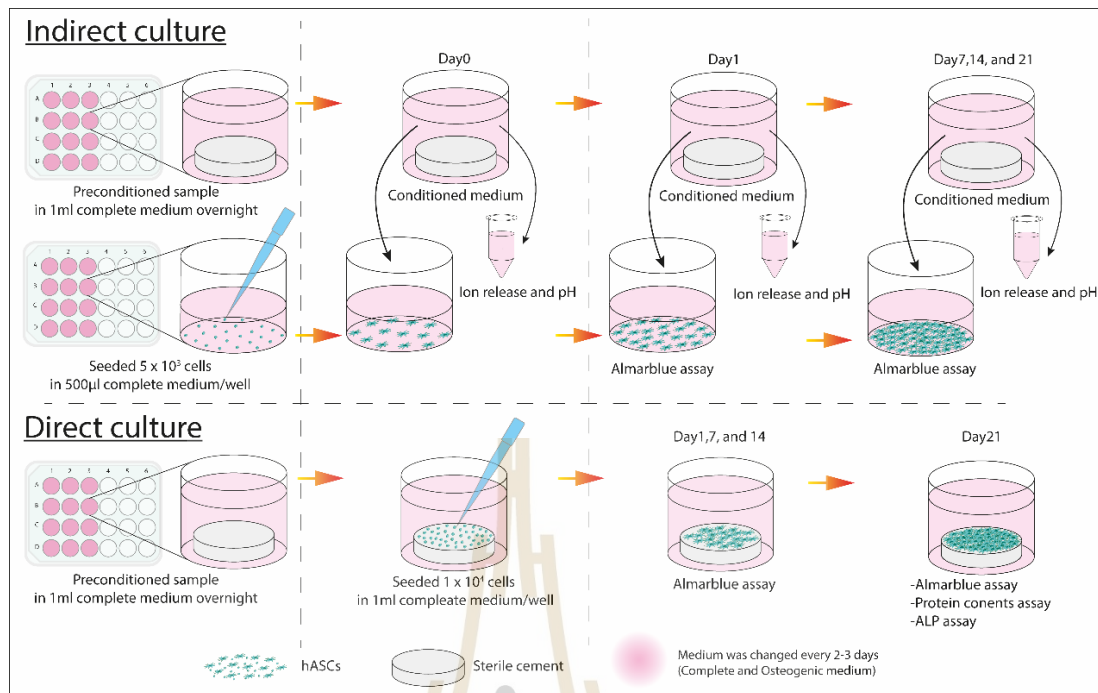


Figure 6.1 Schematic drawing illustrating the procedure of two different hASCs culture conditions (Indirect and Direct culture).

6.2.4.2 Indirect cell culture

Prior to testing, the cement powder was sterilized by dry heat sterilization at 121 °C for 10 h. The cement liquid was sterilized by membrane filtration using a 0.22 µm sterile filter. For both indirect and direct culture, the cement discs were fabricated with a diameter of 2 mm and a height of 12 mm. As shown in Figure 6.1, cement discs were incubated in 1ml complete medium overnight to rinse debris and equilibrate the samples before testing. In the next day, 5x10³ cells suspended in 500 µl complete medium were seeded into a 24-well tissue culture plate and allowed to attach on the plate overnight. Meanwhile, the medium soaked samples were collected and replaced with the new 500 µl complete and osteogenic medium every 2-3 days. The collected media was used as a conditioned medium for each cement condition. The osteogenic medium consisted of -OS medium supplemented with 0.15 mM Ascorbic acid, 0.01 µM Dexamethasone, 10 mM β -glycerophosphate, and 10 nM Vitamin D as osteogenic stimuli and is therefore indicated as +OS medium. The

medium soaked with cells in tissue plate was replaced every 2-3 days by the conditioned medium of each cement condition.

6.2.4.3 Direct cell culture

As presented in Figure 6.1, the cement discs were incubated in 1ml -OS medium overnight prior to cell seeding. 1×10^4 cells suspended in 15 μ l -OS medium was seeded onto the cement discs and allowed to attach for 15 min. The glass coverslip was used as the control condition. The fresh -OS and +OS medium were added to each well to make 1 ml in total. The samples were cultured with cells over times. The culture medium was changed every 2-3 days.

6.2.4.4 pH changes and ion concentration in culture medium

The pH changes of the cement-conditioned medium at each time point were measured by an electrolyte-type pH meter (Denver pH/mV/Temp. Meter, UB-10). To determine the ions releasing/adsorption of cement discs, an aliquot (400 μ l) of the cement-conditioned medium at day 0, 1, 7, 14, and 21 was centrifuged and collected. Then, the obtained supernatant was analysed by Inductively coupled plasma optical emission spectrometry (ICP-OES: Optima 8000, PerkinElmer).

6.2.4.5 Alamarblue assay

For cell proliferation, the metabolic activity was measured using the AlamarBlue assay. For indirect culture, the proliferation of hASCs cultured with cement-conditioned medium was compared with the appropriate controls (hASCs cultured with fresh -OS and +OS media) at 1, 7, 14, and 21 days. For direct culture, cements were transferred to a new well to selectively assess only the viability of cells growing on the samples and to exclude any interference from cells growing on the plastic well for direct culture system. On days 1, 7, 14, and 21, the medium was removed and replaced by 10% of reagent (AlamarBlue; Thermo Fisher Scientific Inc) in complete medium following the manufacturer's protocol. The plates were incubated at 37°C and 5% CO₂ for 2.5 h. Following incubation, 200 μ l of each well was transferred in duplicate to a 96-well plate. Fluorescence was read at the excitation of 540 nm and emission of 600 nm with a Wallac Victor II plate reader.

6.2.4.6 BCA protein assay

After the alamarblue assay was completed at day 21, all samples were rinsed with PBS for several times. Samples were lysed in deionized (DI) water by 3 times freeze-thawed process in the refrigerator at -80°C and in water bath at 37°C . 10 μl sample lysates were transferred in duplicate to a 96-well plate and mixed with 200 μl working solution (BCA Protein Assay; Pierce Biotechnology Inc, Waltham, MA), following the manufacturer's protocol. The plates were incubated at 37°C and 5% CO_2 for 30 min. Afterward, the total protein content was quantified with the absorbance wavelength of 570 nm.

6.2.4.7 Alkaline phosphatase assay

After culturing for 21 days, the osteogenic potential of cells cultured on samples was tested by Alkaline phosphatase (ALP assay, Sigma-Aldrich) activity. 50 μl sample lysates were transferred in duplicate to a 96-well plate and incubated with 100 μl substrate solution (1 mM p-nitrophenyl phosphate dissolved in an alkaline buffer) at 37°C and 5% CO_2 until the solution changed to yellow. The ALP activity was read with the absorbance wavelength of 405 nm and normalized by the protein content.

6.2.5 Statistical analysis

One-way ANOVA coupled with Tukey's multiple comparison test was used for statistical analysis of the mechanical properties, cell proliferation, and differentiation. The statistical analysis was performed using GraphPad Prism 8 software. Differences were considered significant with $p < 0.05$ and the results were presented as mean \pm standard deviation

6.3 Result and discussion

6.3.1 Characterization of n-BG

Nanosize spherical bioactive glass (n-BG) with $80\text{SiO}_2\text{-}15\text{CaO-}5\text{P}_2\text{O}_5$ was successfully prepared by the wet chemical process. The morphology of n-BG was a spherical shape with porous structure observed by SEM and TEM techniques, as shown

in Figure 6.2 and 6.3, respectively. The average particle size of n-BG was 122 ± 15 nm with narrow size distribution, ranging from 80 to 170 nm, as shown in Figure 6.4. In addition, XRD pattern of n-BG presented amorphous phase (Figure 6.5).

The synthesis of n-BG has been investigated using several methods, which resulted in various microstructures of n-BG (Wang, 2019). It was found that the porous structure of n-BG could be controlled by CTAB content with a critical micelle concentration value of CTAB at 1 mM in water (Javadian, 2013). In addition, the higher CTAB content could affect their characteristics, resulting in the long-rod shape (1-6 mM CTAB) (Li, 2015) and more porous structure with a higher specific surface area (0.6-27 mM CTAB) (Gupta, 2016). Hu et al. (Hu, 2014) also demonstrated that a higher CTAB content of 3.3-5.9 mM resulted in more condensed and smaller nanosize of BG particles ranging from 294-187 nm. This could be evidence of the CTAB contents influencing the structure of n-BG. In addition, the difference in n-BG structure could also be correlated to the different NH_4OH concentrations or reactant addition time intervals, as reported in (Kesse, 2019). Here, the n-BG particles with porous structure (CTAB = 5mM) were added to the PAA incorporated apatite/ β -TCP cement to improve its poor apatite phase conversion and bioactivity, as evidenced in the previous study (Thaitalay, 2021). It was reported that the high specific surface area of porous n-BG could enhance the apatite-like formation, resulting in a greater bioactivity (Yan, 2004). Furthermore, more viable cells were found with nanosize (Lei, 2012) and spherical shape of BG (Lei, 2011).

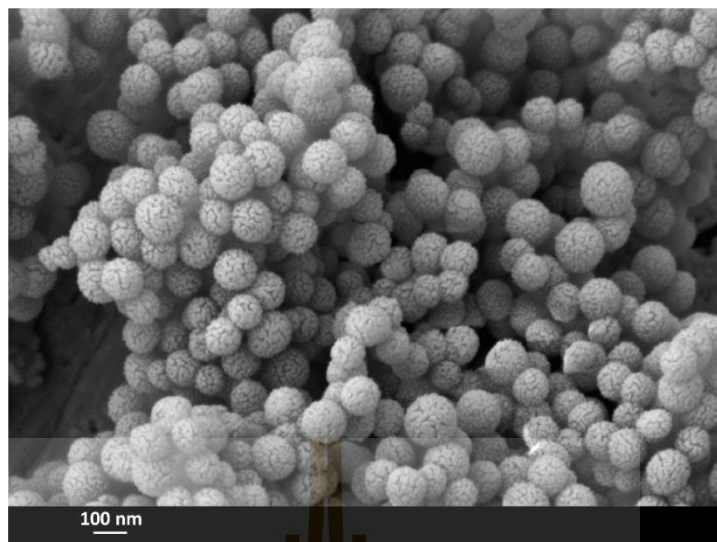


Figure 6.2 SEM image of n-BG powders, magnification of x50,000.

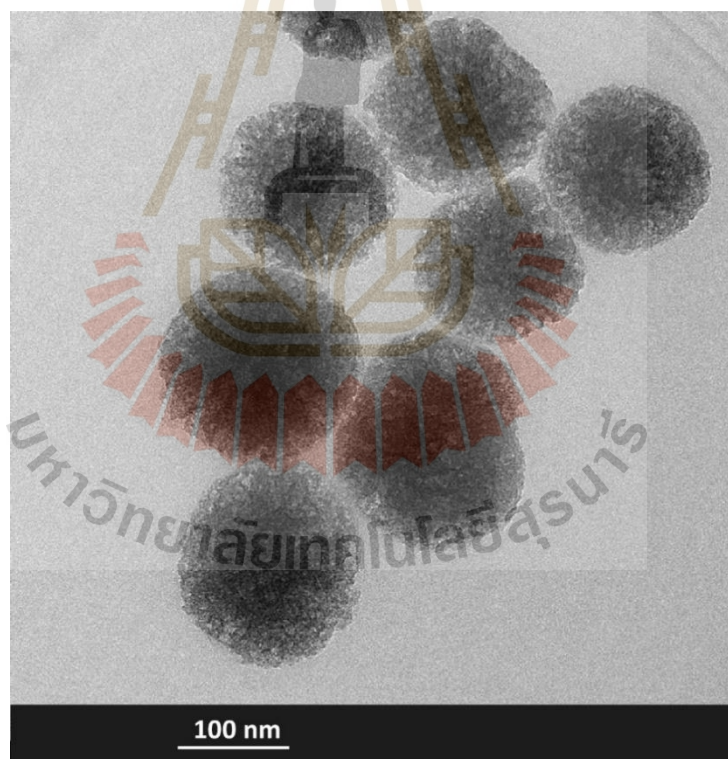


Figure 6.3 TEM image of n-BG powders, magnification of x100,000.

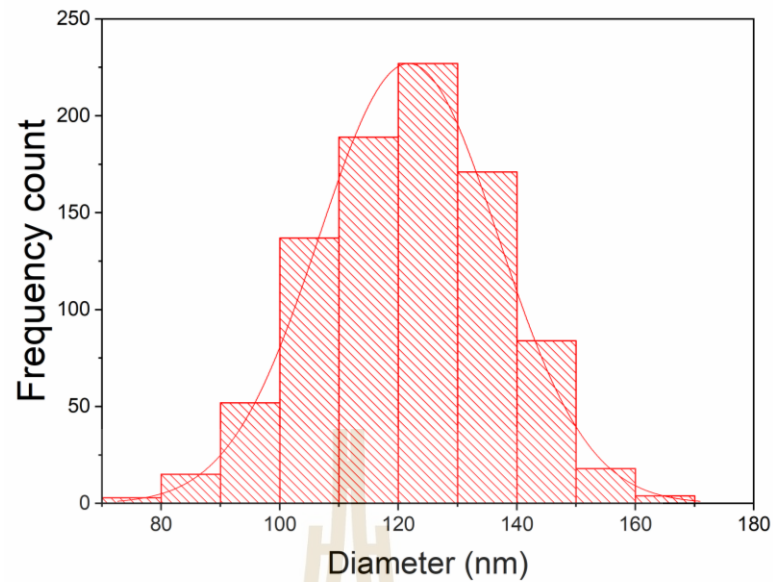


Figure 6.4 Particle size distribution of n-BG powders.

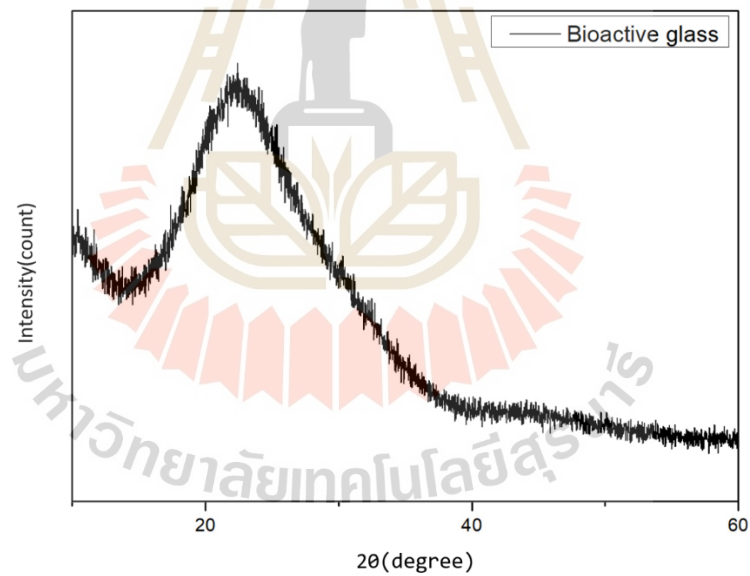


Figure 6.5 XRD pattern of n-BG powders.

6.3.2 Setting time measurement

Figure 6.6 shows that both initial (t_i) and final (t_f) setting times were reduced with the increase of 0-1.5wt.% n-BG powder. Khairoun et al. (Khairoun, 1998) reported that the approximate initial (< 8 min) and final (< 15 min) setting times of

CPCs were clinically required for orthopaedic applications. The initial and final setting times of 1 wt.% ($t_i = 9 \pm 1$ min, $t_f = 18 \pm 1$ min) and 1.5 wt.% ($t_i = 7 \pm 1$ min, $t_f = 14 \pm 2$ min) n-BG added cement were close to the clinical requirements.

The addition of BG into CPCs has been evaluated in some previous works (Lee, 2016, Medvecky, 2017, Stulajterova, 2017, Hasan, 2019), in which the BG could either accelerate or retard the setting time depending on the cement formula. Moreover, the porous structure of BG nanospheres could adsorb the cement liquid, providing lower liquid content in the setting reaction. This could explain the decreased setting time of n-BG incorporated cement in the current study. In addition, the reduced setting time could be attributed to the extra Ca ions sourcesupplied from n-BG, accelerating the setting reaction of cement. These results are consistent with previous findings (Sadiasa, 2014), which reported that the addition of BG increased the source of Ca ions, resulting in shortening the setting time of cement. In addition, El-Fiqi et al. (El-Fiqi, 2015) have explained the significant change in setting time of the mesoporous BG incorporated α -TCP based cement. According to their results, the setting time of BG modified cement decreased with the increasing of BG content, which could be due to the increased rate of HA formation, liquid absorption/adsorption ability of BG, and Ca ions releasing. Their findings could be attributed to the result of this current work, which showed that the addition of 0-1.5 wt.% BG to apatite/ β -TCP cement reduced the setting time.

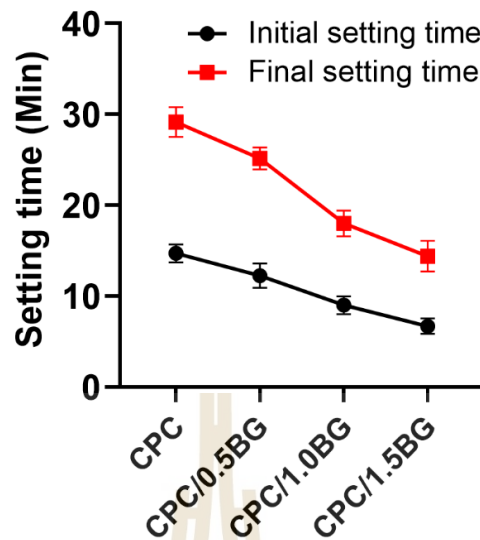


Figure 6.6 Initial and final setting time of polymeric apatite/ β -TCP cement containing the different n-BG contents.

6.3.3 Mechanical testing

After samples soaking in SBF solution for 7 days, the mechanical testing of cement were investigated. The result showed that the compressive strength of 1 wt.% n-BG incorporated cement (CPC/1.0BG, 49.9 ± 5.6 MPa) was significantly higher than that of the control cement (CPC, 37.5 ± 3.2 MPa), as shown in Figure 6.7. Nevertheless, there was no statistical difference between the young's modulus of n-BG incorporated cement and pure cement, as presented in Figure 6.8.

According to our previous work (Thaitalay, 2021), the mechanical properties of the composite cement were tested after soaking in SBF solution as simulated in the biological environment. It was determined that the setting reaction of cement nearly completed (major phase of HA formation) with a highest strength up to 7 days. Therefore, the compressive strength of the samples in this experiment was measured after soaking in SBF solution for 7 days. This prolonged setting reaction was affected by the PAA encapsulated some of the α -TCP powder. In addition, the use of large partical size of starting α -TCP (6 ± 0.13 μm) could also affect the longer setting reaction, which was similar to the size of α -TCP ($4 \mu\text{m}$) in the previous study (Zamanian,

2012). Generally, CPCs possess different degrees of compressive strength, which could be in range of 10-60 MPa (brushite cement) or reach up to 75 MPa (apatite cement) (Schumacher and Gelinsky, 2015). Thus, the compressive strength of cement could be influenced by various parameters, such as cement composition, liquid to powder ratio, particle sizes of starting powder, and additives (Dorozhkin, 2008). Our previous study (Thaitalay, 2021) found that the presence of PAA could form a crosslinked reaction with the starting cement powder, resulting in a significantly increased compressive strength (from 20 to 40 MPa) of apatite/ β -TCP cement. This is consistent with the results in this current study on the control PAA incorporated apatite/ β -TCP cement (CPC, 38 MPa). Afterward, the compressive strength of CPC was increased by the addition of n-BG (up to 50 MPa). This could suggest that the porous structure of cement was filled by the addition of n-BG, resulting in the denser compaction of the microstructure. This finding is supported by the previous works on BG reinforced TTCP cement (Medvecky, 2017) and 45S5 bioactive modified TTCP/DCPA cement (Yu, 2013). They reported that the addition of the number of fine BG particles into cement could reduce the larger pore in its structure. Afterward, the compressive strength was increased due to the more compact structure. Besides, the higher compressive strength of BG modified cement could be attributed to the greater HA formation in the structure with respect to the control cement, as witnessed by the result of phase composition analysis. Hence, the BG degraded and enhanced the HA formation on the particle surface of BG. This behaviour could induce the entanglement of HA nanocrystals into the cement matrix strengthening the set cement.

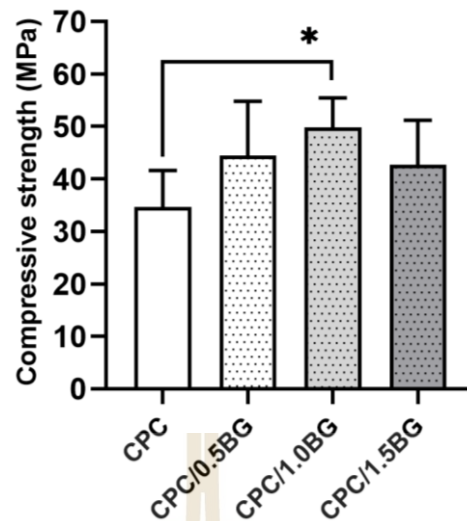


Figure 6.7 Compressive strength of cement containing the different n-BG contents after immersion in the SBF solution for 7 days.

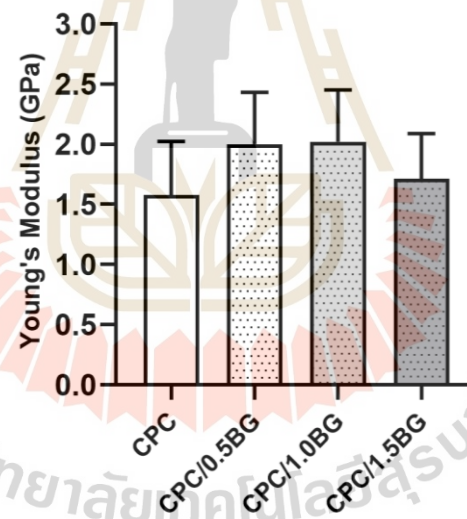


Figure 6.8 Young's modulus of cement containing the different n-BG contents after immersion in the SBF solution for 7 days.

6.3.4 Phase composition analysis

XRD patterns (Figure 6.9) of cement containing 0-1.5 wt.% n-BG powder revealed the phase structures following the datasheet numbers 09-0432 (HA), 29-0359 (α -TCP), 09-0169 (β -TCP), 47-1743 (CaCO_3), and 70-0359 (DCPA) of the powder diffraction standards. After immersion in SBF for 7 days, XRD patterns of all samples

revealed significant peaks of HA and β -TCP with other residuals of the starting components (α -TCP, DCPA, and CaCO_3). Moreover, the addition of n-BG material to cement affected HA phase formation, which was supported by phase composition, as shown in Figure 6.10. The percentage of HA phases in these cements for 0, 0.5, 1.0, and 1.5 wt.% BG were 49.6, 54.6, 56.9, and 58.7 wt.%, respectively.

After soaking in SBF solution at 37 °C for 7 days, the main product of these n-BG incorporated cement consisted of apatite/CD-HA and β -TCP with respect to remaining phases (α -TCP, DCPA, and CaCO_3) as the residuals. This aspect was similar to the previous study (Rattanachan, 2020). It was determined that the residuals of the other starting powder were still detected after 7 days in the setting cement, including α -TCP, DCPA, and CaCO_3 . Afterwards, the complete reaction of cement (β -TCP+HA) was detected after 3 months. Here, it was found that the incorporation of n-BG in cement supported the higher content of HA phase conversion as compared with the control cement without n-BG in this study, as shown in Figure 6.10. A previous work (El-Fiqi, 2015) reported that the acceleration of HA formation could be related to the higher Ca^{2+} released from BG powder in the setting reaction of cement. This explanation could correlate to the result in this current work. Moreover, the incorporation of n-BG could possibly promote the HA formation in the cement matrix due to its excellent bioactivity. Another assumption could be that the porous structure of n-BG adsorbed some PAA in the cement liquid, resulting in less PAA reacting with α -TCP and other components in the cement powder. Subsequently, this aspect could allow more phase conversion from α -TCP to HA. This consideration could be supported by the previous work (Thaitalay, 2021), where the higher PAA content in apatite/ β -TCP cement inhibited the HA phase transformation.

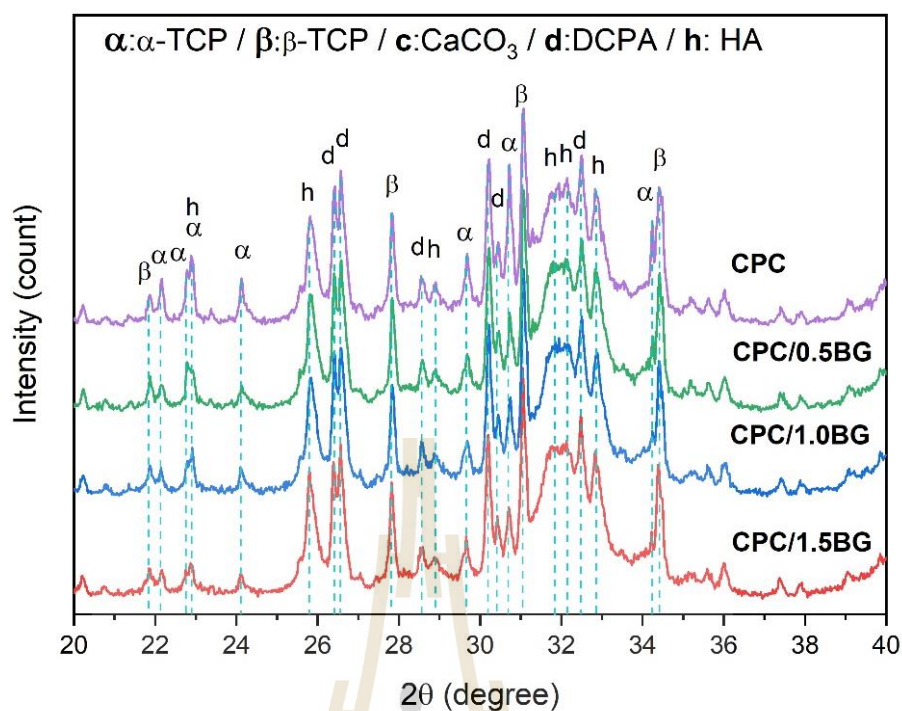


Figure 6.9 XRD patterns of the apatite/ β -TCP cement containing the different n-BG contents after immersion in SBF solution for 7 days.

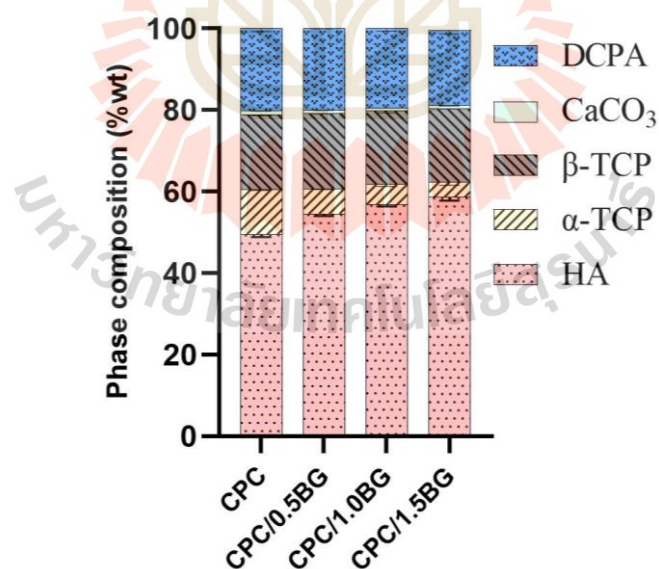


Figure 6.10 Phase composition of apatite/ β -TCP cement containing the different n-BG contents after immersion in SBF solution for 7 days. The experiment was repeated in duplicate with $n = 6$.

6.3.5 Morphology analysis

Figure 6.11 exhibits SEM micrographs of the sample surfaces immersed in SBF solution at 37 °C for 1 and 14 days, respectively. After 1 day of immersion, the rough surface of all samples was observed, presenting fine particles of each cement reactant. The needle-like crystals formation was found on the surface of the sample for 0.5 and 1 wt.% n-BG incorporated cement (CPC/0.5BG and CPC/1.0BG) and became denser covered on the surface of the sample for 1.5 wt.% n-BG incorporated cement (CPC/1.5BG) after immersion in SBF for 14 days. In addition, the fracture surface of each condition presented a flower-like crystals structure and irregular shape of other remaining starting powders after 14 days of incubation.

The bioactivity of bioactive materials has been evaluated by bone-like HA formation on the sample surface in SBF solution (Kokubo and Takadama, 2006). Figure 6.11 shows that the control sample slightly changed after immersion in SBF for 14 days. This observation is similar to the previous result (Thaitalay, 2021), indicating the poor bioactivity of PAA incorporated apatite/ β -TCP cement. In the previous research (Lee, 2016), the improved bioactivity of CPCs by adding BG has been investigated. Nezafati et al. (Nezafati, 2013) showed excellent bioactivity of 15 wt.% BG fibres incorporated CPCs (TTCP/DCPD based cement) after the sample soaking in SBF solution at different time points. They reported that the micro and nanoparticles of apatite grew up and distributed on the entire sample surface after 3, and 7 days immersion. However, the morphology of the surface (SEM) of BG incorporated cements (day 14) could be considered as either the higher apatite conversion (Rietveld refinement at day 7) or the denser needle-like crystal formation on the sample surface when increasing n-BG content in the cement. In order to avoid this confusion, SEM images of each fractured sample with a similar structure (flower-like apatite crystal conversion with other unreacted starting powder) were clearly different from the surface of each condition. As a result, this confirmed that the addition of n-BG could improve the bioactivity of the control sample, resulting in the more crystal-like particles formation on the sample after 14 days of soaking in SBF.

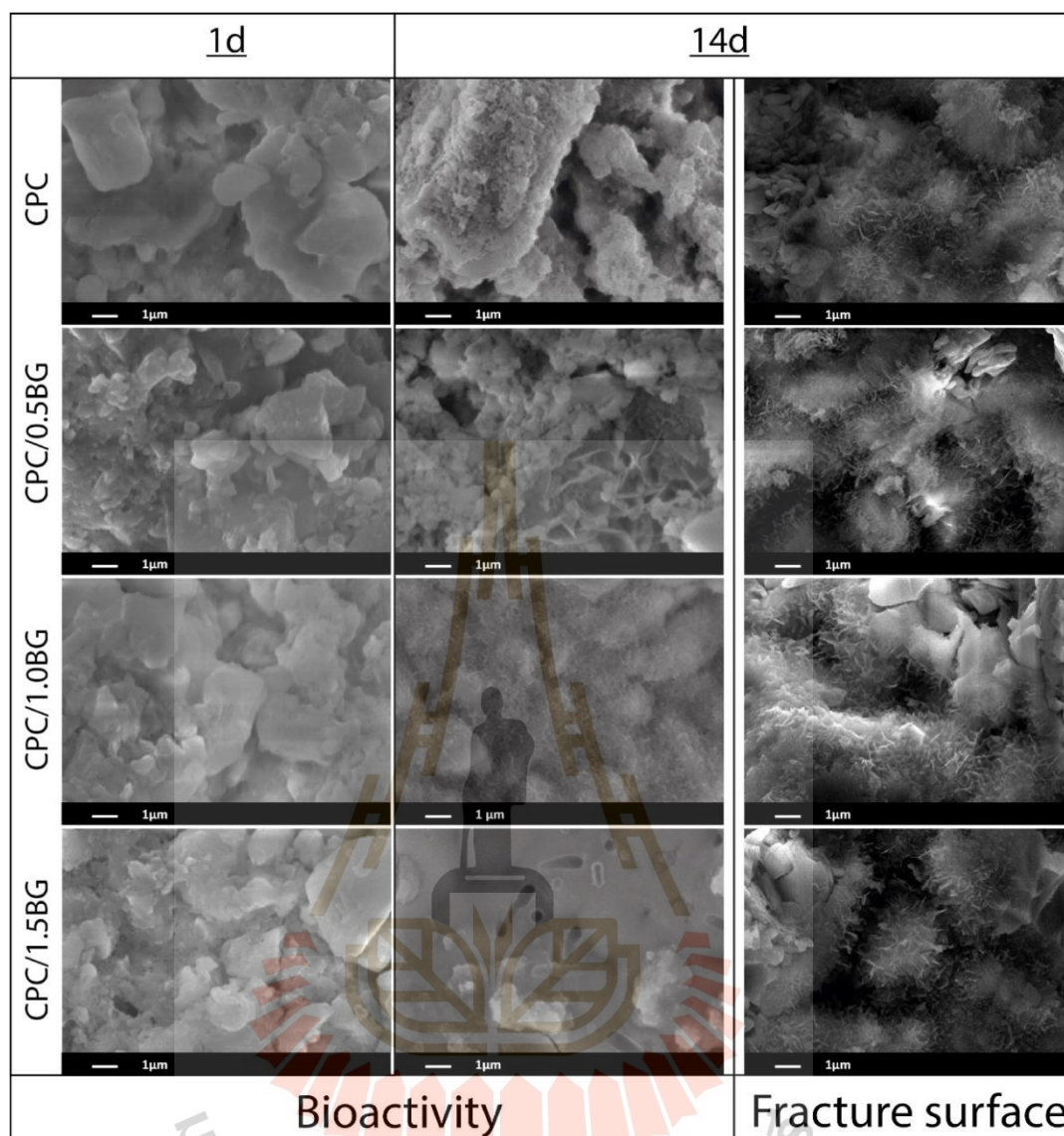


Figure 6.11 SEM micrographs of the surface (1 and 14 days) and fracture (14 days) of the cements with different n-BG concentrations from 0-1.5 wt.% soaking in SBF solution at different time points, magnification of x10,000.

6.3.6 *In vitro* testing

6.3.6.1 Ion releasing/adsorption and pH measurement

The pH change and ions concentration of cell culture media soaking cement over 21 days were detected to determine the influence of cement with the surrounding environment on cell responses. The pH and ion changes (Figure 6.12) in both -OS and +OS medium presented a similar trend. The pH changes of

control CPC-conditioned medium exhibited more acidic than that of the CPC/1.0BG-conditioned medium during incubation. From the incubation period, the pH change of control cement was in a range from 8.87 to 8.55 (-OS) and 8.9 to 8.56 (+OS). After the sample soaking in media for 21 days, the pH value of CPC/1.0BG-conditioned medium was in a range from 8.9 to 8.6 (-OS) and 8.9 to 8.59 in (+OS). Figure 6.13-6.17 presents that the released Ca, P, and Si ions in the control CPC-conditioned medium were in the approximate range of 0.18-0.36 mM, 0.39-1.03 mM, and 0.17-0.56 mM, respectively. Meanwhile, the released Ca (0.16-0.69 mM), P (0.10-0.99 mM), and Si (1.04-1.46 mM) ions in CPC/1.0BG-conditioned medium was recorded during the incubation from 1 to 21 days. The CPC/1.0BG released more Ca ions to the medium than the control CPC during 21 days of incubation. For PO_4^{3-} and Na^+ , the initial burst was highly detected during the early stage of day 0 and 1. Afterward, the PO_4^{3-} slightly increased from 7 to 21 days. For Si ions, the cumulative release was intensively found in CPC/1.0BG with respect to the control one. On the other hand, Mg ions in culture medium were adsorbed by both control CPC and CPC/1.0BG, presenting negative values after blank (culture medium) subtraction.

Among various concentrations of n-BG content in cement, CPC/1.0BG was selected due to its highest strength with other appropriate physical performance in this current work. It should be noted that the pH change in the culture medium was related to the ion release/adsorption ability of cement samples. Subsequently, the more basic culture medium at the initial time of incubation (day 0-1) could be attributed to the excessive residual Na^+ and PO_4^{3-} from the cement liquid of 1M Na_2HPO_4 (pH is approximately 8.92). After that, the pH of both cement conditions slightly decreased to the equilibrium pH of the control medium, which could be a more favourable environment for cell proliferation over time as witnessed in rapid growth after 21 days incubation in the direct culture (Figure 6.19). In addition, the higher pH trend of n-BG added cement in this work could be related to the previous works of BG doped apatite cement (El-Fiqi, 2015) and BG doped apatite/PLGA cement (Renno, 2013), as compared with the control cement. They reported that the BG particles in

the cement released more inorganic ions to culture medium, resulting in the higher pH trend of BG added cement. It was found that both CPC and CPC/1.0BG could adsorb the ions, showing the depletion of Mg ions during the incubation. This adsorption ability of both cements is correlated with the previous work (Schamel, 2017), indicating the ions depletion of Ca^{2+} and Mg^{2+} after immersion of brushite/monetite cement in cell culture medium for 7 days.

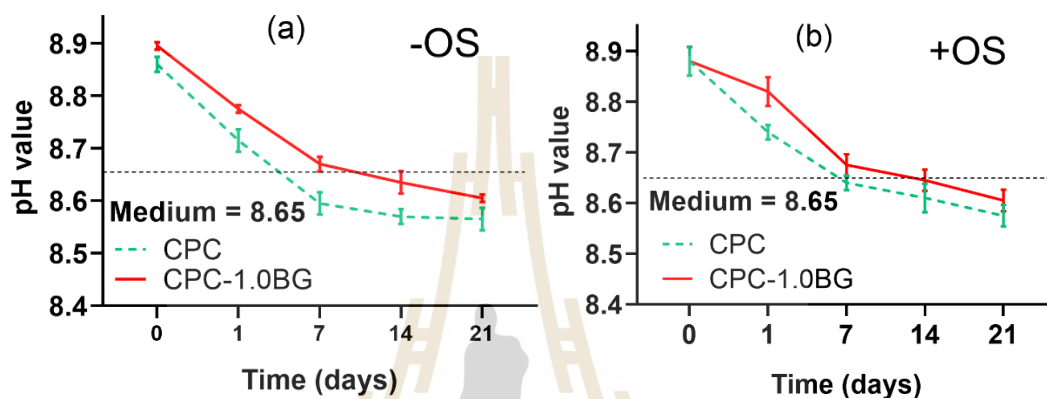


Figure 6.12 pH change in (a) control (-OS) and (b) osteogenic (+OS) media after soaking samples in cell culture media at different immersion time points (Day 0 is preconditioned overnight).

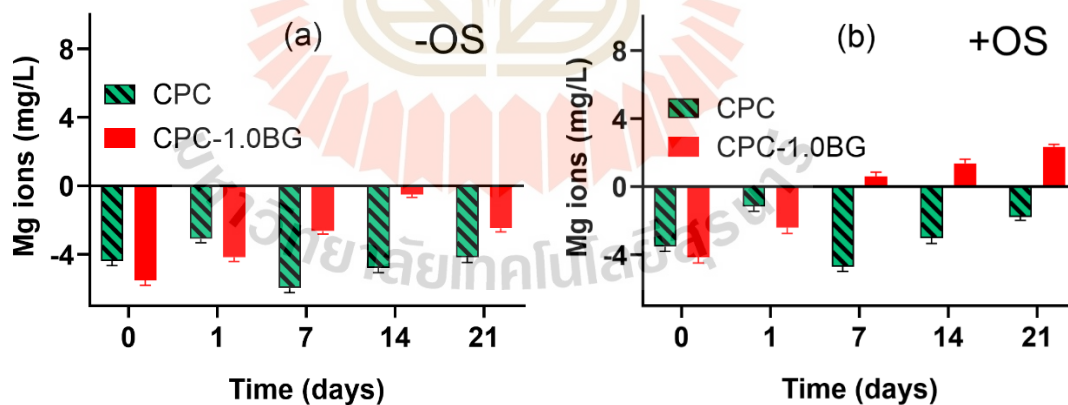


Figure 6.13 Ion changes of Mg ions in (a) control (-OS) and (b) osteogenic (+OS) media. All ions of each condition were subtracted by the control cell culture medium as a blank, showing the ions in the medium adsorbed by samples (negative values) and ions released from sample to medium (positive values).

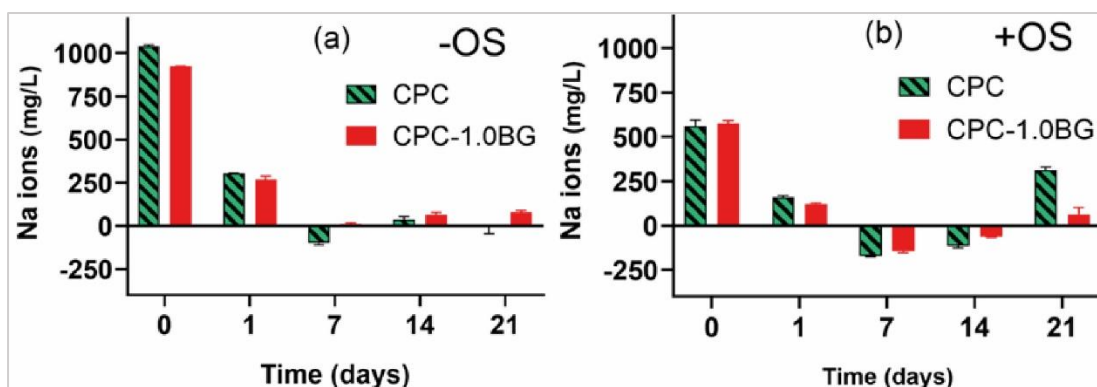


Figure 6.14 Ion changes of Na ions in (a) control (-OS) and (b) osteogenic (+OS) media. All ions of each condition were subtracted by the control cell culture medium as a blank, showing the ions in the medium adsorbed by samples (negative values) and ions released from sample to medium (positive values).

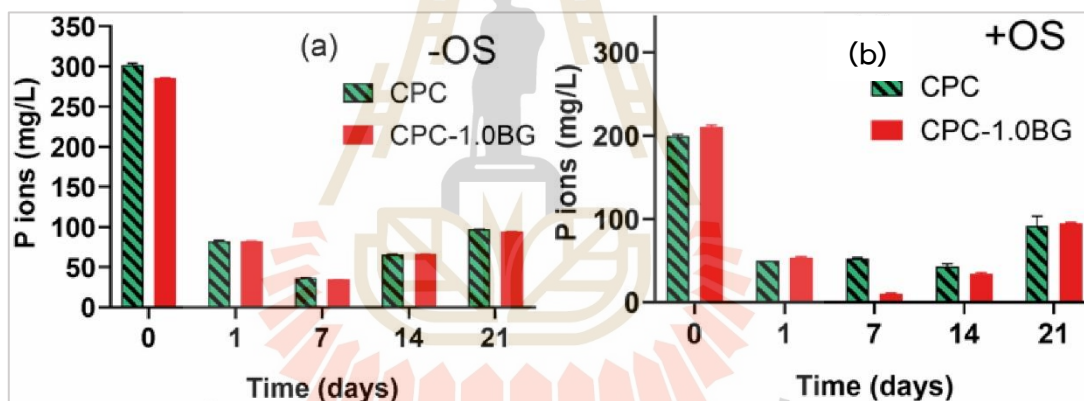


Figure 6.15 Ion changes of P ions in (a) control (-OS) and (b) osteogenic (+OS) media. All ions of each condition were subtracted by the control cell culture medium as a blank.

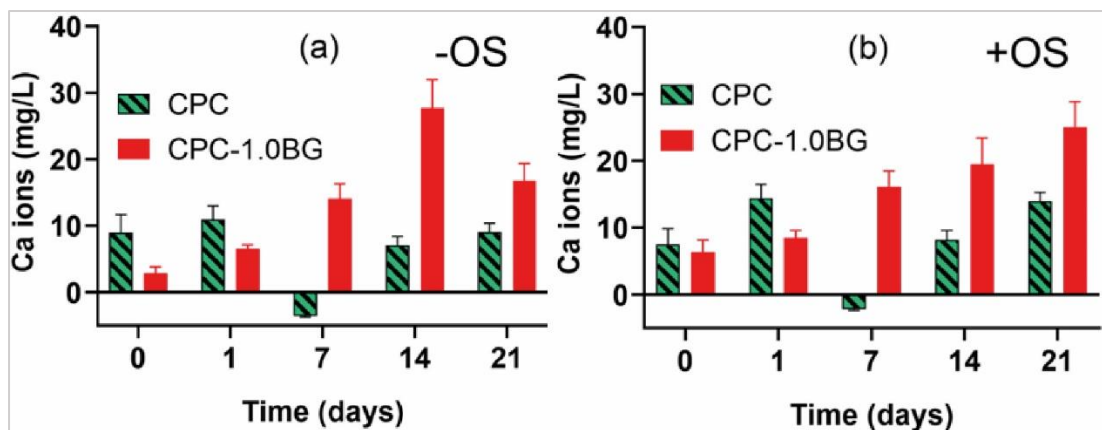


Figure 6.16 Ion changes of Ca ions in (a) control (-OS) and (b) osteogenic (+OS) media. All ions of each condition were subtracted by the control cell culture medium as a blank, showing the ions in the medium adsorbed by samples (negative values) and ions released from sample to medium (positive values).

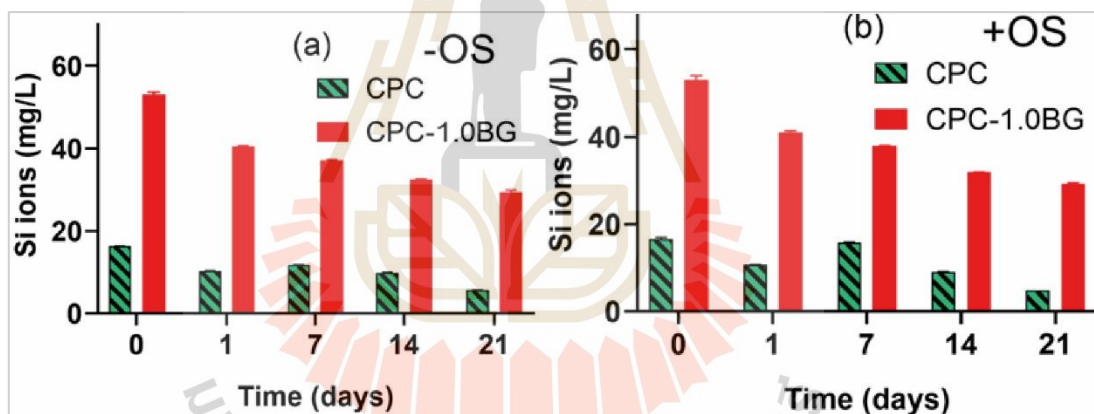


Figure 6.17 Ion changes of Si ions in (a) control (-OS) and (b) osteogenic (+OS) media. All ions of each condition were subtracted by the control cell culture medium as a blank.

6.3.6.2 Indirect cell culture: metabolic activity

The indirect culture setting was performed to determine the influence of ions sequestration by CPC and CPC/1.0BG on hASCs growth during the same time spans followed for direct culture. 5×10^3 hASCs were incubated with 500 μ l of cement-conditioned medium, as compared with the control (fresh medium). During the incubation time, the proliferation rate of hASCs cultured with cement-

conditioned media was significantly lower than that of the fresh media control (both the -OS and +OS media) (Figure 6.18). Besides, there was no significant difference in metabolic activity between the -OS and +OS conditions of both cements, nullifying the proliferative boost linked to osteogenic stimuli (Bruder, 1997).

This decrease in hASCs viability was related to the adsorption ability of CPC and CPC/1.0BG, capturing and sequestering the ions of the culture medium. In a comparable experimental setting, Klimek et al. (Klimek, 2016) ascribed the reduction of osteoblast viability to the lower levels of ions in the medium conditioned from HA due to its high adsorption capacity, resulting in the depletion of Ca^{2+} , Mg^{2+} , and HPO_4^{2-} after soaking sample in the medium. In addition, essential proteins for cell metabolism could be adsorbed by BG incorporated CPCs (El-Fiqi, 2015), and HA nanoparticles (Swain and Sarkar, 2013). Moreover, the osteogenic factors in the +OS medium could also be adsorbed by both cements, determining the null difference in the metabolic activity of cells grown in -OS and +OS medium. At last, the results on protein contents and ALP activities of indirect testing were not reliable due to the low values falling under the standard curves of the assays, further confirming the hypothesis of a sequestration of growth factors and osteogenic cues by the cements.

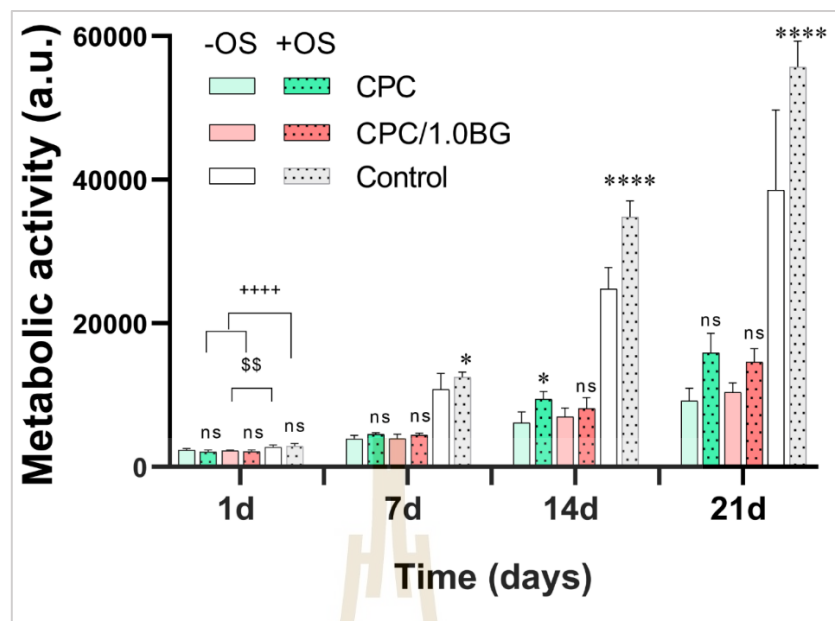


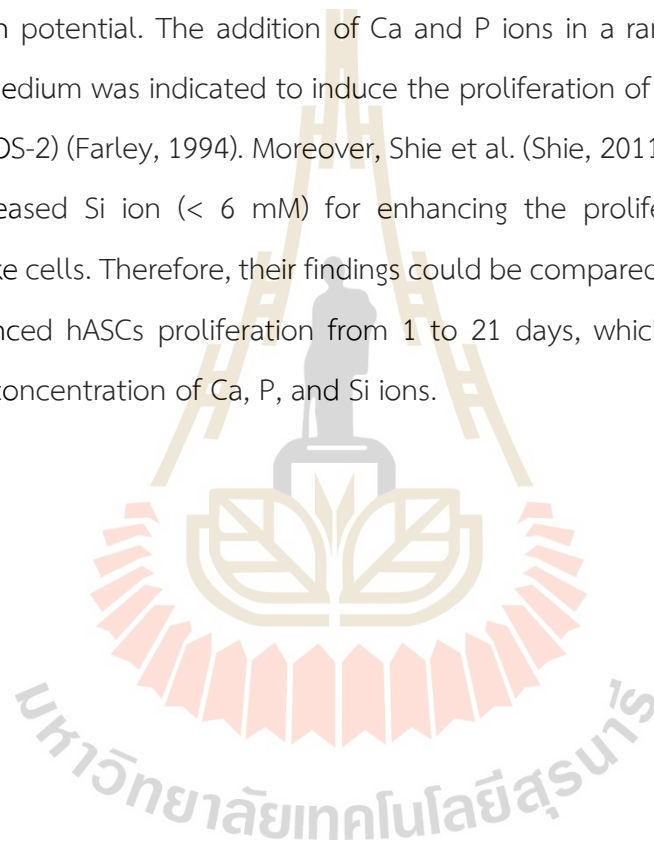
Figure 6.18 Indirect culture: hASCs proliferation on tissue plastic plate cultured with sample-conditioned medium at different time points (The comparison between complete (-OS) and osteogenic (+OS) medium within each condition (CPC, CPC/1.0BG, and control) is shown as ns = no significance, * $p < 0.05$, and **** $p < 0.0001$ / The comparison among samples grown in -OS medium as \$\$ $p < 0.01$ / The comparison among samples grown in +OS medium as **** $p < 0.0001$).

6.3.6.3 Direct cell culture: metabolic activity

The metabolic activity of hASCs loaded on all samples continuously increased during time (Figure 6.19). At day 7 (CPC) and 14 (CPC/1.0BG and coverslip control) the difference between cell metabolic activity in -OS and +OS medium became significant, confirming the higher proliferation rate following osteogenic induction. In addition, both cements stimulated the proliferation of hASCs, with CPC (+OS) and CPC/0.1BG (-OS and +OS medium), exhibiting a statistically greater metabolic activity than the respective coverslip control after 21 days of incubation. Probably the opposite trend of hASCs proliferation between direct and indirect culture depends on the facts that during direct culture, the cements can release the adsorbed

ions and osteogenic factors preserving their positive effect on cell metabolism. Moreover, the porous n-BG in CPC/1.0BG could adsorb more ions and osteogenic inducers, resulting in less essential proteins for cells in +OS when compared with CPC. This was explained by the ICP results with more adsorbed Mg/or less released Ca at day 0 and 1.

In this work, it has been shown that the ion release/adsorption played an important role in hASCs viability, proliferation, and possibly in their differentiation potential. The addition of Ca and P ions in a range between 0.2 to 2 mM to the medium was indicated to induce the proliferation of human osteosarcoma cell lines (SaOS-2) (Farley, 1994). Moreover, Shie et al. (Shie, 2011) indicated the crucial range of released Si ion (< 6 mM) for enhancing the proliferation rate of MG63 osteoblast-like cells. Therefore, their findings could be compared to the current results of the enhanced hASCs proliferation from 1 to 21 days, which was induced by an appropriate concentration of Ca, P, and Si ions.



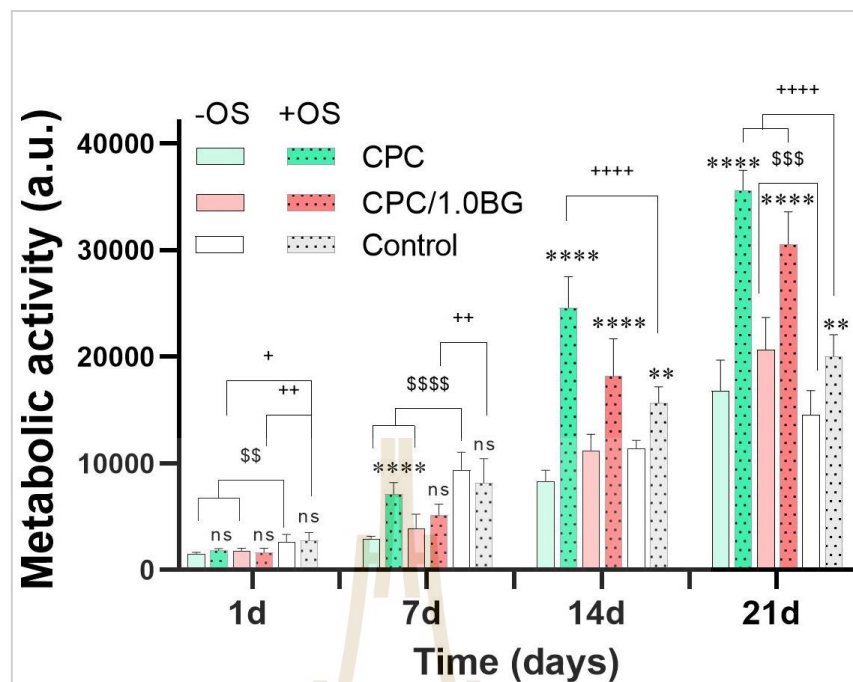


Figure 6.19 Direct culture: hASCs proliferation on samples. The comparison between complete (-OS) and osteogenic (+OS) medium within each condition (CPC, CPC/1.0BG, and control) is shown as ns = no significance, ** $p < 0.01$, and **** $p < 0.0001$ / The comparison among samples grown in -OS medium as \$ $p < 0.01$, \$\$\$ $p < 0.001$, and \$\$\$\$ $p < 0.0001$ / The comparison among samples grown in +OS medium as + $p < 0.05$, ++ $p < 0.01$, and ++++ $p < 0.0001$).

6.3.6.4 Direct cell culture: total protein contents

At day 21, cell lysates were quantified for total protein concentrations (BCA protein contents assay). The protein contents reflect the number of cells, indeed for each sample the results (Figure 6.20) showed a similar trend to the AlamarBlue assay at the same time point (Figure 6.19).

The analysed protein content of hASCs at day 21 could correlate with the number of viable cells on the samples, providing the additional supportive results respect to the metabolic activity. The result showed that hASCs seemed to favour both CPC and CPC/1.0BG more than the coverslip in both -OS and +OS media.

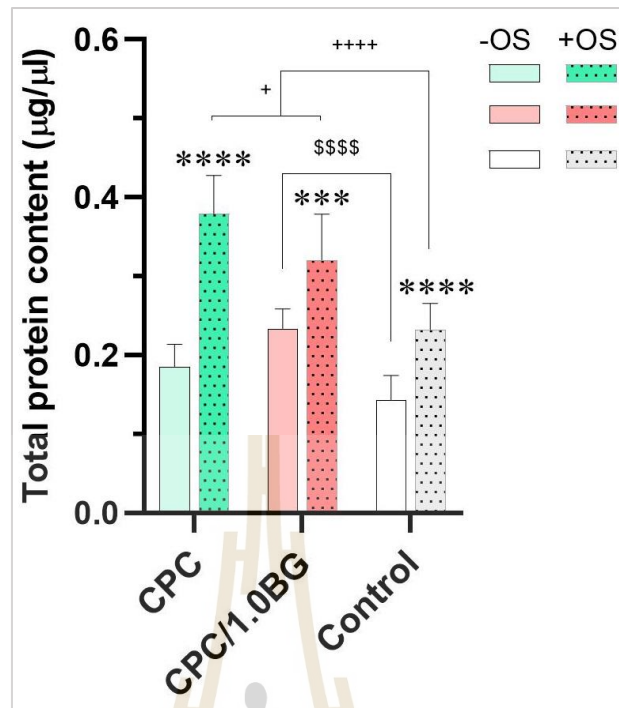


Figure 6.20 Direct culture: hASCs protein content (day 21) on samples. The comparison between complete (-OS) and osteogenic (+OS) medium within each condition (CPC, CPC/1.0BG, and control) is shown as *** $p < 0.001$ and **** $p < 0.0001$. The comparison among samples grown in -OS medium as \$\$\$\$ $p < 0.0001$. The comparison among samples grown in +OS medium as + $p < 0.05$ and ++++ $p < 0.0001$.

6.3.6.5 Direct cell culture: ALP activity

All samples presented the higher level of ALP activity when cultured in the +OS medium as compared with -OS medium. In details, the fold-increase of ALP activities of cells on CPC, CPC/1.0BG, and coverslip control were approximately 8-fold, 10-fold, and 4-fold, respectively. No statistical difference was observed between different +OS samples.

Apart from cell viability and proliferation, osteogenic commitment of hASCs was inferred monitoring ALP activity as an early bone marker. In this work, the higher fold-increase of ALP in both cements could be attributed to higher Ca (0.23-0.63 mM) and P (~1 mM) ion released from cement to medium, as compared with the

coverslip control at day 21. This was supported by the previous works, presenting the enhanced differentiation of MG63 cells with the extracellular Ca (0.4-1.4 mM) ions (Engel, 2008) and SaOS-2 cells with P (0.2-2 mM) ions (Farley, 1994). Moreover, the higher fold-increased ALP activity of CPC/1.0BG could be attributed to the higher Si ions released (~ 1 mM), as compared with the control CPC. This consideration could be in agreement with other previous studies, demonstrating the increased differentiation of SaOS-2 (Mestres, 2012) and rat bone marrow stromal cells (rBMSC) (Radin, 2005) by the extracellular Si ions ranging from 1 to 1.5 mM. However, it should be noted that the higher fold increase of ALP activity in both CPC and CPC/1.0BG could be attributed to a lower basal value in -OS medium respect to coverslips. Based on the *in vitro* testing of cells incorporated with biomaterials, cell differentiation could be stimulated either by the environment surrounding cells (scaffold), or osteogenic factors added to the culture medium, or both (Wei and Ding, 2016). In addition, the differentiation could be due to the combined influence of biomaterials and some biochemical signals, as presented in the previous works. It has previously reported a greater ALP activity in hASCs incorporated with porous HA block (de Girolamo, 2009) and HA/ β -TCP scaffold (Canciani, 2016) cultured with the osteogenic medium, as compared with the control. However, the current finding of 1 wt.% n-BG modified PAA-apatite/ β -TCP cement demonstrated a higher fold-increase in ALP activity, which could be predictive of a higher possibility for osteogenesis and/or new bone formation. Although this early bone marker was positively exhibited in the presence of n-BG added cement, further experiments assessing both gene and protein expression of key osteogenic markers, such as the transcription factors Runx2 and Osterix, the hormone Osteocalcin and several extracellular matrix constituents (e.g. Osteopontin and Collagen I), would be necessary to corroborate the current results. Moreover, data obtained under static culture conditions should be validated in more complex *in vitro* dynamic systems and at last tested with appropriate *in vivo* models.

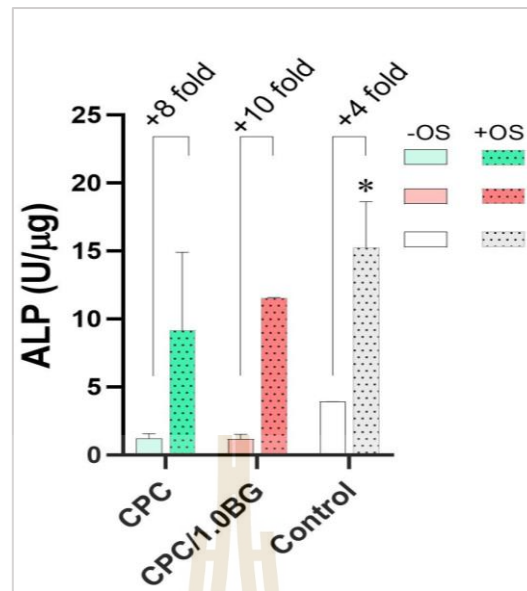
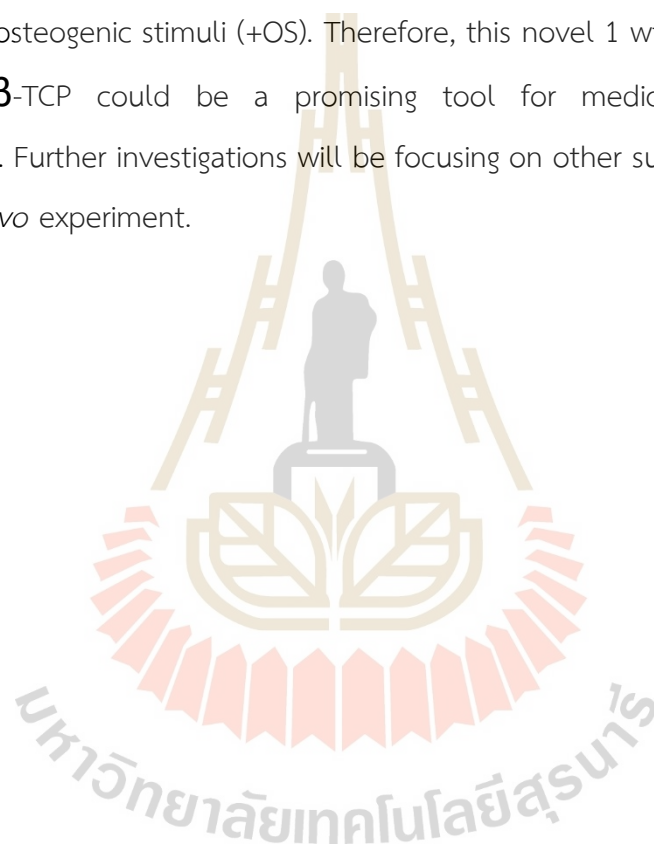


Figure 6.21 Direct culture: hASCs differentiation (day 21) on samples. The comparison between complete (-OS) and osteogenic (+OS) medium within each condition (CPC, CPC/1.0BG, and control) is shown as * $p < 0.05$.

6.4 Conclusions

In the present study, this has shown several advantages of adding the nano particle-BG with porous structure to PAA-apatite/ β -TCP cement with improved mechanical properties, faster setting reaction, and excellent hASCs biocompatibility. The results presented the optimized concentration of 0.5-1.5 wt.% n-BG in cement, showing the highest compressive strength at 1 wt.% n-BG content in this study. Besides, the higher n-BG content decreased the setting time. Afterwards, HA phase conversion was enhanced after immersion in the SBF solution for 7 days. Consequently, the bioactivity was improved by increasing n-BG contents after soaking samples over 14 days. Nevertheless, the *in vitro* testing of indirect culture demonstrated the slow rate of hASCs proliferation on both unmodified and n-BG-modified cement, as compared with the control medium. On the contrary, hASCs viability and proliferation rate were induced by the presence of both control CPC (+OS) and CPC/1.0BG (-OS and +OS medium) in the direct culture, indicating the significantly higher metabolic activity and

protein concentration over 21 days of incubation, as compared with the coverslip control. The superior cell viability and proliferation rate on both cements imply that a more favourable cell condition might increase the osteogenic differentiation compared with cells on coverslips. Also, the CPC/1.0BG seemed to be a more suitable environment than CPC due to the greater Ca and Si ions release from CPC/1.0BG (reduced the acidification of pH), resulting in higher hASC viability/proliferation in complete (-OS) and osteogenic (+OS) medium, and fold-increase of ALP activity in the presence of osteogenic stimuli (+OS). Therefore, this novel 1 wt.% nano-BG modified PAA-apatite/ β -TCP could be a promising tool for medical applications and orthopaedics. Further investigations will be focusing on other supportive assays along with the *in vivo* experiment.



CHAPTER VII

SELF-SETTING NANO-BIOACTIVE GLASS ADDED POLYMERIC APATITE/ β -TCP CEMENT FOR BONE FIXATION AND REGENERATION

In this work, different modified apatite/beta-tricalcium phosphate (β -TCP) cements were evaluated regarding their physical properties and the responses of primary human osteoblast cells (HObs) and mesenchymal stem cells (MSCs). Although polyacrylic acid (PAA) increased mechanical properties of the cement, it could cause poor apatite phase formation, a prolonged setting time, and a lower degradation rate. Consequently, bioactive glass (BG) was added to PAA/cement to improve its physical properties, such as mechanical properties, setting time, and degradation. For in vitro testing, HObs viability was assessed under two culture systems with cement-preconditioned medium (indirect) and with cement (direct). HObs viability was examined in direct contact with cements treated by different prewashing conditions. Thus, HObs presented more well-spread morphology on cement soaked in medium overnight, as compared with other prewashing regimes. In addition, the proliferation, differentiation, and total collagen production of both HObs and MSCs adhered to the cement were detected. Cells adhered to cements showed excellent proliferation in PAA/cement and PAA/BG/cement. Furthermore, the higher released Si ion and lower acidosis of PAA/BG/cement-conditioned medium resulted in an increase in osteogenic differentiation (HObs and MSCs) and enhanced collagen production (HObs in osteogenic medium and MSCs in control medium). Therefore, these results suggest that BG incorporated PAA/apatite/ β -TCP cement could be a promising formula for medical applications.

7.1 Research background, rationale, and significance

Synthetic bone graft substitute is attractive due to the limited availability of autografts and their associated costs (Matassi, 2011, Wang and Yeung, 2017). Calcium phosphate cements (CPCs) are one of the most promising biomaterials due to their remarkable bioactive and biocompatible properties for use in biomedical applications and orthopedics (Xu, 2017). CPCs could be separated in two different types of the end-setting products: hydroxyapatite/calcium deficient hydroxyapatite (HA/CDHA, apatite) and dicalcium dihydrate (DCPD brushite) (O'Neill, 2017). Although the apatite cement has been predominantly studied due to HA/CDHA is similar to the bone mineral compounds (O'Hara, 2014), its degradation was slower with respect to brushite cement (Apelt, 2004). This led to the lack of porosity of apatite cement, resulting in the new bone formation occurred on the surface of cement rather than the inside (Frankenburg, 1998). It was found that biphasic cement became a promising idea for increasing porosity due to the high in vivo resorption of β -TCP content (Daculsi, 1998). In addition, previous work revealed a positive result of biphasic calcium phosphate cement (HA/ β -TCP) augmented in the rabbit's tibial crest, indicating an approximately 2-fold increase of the new bone growth after 2 weeks of operation with respect to the control without augmentation (Rattanachan, 2020).

Although the presence of β -TCP content increased the degradation rate of cement, the compressive strength was decreased (Sariibrahimoglu, 2014, Srakaew and Rattanachan, 2014). It was noted that several parameters could improve the mechanical performance of cement, such as the incorporation of polymers, a decrease in porosity and liquid to powder ratio (Dorozhkin, 2008). The poor mechanical properties of cement were improved by the reinforcement of polymer (Canal and Ginebra, 2011), which could be used in a various forms of both liquid or solid (Geffers, 2015). In the previous findings (Thaitalay, 2021), the compressive strength of apatite/ β -TCP cement was increased with the addition of PAA aqueous solution in appropriate concentration ratio. It was revealed that the higher compressive strength of PAA-cement was influenced by the crosslink reaction between cement powder reacted

with the functional group of PAA. However, the higher concentration of PAA significantly decreased the phase conversion and bioactivity of cement.

To improve the bioactivity of cement, the addition of BG has become promising due to its excellent bioactive and biocompatible properties in both *in vitro* and *in vivo* testing (Hoppe, 2011). The previous work in chapter VI improved the bioactivity and poor phase conversion of the PAA/apatite/ β -TCP cement by adding BG ranging from 0.5-1.5 wt.%. It was found that 1.0 wt.% BG significantly improved the compressive strength of cement, including other appropriate physical properties, enhanced bioactivity, and induced osteogenic differentiation of adipose-derived stem cell *in vitro* biocompatibility. The presence of BG in cement could induce the growth factor delivery (Schumacher, 2017) and protein absorption aspect (El-Fiqi, 2015) due to its high specific surface area. This could result in the enhanced osteogenic differentiation *in vitro* of bone marrow mesenchymal stem cells (BMSCs) on BG/cement composite loaded with growth factor (rhBMP-2). Although some researchers have exhibited the excellent biological performances of BG incorporated cement (Sadiasa, 2014, Lee, 2016), a decrease in cell viability of rat primary Mesenchymal Stem cells (rMSCs) on 45S5-BG/apatite cement was detected (Stulajterova, 2017).

Based on previous cement development in chapter V and VI, we have created a novel apatite/ β -TCP cement modified with PAA and BG to improve its mechanical and biological characteristics for use in bone replacement. This present work characterized the physical properties of three different developed cements and further described their influence on HObs and MSCs responses. The cement from previous work (Rattanachan, 2020) was used as a control condition due to it revealed excellent results both *in vitro* and *in vivo* performances. Herein, HObs were cultured both with cement-conditioned media (indirect) and in direct contact with three different developed cements (direct). In addition, HObs viability in direct culture was observed on cement treated with different prewashing and preconditioning regimes. Finally, the resulted demonstrated the significant effect of ion release/adsorption aspects of these developed cements on HObs and MSCs, including cell proliferation, differentiation, and

extracellular matrix production, which will be more understandable and beneficial for further *in vivo* analysis.

7.2 Experimental procedure

7.2.1 Preparation of precursors

Alpha-tricalcium phosphate (α -TCP) and precipitated hydroxyapatite (PHA) were produced by the precipitation method. Briefly, the aqueous solution of calcium nitrate ($\text{Ca}(\text{NO}_3)_2 \cdot 4\text{H}_2\text{O}$) was mixed with phosphoric acid (H_3PO_4), followed by adding ammonia solution (NH_4OH) to adjust pH to 10.5. After mixing, the obtained white precipitated particle was filtered and washed with deionized water several times. The obtained particle was calcined at 1400 °C for 1 h (α -TCP) and then at 600 °C for 2 h (PHA). BG powder with porous structure was synthesized by the sol-gel method (Hu, 2014). Briefly, Cetyltrimethyl-ammonium Bromide (CTAB), ammonia solution (NH_4OH), tetraethyl orthosilicate (TEOS), triethylphosphate (TEP), and calcium nitrate tetrahydrate (CN) were dissolved in deionized water and absolute ethanol (EtOH) to produce the BG system of $80\text{SiO}_2:15\text{CaO}:5\text{P}_2\text{O}_5$. The obtained particle was calcined at 650 °C for 3 h.

7.2.2 Preparation of cement

Apatite/ β -TCP cement powder consisted of 62.5 wt.% α -TCP, 26.8 wt.% dicalcium phosphate anhydrous (DCPA), 8.9 wt.% calcium carbonate (CaCO_3), 1.8 wt.% precipitated hydroxyapatite (PHA), 20 wt. β -TCP, and 1 wt.% chitosan fiber. The compositions of three different apatite/ β -TCP cements were produced by mixing different solid and liquid phases, as given in Table 1. The sample was prepared by mixing the cement powder and liquid, following the topic 3.2.3.1 of Chapter III.

Table 7.1 Compositions of cement with different solid and liquid phase, and L/P ratio.

Cement group	Solid phase		Liquid phase	L/P ratio (mL/g)
	CaP (wt.%)	BG (wt.%)		
CPC	100	-	1M Na ₂ HPO ₄ + NaH ₂ PO ₄ (Mixed solution at pH 7.4)	0.40
p-CPC	100	-	1M Na ₂ HPO ₄ + 10 w/w% PAA (3:1 v/v ratio)	0.35
p-CPC/BG	100	1	1M Na ₂ HPO ₄ + 10 w/w% PAA (3:1 v/v ratio)	0.35

CaP, Apatite/ β -TCP powder; BG, Nano-bioactive glass; Na₂HPO₄, Disodium hydrogen phosphate; NaH₂PO₄, Sodium dihydrogen phosphate; PAA, Polyacrylic acid; L/P ratio, Liquid to powder ratio.

7.2.3 Properties testing and characterization of cement

The procedure and condition analysis of setting time, phase composition (XRD, Rietveld refinement), FT-IR, mechanical properties (compressive strength and young's modulus), and sample morphology analysis (fracture surface and bioactivity) were explained in Chapter III (Topic 3.2).

7.2.4 Injectability testing

2g cement paste was extruded through the syringe with the capacity of 5ml (1.8 mm internal diameter), in which each condition was tested twice. After 1.5 min of mixing and transferring cement paste in the syringe, the cement paste was tested at a controlled speed of 15mm/min using the universal testing machine (UTM, UH-100A) with a 5 kN load cell. The injection force was recorded until a maximum force of 300 N was reached. The percentage of injectability was calculated, as followed Equation 7.1 (Arkin, 2021).

$$\% \text{ Injectability} = \frac{W_p - W_f}{W_p - W_s} \times 100 \quad (7.1)$$

Where the W_p is the weight of syringe full of cement paste, W_f is the weight of syringe after injection test with remaining paste, W_s is the weight of the empty syringe

7.2.5 Degradation

The samples were soaked in SBF solution at 37 °C for different periods of time with a surface area to volume ratio of 10 mm²/ml. The SBF was changed every 3 days. After incubation, the samples were dried in the oven at 60 °C overnight. The weight of each sample was measured before and after soaking in SBF solution. The degradation of all samples was indicated by the percentage of weight loss after immersion in SBF at different time points, which was calculated as followed Equation 7.2 (Rattanachan, 2018).

$$\% \text{ Weight loss} = \frac{W_i - W_a}{W_i} \times 100 \quad (7.2)$$

Where the W_i is the weight sample before soaking in SBF solution, W_a is the weight of sample after soaking in SBF solution.

7.2.6 Nitrogen adsorption/desorption analysis

To investigate the porosity and specific surface area of cement, the N₂ adsorption-desorption isotherms of each sample were evaluated using Brunauer-Emmett-Teller (BET, Bel Sorp mini II). Prior to measurement, the samples were degassed at 120 °C for 6 h under vacuum. The pore volume distribution of each sample was derived from the desorption isotherm by Barrett-Joyner-Halenda (BJH) method with a relative pressure ranging from 0.0 to 1.0.

7.2.7 *In vitro* biocompatibility

7.2.7.1 Cell culture conditions

Human osteoblast cells (HObs) (Lot No.C-12720, Promocell) were grown in Osteoblast basal medium (Promocell) containing 1% antibiotic antimycotic solution. Mesenchymal stem cells (MSCs) (Lot No.6F4392, Lonza) were grown in Mesenchymal Stem Cell Growth Medium 2 (Promocell) containing 1% antibiotic antimycotic solution. The growth medium was changed every 4 days. Both cells were maintained at 37 °C and 5% CO₂ until reaching 70% confluence, and passage 4-7 of HObs and passage 7-9 of MSCs were used in the experiment. The control (OS-) and stimulated (OS+) medium were used for both cell responses to the cement in this study. For the control (OS-) medium, Dulbecco's Modified Eagle's Medium (DMEM) with 1000 mg/l /glucose, L-glutamine, and sodium bicarbonate were supplemented with 10% fetal bovine serum (FBS) and 25 µM Ascorbic acid. For the stimulated osteogenic (OS+) medium, 10 nM Dexamethasone and 10mM β-glycerophosphate were added to the OS- medium.

7.2.7.2 Live/Dead assay

According to the sample preparation, the cement powder was sterile by dry heat sterilization (121 °C for 10 h) and the cement liquid by membrane filtration (0.22 µm sterile filter). The samples were prepared at a size of 12 mm diameter and 2 mm height. Prior to testing with cells, the samples were prepared in different incubation processes, as shown in Table 7.2.

For the indirect culture, 1ml of OS- medium containing 2×10^4 HObs was seeded onto a glass coverslip in each well of a 24-well plate. Cells were incubated overnight, and the culture medium was removed and replaced with 800 µl preconditioned media from each cement sample (Soaked medium in Table 7.2), then cultured in 37 °C, 5% CO₂ incubator for 24 h.

Table 7.2 Conditions of cement with different preparation process.

Conditions	Procedure
Untreated	Sample as prepared
Rinsed PBS	Rinsed with 1ml PBS for 3 times (5min each time)
Soaked medium	Rinsed with 1ml PBS for 3 times (5min each time) and soaked with 1ml OS- medium overnight

PBS, Phosphate buffered saline; OS-, control medium

For the direct culture, 2×10^4 HObs or MSCs suspended in 1 ml OS- medium were seeded into each well, containing samples from different preparation processes. Each condition was performed in duplicate and incubated at 37 °C, 5% CO₂ for 1 and 7 days. The culture medium was changed every 3 days. At certain time points (1 and 7 days), cell viability of HObs and MSCs was assessed using the Live/Dead assay (Invitrogen). Live/Dead staining solution was prepared by adding 10 µl ethidium homodimer-1 and 1 µl calcein-AM to 5 ml PBS. After incubating samples for 1 and 7 days, the medium was removed and washed with 1 ml PBS. The samples were incubated with 500 µl Live/Dead solution in the incubator for 20 min and visualized using fluorescence microscope (Nikon Eclipse 50i).

7.2.7.3 pH changes, ion release/adsorption, and surface roughness

After soaking sample in 1 ml OS- medium overtime, samples preconditioned medium (Day 0) and samples conditioned medium (Day 1, 7, 14, and 21) were collected for ion release/adsorption testing. The medium was changed three times a week. The ion concentration of the culture medium was detected by Inductively coupled plasma optical emission spectrometry (ICP-OES: Optima 8000, PerkinElmer). The pH of the samples preconditioned, and conditioned medium were measured by Electrolyte-type pH meter (Denver pH/mV/Temp. Meter, UB-10). After

incubating cement overnight, the surface roughness of cement was analyzed using White light interferometer (Contour GT, Veeco).

7.2.7.4 Cell morphology

After incubating cells on samples in the OS- medium for 7 days, cell attachment was assessed by SEM analysis and F-actin staining. For SEM analysis, the culture medium was removed, and samples washed with PBS twice. Samples with cells were fixed with 1.5% glutaraldehyde in 0.1M phosphate buffer for 30 minutes at 4°C, followed by dehydration through the increasing concentrations of ethanol (From 50 to 100%). The ethanol was replaced with hexamethyldisilazane and then removed to dry in the fume hood. The samples were mounted on stubs and coated with 3 nm of Gold/Palladium. The cell attachment on samples was imaged by using SEM (Tescan Vega) equipped with a Tescan Vega3 software. For F-actin staining, samples with cells were fixed with 4% paraformaldehyde for 10 min, followed by washing with PBS three times. Samples were incubated with 0.2% Triton X-100 for 5 min and then rinsed with PBS three times. The actin cytoskeleton (Green) of cells was stained with Alexa Fluor™ 488 Phalloidin (Invitrogen) for 60 min, and the nucleus (Blue) was stained with Molecular Probes™ DAPI (Invitrogen) reagent for 5 min. Finally, the samples were rinsed with PBS three times and viewed on a fluorescence microscope (Nikon Eclipse 50i). Each condition was performed in duplicate for SEM and F-actin staining.

7.2.7.5 Cell proliferation

Prior to cell seeding, samples were rinsed with 1 ml PBS 3 times and incubated in 1 ml OS- medium overnight. For HObs and MSCs, the cell density of 2×10^4 cells in 1 ml OS- medium was separately seeded in each well containing 1 cement sample and incubated at 37 °C and 5% CO₂ for different periods. The medium was changed three times a week. Each cement condition was performed in triplicate with five different plates, as labeled day1, 7, 14, 21, and 28. For both HObs and MSCs, the AlamarBlue assay was used to detect the metabolic activity of cells at each time point. After incubating the sample at each time point, samples were transferred to the new 24-well plate and incubated with 1 ml of 10 vol.% AlamarBlue solution (5mg

Resazurin salt/ 40 ml sterile PBS, Sigma) in OS- medium. The plates were incubated at 37 °C and 5% CO₂ for 2 h. Following incubation, 200 µl of each well was transferred in triplicate to a 96-well plate. The fluorescence was read by a microplate reader (FLUOstar OPTIMA, BMG Labtech) at 544 nm excitation and 590 nm emission. The samples were washed by PBS twice and stored at -80°C for further analysis.

7.2.7.6 DNA quantification

The DNA content of both HObs and MSCs on samples was determined by using Quant-iT™ PicoGreen™ dsDNA assay kit (Thermo Fisher Scientific). After the AlamarBlue assay, 1 ml deionized water (DI) was added to each sample and subjected to three freeze-thaw cycles. The obtained cell lysates were used for DNA and Alkaline phosphatase (ALP) quantification. For PicoGreen assay, 100 µl cell lysates of each sample were transferred to a 96-well plate in triplicate, followed by the addition of 100 µl PicoGreen working solution. The fluorescence was read by a microplate reader (FLUOstar OPTIMA, BMG Labtech) at 485 nm excitation and 520 nm emission. The DNA content was estimated as compared with the standard curve following the manufacturer's instructions.

7.2.7.7 Alkaline phosphatase (ALP) assay

To evaluate the osteogenic differentiation of HObs and MSCs, the level of ALP assay was performed under the OS- and OS+ medium condition. The remaining cell lysate after the PicoGreen assay was also used for ALP activity quantification. Briefly, 20µl cell lysates were transferred to a 96-well plate in triplicate, and then added 200 µl p-Nitrophenyl phosphate (pNPP) substrate solution to each well. The SIGMA FAST™ pNPP (Gold and silver tablet, Sigma Aldrich) enzyme substrate solution was prepared according to the the manufacturer's instructions. A 96-well plate containing the mixture of cell lysates with pNPP solution was read by microplate reader (Multiskan Ascent, Labsystems) at 405 nm every 30 sec for 30 min. Finally, the ALP activity was normalized by the DNA content.

7.2.7.8 Total collagen secretion

The total collagen production of HObs and MSCs on sample was analyzed by using a total collagen assay (QuickZyme Biosciences). 2×10^4 cells/sample was cultured in OS- and OS+ medium and incubated at 37 °C and 5% CO₂ for 14 and 28 days, respectively. Samples were transferred to the new 24-well plate and washed with PBS twice, followed by adding 500 µl 0.25% trypsin/EDTA to each well and incubating at 37 °C for 30 min. Samples were hydrolysed at 95 °C for 20 h with 12M HCl and compared with the standard curve following the manufacturer's instructions. The obtained solution was diluted with DI water at a volume ratio of 2:1. Afterward, 35 µl sample solution and 75 µl assay buffer were transferred to 96-well plate and incubated at room temperature for 20 min, followed by adding 75 µl assay reagents and incubated at 60 °C for 1 h. The well plate was read at a wavelength of 570 nm by using microplate reader (Multiskan Ascent, Labsystems).

7.2.7.9 Statistical analysis

In this study, the statistical significances were analyzed by using GraphPad Prism 8 software (GraphPad Software, USA). The statistical comparison between each data group was performed by One-way ANOVA coupled with Tukey's multiple comparison test at the interval with the confidence interval of $p < 0.05$. The results were presented as mean \pm standard deviation (SD).

7.3 Result and discussion

7.3.1 Setting time measurement

The handling properties of different cement formulations were measured, including setting time and injectability. Figure 7.1 presented the setting time of three cements with different liquid to powder ratio (L/P) of 0.35 and 0.40. The control CPC exhibited the initial and final setting time of 6.0 ± 1.4 min and final setting time of 13.5 ± 0.7 min with L/P ratio of 0.40. Meanwhile the control CPC could not be formed and measured using L/P ratio of 0.35. The initial and final setting time of p-CPC were 16.5 ± 0.7 min and 28.5 ± 0.7 min (0.35 L/P ratio), and 18.8 ± 1.1 min and 42.5 ± 3.5 min

(0.40 L/P ratio). As compared with p-CPC, the presence of BG in cement decreased setting time in both L/P ratio of 0.35 (initial; 9.5 ± 0.7 min, final; 20.0 ± 1.4 min) and 0.40 (initial; 12.8 ± 0.4 min, final; 35.0 ± 1.4 min). As a result, the CPC sample could not be prepared with L/P ratio of 0.35. In addition, the setting time of p-CPC and p-CPC/BG was substantially longer than the required setting time (initial time < 8 min, final time < 15 min) for use in orthopaedic applications (Khairoun, 1998). Therefore, the appropriate L/P ratios of 0.40 ml/g (CPC) and 0.35 ml/g (p-CPC and p-CPC/BG) were fixed for further analysis.

This recent work investigated and described the influence of three different apatite/ β -TCP cements on physical properties and cellular behaviours. PAA and BG components were introduced in the cement to improve some limited performances, such as low mechanical properties as previously described. It was found that PAA reduced pH of cement liquid (data shown in Table 5.1 of Chapter V). Thus, the lower pH of cement liquid could affect the dissolution of cement powder, as shown in the solubility diagram of calcium phosphate salt (Chow, 2001). In addition, PAA could increase the viscosity of cement liquid, resulting in poor mobility of ion dissolved in cement liquid (Majekodunmi and Deb, 2007). Afterward, this poor ion mobility could be related to poor solubility of cement powder. This poor solubility of cement powder could affect the setting reaction of PAA incorporated cement, presenting the increased setting time of both p-CPC and p-CPC/BG in this current work. In the previous work (Sadiasa, 2014), the addition of BG to cement increased the amount of Ca ions in the cement, resulting in a faster setting time. Moreover, the reduced setting time of BG added cement could be due to the increased rate of hydroxyapatite formation, and liquid absorption/adsorption ability of BG in the cement (El-Fiqi, 2015). This aspect could be attributed to the current result, indicating the decreased setting time of p-CPC/BG with respect to p-CPC.

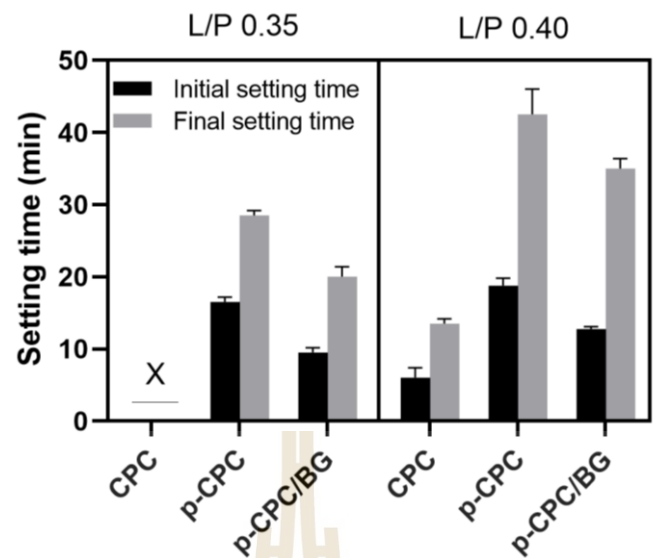


Figure 7.1 Setting time of all cement conditions at different L/P ratio of 0.35 and 0.40. The unmoldable sample was denoted as X.

7.3.2 Injectability

For injectability testing, all cement paste condition could be extruded through a 5ml syringe with an internal diameter of 1.8 mm. As compared with the control CPC ($74.1 \pm 2.5\%$), the presence of PAA in cement improved the injectability of $85.5 \pm 2.7\%$ for p-CPC and $82.9 \pm 1.0\%$ for p-CPC/BG.

According to the result of setting time measurement, the decreased setting time of BG incorporated cement had no significant impact on injectability when compared between p-CPC and p-CPC/BG. The injectability of cement could be affected by various factors, such as setting reaction, and L/P ratio, (O'Neill, 2017) etc. Elena et al. (Burguera, 2008) revealed that the injectability of cement could be increased by increasing L/P ratio. Although the control CPC (0.40) had a higher L/P ratio, it was less injectable than both p-CPC and p-CPC/BG (0.35). This improved injectability of p-CPC and p-CPC/BG could be correlated to the prolonged setting time of PAA incorporated cement.

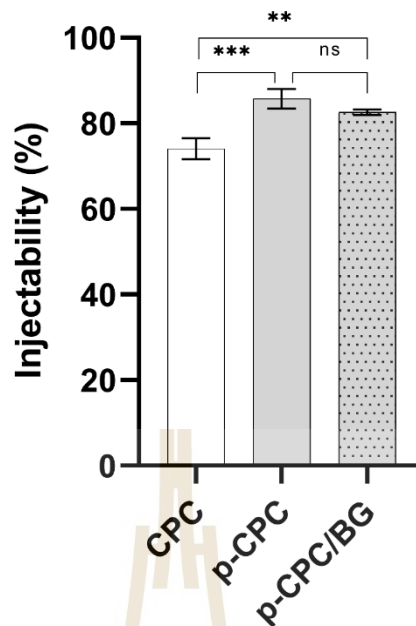


Figure 7.2 Injectability percentage of each cement condition with an appropriate selective L/P ratio (0.35; p-CPC and p-CPC/BG, 0.40; CPC). The statistical comparison among sample conditions: ns = no significance, ** $p < 0.01$, and *** $p < 0.001$.

7.3.3 Mechanical testing

Figure 7.3 and 7.4 presents the mechanical properties (Compressive strength and Young's modulus) of each cement after immersion in SBF solution over 28 days. The results showed that the compressive strength of all samples increased dramatically after soaking in SBF solution for 7 days. Afterward, the compressive strength of both control cement (CPC) and polymeric cement (p-CPC) remained stable until 28 days of incubation. Meanwhile, the compressive strength of bioactive glass added polymeric cement (p-CPC/BG) slightly decreased from 7 to 28 days of incubation, which could be attributed to the degradation of BG during incubation. Young's modulus exhibited the same trend, as compared with the compressive strength.

In the previous study (Thaitalay, 2021), the addition of PAA into cement indicated the crosslink reaction between functional group of PAA and cement powder,

resulting in the enhanced compressive strength. This is relevant to the current results, presenting the higher compressive strength and young's modulus of p-CPC and p-CPC/BG cement when compared with the control CPC (Figure 7.3 and 7.4). Besides, the presence of BG in cement increased the mechanical properties of polymeric cement (p-CPC), resulting in superior mechanical properties of p-CPC/BG. This could suggest that the BG particles filled the porous structure of the cement, producing a denser microstructure. This assumption could be relevant to previous work on BG modified TTCP (Medvecký, 2017) and TTCP/DCPA cement (Yu, 2013). They reported that increasing the amount of BG particles reduced the pore size in the structure of cement, resulting in enhanced compressive strength. Furthermore, it should be noted that the difference in L/P ratio among cement conditions could also influence on the mechanical properties.

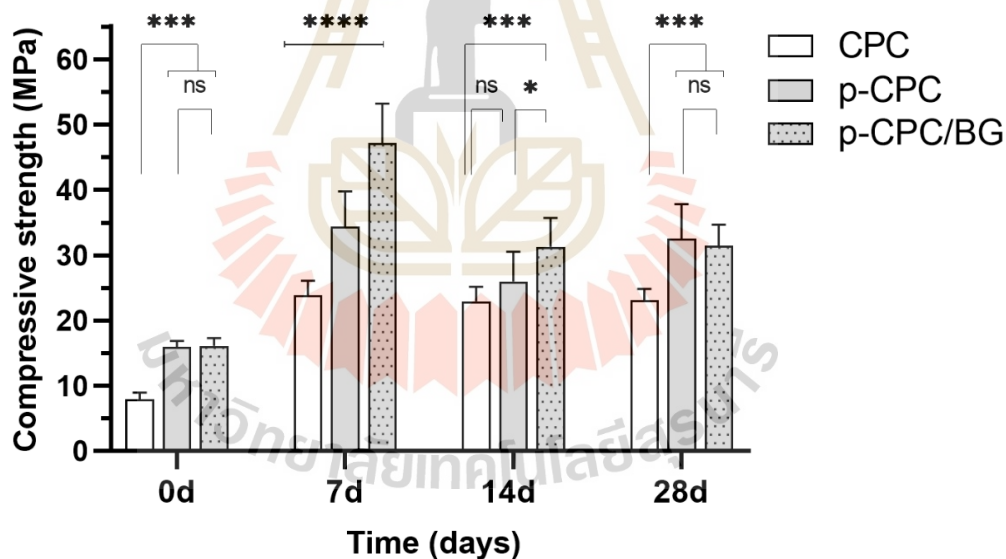


Figure 7.3 Compressive strength of each cement condition after immersion in SBF solution over 28 days. The statistical comparison among sample conditions is shown as ns = no significance, * $p < 0.05$, *** $p < 0.001$, and **** $p < 0.0001$.

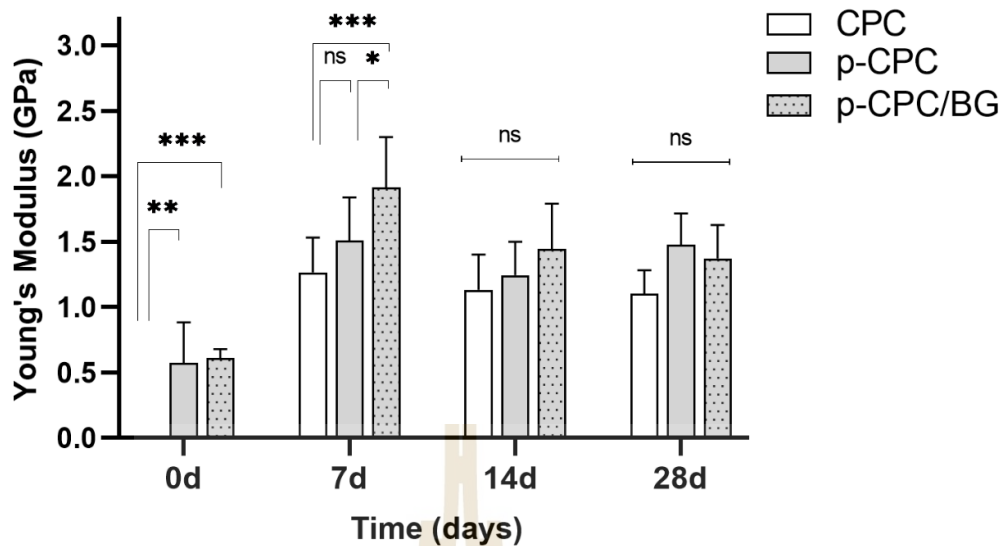


Figure 7.4 Young's Modulus of each cement condition after immersion in SBF solution over 28 days. The statistical comparison among sample conditions is shown as ns = no significance, * $p < 0.05$, ** $p < 0.01$, and *** $p < 0.001$.

7.3.4 Phase composition analysis

XRD patterns indicated phase compositions of three different cements, as followed the data sheet numbers of 09-0432 (HA), 29-0359 (α -TCP), 09-0169 (β -TCP), 47-1743 (CaCO_3), and 70-0359 (DCPA). The results presented the phase conversion of the starting powder to HA as one of the main setting products with respect to other residual phases over 28 days of incubation. After forming cement (0 day), the percentage of HA phase in these cements (0d) for CPC, p-CPC, and p-CPC/BG were 17.0, 14.2, and 16.3 wt.%, respectively. Afterward, the HA phase conversion of all cement conditions continuously increased, while other remaining phases gradually decreased after immersion in SBF solution from 7 to 28 days. According to the phase change in set cement, remaining DCPA, β -TCP, and CaCO_3 phases of all condition continuously decreased over 28 days of incubation. The control CPC showed fewer remaining DCPA in set cement over times when compared with p-CPC and p-CPC/BG.

Based on phase transformation, it was reported that the PAA could cover the surface of the cement powder, resulting in the less α -TCP phase converted into HA (Thaitalay, 2021). This is correlated to the current work, presenting the less converted HA phase in PAA incorporated cement (p-CPC), as compared with the control CPC from 0 to 28 day. In addition, the presence of PAA appeared to interfere and encapsulate other particles, resulting in the more remaining phases in cement matrix for DCPA (day 7 to 28) and CaCO_3 (day0) of p-CPC and p-CPC/BG and that for β -TCP (day0 to 28) of p-CPC when compared with the control CPC. Afterward, the BG content was added to p-CPC in order to enhance the phase conversion of HA. It was reported that the HA formation in the cement matrix was enhanced by the addition of BG due to the BG particles degraded and released more Ca^{2+} during the setting reaction of cement (El-Fiqi, 2015). Therefore, this feature could improve the poor phase conversion of p-CPC, indicating the higher converted HA phase of p-CPC/BG at 0 day.

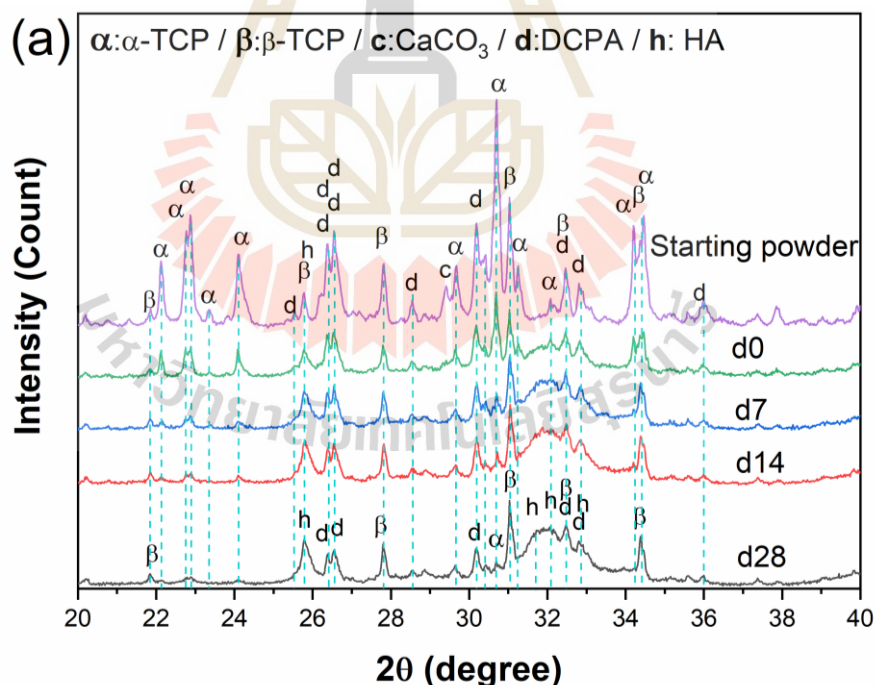


Figure 7.5 XRD patterns of (a) CPC, (b) p-CPC, and (c) p-CPC/BG cement after immersion in SBF solution over 28 days.

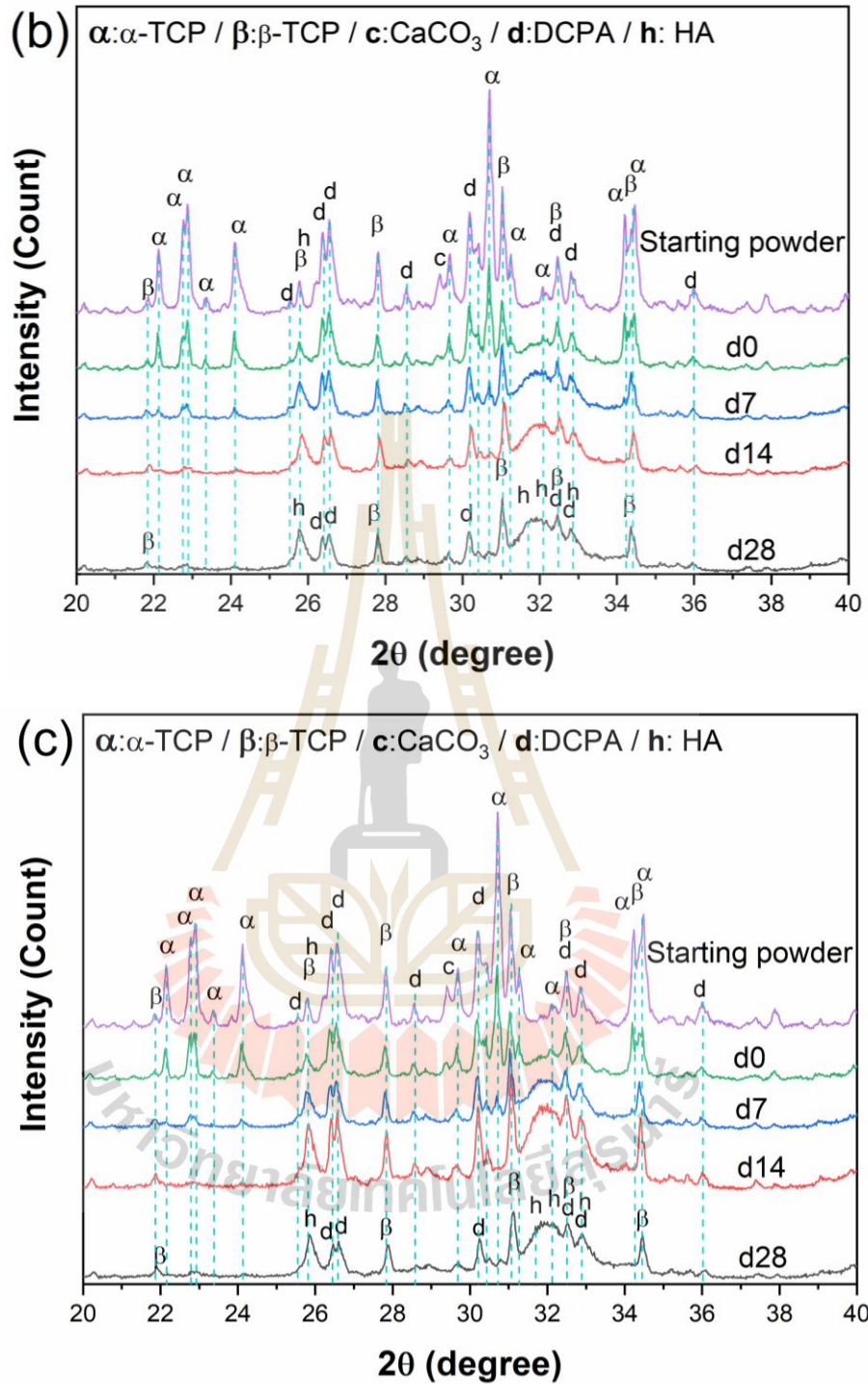


Figure 7.5 XRD patterns of (a) CPC, (b) p-CPC, and (c) p-CPC/BG cement after immersion in SBF solution over 28 days. (continued)

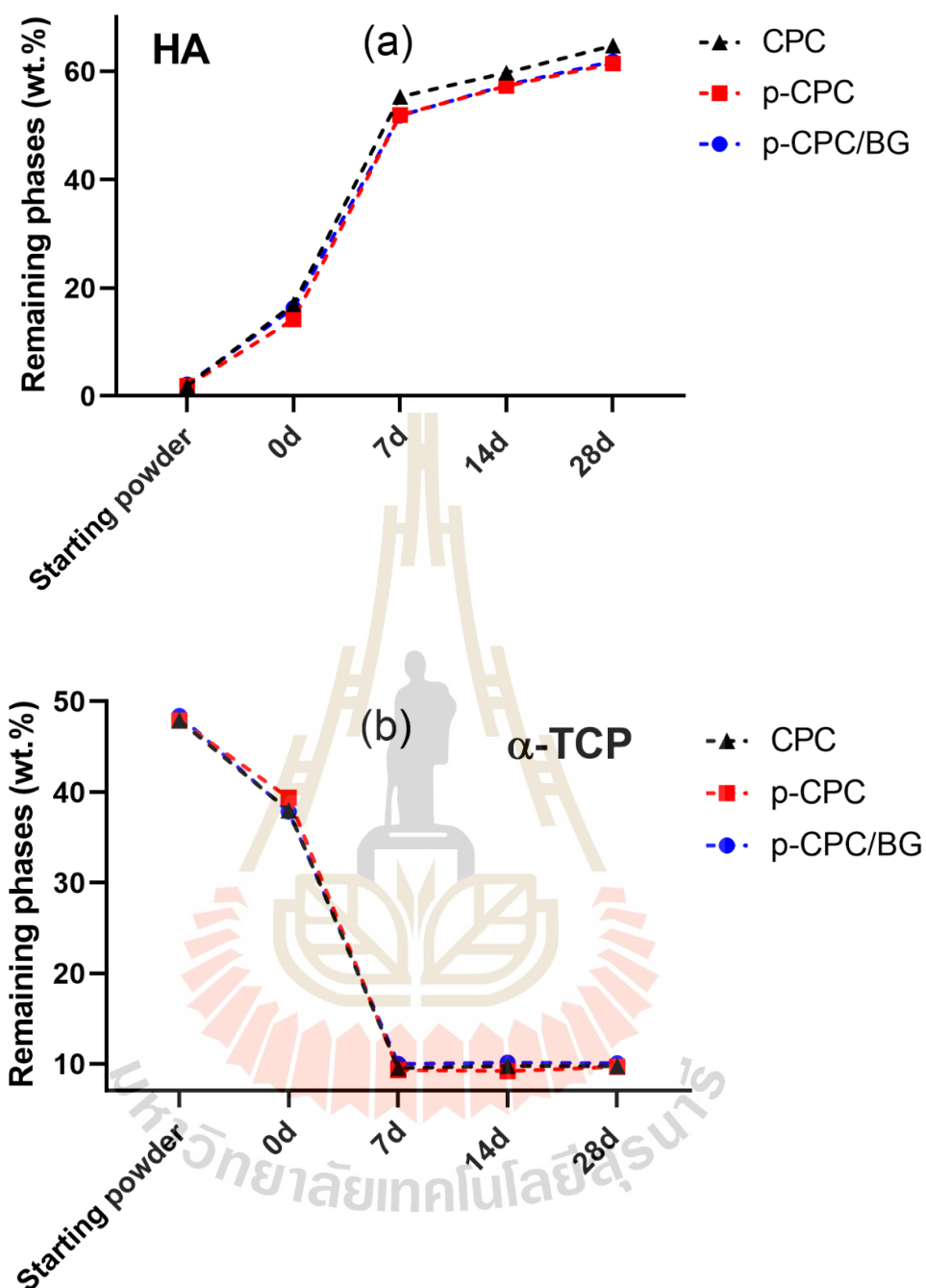


Figure 7.6 Remaining phases of (a) HA, (b) α -TCP, (c) DCPA, (d) CaCO_3 , and (e) β -TCP in cement matrix of each cement condition after immersion in SBF solution over 28 days.

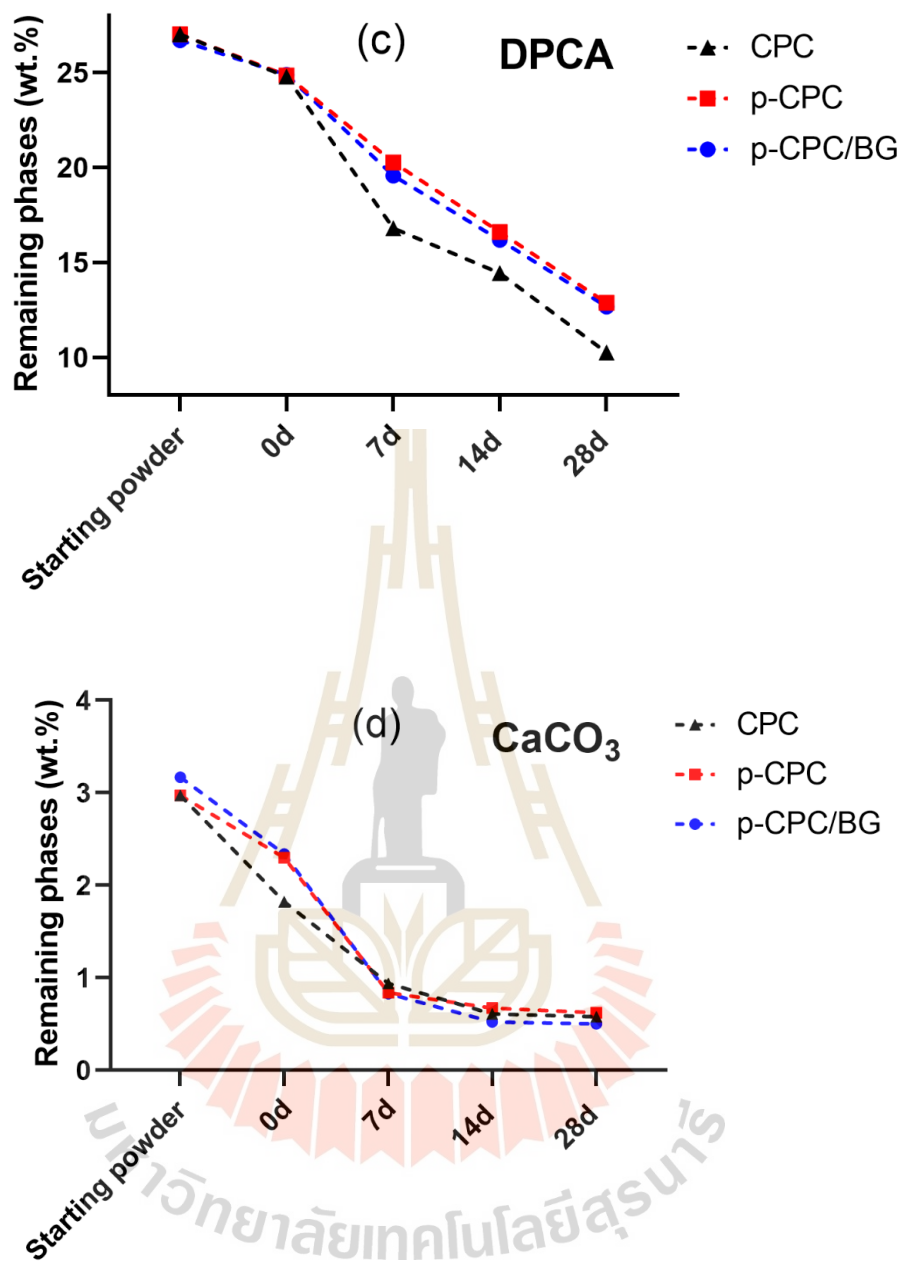


Figure 7.6 Remaining phases of (a) HA, (b) α -TCP, (c) DCPA, (d) CaCO₃, and (e) β -TCP in cement matrix of each cement condition after immersion in SBF solution over 28 days. (continued)

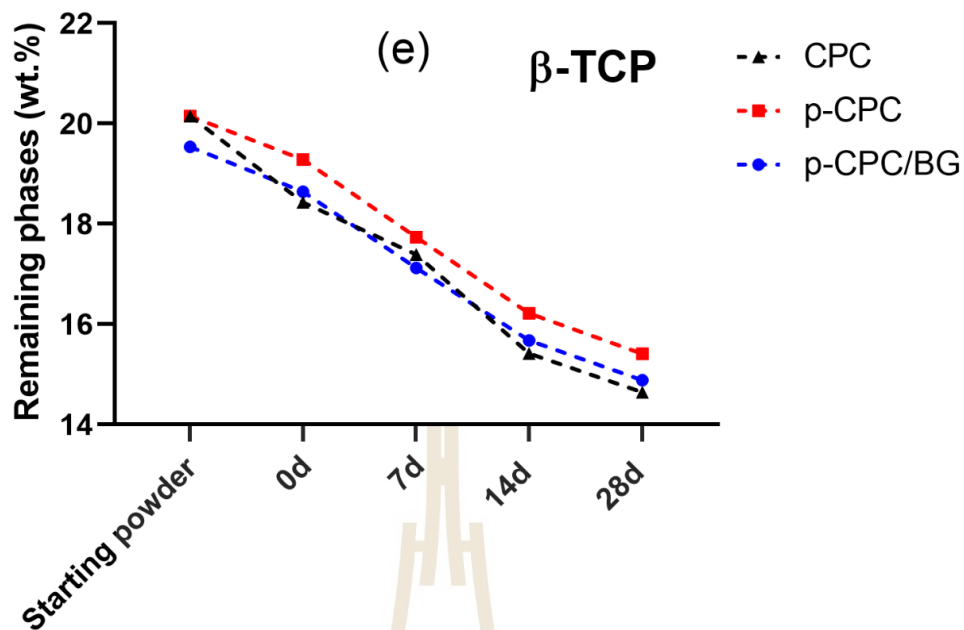


Figure 7.6 Remaining phases of (a) HA, (b) α -TCP, (c) DCPA, (d) CaCO_3 , and (e) β -TCP in cement matrix of each cement condition after immersion in SBF solution over 28 days. (Continued)

7.3.5 FT-IR

Figure 7.7 presents FT-IR spectra of each cement condition before and after soaking in SBF solution for 28 days. The results showed that there were no significant differences among the three cements, which were similar to the XRD results. The peak of starting cement powder indicated different functional groups, consisting of major α -TCP (550, 583, 1025, and 1039 cm^{-1}), CaCO_3 (857 cm^{-1}), and poor HA (960 cm^{-1}) peaks. After forming cement (d0), the FT-IR spectrum of set cement slightly changed, detecting α -TCP and HA peaks with disappeared CaCO_3 . Afterward, intense peaks of HA (470, 561, 600, 873, 960, 1020, 1415, and 1453 cm^{-1}) were indicated during 28 days of incubation (d7-28). This could be attributed to the phase transformation of α -TCP to HA after the cement has set, which was supported by the XRD results.

In this study, α -TCP (550, 583, 1025, and 1039 cm^{-1}) peaks were supported by previous works (Carrodegua and De Aza, 2011, Kolmas, 2015), indicating anti-

symmetric P-O bending (ν_4 , 551 and 585 cm^{-1}) and stretching (ν_3 , 1025 and 1039 cm^{-1}) triply degenerate. In addition, the peak of CaCO_3 (857 cm^{-1}) in the starting cement powder was consistent with the C-O bending vibration of 857 cm^{-1} (Islam, 2012, Zhu, 2014). Furthermore, the converted HA peaks (470, 561, 600, 873, 960, 1020, 1415, and 1453 cm^{-1}) were indicated after soaking in SBF solution for 28 days. These peaks were relevant to previous studies (Rehman and Bonfield, 1997, Smolen, 2013), which assigned them to symmetric O-P-O bending vibration (ν_2 : 470 cm^{-1} and ν_4 : 601 cm^{-1}), anti-symmetric P-O stretching (ν_1 , 962 cm^{-1}) and bending (ν_4 , 561 cm^{-1}) vibrations, asymmetric P-O stretching (ν_3 , 1022 cm^{-1}), and carbonate (ν_3 , 1417 and 1455 cm^{-1}). This could be related to the phase transformation of α -TCP to HA after cement has set (d0) and been incubated in SBF solution over 28 days (d7-28).

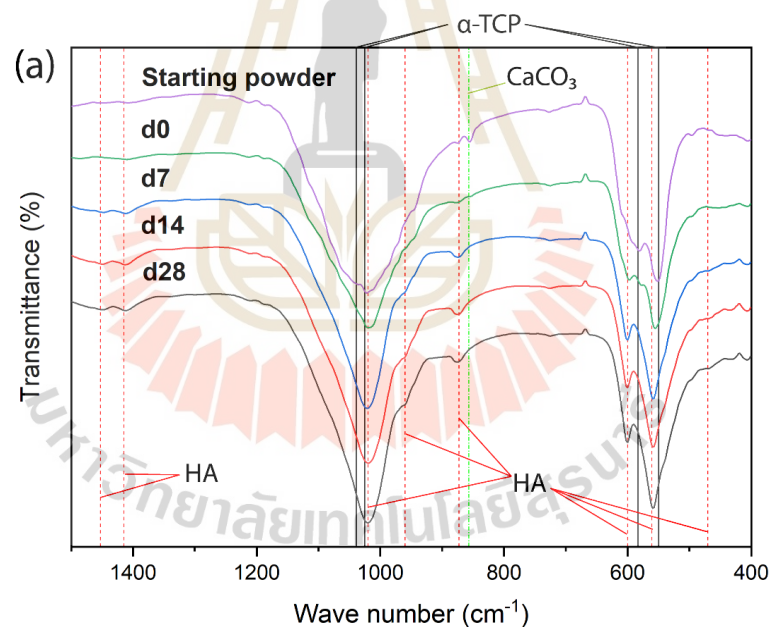


Figure 7.7 FTIR patterns of (a) CPC, (b) p-CPC, and (c) p-CPC/BG cement after immersion in SBF solution over 28 days.

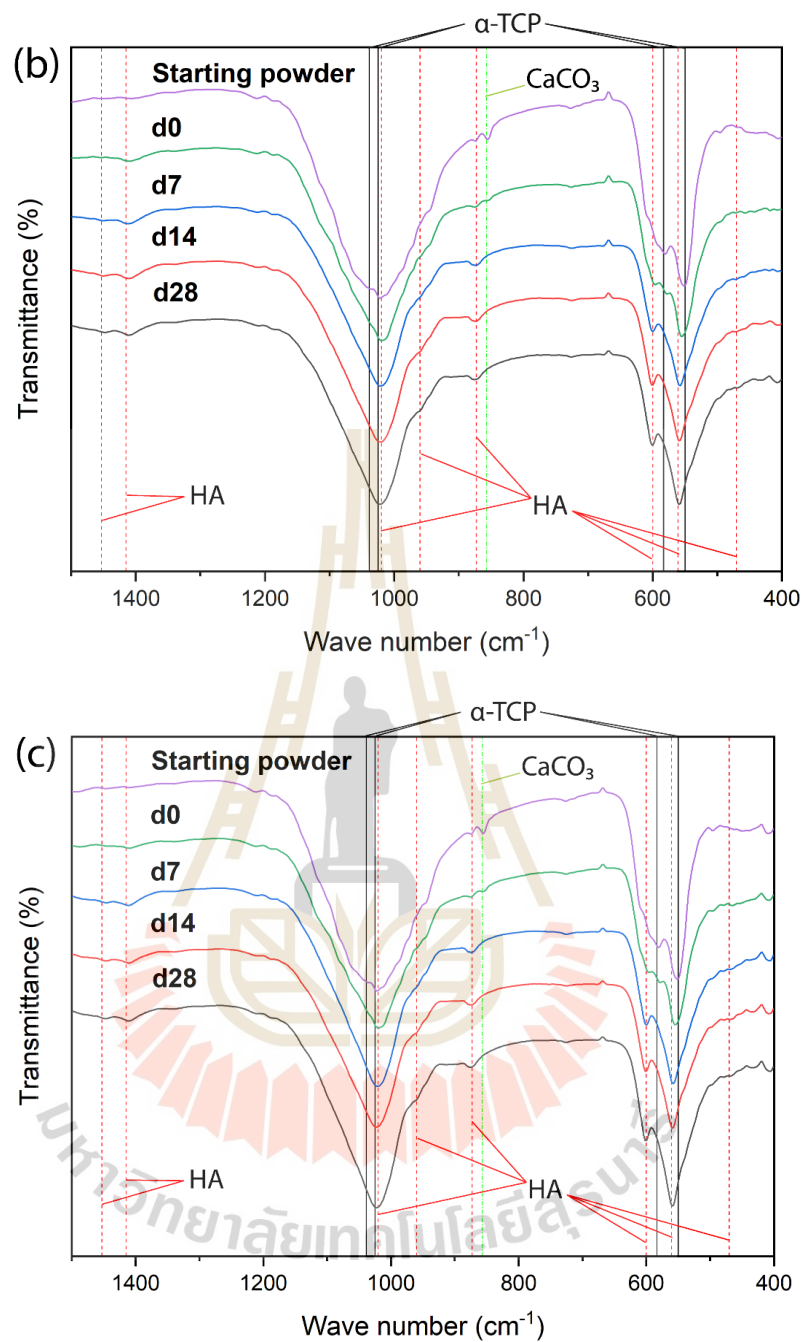


Figure 7.7 FTIR patterns of (a) CPC, (b) p-CPC, and (c) p-CPC/BG cement after immersion in SBF solution over 28 days. (Continued)

7.3.6 Degradation

The weight loss percentage of control CPC was higher than both p-CPC and p-CPC/BG after 7 days of incubation. Afterward, weight loss percentage of all samples increased and remained constant from 14 to 28 days of incubation.

According to the phase composition results, PAA encapsulated some of the starting powder. This aspect also reduced the degradation of p-CPC (7 to 28 days) and p-CPC/BG (7 days) during the incubation, as shown in Figure 7.8. Moreover, the presence of degradable BG in cement also increased the degradation of cement, resulting in the higher weight loss of p-CPC/BG with respect to p-CPC (14 to 28 days). This feature was consistent with the previous result (Liu, 2008), showing superior degradation of BG added apatite cement with respect to the control cement without BG. However, the fewer remaining β -TCP phases in CPC and p-CPC/BG in the cement matrix could also reflect the superior degradation with respect to the p-CPC.

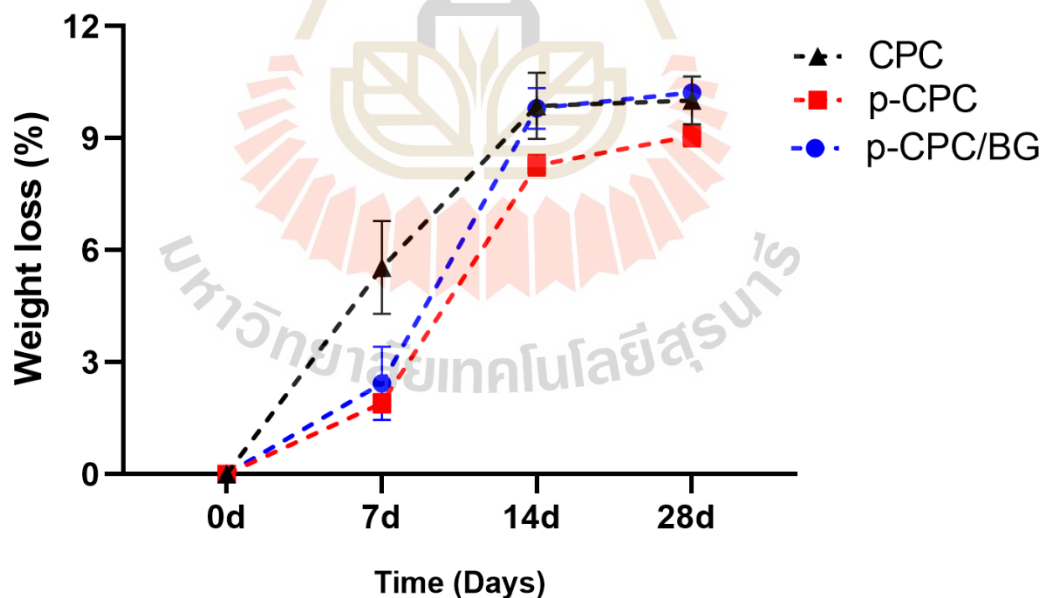


Figure 7.8 Weight loss percentage of each cement condition after immersion in SBF solution over 28 days.

7.3.7 Nitrogen adsorption/desorption analysis

The N₂ adsorption-desorption isotherms of three cements were analysed before and after immersion in SBF solution for 28 days, as shown in Figure 7.9 (a). The isotherm of all cements could be considered as type IV with H3 hysteresis loop, reflecting the mesopore and macropore structure according to the IUPAC classification (Sing, 1985, Murugesu, 2017). The pore size distribution of all cement ranged from 2.4-190.5 nm, indicating mesopore and macropore. The total pore volume of all conditions rapidly increased, in which the significant change could be measured only in macropore of the control CPC over 28 days of incubation. In addition, the macropore of CPC was higher than both p-CPC and p-CPC/BG at 28 days. Meanwhile, p-CPC and p-CPC/BG presented greater mesopore when compared with the control CPC. The specific surface area of all cement was not statistically difference after forming cement (0d). Afterward, the surface area of both p-CPC and p-CPC/BG was higher than that of the control CPC.

As a result, there was no significant difference in total pore volume among each cement condition before and after immersion in SBF for 28 days. However, the macropore in CPC was significantly lower than that in p-CPC and p-CPC/BG after forming cement at 0 day. This lower macropore volume in control CPC could be attributed to the higher entangled CDHA precipitation in the set cement, as evidenced in the phase composition result. This aspect could lead to a more compact structure in the cement matrix of CPC, resulting in less macropore volume when compared with p-CPC, and p-CPC/BG. This consideration could be supported by the previous works (Fernández, 1996, Ginebra, 1997, Vlad, 2012, Vojtova, 2019). They reported that the growth of precipitated CDHA crystal in the set cement formed a more compact cement microstructure, resulting in a smaller pore in the cement matrix. After 28 days of incubation, the greater macropore volume could be correlated to the higher DCPA degradation in CPC, as compared with p-CPC and p-CPC/BG. Thus, the higher degradation could result in more supersaturated with respect to phosphate and calcium ions (Ginebra, 2004). This could explain the more precipitated CDHA growth in

CPC (64.8 wt.%) when compared with p-CPC (61.4 wt.%) and p-CPC/BG (61.9 wt.%), as witnessed in the phase composition result at 28 days of incubation. A previous work (Vojtova, 2019) reported that the higher CDHA precipitation in the cement matrix could reduce the pore size in the cement. This explanation could relate to the result in this current work, indicating lower mesopore in CPC when compared with p-CPC and p-CPC/BG. Consequently, the lower mesopore could lead to the lower specific surface area in CPC, as compared with other ones.

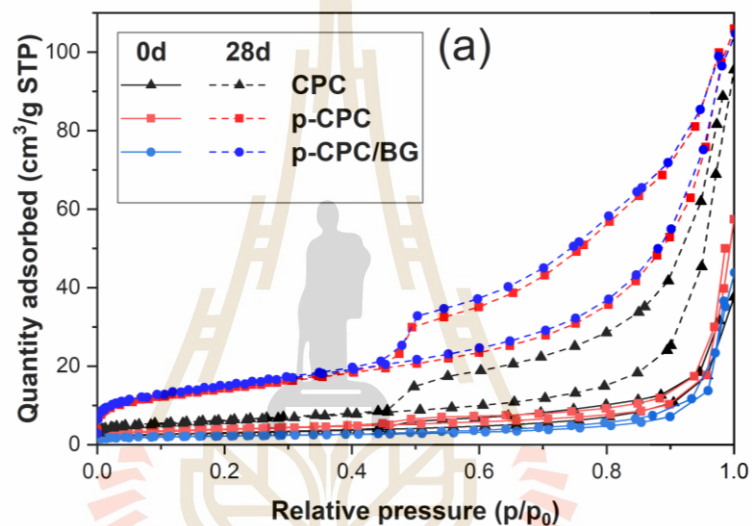


Figure 7.9 (a) N_2 adsorption-desorption isotherms and (b) pore size distribution curves of each cement condition, as comparing samples before (0d) and after immersion in SBF for 28 days (28d).

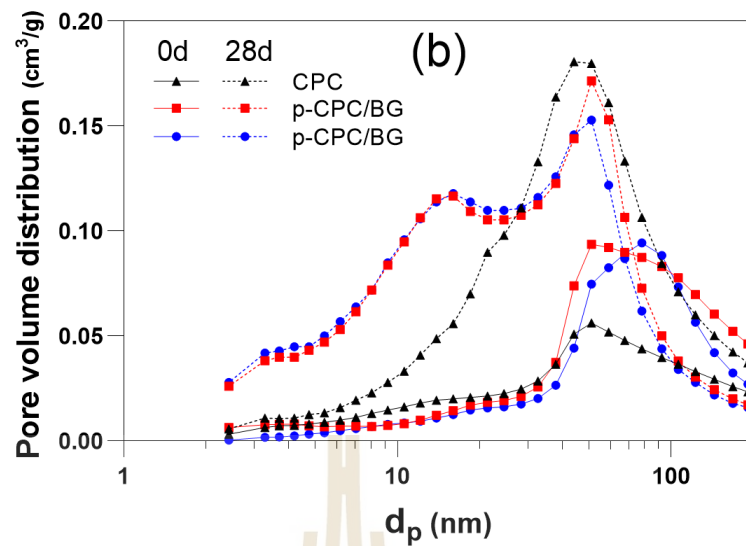


Figure 7.9 (a) N_2 adsorption-desorption isotherms and (b) pore size distribution curves of each cement condition, as comparing samples before (0d) and after immersion in SBF for 28 days (28d) (Continued).

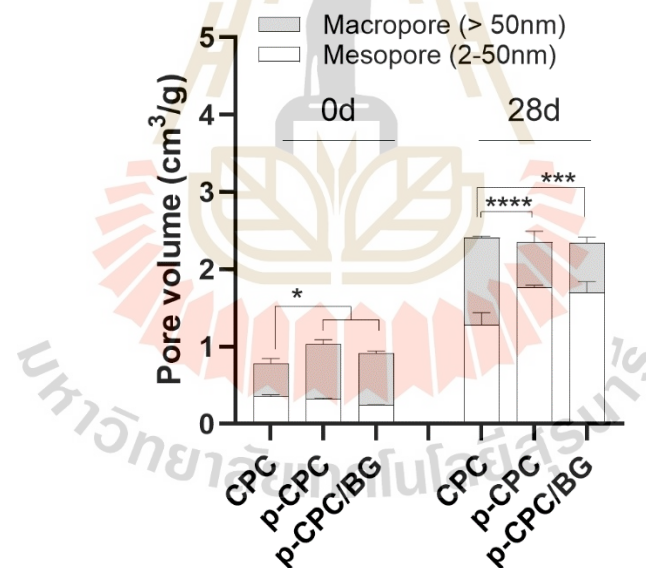


Figure 7.10 Cumulative pore volume (Macropore and mesopore) of each cement condition, as comparing samples before (0d) and after immersion in SBF for 28 days (28d). The statistical comparison among sample conditions is shown as * $p < 0.05$, *** $p < 0.001$, and **** $p < 0.0001$.

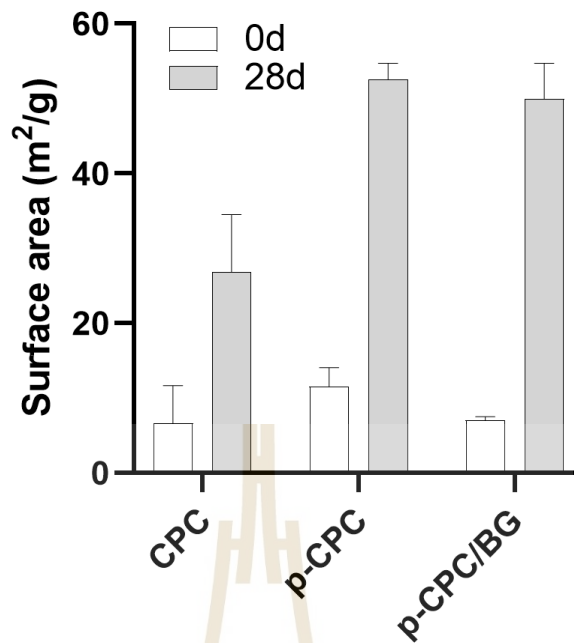


Figure 7.11 Specific surface area of each cement condition, as comparing samples before (0d) and after immersion in SBF for 28 days (28d).

7.3.8 Cement morphology analysis

SEM images exhibit the fracture and surface of each cement condition before and after soaking in SBF solution at different time points. For the fractured samples, all cement conditions displayed a similar structure. At x100 magnification, the presence of chitosan fiber could be observed in all fractured samples. Meanwhile, the higher number of micropores could be noticeable when increasing incubation time with respect to the unsoaked samples (d0). At x5000 magnification, all fractured cements at 0 day exhibited flower-like crystal and irregularly shaped structures of other remaining cement powders. After soaking cement in SBF solution for 7 to 28 days, more flower-like crystal structures were found as compared with the unsoaked cement. For bioactivity, the surface of samples was observed in order to detect the crystal-like structures deposited on the sample at each time point. The sample surface of three cements showed a similar structure at day 0, presenting the irregular structure of starting cement powder. After incubating the sample in SBF solution, the needle-

like crystal formation was clearly observed for CPC, p-CPC/BG, and p-CPC at days 7, 14, and 28, respectively.

As a result, the number of micropores in the fractured cements was observed after sample incubation in SBF solution, representing the degradable ability of these cements. This feature could support the results of weight loss percentage and porosity. In addition, the more flower-like crystal structures were found when increasing the soaking time, which could describe the higher converted HA phases in these cements. This aspect could be supported by the results of phase composition and FT-IR, indicating the higher converted HA after soaking in SBF solution for 28 days. Apart from the fractured samples, bone-like HA deposition on the sample surface in SBF solution was used to assess the bioactivity of bioactive compounds (Kokubo and Takadama, 2006). It was found that the needle-like structures were observed on CPC after day 7, which became denser from day 14 to 28. Meanwhile, the needle-like structures on p-CPC and p-CPC/BG were also discovered after days 28 and 14, respectively. This could represent the superior bioactive ability of each sample in the following order: CPC, p-CPC/BG, and p-CPC. The poor bioactivity of p-CPC was consistent with the results in the previous Chapter V, indicating the poor bioactivity of PAA incorporated cement. However, the poor bioactivity of p-CPC could be improved by the addition of BG into cement (p-CPC/BG), which was relevant to the results in Chapter VI. The superior bioactivity of CPC and p-CPC/BG was related to the higher weight loss percentage, which could consequently release more Ca (CPC and p-CPC/BG) and P (CPC) ions with respect to the p-CPC. Thus, these higher Ca and P ions in CPC and p-CPC/BG could facilitate the higher HA formation on the cements.

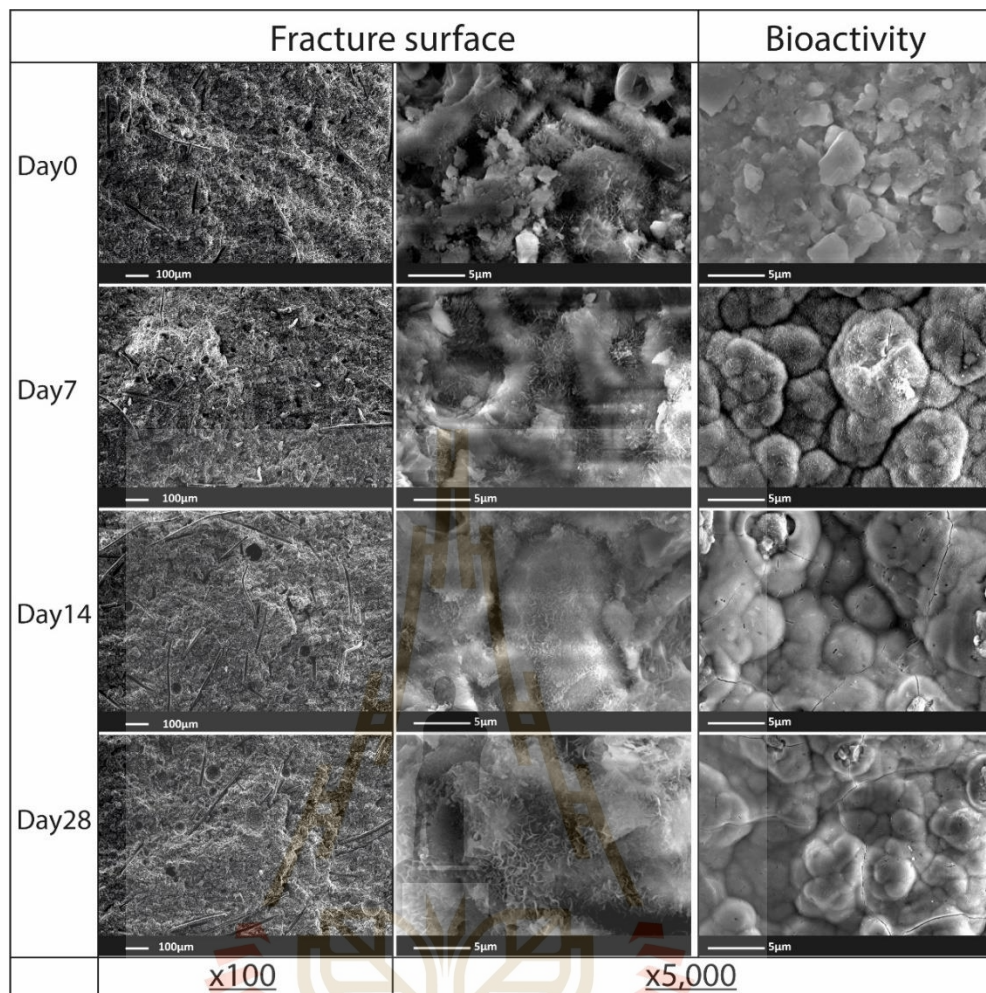


Figure 7.12 SEM micrographs of the fracture (magnification of x100 and x5,000) and surface (magnification of x5,000) of the CPC cement before and after soaking in SBF solution over 28 days.

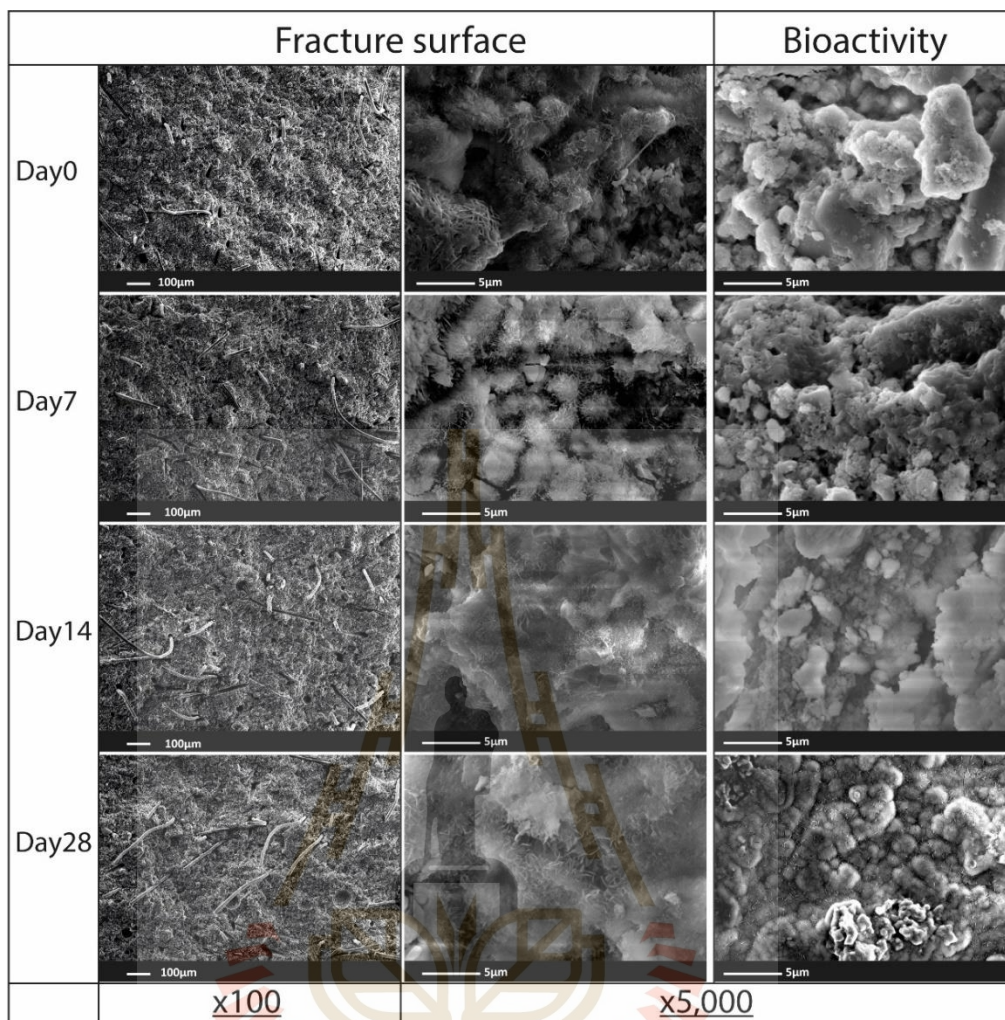


Figure 7.13 SEM micrographs of the fracture (magnification of x100 and x5,000) and surface (magnification of x5,000) of the p-CPC cement before and after soaking in SBF solution over 28 days.

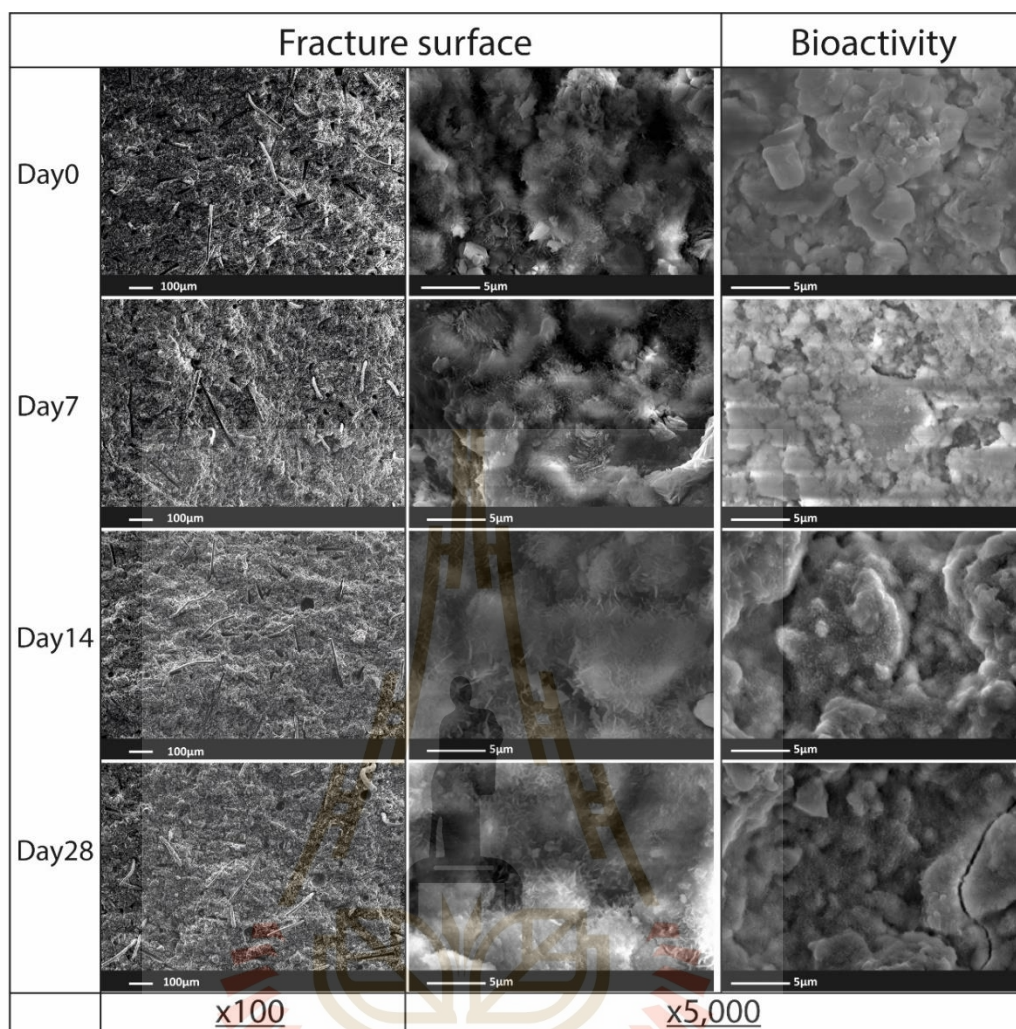


Figure 7.14 SEM micrographs of the fracture (magnification of x100 and x5,000) and surface (magnification of x5,000) of the p-CPC/BG cement before and after soaking in SBF solution over 28 days.

7.3.9 *In vitro* biocompatibility

7.3.9.1 Live/dead assay

For indirect culture, HObs were cultured on coverslips for 1 day with samples-preconditioned medium (Day0) to determine the effect of the environment surrounding the cement on cell viability. In Figure 7.15, live/dead staining presented more viable cells (Green fluorescence) in the p-CPC, p-CPC/BG conditioned medium, as compared with the control CPC. Meanwhile, all conditions exhibited a

similar trend of dead cells (Red fluorescence). However, the viable cells in the control medium were higher than all cement-preconditioned media.

Herein, all cement conditions also appeared to adsorb the essential ions/or proteins, as witnessed in the depletion of Mg ions during the incubation (Figure 7.22 (e)). Therefore, the adsorption aspect of these cements could be responsible for the lower density of viable cells in cement-preconditioned media, as compared with the control medium. This consideration could be supported by the previous work (Klimek, 2016). They attributed the decrease in osteoblast viability to the reduced levels of ions (Ca^{2+} , Mg^{2+} , and HPO_4^{2-}) in the extracted medium of HA after soaking the sample in the medium due to its high adsorption capacity. Besides, the essential proteins for cell metabolism could be adsorbed by nano-powder HA (Swain and Sarkar, 2013), and BG doped apatite cement (El-Fiqi, 2015).

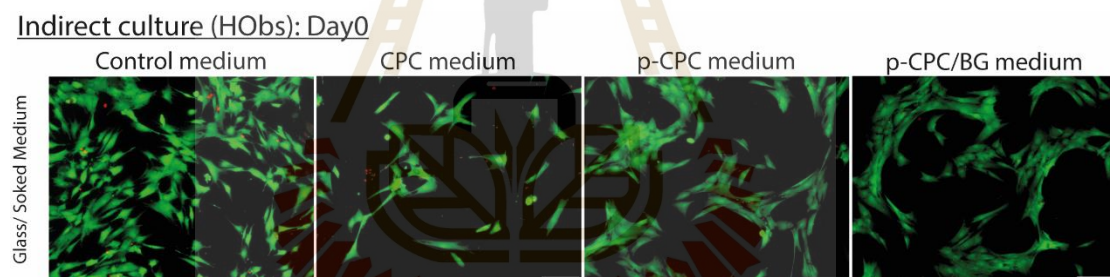


Figure 7.15 Live/Dead assay of HObs on coverslip cultured with preconditioned media and control medium for 1 day (Day0), magnification of x10. Green stain represents live cells and red stain represents dead cells. The scale bar was 100 μm .

For the direct culture, HObs were cultured on top of three cement from different preparations, as described in Table 7.1. After 1 day of incubation (Figure 7.16), live/dead staining exhibited more extended HObs adhesion on the cement in a soaked medium condition, as compared with the untreated and rinsed PBS conditions. After 7 days of culture (Figure 7.17), HObs maintained a spread morphology on all cements (Soaked medium condition) and displayed more elongated cells. It was found

that only CPC presented most of dead HObs in the untreated and rinsed PBS conditions after 7 days of incubation. Afterward, MSCs were cultured on each cement samples (Soaked medium condition) for 1 and 7 days (Figure 7.18). The MSCs elongation on each cement condition presented a similar trend to the results of HObs. However, both HObs and MSCs presented more well-spread on the glass slip with respect to all cement conditions.

HObs were cultured on cement samples from different preparations to determine the influence of the cement and any residuals released on cell responses. In a comparable experimental procedure, Kunisch et al. (Kunisch, 2017) investigated cell responses to cements from different preparations, indicating more viable cells on the PBS-prewashed cement with respect to the fresh cement. Furthermore, the incubation of cement in cell culture medium could inhibit any harmful components or ions after the setting of cement, resulting in a higher cell number and activity (Schamel, 2017). Their findings could be correlated to the present work, showing the more extended HObs in the prewashed conditions of cement/rinsed PBS and cement/soaked medium with respect to untreated cement condition. It could be noted that the process of prewashed cement (soaked in medium overnight) could rinse the released excessive ions or residuals from cement and allow cement to adsorb some essential ions/protein from the medium, which become favorable for cell adhesion. Although the adsorption aspect of cement resulted in low viable cells in the cement-preconditioned medium in the (indirect), this could allow cell adhesion and spread in direct contact to cement (direct). Since cement has already adsorbed ions and essential proteins from the medium after soaking cement in the medium overnight, which could facilitate cell viability and proliferation. Therefore, the cement soaked in medium overnight was used for further experiments. Among each cement condition, cells exhibited greater elongation in the following order: CPC, p-CPC, and p-CPC/BG. The number of rounded shapes of HObs in p-CPC/BG could be attributed to the higher concentration of Si (1.5 mM at 1 day, Figure 7.22 (c)) in the medium. These findings are relevant to the previous work (Shie, 2011), presenting a more rounded

shape of human osteoblast-like cells (MG63 cells) in the medium with a higher extracellular Si (from 2 to 6 mM), as compared with well-spread cells in the control medium. Besides, Stulajterova et al. (Stulajterova, 2017) found more rounded rat primary Mesenchymal Stem cells (rMSCs) in 7.5-15 wt.% BG (45S5) incorporated TTCP based cement with the released Si ions (0.28-5.05 mM), as compared with the control cement.

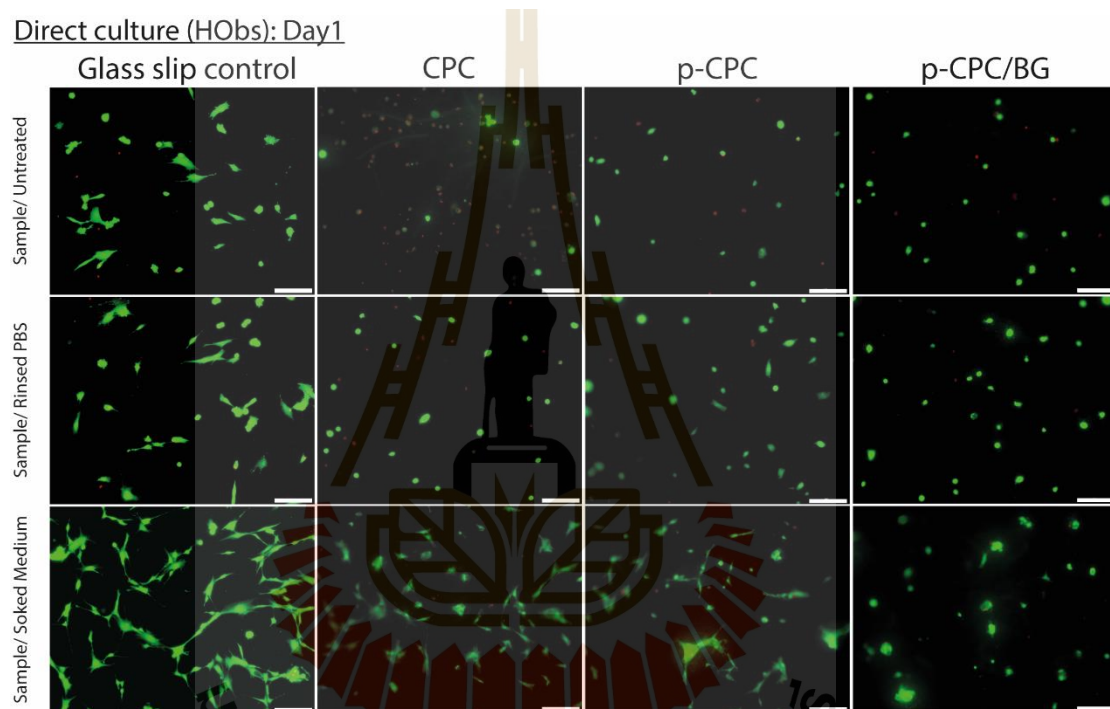


Figure 7.16 Live/Dead assay of HObs cultured on each cement condition with different sample preparation for 1 day, magnification of x10. Green stain represents live cells and red stain represents dead cells. The scale bar was 100 μm .

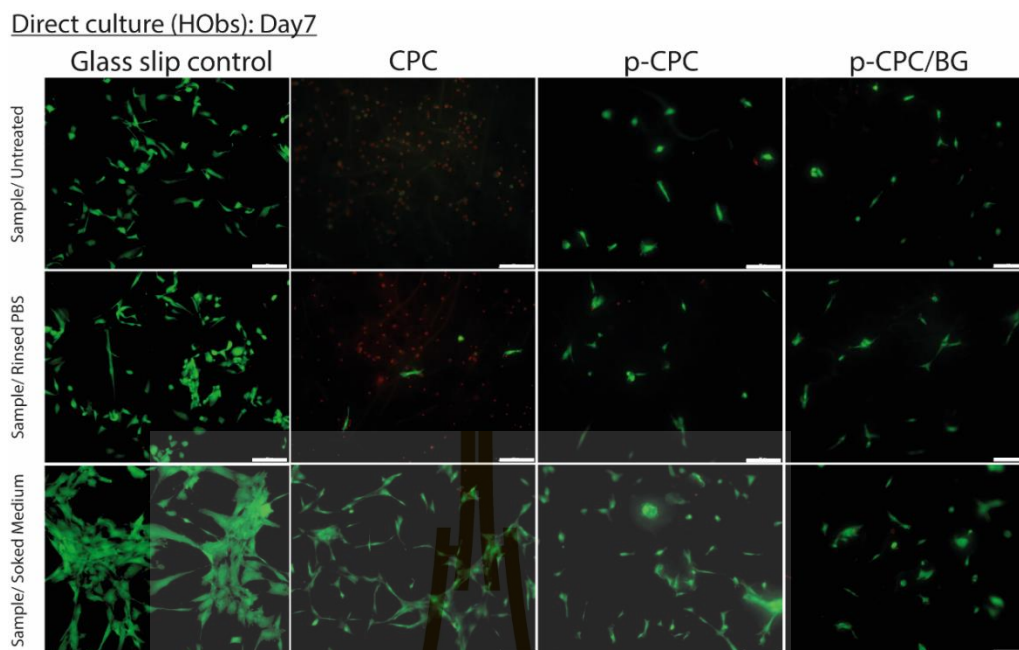


Figure 7.17 Live/Dead assay of HObs cultured on each cement condition with different sample preparation for 7 days, magnification of x10. Green stain represents live cells and red stain represents dead cells. The scale bar was 100 μm .

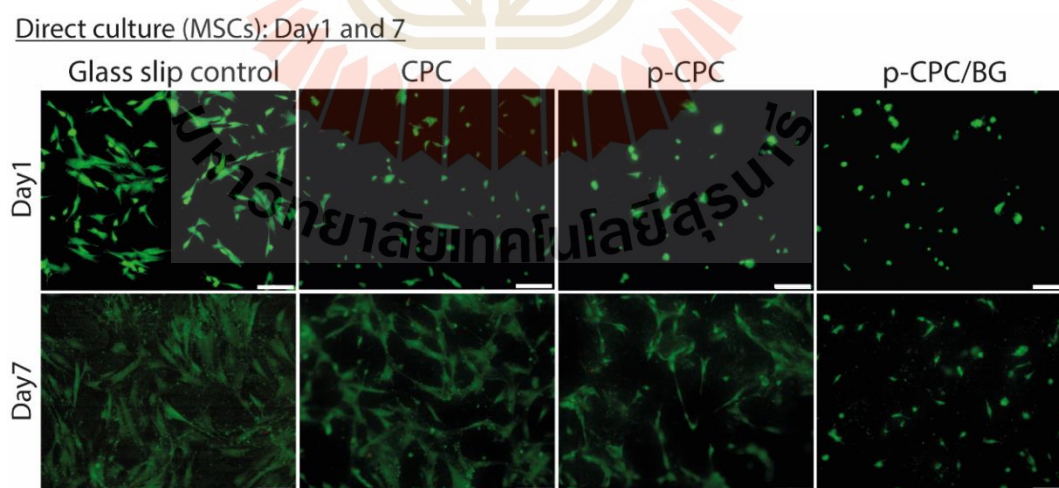


Figure 7.18 Live/Dead assay of MSCs cultured on each cement condition with different sample preparation for 1 (Day1) and 7 (Day7) days, magnification of x10. Green stain represents live cells and red stain represents dead cells. The scale bar was 100 μm .

7.3.9.2 Cell morphology

After 7 days of culture, the spreading morphology of HObs and MSCs on cement (Soaked medium condition) was observed (Figure 7.19 and 7.20), showing the nuclei (Blue) and actin filaments (Green) in the cytoplasm. All cement conditions revealed similar actin fibre spreading and filament elongation of HObs and MSCs. However, p-CPC/BG showed less spread of HObs with respect to other conditions. In addition, SEM images presented superior HObs spreading on each cement condition in the following order: CPC, p-CPC, and p-CPC/BG. Furthermore, MSCs showed similar spreading on all cement conditions.

HObs and MSCs were stained with DAPI and Phalloidin to observe the formation of cytoskeleton actin fibres after culture with cement for 7 days, presenting well-spread actin filaments in all conditions. The morphology and adhesion of HObs on all cement were also detected by SEM images, showing a similar trend and supporting the fluorescence staining results. In this work, the poor stretching of actin fibres of HObs in p-CPC/BG could be affected by the excessive Si ions (1.9-1.3 mM) released from cement to the medium from 0 to 7 days. The released Si ions in this present work was much higher than the previous work (Li, 2015). They found that the released Si ions of approximately 0.2 mM could result in well-spread actin fibres of bone marrow stromal cells (BMSCs) on the mesoporous BG added calcium phosphate cement scaffold. The well-spread and elongated actin fibres of rat osteoblast cells (MC3T3-E1) (Axrap, 2016) and osteoblast-like cells (MG63) (Sadiasa, 2014) were also detected in other studies of BG added calcium phosphate cement.

Direct culture (HObs): Day7

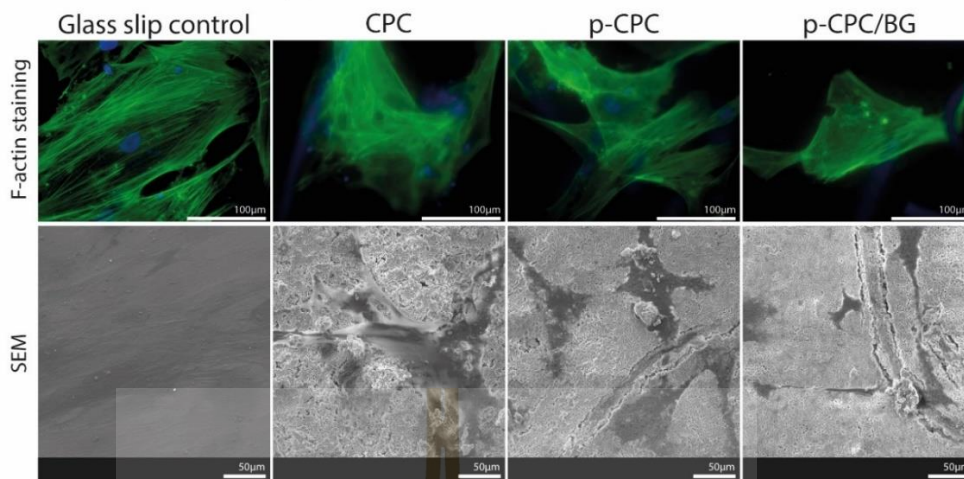


Figure 7.19 HObs morphology cultured on each cement condition with control medium for 7 days. 2D images of cells spreading stained with phalloidin for actin cytoskeleton (green) and DAPI for the nucleus (blue), original magnification of x40. SEM images show cells adhesion on each cement at magnification of x1000.

Direct culture (MSCs): Day7

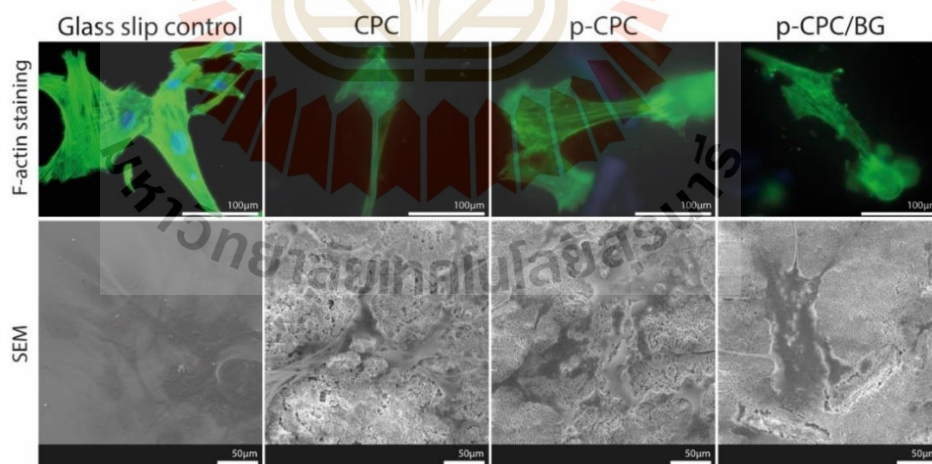


Figure 7.20 MSCs morphology cultured on each cement condition with control medium for 7 days. 2D images of cells spreading stained with phalloidin for actin cytoskeleton (green) and DAPI for the nucleus (blue), original magnification of x40. SEM images show cells adhesion on each cement at magnification of x1000.

7.3.9.3 pH changes, ion release/adsorption, and surface roughness

As a result, pH trend of all cement conditioned media appeared more acidic after soaking in the medium for 21 days, as compared with the control medium. The result showed that the pH of all samples was in a range of 8.79 to 8.36 (CPC), 8.88 to 8.57 (p-CPC), and 8.90 to 8.61 (p-CPC/BG). All cements presented both release (White area: positive value) and adsorption (Grey area: negative value) ability after the values were subtracted by the control medium. For control CPC-conditioned media, the released Ca, P, and Si ions were in a range of 0.24-0.49 mM, 0.82-4.04 mM, and 0.15-0.53 mM, respectively. The p-CPC released ions to the culture media ranging from 0.21-0.32 mM Ca ion, 0.47-2.63 mM P ion, and 0.19-0.59 mM Si ion. Besides, the released Ca (0.12-0.59 mM), P (0.24-2.62 mM), and Si (1.05-1.91 mM) ions of p-CPC/BG was indicated during the incubation from 1 to 21 days. For Si ions, the cumulative release was the most prominent in p-CPC/BG with respect to the other ones. All cement released a large amount of PO_4^{3-} into the medium at 0 day and rapidly reduced to 1 day, which then slightly increased to 21 days. Furthermore, the initial burst of Na^+ was clearly seen throughout the early stages of 0 and 1 day. In contrast, Mg ions in the culture medium were absorbed by all cement conditions, resulting in negative results after subtracting the blank (culture medium). After soaking cement in medium overnight, there was no significant difference in surface roughness among each cement condition, as presented in Figure 7.23.

Herein, it was found that each sample presented different pH changes of culture medium during incubation. p-CPC/BG exhibited a higher pH trend with respect to other conditions. This result is relevant to the previous work of BG doped apatite cement (El-Fiqi, 2015) and BG doped apatite/PLGA cement (Renno, 2013). They reported that the higher pH trend was influenced by the more inorganic ions in the BG particles released into the medium. Meanwhile, the pH of the control CPC was more acidic than the other samples. It is noteworthy that the pH change in the culture medium was correlated to the ion release/adsorption feature of cement. Thus, the higher acidic value of CPC medium could be related to redundant residual

P and Na ions from the cement liquid mixture of 1M Na_2HPO_4 and 1M NaH_2PO_4 (total pH = 7.4) and the high degradation of DCPA powder. This could result in the higher released P ions when compared with other samples during 28 days of cultivation. In addition, the higher Ca ions of CPC and p-CPC/BG could be related to the higher degradation of β -TCP content (shown in weight loss results) with respect to p-CPC. Furthermore, these cements also presented the adsorption ability, representing the depletion of Mg ions over time of samples incubation. This feature is consistent with the previous study (Klimek, 2016). Apart from ions and pH changes, it should be noted that the different morphology of HObs may not be influenced by the microstructure of each sample as there was no significant difference in surface roughness among each cement condition.

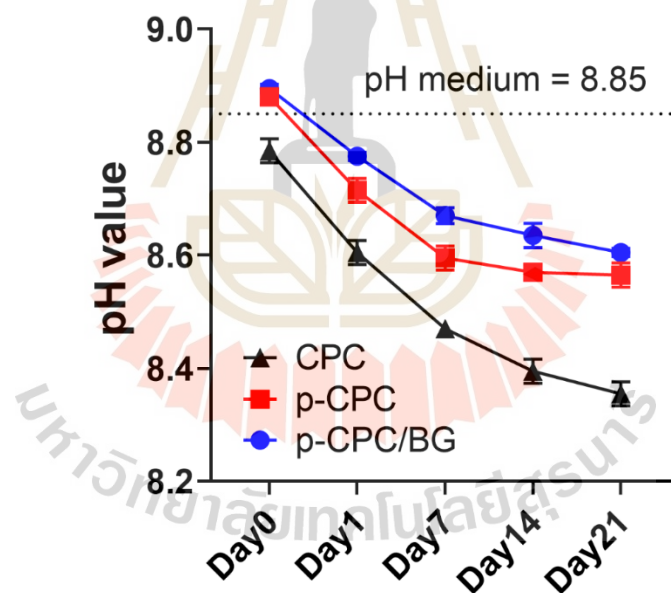


Figure 7.21 pH value of sample-conditioned medium after soaking in culture medium at different time points.

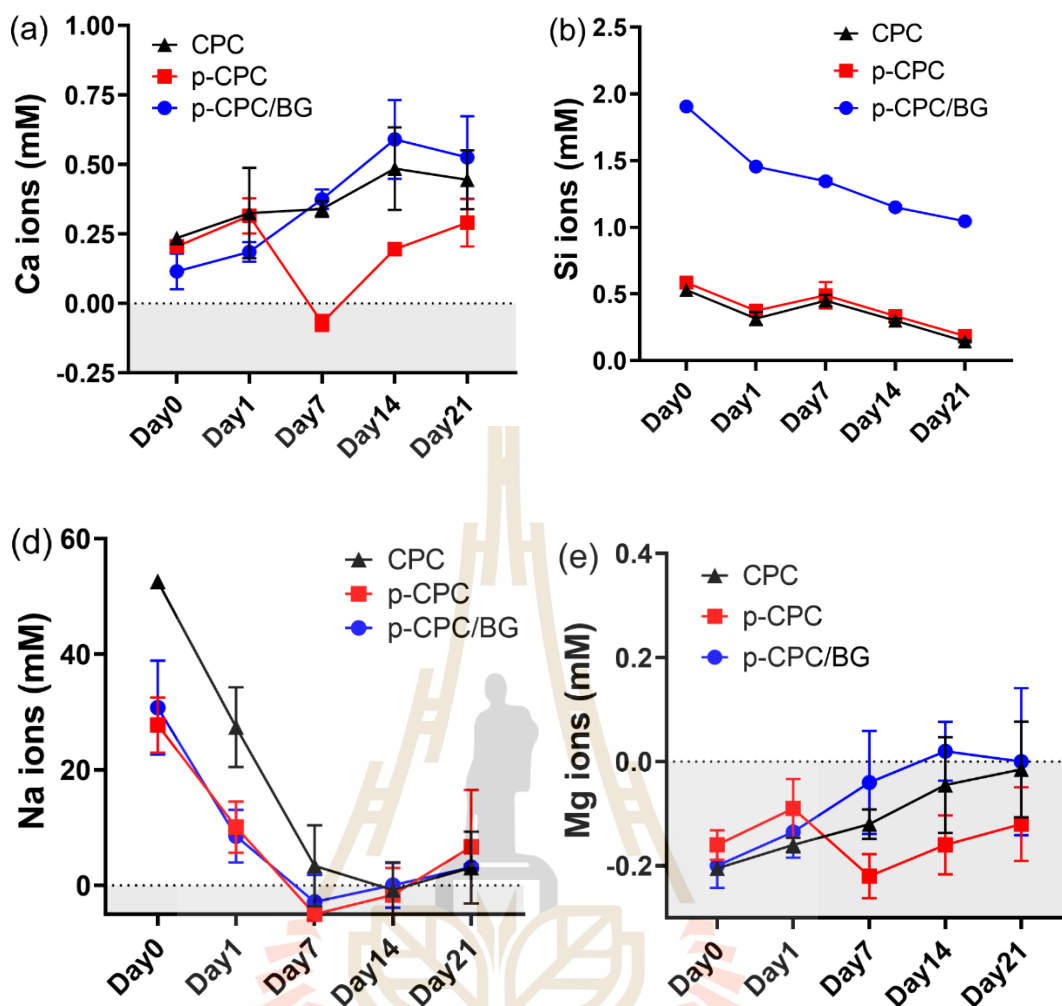


Figure 7.22 Ion changes of (a) Ca, (b) Si, (c) P, (d) Na, and (e) Mg ions of sample-conditioned medium after soaking in culture medium at different time points. All ions of each condition were subtracted by the control cell culture medium as a blank, showing the ions in the medium adsorbed by samples (Grey area: negative value) and ions released from sample to medium (White area: positive value).

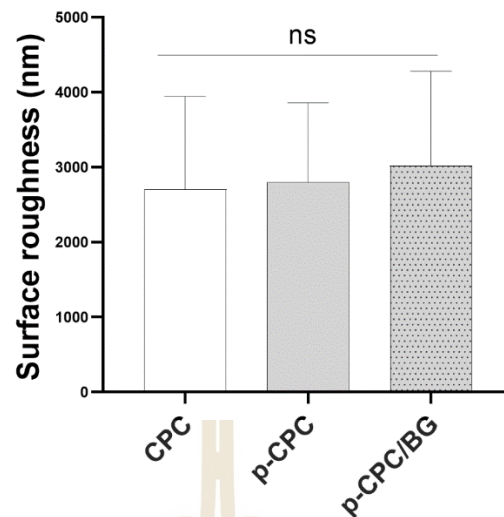


Figure 7.23 Surface roughness of each cement condition after immersion in culture medium overnight.

7.3.9.4 Cell proliferation and Picogreen DNA quantification

The results presented the metabolic activity and DNA content of both HObs and MSCs adhered to the cement and glass slip control. For HObs, there was no significance different of cellular metabolic activity among three cement conditions at 1 day of culture. In addition, the metabolic activity of HObs on p-CPC, p-CPC/BG cement and glass slip control significantly increased, while the CPC showed a consistent level of metabolically active cells from 7 to 28 days. The DNA contents of HObs presented a similar trend with respect to the result of metabolic activity. For MSCs, the metabolic activity of cells on all cements and glass slip control rapidly increased over 28 days of incubation. A similar trend of MSCs grew on samples was also detected by the DNA content when compared with the metabolic activity result.

As a result, the higher acidosis of the CPC medium could affect the cell viability and proliferation, demonstrating less viable HObs (Indirect: day 0 and Direct: day 1, cement/untreated) and poor proliferation rate (metabolic activity and DNA contents) of both HObs and MSCs with respect to other samples. This is consistent with the previous studies, exhibiting a reduced proliferation rate of mouse-osteoblast

cells (MC3T3-E1) (Galow, 2017) and primary human bone marrow mesenchymal stem cells (hBMMSCs) (Wu, 2016) cultured in the acidic medium. However, MSCs in this work could tolerate the acidic pH of the CPC medium, as witnessed in the result of MSCs proliferation. Apart from pH changes in culture medium, ion changes could also influence the proliferation of both cells. Previous work (Farley, 1994) found that Ca ions also played an important role in cellular responses, as evidenced by increased proliferation of SaOS-2 human osteosarcoma cell lines (Ca ions, 0.2-2.0 mM). Although their findings were in a similar range with the released Ca ions (0.1-0.6 mM) in the current study, this Ca concentration did not appear to affect any specific responses in both HObs and MSCs. This could be due to other important features of ions release/adsorption and pH changes which have already had an impact on cell behaviour. As a result, P ions (0.8-1.5 mM) in the CPC medium could inhibit the proliferation of HObs and MSCs, presenting the lower viable HObs and MSCs with respect to other conditions over 28 days of incubation. Current results are in contrast with the previous work (Kanatani, 2002), revealing enhanced proliferation of osteoblastic cells when increasing extracellular P ions (1.5-4.0 mM) in the medium. Thus, the low proliferation of HObs and MSCs of CPC in the current work could be influenced by the more acidic environment as mentioned above.

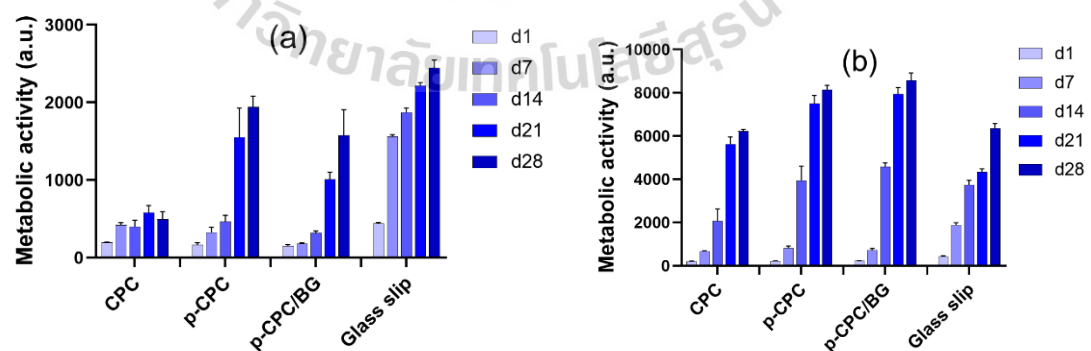


Figure 7.24 Metabolic activity of (a) HObs and (b) MSCs cultured for 1, 7, 14, 21, and 28 days in the control medium.

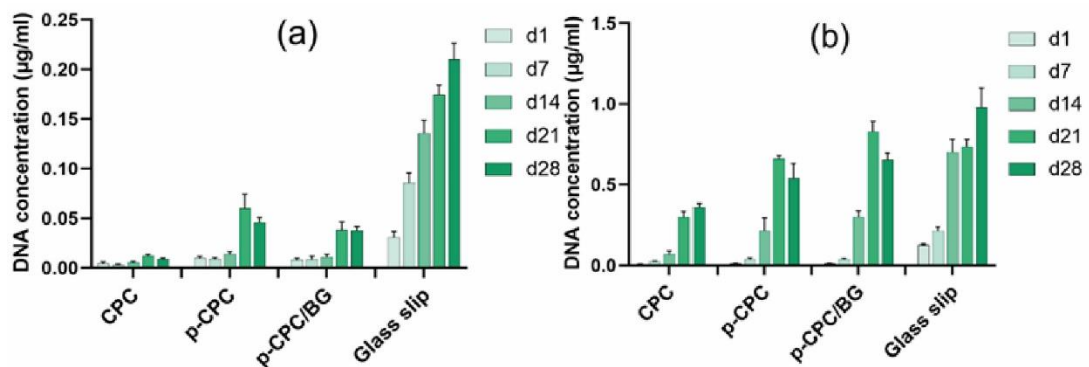


Figure 7.25 DNA content of (a) HObs and (b) MSCs cultured for 1, 7, 14, 21, and 28 days in the control medium.

7.3.9.5 Alkaline phosphatase (ALP) assay

ALP activities of HObs and MSCs adhered to cement and glass slip control were evaluated, as shown in Figure 7.26 (a) and (b), respectively. For HObs, there was no significant difference in ALP activity among three cements and glass slip control after culture in the control medium (OS-) from 1 to 28 days. In the osteogenic medium (OS+), the ALP contents slightly increased in p-CPC, p-CPC/BG, and glass slip control, indicating superior ALP activity when compared with the CPC at 28 days of culture. In addition, the ALP activity of p-CPC/BG in OS+ medium was significantly higher than that in OS- medium after 28 days of incubation. For MSCs cells, the ALP expression could be detected only in OS- medium for p-CPC, p-CPC/BG, and glass slip control and that in OS+ medium for p-CPC/BG and glass slip control. Furthermore, p-CPC/BG presented the higher level of ALP contents in OS+ medium when compared with the OS- medium.

The increase in ALP activity was determined as the osteogenic differentiation of MSCs into osteoblasts (Liu, 2018). ALP activity is also produced by osteoblasts, which encourages the bone mineralization (Bilgiç, 2020). As a result, the acidosis of CPC medium could significantly influence the ALP expression, resulting in no ALP activity of HObs in OS+ medium (day 28) and MSCs in both OS- and OS+ medium (day 1 to 28). This behaviour could be attributed to the more acidosis in CPC

medium with respect to other samples. Thus, this lower pH could down-regulate the ALP production of both cells. This consideration is consistent with the earlier studies, presenting the lower ALP level of osteoblast-like cells (Ramp, 1994) and dental pulp stem cells (DPSC) (Massa, 2017) when cultured in the more acidic medium. Surprisingly, the enhanced osteogenic differentiation of both HObs and MSCs was detected only in the p-CPC/BG, showing a significant fold-increased ALP level with the presence of osteogenic inducers (OS+). In addition, ALP p-CPC/BG showed superior ALP level in OS+ medium when compared with the glass slip control. This aspect could be influenced by the appropriate range of extracellular Si ions (1.1-1.5 mM) from p-CPC/BG released into the medium, enhancing the ALP level of HObs (28 days) and MSCs (1 and 7 days) after culture in OS+. This could be supported by previous work showing that extracellular Si ions ranging from 1 to 1.5 mM promoted differentiation of SaOS-2 (Mestres, 2012) and rMSCs (Radin, 2005). However, it is still unclear why the MSCs could produce ALP enzymes only in the p-CPC cultured in OS- medium, but not in OS+ medium. This could be related to the low number of viable cells cultured in OS+, which were not enough to support the ALP induction.

Figure 7.27 (a) and (b) shows the total collagen contents of HObs and MSCs after culture in both OS- and OS+ media for 14 and 28 days. The total collagen production slightly increased from 14 to 28 days in all cement conditions. HObs presented a similar level of total collagen content in OS- medium. Meanwhile, the total collagen expression of the CPC was significantly lower than that of p-CPC (28 days), p-CPC/BG (14 and 28 days), and glass slip control (14 and 28 days) in OS+ medium. For MSCs, the total collagen expression in p-CPC/BG (14 and 28 days) was significantly greater than that of p-CPC in the OS- medium. In addition, the control CPC showed higher total collagen contents than p-CPC and p-CPC/BG after 14 days of culture in the OS+ medium. When compared between two condition media, the greater total collagen content was detected in CPC cultured in OS+ medium at 14 days. However, the total collagen level in p-CPC/BG significantly reduced of culture in OS+ medium, as compared with the OS- medium at 28 days.

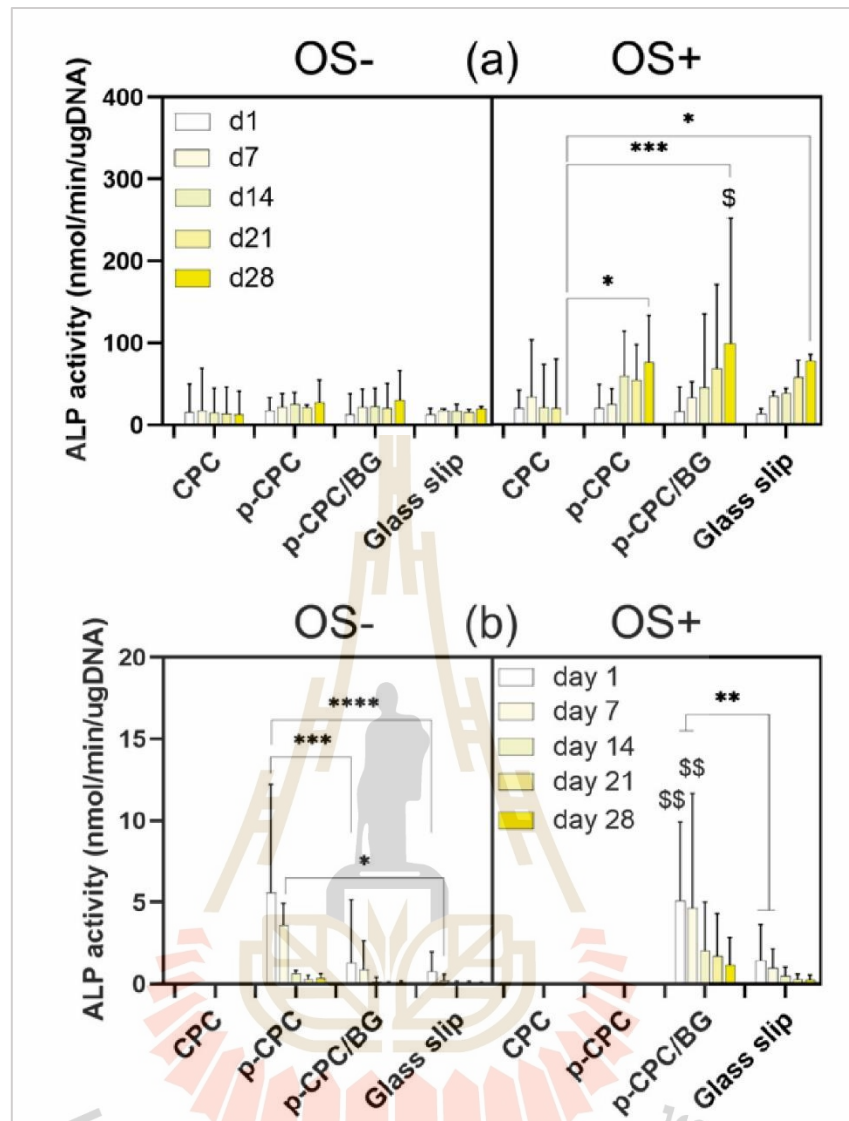


Figure 7.26 ALP activity of (a) HObs and (b) MSCs cultured on cement sample with control medium (OS-) and osteogenic medium (OS+) for 1, 7, 14, 21, and 28 days (The statistical comparison among sample conditions is shown as * $p < 0.05$, ** $p < 0.01$, *** $p < 0.001$, and **** $p < 0.0001$ / The comparison between complete (OS-) and osteogenic (OS+) medium as $^{\$}p < 0.05$ and $^{\$\$}p < 0.01$).

7.3.9.6 Total collagen secretion

It was noted that osteoblastic cells secrete collagen with essential proteins constituted in the extracellular matrix, facilitating new bone formation

(McNamara, 2017). For HObs, CPC exhibited a lower collagen level (OS+ medium), which could be influenced by the more acidic pH of CPC-conditioned medium with respect to other conditions. Our assumption could be supported by previous studies showing lower collagen production when cells were cultured in a more acidic medium (Kohn, 2002). However, the higher released P ions of CPC could result in the higher collagen production (d14, OS+ medium) with respect to other conditions, p-CPC and p-CPC/BG. Current results could be correlated to the previous work (Schäck, 2013), exhibiting enhanced collagen levels of MSCs cultured in medium containing extracellular P ions. Herein, the high concentration of Si in p-CPC/BG could also result in higher secreted collagen (OS- medium) with respect to p-CPC. This aspect was comparable with previous studies (Reffitt, 2003, Shie, 2011), revealing the enhanced collagen production of osteoblast-like cells and human bone marrow stromal cells cultured in the medium with extracellular Si ions. Although the p-CPC/BG supported ALP and collagen expression of HObs and MSCs under static culture, further investigations into dynamic culture systems with other gene expression tests, including *in vivo* testing, would be advantageous for the current results.

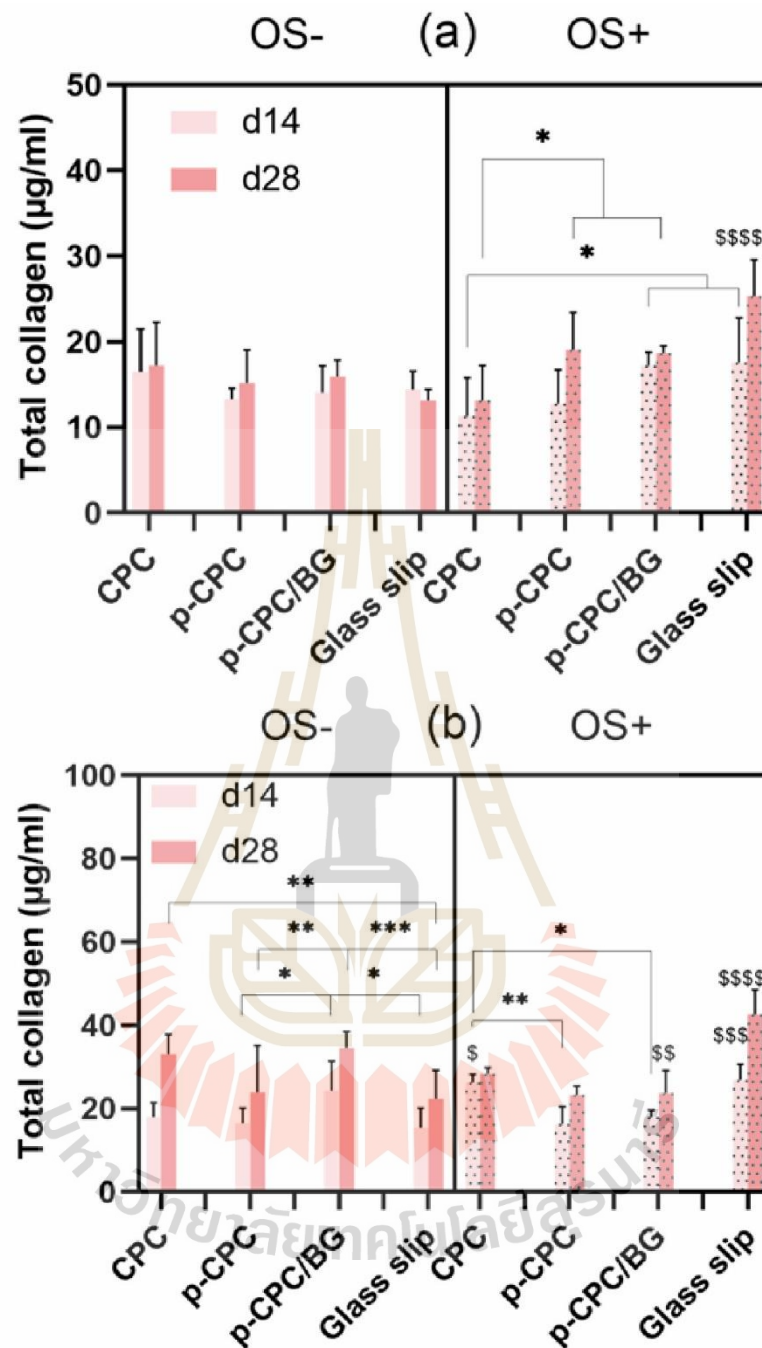


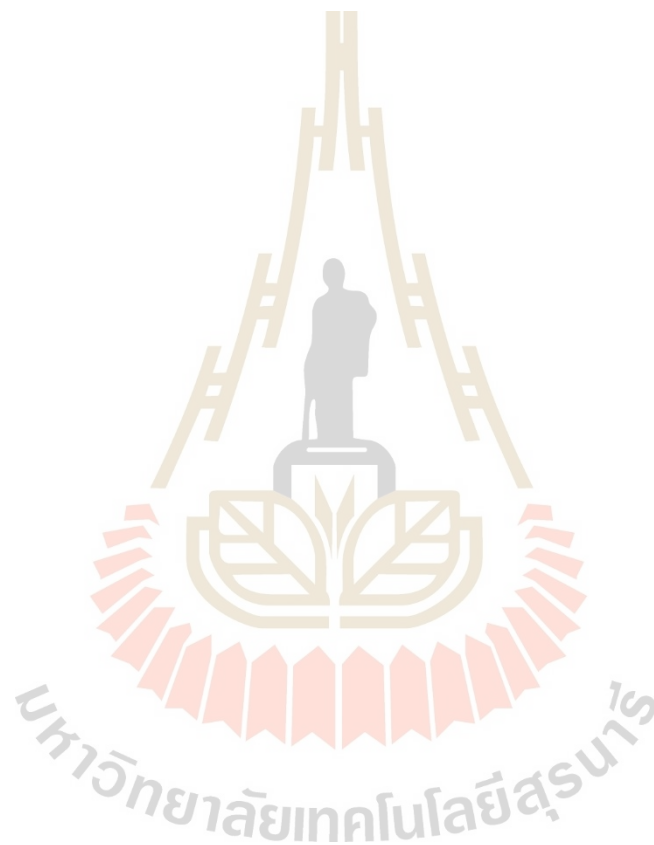
Figure 7.27 Total collagen secretion of (a) HObs and (b) MSCs cultured on cement sample with control medium (OS-) and osteogenic medium (OS+) for 14 and 28 days (The statistical comparison among sample conditions is shown as * $p < 0.05$, ** $p < 0.01$, and *** $p < 0.001$ / The comparison between complete (OS-) and osteogenic (OS+) medium as $^{\$}p < 0.05$, $^{\$\$}p < 0.01$, and $^{\$ \$ \$}p < 0.001$).

7.4 Conclusions

This work investigated the incorporation of PAA (liquid phase) and BG (powder phase) into apatite/ β -TCP cement, indicating its improved physical properties and enhanced *in vitro* cellular activities of HObs and MSCs on the cement. The addition of PAA in the cement retarded the setting time, which the prolonged setting time of p-CPC could be decreased by the addition of BG (p-CPC/BG). Besides, the injectability percentage of p-CPC/BG was still higher than the control CPC. The mechanical properties of cement were significantly improved with the presence of PAA coupled with BG during the incubation in SBF solution. However, PAA could slightly interfere the phase conversion and degradation of DCPA and β -TCP in the cement, resulting in less phase of HA formation and weight loss percentage in both p-CPC and p-CPC/BG with respect to CPC. This led to the more mesopore (less converted HA) and less macropore (less degraded DCPA) in p-CPC and p-CPC/BG. Thus, the higher mesopore resulted in a higher specific surface area with respect to the control CPC after 28 days of incubation in SBF solution. Furthermore, the poor degradation of p-CPC could be related to the fewer released ions for the HA deposition on the surface of the sample, indicating poor bioactivity.

For *in vitro* testing, we determined the influence of cement (direct) and the conditioned medium from the cement (indirect) on cell viability. All cements presented the ion release/adsorption characteristic after soaking cement in the medium over time. This adsorption feature resulted in less viable HObs cultured in cement-conditioned medium (indirect) when compared with the control medium. CPC-medium (higher Na and P ions) resulted in less viable HObs with respect to other conditions. For direct culture, HObs viability on cement from different prewashed-procedure was examined. Cement/Soaked medium condition showed the more spread cells adhered on cements with respect to other sample preparation. At 7 days, HObs and MSCs presented well-spread on cement, revealing the elongated actin filaments in the cytoplasm. Afterward, the proliferation, differentiation, and total collagen secretion of HObs and MSCs were investigated. The higher released Si ion and lower

acidification of p-CPC/BG appeared to be more appropriate environment for cells, resulting in the enhanced osteogenic differentiation (HObs and MSCs) and total collagen production (HObs in OS+ and MSCs in OS-). Therefore, the presence of PAA coupled with BG in this apatite/ β -TCP cement could be promising for biomedical applications and bone engineering, which will be further characterized in other supportive gene expression assays, including *in vivo* testing.



CHAPTER VIII

CONCLUSIONS

This work aimed to find the new potential formula of calcium phosphate cement for use in bone tissue engineering under load-bearing conditions. In addition, this new formula required some major starting precursors (alpha-tricalcium phosphate, α -TCP), which could be successfully prepared in-house using the new technique. Moreover, the influence of the particle size of α -TCP and the selective sterilization process with the appropriate conditions on this cement was estimated. For the cement formula, the presence of a biopolymer (polyacrylic acid, PAA) and a bioactive component (bioactive glass, BG) significantly improved the physical and biological properties of apatite/beta-tricalcium phosphate (β -TCP) cement. These developments and enhancements could be summarized in the following sections.

8.1 Effect of different synthesis of α -TCP powder on physical properties of apatite/ β -TCP cement

The result showed that the high purity phase of α -TCP powder could be successfully produced by different syntheses of both traditional solid state and wet chemical reaction methods. It was found α -TCP from both methods (α -solid and α -wet) exhibited no significant difference in phase composition, chemical functional groups, and morphology. Afterward, both α -solid and α -wet were used as one of the starting cement powders to prepare the cement samples (CPC-solid and CPC-wet) for their physical testing, including phase conversion, compressive strength, morphology (fracture surface, and bioactivity). Thus, both CPC-solid and CPC-wet presented similar performances. This confirmed that the wet chemical reaction could be an optional process to obtain the high purity phase of α -TCP powder. Moreover, this wet chemical reaction technique reduced time and cost of manufacture with respect to the conventional solid state reaction.

8.2 Effect of particle size of α -TCP and dry heat sterilization on physical properties of apatite/ β -TCP cement

For particle size of α -TCP parameter, smaller size of α -TCP resulted in decreased setting time, increased compressive strength, and enhanced calcium deficient hydroxyapatite (CDHA) transformation of apatite/ β -TCP cement. For dry heat sterilization parameter, it was found that phase composition of both starting cement powder and set cement samples after soaking in SBF solution for 7 days were not influenced by the higher temperature, ranging from 121 to 170 °C. In addition, FT-IR spectra of chitosan fiber from different sterilized temperature were similar. Meanwhile, the color of chitosan fiber was slightly darker when increasing temperature, reflecting the damage of the chitosan fiber. Consequently, the compressive strength of sterilized cement (140-170°C) was decreased. Herein, the sterilized condition (121°C soaked for 10h) exhibited no statistical difference in compressive strength, setting time, pH changes, and bioactivity of cement when compared with the control non-sterilized cement. Therefore, this assured that the sterilized condition at 121 °C for 10 h could be an appropriate process for the sterilization of the cement powder formula in this study.

8.3 Effect of PAA added into apatite/ β -TCP cement on its physical properties and cytotoxicity

The combination of PAA (0-50 v/v%) and disodium hydrogen phosphate (Na_2HPO_4) was optimized in an appropriate ratio to improve the mechanical strength of this cement formula. Thus, 30 v/v% PAA cement at 0.35 L/P ratio presented the shortest setting time (initial setting time: 11.8 ± 2.5 min, and final setting time: 54.7 ± 2.3 min) and the highest compressive strength (40.3 ± 5.9 MPa) with respect to other conditions. Meanwhile, the phase conversion of cement into CDHA could be maintained with the concentration of PAA content in cement ranging from 10 to 40 v/v%. In addition, the higher PAA showed less HA deposition on cement (poor bioactivity). However, 30 v/v% PAA was still bioactive, indicating some HA deposited on the surface of cement. Furthermore, 30 v/v% PAA presented higher viability of

fibroblast cells than control cement without PAA (day 1) and a commercial product of biphasic granules (day 7). Afterward, the concentration of PAA ranging from 25 to 35 was investigated, showing the higher compressive strength at 25 v/v% PAA (44.2 ± 4.2 MPa) Therefore, 25 v/v% PAA was used for further analysis.

8.4 Effect nano-BG added into polymeric apatite/ β -TCP cement on its physical performances and adipose-derived stem (ASC) cells behaviors

The poor phase conversion and bioactivity of polymeric apatite/ β -TCP cement were continuously improved by the addition of porous nanoparticle-BG (122 ± 15 nm) from 0 to 1.5 wt.%. The higher nano-BG concentration resulted in decreased setting time, enhanced CDHA conversion, and promoted bioactivity of polymeric apatite/ β -TCP cement. The highest compressive strength (49.9 ± 5.6 MPa) and Young's modulus (10.1 ± 2 GPa) were found at 1wt.% nano-BG when compared with other conditions. The initial and final setting times of 1 wt.% nano-BG cement were 9 ± 1 min and 18 ± 1 min, respectively. Afterward, the promising formula of 1 wt.% nano-BG was selected for further biological testing with human adipose-derived stem (hASC) cells. It was found that both unmodified and 1 wt.% nano-BG cements adsorbed some essential ions (Mg^{2+}) and proteins from the culture medium. This resulted in lower metabolic activity and protein content of hASCs as compared with the control culture medium (indirect culture). For direct culture, 1 wt.% nano-BG cement with extra released Ca (0.16-0.69 mM), P (0.10-0.99 mM), and Si (1.04-1.46 mM) ions enhanced the metabolic activity and protein content of hASCs in both control (-OS) and osteogenic (+OS) medium. In addition, 1 wt.% nano-BG cement showed the higher osteogenic differentiation of hASCs with respect to the glass coverslip control. Thus, promising formula of 1 wt.% nano-BG cement was selected for further experiments.

8.5 Nano-BG incorporated polymeric apatite/ β -TCP cement for bone regeneration

In this section, the physical and biological performance of nano-BG added polymeric apatite/ β -TCP (p-CPC/BG) cement was comprehensively indicated. This

formula was compared with both polymeric apatite/ β -TCP (p-CPC) and unmodified apatite/ β -TCP (CPC) cement. The prolonged setting time and lower HA conversion of p-CPC were improved by the addition of nano-BG. p-CPC/BG showed two major phases of apatite and β -TCP after 28 days of incubation with a few DCPA residuals. The injectability of p-CPC/BG ($82.9 \pm 1.0\%$) was higher than that of CPC ($74.1 \pm 2.5\%$). During the incubation in SBF solution, the compressive strength and Young's modulus of p-CPC/BG were significantly higher than those of p-CPC and CPC. The presence of nano-BG improved the poor degradation and bioactivity of p-CPC. However, poor degradation of DCPA (less macropore) and HA phase conversion (higher mesopore) in both p-CPC and p-CPC/BG led to a higher specific surface area with respect to the control CPC. There was no significant difference in surface roughness among the three cements.

In in vitro experiments, primary human osteoblast (HOB) and mesenchymal stem cell (MSC) responses to three cements were investigated. All cements appeared to absorb some essential ions (Mg^{2+}) and proteins, resulting in less viable HOBs cultured with cement-preconditioned medium (in direct culture) when compared with control culture medium. However, all cements were not harmful to both cells, presenting viable HOBs and MSCs and actin filament formation in the cell cytoplasm after 7 days of cultivation. Afterward, the strong acidic surrounding environment of CPC showed poor proliferation of both cells. Meanwhile, HOBs and MSCs rapidly grew on both p-CPC and p-CPC/BG. Consequently, the significant fold-increase in osteogenic differentiation of both HOBs and MSCs was detected in only p-CPC/BG, demonstrating the statistical upregulation of ALP levels in the presence of osteogenic stimuli (+OS medium). In addition, the superior total collagen secretion of MSCs was measured in p-CPC/BG when compared with p-CPC in -OS medium. This enhanced osteogenic differentiation (HOBs and MSCs) and total collagen secretion (HOBs in +OS and MSCs in -OS) could be attributed to the higher released Si ion and lower acidification of the medium with respect to other cement conditions. This could suggest that the appropriate concentration of both 25 v/v% PAA (liquid) and 1 wt.% nano-BG (powder) incorporated into this apatite/ β -TCP cement could be a promising tool for bone repair and fixation. Further experiments will concentrate on other critical in vitro gene

expression analysis and in vivo testing in order to supplement the current work with more comprehensive results in the biological performance of this formula.



REFERENCES

- Apelt, D., Theiss, F., El-Warrak, A. O., Zlinszky, K., Bettschart-Wolfisberger, R., Bohner, M., Matter, S., Auer, J. A., and von Rechenberg, B. (2004). In vivo behavior of three different injectable hydraulic calcium phosphate cements. **Biomaterials**. 25(7-8): 1439-1451.
- Arahira, T., Maruta, M., and Matsuya, S. (2017). Characterization and in vitro evaluation of biphasic α -tricalcium phosphate/ β -tricalcium phosphate cement. **Materials Science and Engineering: C**. 74: 478-484.
- Arkin, V. H., Narendrakumar, U., Madhyastha, H., and Manjubala, I. (2021). Characterization and In Vitro Evaluations of Injectable Calcium Phosphate Cement Doped with Magnesium and Strontium. **ACS Omega**. 6(4): 2477-2486.
- Arora, S., Lala, S., Kumar, S., Kumar, M., and Kumar, M. (2011). Comparative degradation kinetic studies of three biopolymers: Chitin, chitosan and cellulose. **Archives of Applied Science Research**. 3: 188-201.
- Axrap, A., Wang, J., Liu, Y., Wang, M., and Yusuf, A. (2016). Study on adhesion, proliferation and differentiation of osteoblasts promoted by new absorbable bioactive glass injection in vitro. **Eur Rev Med Pharmacol Sci**. 20(22): 4677-4681.
- Ayre, W. N., Denyer, S. P., and Evans, S. L. (2014). Ageing and moisture uptake in polymethyl methacrylate (PMMA) bone cements(). **Journal of the Mechanical Behavior of Biomedical Materials**. 32(100): 76-88.
- Baer, P. C., and Geiger, H. (2012). Adipose-derived mesenchymal stromal/stem cells: tissue localization, characterization, and heterogeneity. **Stem Cells International**. 2012: 812693.
- Bilgiç, E., Boyacıoğlu, Ö., Gizer, M., Korkusuz, P., and Korkusuz, F. (2020). Chapter 6 - Architecture of bone tissue and its adaptation to pathological conditions.

- Comparative Kinesiology of the Human Body. Angin, S. and Şimşek, I. E., Academic Press: 71-90.
- Bohner, M., Malsy, A. K., Camiré, C. L., and Gbureck, U. (2006). Combining particle size distribution and isothermal calorimetry data to determine the reaction kinetics of α -tricalcium phosphate–water mixtures. **Acta Biomaterialia**. 2(3): 343-348.
- Brown, W. E. (1987). A New Calcium Phosphate, Water-setting Cement. **Cem. Res. Prog.**: 351-379.
- Brown, W. E., and Chow, L. C. (1983). **J. Dent. Res.** 62.
- Bruder, S. P., Jaiswal, N., and Haynesworth, S. E. (1997). Growth kinetics, self-renewal, and the osteogenic potential of purified human mesenchymal stem cells during extensive subcultivation and following cryopreservation. **J Cell Biochem**. 64(2): 278-294.
- Brunner, T. J., Bohner, M., Dora, C., Gerber, C., and Stark, W. J. (2007). Comparison of amorphous TCP nanoparticles to micron-sized α -TCP as starting materials for calcium phosphate cements. **Journal of Biomedical Materials Research Part B: Applied Biomaterials**. 83B(2): 400-407.
- Burguera, E. F., Xu, H. H. K., and Sun, L. (2008). Injectable calcium phosphate cement: effects of powder-to-liquid ratio and needle size. **Journal of biomedical materials research. Part B, Applied biomaterials**. 84(2): 493-502.
- Burguera, E. F., Xu, H. H. K., and Weir, M. D. (2006). Injectable and rapid-setting calcium phosphate bone cement with dicalcium phosphate dihydrate. **J. Biomed. Mater. Res. Part B Appl. Biomater.** . 77B(1): 126-134.
- C.L. Camiré, U. G., W. Hirsiger, M. Bohner, (2005). Correlating crystallinity and reactivity in an α -tricalcium phosphate. **Biomaterials** 26 (2005) 2787–2794.
- Camiré, C. L., Gbureck, U., Hirsiger, W., and Bohner, M. (2005). Correlating crystallinity and reactivity in an α -tricalcium phosphate. **Biomaterials**. 26(16): 2787-2794.

- Camiré, C. L., Nevsten, P., Lidgren, L., and McCarthy, I. (2006). The effect of crystallinity on strength development of alpha-TCP bone substitutes. **J Biomed Mater Res B Appl Biomater.** 79(1): 159-165.
- Camiré, C. L., Nevsten, P., Lidgren, L., and McCarthy, I. (2006). The effect of crystallinity on strength development of α -TCP bone substitutes. **Journal of Biomedical Materials Research Part B: Applied Biomaterials.** 79B(1): 159-165.
- Camiré, C. L., Saint-JEAN, S. J., Hansen, S., McCarthy, I., and Lidgren, L. (2005). Hydration Characteristics of α -tricalcium Phosphates: Comparison of Preparation Routes. **Journal of Applied Biomaterials and Biomechanics.** 3(2): 106-111.
- Campana, V., Milano, G., Pagano, E., Barba, M., Cicione, C., Salonna, G., Lattanzi, W., and Logroscino, G. (2014). Bone substitutes in orthopaedic surgery: from basic science to clinical practice. **Journal of Materials Science: Materials in Medicine.** 25(10): 2445-2461.
- Canal, C., and Ginebra, M. P. (2011). Fibre-reinforced calcium phosphate cements: A review. **Journal of the Mechanical Behavior of Biomedical Materials.** 4(8): 1658-1671.
- Canciani, E., Dellavia, C., Ferreira Espinoza, L., Giannasi, C., Carmagnola, D., Carrassi, A., and Brini, A. (2016). Human Adipose-Derived Stem Cells on Rapid Prototyped Three-Dimensional Hydroxyapatite/Beta-Tricalcium Phosphate Scaffold. **J. Craniofac. Surg.** 27.
- Carrodeguas, R. G., and De Aza, S. (2011). α -Tricalcium phosphate: Synthesis, properties and biomedical applications. **Acta Biomaterialia.** 7(10): 3536-3546.
- Catti, M., Ferraris, G., and Mason, S. A. (1980). Low-temperature ordering of hydrogen atoms in CaHPO_4 (monetite): X-ray and neutron diffraction study at 145 K. **Acta Cryst. B.** 36(2): 254-259.
- Chen, C.-K., Ju, C.-P., Lee, J.-W., and Lin, J.-H. (2013). Effect of Gamma Radiation on Properties of a Calcium Phosphate-Calcium Sulfate Composite Cement. **MATERIALS TRANSACTIONS.** 54: 1160-1165.

- Chen, W.-C., Ju, C.-P., Wang, J.-C., Hung, C.-C., and Chern Lin, J.-H. (2008). Brittle and ductile adjustable cement derived from calcium phosphate cement/polyacrylic acid composites. **Dent Mater.** 24(12): 1616-1622.
- Chen, Y. Z., Lü, X. Y., and Liu, G. D. (2012). A novel root-end filling material based on hydroxyapatite, tetracalcium phosphate and polyacrylic acid. **Int Endod J.** 46.
- Chow, L. C. (2001). Solubility of calcium phosphates. **Monogr Oral Sci.** 18: 94-111.
- Chow, L. C., Markovic, M., and Takagi, S. (1999). Formation of Hydroxyapatite in Cement Systems: Effects of Phosphate. **Phosphorus Sulfur Silicon Relat Elem.** 144(1): 129-132.
- CORSETTI, A., BAHUSCHEWSKYJ, C., PONZONI, D., LANGIE, R., SANTOS, L. A. d., CAMASSOLA, M., NARDI, N. B., and PURICELLI, E. (2017). Repair of bone defects using adipose-derived stem cells combined with alpha-tricalcium phosphate and gelatin sponge scaffolds in a rat model. **J. Appl. Oral Sci.** 25: 10-19.
- Daculsi, G. (1998). Biphasic calcium phosphate concept applied to artificial bone, implant coating and injectable bone substitute. **Biomaterials.** 19(16): 1473-1478.
- Dai, R., Wang, Z., Samanipour, R., Koo, K.-I., and Kim, K. (2016). Adipose-Derived Stem Cells for Tissue Engineering and Regenerative Medicine Applications. **Stem Cells Int.** 2016: 6737345-6737345.
- Dash, M., Chiellini, F., Ottenbrite, R. M., and Chiellini, E. (2011). Chitosan—A versatile semi-synthetic polymer in biomedical applications. **Progress in Polymer Science.** 36(8): 981-1014.
- de Girolamo, L., Lopa, S., Arrigoni, E., Sartori, M. F., Baruffaldi Preis, F., and Brini, A. (2009). Human adipose-derived stem cells isolated from young and elderly women: Their differentiation potential and scaffold interaction during in vitro osteoblastic differentiation. **Cytotherapy.** 11: 793-803.
- Dorozhkin, S. V. (2008). Calcium orthophosphate cements for biomedical application. **Journal of Materials Science.** 43(9): 3028-3057.

- Dorozhkin, S. V. (2013). Self-Setting Calcium Orthophosphate Formulations. **J. Funct. Biomater.** 4(4): 209-311.
- Dorozhkin, S. V. (2017). A history of calcium orthophosphates (CaPO₄) and their biomedical applications. **Morphologie.** 101(334): 143-153.
- Duncan, J., MacDonald, J. F., Hanna, J. V., Shirotsaki, Y., Hayakawa, S., Osaka, A., Skakle, J. M. S., and Gibson, I. R. (2014). The role of the chemical composition of monetite on the synthesis and properties of α -tricalcium phosphate. **Mater. Sci. Eng. C.** 34: 123-129.
- Duncan, J., MacDonald, J. F., Hanna, J. V., Shirotsaki, Y., Hayakawa, S., Osaka, A., Gibson, I. R. (2014). The role of the chemical composition of monetite on the synthesis and properties of α -tricalcium phosphate. **Mater. Sci. Eng. C.** 34: 123-129.
- Durucan, C., and Brown, P. W. (2002). Reactivity of α -tricalcium phosphate. **Journal of Materials Science.** 37(5): 963-969.
- El-Fiqi, A., Kim, J.-H., Perez, R. A., and Kim, H.-W. (2015). Novel bioactive nanocomposite cement formulations with potential properties: incorporation of the nanoparticle form of mesoporous bioactive glass into calcium phosphate cements. **J. Mater. Chem. B.** 3(7): 1321-1334.
- Engel, E., Del Valle, S., Aparicio, C., Altankov, G., Asin, L., Planell, J. A., and Ginebra, M. P. (2008). Discerning the role of topography and ion exchange in cell response of bioactive tissue engineering scaffolds. **Tissue Eng. Part A.** 14(8): 1341-1351.
- Famery, R., Richard, N., and Boch, P. (1994). Preparation of α - and β -tricalcium phosphate ceramics, with and without magnesium addition. **Ceramics International.** 20(5): 327-336.
- Fariña, N. M., Guzón, F. M., Peña, M. L., and Cantalapiedra, A. G. (2008). In vivo behaviour of two different biphasic ceramic implanted in mandibular bone of dogs. **J Mater Sci Mater Med.** 19(4): 1565-1573.
- Farley, J. R., Hall, S. L., Tanner, M. A., and Wergedal, J. E. (1994). Specific activity of skeletal alkaline phosphatase in human osteoblast-line cells regulated by

phosphate, phosphate esters, and phosphate analogs and release of alkaline phosphatase activity inversely regulated by calcium. **J Bone Miner Res.** 9(4): 497-508.

Fernández, E., Boltong, M. G., Ginebra, M. P., Bermúdez, O., Driessens, F. C. M., and Planell, J. A. (1994). Common ion effect on some calcium phosphate cements. **Clin. Mater.** 16(2): 99-103.

Fernández, E., Ginebra, M. P., Boltong, M. G., Driessens, F. C. M., Planell, J. A., Ginebra, J., De Maeyer, E. A. P., and Verbeeck, R. M. H. (1996). Kinetic study of the setting reaction of a calcium phosphate bone cement. **Journal of Biomedical Materials Research.** 32(3): 367-374.

Frankenburg, E. P., Goldstein, S. A., Bauer, T. W., Harris, S. A., and Poser, R. D. (1998). Biomechanical and histological evaluation of a calcium phosphate cement. **J Bone Joint Surg Am.** 80(8): 1112-1124.

Gallinetti, S., Canal, C., and Ginebra, M.-P. (2014). Development and Characterization of Biphasic Hydroxyapatite/ β -TCP Cements. **J. Am. Ceram. Soc.** 97(4): 1065-1073.

Galow, A.-M., Rebl, A., Koczan, D., Bonk, S. M., Baumann, W., and Gimsa, J. (2017). Increased osteoblast viability at alkaline pH in vitro provides a new perspective on bone regeneration. **Biochemistry and Biophysics Reports.** 10: 17-25.

Gbureck, U., Barralet, J. E., Radu, L., Klinger, H. G., and Thull, R. (2004). Amorphous α -Tricalcium Phosphate: Preparation and Aqueous Setting Reaction. **Journal of the American Ceramic Society.** 87(6): 1126-1132.

Gbureck, U., Spatz, K., Thull, R., and Barralet, J. E. (2005). Rheological enhancement of mechanically activated α -tricalcium phosphate cements. **Journal of Biomedical Materials Research Part B: Applied Biomaterials.** 73B(1): 1-6.

Geffers, M., Groll, J., and Gbureck, U. (2015). Reinforcement Strategies for Load-Bearing Calcium Phosphate Biocements. **Materials.** 8(5): 2700.

- Geffers, M., Groll, J., and Gbureck, U. (2015). Reinforcement Strategies for Load-Bearing Calcium Phosphate Biocements. **Materials (Basel, Switzerland)**. 8(5): 2700-2717.
- Ginebra, M. P. (2008). Chapter 10 - Calcium phosphate bone cements. *Orthopaedic Bone Cements*. Deb, S., Woodhead Publishing: 206-230.
- Ginebra, M. P., Boltong, M. G., Fernández, E., Planell, J. A., and Driessens, F. C. M. (1995). Effect of various additives and temperature on some properties of an apatitic calcium phosphate cement. **Journal of Materials Science: Materials in Medicine**. 6(10): 612-616.
- Ginebra, M. P., Canal, C., Espanol, M., Pastorino, D., and Montufar, E. B. (2012). Calcium phosphate cements as drug delivery materials. **Adv. Drug Deliv. Rev.** 64(12): 1090-1110.
- Ginebra, M. P., Driessens, F. C. M., and Planell, J. A. (2004). Effect of the particle size on the micro and nanostructural features of a calcium phosphate cement: a kinetic analysis. **Biomaterials**. 25(17): 3453-3462.
- Ginebra, M. P., Fernández, E., Boltong, M. G., Planell, J. A., Bermúdez, O., and Driessens, F. C. M. (1994). Compliance of a Calcium Phosphate Cement with Some Short-term Clinical Requirements. *Bioceramics*. Andersson, Ö. H., Happonen, R.-P. and Yli-Urpo, A. Oxford, Pergamon: 273-278.
- Ginebra, M. P., Fernández, E., De Maeyer, E. A. P., Verbeeck, R. M. H., Boltong, M. G., Ginebra, J., Driessens, F. C. M., and Planell, J. A. (1997). Setting Reaction and Hardening of an Apatitic Calcium Phosphate Cement. **Journal of Dental Research**. 76(4): 905-912.
- Gisep, A., Wieling, R., Bohner, M., Matter, S., Schneider, E., and Rahn, B. (2003). Resorption patterns of calcium-phosphate cements in bone. **J Biomed Mater Res A**. 66(3): 532-540.
- Goldberg, M., Smirnov, V., Antonova, O., Khairutdinova, D., Smirnov, S., Krylov, A., Sergeeva, N., Sviridova, I., Kirsanova, V., Akhmedova, S., Zhevnenko, S., and

- Barinov, S. (2018). Magnesium-substituted calcium phosphate bone cements containing MgO as a separate phase: synthesis and in vitro behavior. **Mendeleev Communications**. 28.
- Gupta, N., Santhiya, D., and Aditya, A. (2016). Tailored smart bioactive glass nanoassembly for dual antibiotic in vitro sustained release against osteomyelitis. **J. Mater. Chem. B**. 4(47): 7605-7619.
- Habraken, W., Habibovic, P., Epple, M., and Bohner, M. (2016). Calcium phosphates in biomedical applications: materials for the future? **Materials Today**. 19(2): 69-87.
- Hasan, M. L., Kim, B., Padalhin, A. R., Faruq, O., Sultana, T., and Lee, B.-T. (2019). In vitro and in vivo evaluation of bioglass microspheres incorporated brushite cement for bone regeneration. **Mater. Sci. Eng. C**. 103: 109775.
- Hasirci, V., and Hasirci, N. (2018). Sterilization of Biomaterials. *Fundamentals of Biomaterials*. New York, NY, Springer New York: 187-198.
- Henkel, J., Woodruff, M. A., Epari, D. R., Steck, R., Glatt, V., Dickinson, I. C., Choong, P. F. M., Schuetz, M. A., and Hutmacher, D. W. (2013). Bone Regeneration Based on Tissue Engineering Conceptions — A 21st Century Perspective. **Bone Research**. 1: 216.
- Hoppe, A., Güldal, N., and Boccaccini, A. (2011). A Review of The Biological Response to Ionic Dissolution Products From Bioactive Glasses and Glass-Ceramics. **Biomaterials**. 32: 2757-2774.
- Horiuchi, S., Hiasa, M., Yasue, A., Sekine, K., Hamada, K., Asaoka, K., and Tanaka, E. (2014). Fabrications of zinc-releasing biocement combining zinc calcium phosphate to calcium phosphate cement. **Journal of the Mechanical Behavior of Biomedical Materials**. 29: 151-160.
- Hu, Q., Li, Y., Zhao, N., Ning, C., and Chen, X. (2014). Facile synthesis of hollow mesoporous bioactive glass sub-micron spheres with a tunable cavity size. **Mater. Lett**. 134: 130-133.

- Hurle, K., Neubauer, J., Bohner, M., Doebelin, N., and Goetz-Neunhoeffer, F. (2014). Effect of amorphous phases during the hydraulic conversion of α -TCP into calcium-deficient hydroxyapatite. **Acta Biomaterialia**. 10(9): 3931-3941.
- Ishikawa, K. (2010). Bone Substitute Fabrication Based on Dissolution-Precipitation Reactions. **Materials**. 3(2): 1138-1155.
- Islam, K. N., Zuki, A. B. Z., Ali, M. E., Bin Hussein, M. Z., Noordin, M. M., Loqman, M. Y., Wahid, H., Hakim, M. A., and Abd Hamid, S. B. (2012). Facile Synthesis of Calcium Carbonate Nanoparticles from Cockle Shells. **Journal of Nanomaterials**. 2012: 534010.
- Javadian, S., Ruhi, V., Heydari, A., Asadzadeh Shahir, A., Yousefi, A., and Akbari, J. (2013). Self-Assembled CTAB Nanostructures in Aqueous/Ionic Liquid Systems: Effects of Hydrogen Bonding. **Ind. Eng. Chem. Res.** 52(12): 4517-4526.
- Jeong, J., Kim, J. H., Shim, J. H., Hwang, N. S., and Heo, C. Y. (2019). Bioactive calcium phosphate materials and applications in bone regeneration. **Biomaterials Research**. 23(1): 4.
- Jones, J. R. (2013). Review of bioactive glass: from Hench to hybrids. **Acta Biomater.** 9(1): 4457-4486.
- K, N., R, S., Cholewa-Kowalska, K., Pawlik, J., and Laczka, M. (2011). An in vivo study of the new generation of bioactive glass-ceramics as a bone substitute. **Glass Technology: European Journal of Glass Science and Technology Part A**. 52: 63-66.
- Kadajji, V., and Betageri, G. (2011). Water Soluble Polymers for Pharmaceutical Applications. **Polymers**. 3.
- Kanatani, M., Sugimoto, T., Kano, J., and Chihara, K. (2002). IGF-I mediates the stimulatory effect of high phosphate concentration on osteoblastic cell proliferation. **J Cell Physiol**. 190(3): 306-312.
- Kanter, B., Geffers, M., Ignatius, A., and Gbureck, U. (2014). Control of in vivo mineral bone cement degradation. **Acta Biomaterialia**. 10(7): 3279-3287.

- Kattimani, V. S., Kondaka, S., and Lingamaneni, K. P. (2016). Hydroxyapatite--Past, Present, and Future in Bone Regeneration. **Bone and Tissue Regeneration Insights**. 7: BTRI.S36138.
- Kesse, X., Vichery, C., and Nedelec, J.-M. (2019). Deeper Insights into a Bioactive Glass Nanoparticle Synthesis Protocol To Control Its Morphology, Dispersibility, and Composition. **ACS Omega**. 4(3): 5768-5775.
- Khairoun, I., Boltong, M. G., Driessens, F. C. M., and Planell, J. A. (1997). Effect of calcium carbonate on the compliance of an apatitic calcium phosphate bone cement. **Biomaterials**. 18(23): 1535-1539.
- Khairoun, I., Boltong, M. G., Driessens, F. C. M., and Planell, J. A. (1998). Limited compliance of some apatitic calcium phosphate bone cements with clinical requirements. **Journal of Materials Science: Materials in Medicine**. 9(11): 667-671.
- Khashaba, R. M., Moussa, M. M., Mettenburg, D. J., Rueggeberg, F. A., Chutkan, N. B., and Borke, J. L. (2010). Polymeric-calcium phosphate cement composites-material properties: in vitro and in vivo investigations. **Int J Biomater**. 2010.
- Khashaba, R. M., Moussa, M. M., Mettenburg, D. J., Rueggeberg, F. A., Chutkan, N. B., and Borke, J. L. (2010). Polymeric-Calcium Phosphate Cement Composites-Material Properties: In Vitro and In Vivo Investigations. **Int J Biomater**. 2010: 14.
- Kim, C. H., Park, H.-S., Gin, Y. J., Son, Y., Lim, S.-H., Choi, Y. J., Park, K.-S., and Park, C. W. (2004). Improvement of the biocompatibility of chitosan dermal scaffold by rigorous dry heat treatment. **Macromolecular Research**. 12(4): 367-373.
- Klimek, K., Belcarz, A., Pazik, R., Sobierajska, P., Han, T., Wiglusz, R. J., and Ginalska, G. (2016). "False" cytotoxicity of ions-adsorbing hydroxyapatite — Corrected method of cytotoxicity evaluation for ceramics of high specific surface area. **Mater. Sci. Eng. C**. 65: 70-79.

- Kodera, Y., Maeda, M., Sakurai, M., Novosad, J., and Watanabe, M. (2005). INFLUENCE OF ADDITIVES ON THE MECHANICAL PROPERTIES OF α -TRICALCIUM PHOSPHATE CEMENT. **Phosphorus Res. Bull.** 19: 48-53.
- Kohn, D. H., Sarmadi, M., Helman, J. I., and Krebsbach, P. H. (2002). Effects of pH on human bone marrow stromal cells in vitro: implications for tissue engineering of bone. **J Biomed Mater Res.** 60(2): 292-299.
- Kokubo, T., and Takadama, H. (2006). How useful is SBF in predicting in vivo bone bioactivity? **Biomaterials.** 27(15): 2907-2915.
- Kolmas, J., Kafalak, A., Zima, A., and Ślósarczyk, A. (2015). Alpha-tricalcium phosphate synthesized by two different routes: Structural and spectroscopic characterization. **Ceramics International.** 41(4): 5727-5733.
- Komath, M., Varma, H. K., and Sivakumar, R. (2000). On the development of an apatitic calcium phosphate bone cement. **Bull. Mater. Sci.** 23(2): 135-140.
- Kon, M., Hirakata, L. M., Miyamoto, Y., Kasahara, H., and Asaoka, K. (2005). Strengthening of calcium phosphate cement by compounding calcium carbonate whiskers. **Dent Mater J.** 24(1): 104-110.
- Kumar, P., Vinitha, B., and Fathima, G. (2013). Bone grafts in dentistry. **Journal of Pharmacy & Bioallied Sciences.** 5(Suppl 1): S125-S127.
- Kunisch, E., Gunnella, F., Wagner, S., Dees, F., Maenz, S., Bossert, J., Jandt, K. D., and Kinne, R. W. (2019). The poly (l-lactid-co-glycolide; PLGA) fiber component of brushite-forming calcium phosphate cement induces the osteogenic differentiation of human adipose tissue-derived stem cells. **Biomed Mater.** 14(5): 055012.
- Kunisch, E., Maenz, S., Knoblich, M., Ploeger, F., Jandt, K. D., Bossert, J., Kinne, R. W., and Alsalameh, S. (2017). Short-time pre-washing of brushite-forming calcium phosphate cement improves its in vitro cytocompatibility. **Tissue Cell.** 49(6): 697-710.
- L. Evans, S. (2006). Fatigue of PMMA Bone Cement.

- Laurencin, C., Khan, Y., and El-Amin, S. F. (2006). Bone graft substitutes. **Expert Rev Med Devices**. 3(1): 49-57.
- Lee, S. I., Lee, E. S., El-Fiqi, A., Lee, S. Y., Eun-Cheol, K., and Kim, H. W. (2016). Stimulation of Odontogenesis and Angiogenesis via Bioactive Nanocomposite Calcium Phosphate Cements Through Integrin and VEGF Signaling Pathways. **J. Biomed. Nanotechnol.** 12(5): 1048-1062.
- Legeros, R. Z. (1982). Apatite calcium phosphate : possible restorative materials. **J. Dent Res.** 61(Spec Issue): 343.
- Lei, B., Chen, X., Han, X., and Li, Z. (2011). Unique physical-chemical, apatite-forming properties and human marrow mesenchymal stem cells (HMSCs) response of sol-gel bioactive glass microspheres. **J. Mater. Chem. B.** 21(34): 12725-12734.
- Lei, B., Chen, X., Han, X., and Zhou, J. (2012). Versatile fabrication of nanoscale sol-gel bioactive glass particles for efficient bone tissue regeneration. **J. Mater. Chem. B.** 22(33): 16906-16913.
- Li, N., Jiang, C., Zhang, X., Gu, X., Zhang, J., Yuan, Y., Liu, C., Shi, J., Wang, J., and Li, Y. (2015). Preparation of an rhBMP-2 loaded mesoporous bioactive glass/calcium phosphate cement porous composite scaffold for rapid bone tissue regeneration. **J. Mater. Chem. B.** 3.
- Li, Y., Chen, X., Ning, C., Yuan, B., and Hu, Q. (2015). Facile synthesis of mesoporous bioactive glasses with controlled shapes. **Mater. Lett.** 161: 605-608.
- Lim, L.-Y., Khor, E., and Ling, C.-E. (1999). Effects of dry heat and saturated steam on the physical properties of chitosan. **Journal of Biomedical Materials Research.** 48(2): 111-116.
- Lindroos, B., Suuronen, R., and Miettinen, S. (2011). The potential of adipose stem cells in regenerative medicine. **Stem Cell Rev. Rep.** 7(2): 269-291.
- Liu, C., Chen, C.-W., and Ducheyne, P. (2008). In vitrosurface reaction layer formation and dissolution of calcium phosphate cement-bioactive glass composites. **Biomedical Materials.** 3(3): 034111.

- Liu, H., Wei, L. K., Jian, X. F., Huang, J., Zou, H., Zhang, S. Z., and Yuan, G. H. (2018). Isolation, culture and induced differentiation of rabbit mesenchymal stem cells into osteoblasts. **Exp Ther Med.** 15(4): 3715-3724.
- Liu, T., Xu, J., Pan, X., Ding, Z., Xie, H., Wang, X., and Xie, H. (2021). Advances of adipose-derived mesenchymal stem cells-based biomaterial scaffolds for oral and maxillofacial tissue engineering. **Bioact. Mater.** 6(8): 2467-2478.
- Lode, A., Heiss, C., Knapp, G., Thomas, J., Nies, B., Gelinsky, M., and Schumacher, M. (2017). Strontium-modified premixed calcium phosphate cements for the therapy of osteoporotic bone defects. **Acta Biomaterialia.**
- Lu, H., Zhou, Y., Ma, Y., Xiao, L., Ji, W., Zhang, Y., and Wang, X. (2021). Current Application of Beta-Tricalcium Phosphate in Bone Repair and Its Mechanism to Regulate Osteogenesis. **Frontiers in Materials.** 8.
- Lu, J., Yu, H., and Chen, C. (2018). Biological properties of calcium phosphate biomaterials for bone repair: a review. **RSC Advances.** 8(4): 2015-2033.
- Lu, W., Ji, K., Kirkham, J., Yan, Y., Boccaccini, A. R., Kellett, M., Jin, Y., and Yang, X. B. (2014). Bone tissue engineering by using a combination of polymer/Bioglass composites with human adipose-derived stem cells. **Cell Tissue Res.** 356(1): 97-107.
- Majekodunmi, A. O., and Deb, S. (2007). Poly(acrylic acid) modified calcium phosphate cements: the effect of the composition of the cement powder and of the molecular weight and concentration of the polymeric acid. **J Mater Sci Mater Med.** 18(9): 1883-1888.
- Majekodunmi, A. O., Deb, S., and Nicholson, J. W. (2003). Effect of molecular weight and concentration of poly(acrylic acid) on the formation of a polymeric calcium phosphate cement. **Journal of Materials Science: Materials in Medicine.** 14(9): 747-752.
- Maslen, E. N., Streltsov, V. A., and Streltsova, N. R. (1993). X-ray study of the electron density in calcite, CaCO_3 . **Acta Cryst. B.** 49(4): 636-641.

- Massa, A., Perut, F., Chano, T., Woloszyk, A., Mitsiadis, T. A., Avnet, S., and Baldini, N. (2017). The effect of extracellular acidosis on the behaviour of mesenchymal stem cells in vitro. **Eur Cell Mater.** 33: 252-267.
- Matassi, F., Nistri, L., Chicon Paez, D., and Innocenti, M. (2011). New biomaterials for bone regeneration. **Clinical cases in mineral and bone metabolism : the official journal of the Italian Society of Osteoporosis, Mineral Metabolism, and Skeletal Diseases.** 8(1): 21-24.
- McNamara, L. M. (2017). 2.10 Bone as a Material ☆. *Comprehensive Biomaterials II*. Ducheyne, P. Oxford, Elsevier: 202-227.
- Medvecky, L., Stulajterova, R., Sopcak, T., Giretova, M., and Fáberová, M. (2017). Properties of CaO-SiO₂-P₂O₅ reinforced calcium phosphate cements and in vitro osteoblast response. **Biomed Mater.** 12.
- Meng, D., Dong, L., Yuan, Y., and Jiang, Q. (2018). In vitro and in vivo analysis of the biocompatibility of two novel and injectable calcium phosphate cements. **Regenerative Biomaterials.** 6(1): 13-19.
- Mestres, G., Le Van, C., and Ginebra, M.-P. (2012). Silicon-stabilized α -tricalcium phosphate and its use in a calcium phosphate cement: Characterization and cell response. **Acta Biomaterialia.** 8(3): 1169-1179.
- Mickiewicz, R. A., Mayes, A. M., and Knaack, D. (2002). Polymer-calcium phosphate cement composites for bone substitutes. **J. Biomed. Mater. Res.** 61(4): 581-592.
- Mitzner, E., Pelt, P. A. H. M., Mueller, C., Strohwig, A., and Mueller, W.-D. (2009). Material properties and in vitro biocompatibility of a newly developed bone cement. **Materials Research.** 12: 447-454.
- Miyazaki, K., Horibe, T., Antonucci, J. M., Takagi, S., and Chow, L. C. (1993). Polymeric calcium phosphate cements: analysis of reaction products and properties. **Dental materials : official publication of the Academy of Dental Materials.** 9(1): 41-45.

- Miyazaki, K., Horibe, T., Antonucci, J. M., Takagi, S., and Chow, L. C. (1993). Polymeric calcium phosphate cements: analysis of reaction products and properties. **Dental Materials**. 9(1): 41-45.
- Mondal, S., Mondal, A., Mandal, N., Mondal, B., S. Mukhopadhyay, S., Dey, A., and Singh, S. (2014). Physico-chemical characterization and biological response of Labeo rohita-derived hydroxyapatite scaffold.
- Montufar, E. B., Maazouz, Y., and Ginebra, M. P. (2013). Relevance of the setting reaction to the injectability of tricalcium phosphate pastes. **Acta Biomaterialia**. 9(4): 6188-6198.
- Morejón-Alonso, L., Carrodegua, R., Delgado, J., Pérez, J., and Martínez, S. (2007). Effect of sterilization on the properties of CDHA-OCP- β -TCP biomaterial. **Materials Research-ibero-american Journal of Materials - MATER RES-IBERO-AM J MATER**. 10.
- Morejón-Alonso, L., Ferreira, O. J. B., Carrodegua, R. G., and dos Santos, L. A. (2012). Bioactive composite bone cement based on α -tricalcium phosphate/tricalcium silicate. **J. Biomed. Mater. Res. Part B Appl. Biomater**. 100(1): 94-102.
- Murugesu, M. (2017). Pore Structure Analysis Using Subcritical Gas Adsorption Method.
- Nezafati, N., Moztarzadeh, F., Hesaraki, S., Moztarzadeh, Z., and Mozafari, M. (2013). Biological response of a recently developed nanocomposite based on calcium phosphate cement and sol-gel derived bioactive glass fibers as substitution of bone tissues. **Ceramics International**. 39(1): 289-297.
- O'Hara, R. M., Dunne, N. J., Orr, J. F., Buchanan, F. J., Wilcox, R. K., and Barton, D. C. (2010). Optimisation of the mechanical and handling properties of an injectable calcium phosphate cement. **J Mater Sci Mater Med**. 21(8): 2299-2305.
- O'Neill, R., McCarthy, H. O., Montufar, E. B., Ginebra, M. P., Wilson, D. I., Lennon, A., and Dunne, N. (2017). Critical review: Injectability of calcium phosphate pastes and cements. **Acta Biomater**. 50(Supplement C): 1-19.

- O Majekodunmi, A., and Deb, S. (2007). Poly(acrylic acid) modified calcium phosphate cements: The effect of the composition of the cement powder and of the molecular weight and concentration of the polymeric acid.
- O'Hara, R., Buchanan, F., and Dunne, N. (2014). Chapter 2 - Injectable calcium phosphate cements for spinal bone repair. *Biomaterials for Bone Regeneration*. Dubruel, P. and Van Vlierberghe, S., Woodhead Publishing: 26-61.
- O'Hara, R., Buchanan, F., and Dunne, N. (2014). Injectable calcium phosphate cements for spinal bone repair. *Biomaterials for Bone Regeneration*. Dubruel, P. and Van Vlierberghe, S., Woodhead Publishing: 26-61.
- Oliveira, I. R. d., Andrade, T. L. d., Parreira, R. M., Jacobovitz, M., and Pandolfelli, V. C. (2015). Characterization of Calcium Aluminate Cement Phases when in Contact with Simulated Body Fluid. *Materials Research*. 18: 382-389.
- Pan, Z., Jiang, P., Fan, Q., Ma, B., and Cai, H. (2007). Mechanical and biocompatible influences of chitosan fiber and gelatin on calcium phosphate cement. *Journal of Biomedical Materials Research Part B: Applied Biomaterials*. 82B(1): 246-252.
- Pan, Z. H., Cai, H. P., Jiang, P. P., and Fan, Q. Y. (2006). Properties of a Calcium Phosphate Cement Synergistically Reinforced by Chitosan Fiber and Gelatin. *Journal of Polymer Research*. 13(4): 323.
- Perez, R. A., Kim, H.-W., and Ginebra, M.-P. (2012). Polymeric additives to enhance the functional properties of calcium phosphate cements. *Journal of Tissue Engineering*. 3(1): 2041731412439555.
- Phetnin, R., and Rattanachan, S. T. (2015). Preparation and antibacterial property on silver incorporated mesoporous bioactive glass microspheres. *J Solgel Sci Technol*. 75(2): 279-290.
- Phetnin, R. B., Suksaweang, S., Giannasi, C., Brini, A. T., Niada, S., Srisuwan, S., and Rattanachan, S. T. (2020). 3D mesoporous bioactive glass/silk/chitosan scaffolds

- and their compatibility with human adipose-derived stromal cells. **Int. J. Appl. Ceram. Technol.** 17(6): 2779-2791.
- Pillai, C. K. S., Paul, W., and Sharma, C. P. (2009). Chitin and chitosan polymers: Chemistry, solubility and fiber formation. **Progress in Polymer Science.** 34(7): 641-678.
- Queiroz, M., Melo, K., Sabry, D., Sasaki, G., and Rocha, H. (2014). Does the Use of Chitosan Contribute to Oxalate Kidney Stone Formation? **Marine drugs.** 13: 141-158.
- Radin, S., Reilly, G., Bhargave, G., Leboy, P. S., and Ducheyne, P. (2005). Osteogenic effects of bioactive glass on bone marrow stromal cells. **J Biomed Mater Res A.** 73(1): 21-29.
- Ramp, W. K., Lenz, L. G., and Kaysinger, K. K. (1994). Medium pH modulates matrix, mineral, and energy metabolism in cultured chick bones and osteoblast-like cells. **Bone and Mineral.** 24(1): 59-73.
- Rattanachan, S. T., Srakaew, N. L., Thaitalay, P., Thongsri, O., Dangviriyakul, R., Srisuwan, S., Suksaweang, S., Widelitz, R. B., Chuong, C. M., Srithunyarat, T., Kampa, N., Kaenkangplo, D., Hoisang, S., Jittimanee, S., Wipoosak, P., Kamlangchai, P., Yongvanit, K., and Tuchpramuk, P. (2020). Development of injectable chitosan/biphasic calcium phosphate bone cement and in vitro and in vivo evaluation. **Biomed Mater.** 15(5): 055038.
- Rattanachan, S. T., Suksaweang, S., Jiang, T. X., Widelitz, R., Chuong, C., and Srakaew, N. L. O. (2018). Self-setting calcium phosphate enhanced with osteoconduction and bioactivity for bone cement. **Chiang Mai Journal of Science.** 45: 2132-2139.
- Reffitt, D. M., Ogston, N., Jugdaohsingh, R., Cheung, H. F. J., Evans, B. A. J., Thompson, R. P. H., Powell, J. J., and Hampson, G. N. (2003). Orthosilicic acid stimulates collagen type 1 synthesis and osteoblastic differentiation in human osteoblast-like cells in vitro. **Bone.** 32(2): 127-135.

- Rehman, I., and Bonfield, W. (1997). Characterization of hydroxyapatite and carbonated apatite by photo acoustic FTIR spectroscopy. **Journal of Materials Science: Materials in Medicine**. 8(1): 1-4.
- Renno, A. C., Nejadnik, M. R., van de Watering, F. C., Crovace, M. C., Zanotto, E. D., Hoefnagels, J. P., Wolke, J. G., Jansen, J. A., and van den Beucken, J. J. (2013). Incorporation of bioactive glass in calcium phosphate cement: material characterization and in vitro degradation. **J Biomed Mater Res A**. 101(8): 2365-2373.
- Sadiasa, A., Sarkar, S. K., Franco, R. A., Min, Y. K., and Lee, B. T. (2014). Bioactive glass incorporation in calcium phosphate cement-based injectable bone substitute for improved in vitro biocompatibility and in vivo bone regeneration. **J Biomater Appl**. 28(5): 739-756.
- Samper Gaitán, A., Rojas Mora, F. A., Diana María, N., and Méndez Moreno, L. M. (2011). Characterising structural, mechanical and cytotoxic properties of coral-based composite material intended for bone implant applications. **Ingeniería e Investigación**. 31: 135-141.
- Santos Jr., J. G. F., Pita, V. J. R. R., Melo, P. A., Nele, M., and Pinto, J. C. (2013). Effect of process variables on the preparation of artificial bone cements. **Brazilian Journal of Chemical Engineering**. 30: 865-876.
- Sariibrahimoglu, K., Leeuwenburgh, S. C., Wolke, J. G., Yubao, L., and Jansen, J. A. (2012). Effect of calcium carbonate on hardening, physicochemical properties, and in vitro degradation of injectable calcium phosphate cements. **J Biomed Mater Res A**. 100(3): 712-719.
- Sariibrahimoglu, K., Wolke, J. G., Leeuwenburgh, S. C., Yubao, L., and Jansen, J. A. (2014). Injectable biphasic calcium phosphate cements as a potential bone substitute. **J Biomed Mater Res B Appl Biomater**. 102(3): 415-422.
- Schäck, L. M., Noack, S., Winkler, R., Wißmann, G., Behrens, P., Wellmann, M., Jagodzinski, M., Krettek, C., and Hoffmann, A. (2013). The Phosphate Source Influences Gene Expression and Quality of Mineralization during In Vitro

- Osteogenic Differentiation of Human Mesenchymal Stem Cells. **PLOS ONE**. 8(6): e65943.
- Schamel, M. (2017). Novel dual setting approaches for mechanically reinforced mineral biocements.
- Schamel, M., Barralet, J. E., Groll, J., and Gbureck, U. (2017). In vitro ion adsorption and cytocompatibility of dicalcium phosphate ceramics. **Biomater. Res.** 21: 10-10.
- Schumacher, M., and Gelinsky, M. (2015). Strontium modified calcium phosphate cements - Approaches towards targeted stimulation of bone turnover.
- Schumacher, M., Henß, A., Rohnke, M., and Gelinsky, M. (2013). A novel and easy-to-prepare strontium(II) modified calcium phosphate bone cement with enhanced mechanical properties. **Acta Biomaterialia**. 9(7): 7536-7544.
- Schumacher, M., Reither, L., Thomas, J., Kampschulte, M., Gbureck, U., Lode, A., and Gelinsky, M. (2017). Calcium phosphate bone cement/mesoporous bioactive glass composites for controlled growth factor delivery. **Biomater. Sci.** 5(3): 578-588.
- Sheikh, Z., Abdallah, M.-N., Hanafi, A. A., Misbahuddin, S., Rashid, H., and Glogauer, M. (2015). Mechanisms of in Vivo Degradation and Resorption of Calcium Phosphate Based Biomaterials. **Materials**. 8(11): 7913-7925.
- Sheikh, Z., Zhang, Y. L., Tamimi, F., and Barralet, J. (2017). Effect of processing conditions of dicalcium phosphate cements on graft resorption and bone formation. **Acta Biomaterialia**. 53: 526-535.
- Shen, D., Fang, L., Chen, X., and Tang, Y. (2011). Structure and properties of polyacrylic acid modified hydroxyapatite/liquid crystal polymer composite. **J. Reinf. Plast. Compos.** 30: 1155-1163.
- Shie, M. Y., Ding, S. J., and Chang, H. C. (2011). The role of silicon in osteoblast-like cell proliferation and apoptosis. **Acta Biomater.** 7(6): 2604-2614.

- Sing, K. S. W. (1985). Reporting physisorption data for gas/solid systems with special reference to the determination of surface area and porosity (Recommendations 1984). **Pure and Applied Chemistry**. 57(4): 603-619.
- Siqueira, R. L., Maurmann, N., Burguêz, D., Pereira, D. P., Rastelli, A. N. S., Peitl, O., Pranke, P., and Zanotto, E. D. (2017). Bioactive gel-glasses with distinctly different compositions: Bioactivity, viability of stem cells and antibiofilm effect against *Streptococcus mutans*. **Materials Science and Engineering: C**. 76: 233-241.
- Smolen, D., Chudoba, T., Malka, I., Kedzierska-Sar, A., Lojkowski, W., Swieszkowski, W., Kurzydłowski, K. J., Kolodziejczyk-Mierzynska, M., and Lewandowska-Szumiel, M. (2013). Highly biocompatible, nanocrystalline hydroxyapatite synthesized in a solvothermal process driven by high energy density microwave radiation. **International journal of nanomedicine**. 8: 653-668.
- Srakaew, N. L. O., and Rattanachan, S. T. (2014). The pH-Dependent Properties of the Biphasic Calcium Phosphate for Bone Cements. **J. Biomimetics, Biomater. Biomed. Eng.** 21: 3-16.
- Srakaew, N. L. O., and Rattanachan, S. T. (2014). The pH-Dependent Properties of the Biphasic Calcium Phosphate for Bone Cements. **Journal of Biomimetics, Biomaterials and Biomedical Engineering**. 21: 3-16.
- Stulajterova, R., Medvecký, L., Giretova, M., Sopčák, T., and Kovalčíková, A. (2017). Effect of bioglass 45S5 addition on properties, microstructure and cellular response of tetracalcium phosphate/monetite cements. **Mater. Charact.** 126: 104-115.
- Sun, H., Liu, C., Liu, H., Bai, Y., Zhang, Z., Li, X., Li, C., Yang, H., and Yang, L. (2017). A novel injectable calcium phosphate-based nanocomposite for the augmentation of cannulated pedicle-screw fixation. **International Journal of Nanomedicine**. 12: 3395-3406.
- Suneelkumar, C., Datta, K., Srinivasan, M., and Kumar, S. (2008). Biphasic calcium phosphate in periapical surgery. **Journal of Conservative Dentistry**. 11(2): 92-96.

- Swain, S. K., and Sarkar, D. (2013). Study of BSA protein adsorption/release on hydroxyapatite nanoparticles. **Appl. Surf. Sci.** 286: 99-103.
- Szymonowicz, M., Korczynski, M., Dobrzynski, M., Zawisza, K., Mikulewicz, M., Karuga-Kuzniewska, E., Zywickab, B., Rybak, Z., and Wiglusz, R. J. (2017). Cytotoxicity Evaluation of High-Temperature Annealed Nanohydroxyapatite in Contact with Fibroblast Cells. **Materials (Basel, Switzerland)**. 10(6): 590.
- Takechi, M., Miyamoto, Y., Momota, Y., Yuasa, T., Tatehara, S., Nagayama, M., and Ishikawa, K. (2004). Effects of Various Sterilization Methods on the Setting and Mechanical Properties of Apatite Cement. **Journal of biomedical materials research. Part B, Applied biomaterials**. 69: 58-63.
- Talaro, K. P. (2008). Foundations in microbiology, Seventh edition. Boston : McGraw-Hill, [2008] ©2008.
- Tan, Y., Liu, Y., Wu, Z., and Tang, H. Preparation of titanium/tricalcium phosphate bone implant materials by spark plasma sintering. **Frontiers in Bioengineering and Biotechnology**.
- Tavares, L., Esparza Flores, E. E., Rodrigues, R. C., Hertz, P. F., and Noreña, C. P. Z. (2020). Effect of deacetylation degree of chitosan on rheological properties and physical chemical characteristics of genipin-crosslinked chitosan beads. **Food Hydrocolloids**. 106: 105876.
- Thaitalay, P., Thongsri, O., Dangviriyakul, R., Srisuwan, S., Talabnin, C., Suksaweang, S., Srakaew, N. L.-o., and Rattanachan, S. T. (2021). Influence of polyacrylic acid (PAA)/Na₂HPO₄ mixture on biphasic calcium phosphate cement: Enhancing strength and cell viability. **Int. J. Appl. Ceram. Technol.** 18(4): 1365-1378.
- Thürmer, M., Silveira Vieira, R., Fernandes, J., Coelho, W., and Dos Santos, L. A. (2012). Synthesis of Alpha-Tricalcium Phosphate by Wet Reaction and Evaluation of Mechanical Properties.

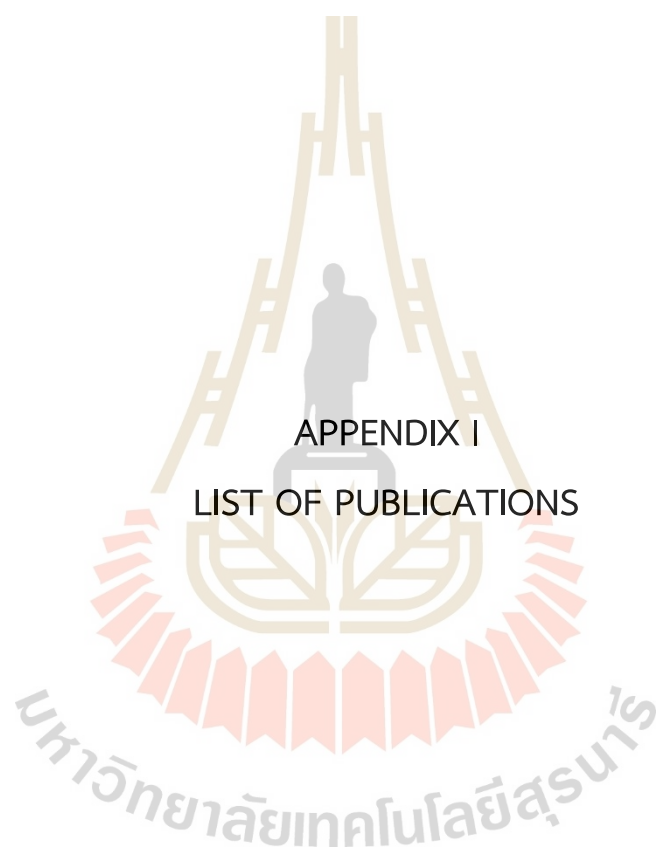
- Thürmer, M. B., Diehl, C. E., Brum, F. J., and dos Santos, L. A. (2013). Development of dual-setting calcium phosphate cement using absorbable polymer. **Artif Organs**. 37(11): 992-997.
- Thürmer, M. B., Diehl, C. E., and dos Santos, L. A. L. (2016). Calcium phosphate cements based on alpha-tricalcium phosphate obtained by wet method: Synthesis and milling effects. **Ceramics International**. 42(16): 18094-18099.
- Thürmer, M. B., Vieira, R. S., Fernandes, J. M., Coelho, W. T. G., and Santos, L. A. (2012). Synthesis of Alpha-Tricalcium Phosphate by Wet Reaction and Evaluation of Mechanical Properties. **Mater. Sci. Forum**. 727-728: 1164-1169.
- Tsai, C. H., Lin, R. M., Ju, C. P., and Chern Lin, J. H. (2008). Bioresorption behavior of tetracalcium phosphate-derived calcium phosphate cement implanted in femur of rabbits. **Biomaterials**. 29(8): 984-993.
- Tsuru, K., Ruslin, Maruta, M., Matsuya, S., and Ishikawa, K. (2015). Effects of the method of apatite seed crystals addition on setting reaction of α -tricalcium phosphate based apatite cement. **Journal of Materials Science: Materials in Medicine**. 26.
- Unosson, J., and Engqvist, H. (2014). Development of a Resorbable Calcium Phosphate Cement with Load Bearing Capacity. **Bioceramics Development and Applications**. 4(1): 1000074.
- Verma, D., Katti, K., and Katti, D. (2006). Experimental investigation of interfaces in hydroxyapatite/polyacrylic acid/polycaprolactone composites using photoacoustic FTIR spectroscopy. **J Biomed Mater Res A**. 77: 59-66.
- Victor, S. P., and Kumar, T. S. S. (2008). Tailoring Calcium-Deficient Hydroxyapatite Nanocarriers for Enhanced Release of Antibiotics. **Journal of Biomedical Nanotechnology**. 4(2): 203-209.
- Vlad, M. D., Gómez, S., Barracó, M., López, J., and Fernández, E. (2012). Effect of the calcium to phosphorus ratio on the setting properties of calcium phosphate

- bone cements. **Journal of Materials Science: Materials in Medicine**. 23(9): 2081-2090.
- Vojtova, L., Michlovska, L., Valova, K., Zboncak, M., Trunec, M., Castkova, K., Krticka, M., Pavlinakova, V., Polacek, P., Dzurov, M., Lukasova, V., Rampichova, M., Suchy, T., Sedlacek, R., Ginebra, M.-P., and Montufar, E. B. (2019). The Effect of the Thermosensitive Biodegradable PLGA–PEG–PLGA Copolymer on the Rheological, Structural and Mechanical Properties of Thixotropic Self-Hardening Tricalcium Phosphate Cement. **International Journal of Molecular Sciences**. 20(2): 391.
- Wagh, A. S. (2016). Chapter 13 - Calcium Phosphate Cements. *Chemically Bonded Phosphate Ceramics (Second Edition)*. Wagh, A. S., Elsevier: 165-178.
- Wang, W., and Yeung, K. W. K. (2017). Bone grafts and biomaterials substitutes for bone defect repair: A review. **Bioactive Materials**. 2(4): 224-247.
- Wang, X. J., Li, Y. B., Jansen, J. A., Li, S. H., and Wolke, J. G. C. (2007). Studies on Non-Quenched Calcium Phosphate Cement: Influences of Quenching and Milling on Setting Characteristic. **Key Engineering Materials**. 330-332: 39-42.
- Wang, Y., Du, X., Liu, Z., Shi, S., and Lv, H. (2019). Dendritic fibrous nano-particles (DFNPs): rising stars of mesoporous materials. **J. Mater. Chem. A**. 7(10): 5111-5152.
- Watanabe, M., Suzuki, H., Mizuno, K., Terada, T., Maeda, M., and Sakurai, M. (2005). EFFECT OF WATER-SOLUBLE ORGANIC POLYMER ON HARDENING OF CALCIUM PHOSPHATE CEMENT. **Phosphorus Res. Bull.** 18: 75-81.
- Watson, K. E., Tenhuisen, K. S., and Brown, P. W. (1999). The formation of hydroxyapatite–calcium polyacrylate composites. **Journal of Materials Science: Materials in Medicine**. 10(4): 205-213.
- Webster, T. J., Ergun, C., Doremus, R. H., Siegel, R. W., and Bizios, R. (2001). Enhanced osteoclast-like cell functions on nanophase ceramics. **Biomaterials**. 22(11): 1327-1333.

- Wei, C.-K., and Ding, S.-J. (2016). Acid-resistant calcium silicate-based composite implants with high-strength as load-bearing bone graft substitutes and fracture fixation devices. **Journal of the Mechanical Behavior of Biomedical Materials**. 62: 366-383.
- Wilson, R., Elliott, J. C., and Dowker, S. E. P. (1999). Rietveld refinement of the crystallographic structure of human dental enamel apatites. **Am. Mineral**. 84: 1406 - 1414.
- Wiltfang, J., Merten, H. A., Schlegel, K. A., Schultze-Mosgau, S., Kloss, F. R., Rupprecht, S., and Kessler, P. (2002). Degradation characteristics of α and β tri-calcium-phosphate (TCP) in minipigs. **Journal of Biomedical Materials Research**. 63(2): 115-121.
- Wu, C., Lu, G., Ji, M., and Wang, X. (2016). Effects of acidosis on the osteogenic differentiation of human bone marrow mesenchymal stem cell. **Int J Clin Exp Med**. 9(12): 23182-23189.
- Wu, T.-Y., Zhou, Z.-B., He, Z.-W., Ren, W.-P., Yu, X.-W., and Huang, Y. (2014). Reinforcement of a new calcium phosphate cement with RGD-chitosan-fiber. **Journal of Biomedical Materials Research Part A**. 102(1): 68-75.
- Xu, H., Eichmiller, F., and Giuseppetti, A. (2000). Reinforcement of a Self Setting Calcium Phosphate Cement With Different Fibers. **J. Biomed. Mater. Res.** . 52: 107-114.
- Xu, H. H. K., Carey, L. E., Simon, C. G., Takagi, S., and Chow, L. C. (2007). Premixed calcium phosphate cements: Synthesis, physical properties, and cell cytotoxicity. **Dent Mater**. 23(4): 433-441.
- Xu, H. H. K., Wang, P., Wang, L., Bao, C., Chen, Q., Weir, M. D., Chow, L. C., Zhao, L., Zhou, X., and Reynolds, M. A. (2017). Calcium phosphate cements for bone engineering and their biological properties. **Bone Res**. 5(1): 17056.
- Yan, X., Huang, X., Yu, C., Deng, H., Wang, Y., Zhang, Z., Qiao, S., Lu, G., and Zhao, D. (2006). The in-vitro bioactivity of mesoporous bioactive glasses. **Biomaterials**. 27(18): 3396-3403.

- Yan, X., Yu, C., Zhou, X., Tang, J., and Zhao, D. (2004). Highly Ordered Mesoporous Bioactive Glasses with Superior In Vitro Bone-Forming Bioactivities. **Angew. Chem. Int. Ed.** 43(44): 5980-5984.
- Yan, X. X., Deng, H. X., Huang, X. H., Lu, G. Q., Qiao, S. Z., Zhao, D. Y., and Yu, C. Z. (2005). Mesoporous bioactive glasses. I. Synthesis and structural characterization. **J. Non-Cryst. Solids.** 351(40): 3209-3217.
- Yang, Q., Troczynski, T., and Liu, D. M. (2002). Influence of apatite seeds on the synthesis of calcium phosphate cement. **Biomaterials.** 23(13): 2751-2760.
- Yang, Y.-M., Zhao, Y.-H., Liu, X.-H., Ding, F., and Gu, X.-S. (2007). The effect of different sterilization procedures on chitosan dried powder. **Journal of Applied Polymer Science.** 104(3): 1968-1972.
- Yashima, M., and Sakai, A. (2003). High-temperature neutron powder diffraction study of the structural phase transition between α and α' phases in tricalcium phosphate $\text{Ca}_3(\text{PO}_4)_2$. **Chem. Phys. Lett.** 372(5): 779-783.
- Yashima, M., Sakai, A., Kamiyama, T., and Hoshikawa, A. (2003). Crystal structure analysis of β -tricalcium phosphate $\text{Ca}_3(\text{PO}_4)_2$ by neutron powder diffraction. **J. Solid State Chem.** 175(2): 272-277.
- Yu, L., Li, Y., Zhao, K., Tang, Y., Cheng, Z., Chen, J., Zang, Y., Wu, J., Kong, L., Liu, S., Lei, W., and Wu, Z. (2013). A novel injectable calcium phosphate cement-bioactive glass composite for bone regeneration. **PloS one.** 8(4): e62570-e62570.
- Yubao, L., Xingdong, Z., and de Groot, K. (1997). Hydrolysis and phase transition of alpha-tricalcium phosphate. **Biomaterials.** 18(10): 737-741.
- Zamanian, A. (2012). The Effect of Paste Concentration on Mechanical and Setting Properties of Calcium Phosphate Bone Cements. **Advanced Chemical Engineering Research.** 1: 1-7.
- Zawadzki, J., and Kaczmarek, H. (2010). Thermal treatment of chitosan in various conditions. **Carbohydrate Polymers.** 80(2): 394-400.

- Zhang, J., Liu, W., Schnitzler, V., Tancret, F., and Bouler, J.-M. (2014). Calcium phosphate cements for bone substitution: Chemistry, handling and mechanical properties. **Acta Biomaterialia**. 10(3): 1035-1049.
- Zhang, J. T., Tancret, F., and Bouler, J. M. (2011). Fabrication and mechanical properties of calcium phosphate cements (CPC) for bone substitution. **Materials Science and Engineering: C**. 31(4): 740-747.
- Zhao, L., Li, J., Zhang, L., Wang, Y., Wang, J., Gu, B., Chen, J., Hao, T., Wang, C., and Wen, N. (2016). Preparation and characterization of calcium phosphate/pectin scaffolds for bone tissue engineering. **RSC Advances**. 6(67): 62071-62082.
- Zhao, R., Xie, P., Zhang, K., Tang, Z., Chen, X., Zhu, X., Fan, Y., Yang, X., and Zhang, X. (2017). Selective effect of hydroxyapatite nanoparticles on osteoporotic and healthy bone formation correlates with intracellular calcium homeostasis regulation. **Acta Biomaterialia**. 59: 338-350.
- Zhu, Y., Zhang, J., Fu, M., Zeng, J., Omari-Siaw, E., and Xu, X.-m. (2014). Calcium Carbonate Nanoparticles Templated by Mixed Polymeric Micelles: Characterization, In Vitro Drug Release and Oral Bioavailability in Beagle Dogs. **LATIN AMERICAN JOURNAL OF PHARMACY**. 33: 1106-1113.
- Zhuang, C., Zhong, Y., and Zhao, Y. (2019). Effect of deacetylation degree on properties of Chitosan films using electrostatic spraying technique. **Food Control**. 97: 25-31.



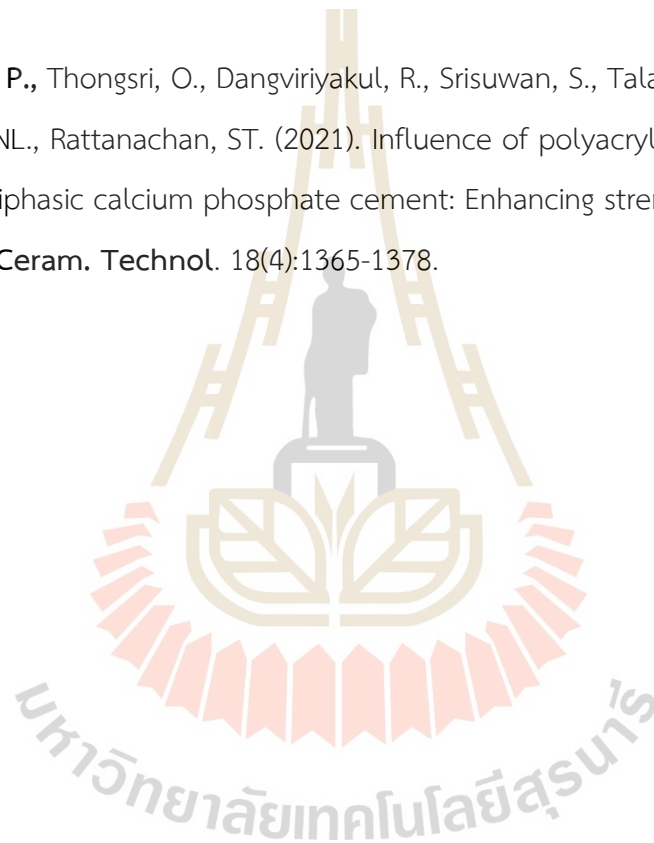
APPENDIX I

LIST OF PUBLICATIONS

มหาวิทยาลัยเทคโนโลยีสุรนารี

LIST OF PUBLICATIONS

1. **Thaitalay, P.**, Srakaew, NL., Rattanachan, ST. (2018): Comparison among alpha-tricalcium phosphate synthesized by solid state reaction and wet chemical reaction for calcium phosphate cements. **Chiang Mai J. Sci.** 45:2123-2131.
2. **Thaitalay, P.**, Thongsri, O., Dangviriyakul, R., Srisuwan, S., Talabnin, C., Suksaweang, S., Srakaew, NL., Rattanachan, ST. (2021). Influence of polyacrylic acid (PAA)/Na₂HPO₄ mixture on biphasic calcium phosphate cement: Enhancing strength and cell viability. **Int. J. Appl. Ceram. Technol.** 18(4):1365-1378.



BIOGRAPHY

Parithat Thaitalay was born on February 26, 1993 in Nakhon Ratchasima, Thailand. In 2015, she received her bachelor's degree in Ceramic Engineering, School of Ceramic Engineering, Institute of Engineering, Suranaree University of Technology (SUT), Nakhon Ratchasima. In the same year, she received the Royal Golden Jubilee Ph.D. Program scholarship from the Thailand Research Fund and started studying for her Ph.D. in the Materials Engineering Program, Institute of Engineering, SUT. During her Ph.D. program, she did short-term research at the University of Manchester, UK for 6 months (May to October 2019). Afterward, she also did another short-term research at the University of Milano, Italy for 6 months (February to July 2020).

